



# **Blood Typing Using Bioactive Paper Devices and Liquid Micro Reactors**

**Thesis in fulfillment of the requirement for the degree of  
Doctor of Philosophy in Chemical Engineering**

**By**

**Lizi Li**

*Master of Science*

**Department of Chemical Engineering**

**Faculty of Engineering**

**MONASH UNIVERSITY**

**October 2015**



*Dedicated to my parents*

*Xiuying Li and Guoguang Li*

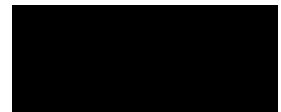




## **Copyright Notice**

Under the Copyright Act 1968, this thesis must be used only under the normal conditions of scholarly fair dealing. In particular no results or conclusions should be extracted from it, nor should it be copied or closely paraphrased in whole or in part without the written consent of the author. Proper written acknowledgement should be made for any assistance obtained from this thesis.

I certify that I have made all reasonable efforts to secure copyright permissions for third party content included in this thesis and have not knowingly added copyright content to my work without the owner's permission.

A solid black rectangular box used to redact the author's signature.

.....

Lizi Li

**This page is intentionally blank**

# TABLE OF CONTENTS

	Page
Table of Contents	iii
General Declaration	ix
Acknowledgments	xi
Abstract	xix
List of Publications and Awards	xv
List of Figures	xix
List of Tables	xxv
List of Abbreviations	xxvii
List of Nomenclature	xxix
<b>Chapter 1 Introduction and Literature Review</b> .....	<b>1</b>
1.1 Introduction .....	3
1.2 Blood grouping techniques.....	6
1.2.1 Blood groups.....	6
1.2.1.1 What is the blood group.....	6
1.2.1.2 Medical and biological significance of blood groups.....	7
1.2.2 Existing blood typing techniques .....	8
1.2.2.1 Blood typing principles.....	8
1.2.2.2 Conventional laboratory blood typing techniques .....	9
1.2.3 Demand for low-cost POC blood typing devices .....	11
1.2.4 Automation of blood typing techniques .....	13
1.3 Paper as substrate for microfluidic devices .....	15
1.3.1 Microfluidic devices.....	15
1.3.1.1 Review of microfluidics .....	15
1.3.1.2 Microfluidic technologies for POC diagnostic devices .....	17
1.3.2 Overview of paper.....	18
1.3.2.1 Production process of paper.....	19
1.3.2.2 Paper chemistry .....	21
1.3.2.3 Paper physics.....	23
1.3.2.4 Comparison of paper with other materials for microfluidic devices .....	24

1.3.3 Development of paper-based microfluidic devices .....	26
1.3.3.1 Fabrication techniques .....	27
1.3.3.2 Detection techniques .....	29
1.4 Paper-based blood typing devices .....	34
1.4.1 Development of paper-based blood typing devices.....	34
1.4.2 Previous studies of fundamentals for paper-based blood typing devices .....	39
1.5 Liquid micro reactors .....	42
1.5.1 Design principles of liquid micro reactors.....	42
1.5.2 Superhydrophobicity for liquid micro reactors for blood typing applications..	44
1.6 Research objectives .....	49
1.7 Thesis outline .....	50
1.8 References.....	54

## **Part I Mechanisms of Paper-Based Blood Typing Devices**

### **Chapter 2 A Study of the Transport and Immobilisation Mechanisms of Human Red Blood Cells in a Paper-Based Blood Typing Device Using Confocal**

<b>Microscopy .....</b>	<b>71</b>
2.1 Abstract.....	75
2.2 Keywords .....	75
2.3 Introduction.....	76
2.4 Experimental .....	79
2.4.1 Materials.....	79
2.4.2 Methods.....	80
2.5 Results and disscussion .....	81
2.5.1 Observation of red blood cells in paper using confocal microscopy.....	81
2.5.2 The activity of the red blood cell antigen after FITC labelling.....	83
2.5.3 Mechanisms of red blood cell immobilisation in antibody-treated paper .....	83
2.5.4 An application study of blood elution patterns in paper using the confocal method .....	86
2.6 Conclusions.....	90
2.7 Supporting information.....	91
2.8 Acknowledgement.....	93
2.9 References.....	93

### **Chapter 3 Revealing the Transport Behaviour of Human Red Blood Cells in Paper Using Scanning Electron Microscopy Combined with Focused Ion Beam**

<b>Milling .....</b>	<b>97</b>
3.1 Abstract .....	101
3.2 Keywords.....	102
3.3 Introduction .....	102
3.4 Experimental section.....	104
3.4.1 Materials .....	104
3.4.2 Methods .....	104
3.4.2.1 Handsheet making .....	104
3.4.2.2 Specimen preparation and SEM observation.....	105
3.4.2.3 FIB tomography setup .....	105
3.4.2.4 Data collection and 3D reconstruction .....	105
3.5 Results and disscussion .....	106
3.5.1 Theoretical background of aqueous fluid transportation in paper network....	106
3.5.2 Capturing the moment that blood penetrates the fibre network in paper .....	107
3.5.3 Construction of 3D FIB-based SEM images of RBCs in paper network.....	109
3.5.4 The pathways of human red blood cells in paper networks .....	111
3.6 Conclusions .....	115
3.7 Acknowledgements.....	115
3.8 References .....	116

### **Chapter 4 Control Performance of Paper-based Blood Analysis Devices through Paper Structure Design .....**

4.1 Abstract .....	123
4.2 Keywords.....	124
4.3 Introduction .....	124
4.4 Experimental section.....	127
4.4.1 Materials .....	127
4.4.2 Methods .....	127
4.5 Results and disscussion .....	129
4.5.1 Isolation of the paper physical structure from the influence of chemical additives and fines .....	129

4.5.2 Characterization of pore size distribution of paper .....	132
4.5.3 Effect of paper's physical structure on lateral elution blood typing performance .....	137
4.5.4 Effect of paper physical structure on vertical flow-through blood typing performance .....	141
4.6 Conclusions.....	145
4.7 Supporting information.....	145
4.8 Acknowledgements .....	148
4.9 References.....	148

## **Part II Blood Typing Devices Based on Liquid Micro Reactors**

<b>Chapter 5 Superhydrophobic Surface Supported Bioassay – An Application in blood Typing.....</b>	<b>155</b>
5.1 Abstract.....	159
5.2 Keywords .....	159
5.3 Introduction.....	160
5.4 Materials and methods .....	163
5.4.1 Fabrication of superhydrophobic Teflon powder surface on polymer film ....	163
5.4.2 Observation of haemagglutination reaction inside the blood sample drop.....	163
5.4.3 Blood typing assay on superhydrophobic surfaces .....	164
5.5 Results and discussion .....	164
5.5.1 Contact angle characterization of the superhydrophobic Teflon powder surface .....	164
5.5.2 Observation of haemagglutination inside the blood sample droplet .....	165
5.5.3 Blood typing using superhydrophobic surfaces as a low-cost supporting substrate.....	166
5.6 Conclusion .....	169
5.7 Supporting information.....	170
5.8 Acknowledgements .....	170
5.9 References.....	170
 <b>Chapter 6 Liquid Marbles as Micro Bio-Reactors for Rapid Blood Typing .....</b>	 <b>173</b>
6.1 Keywords .....	177

6.2 Introduction .....	177
6.3 Experimental.....	178
6.4 Results and disscussion.....	179
6.5 Acknowledgements.....	183
6.6 References .....	184

<b>Chapter 7 Conclusions and Future Work.....</b>	<b>179</b>
---	------------

<b>Appendix I Published First and Co-Authored Papers Included in the Main Body of This Thesis .....</b>	<b>I-1</b>
---	------------

I (1) A study of the transport and immobilization mechanisms of human red blood cells in a paper-based blood typing device using confocal microscopy .....	I-3
I (2) Control performance of paper-based blood analysis devices through paper structure design.....	I-11
I (3) Superhydrophobic surface supported bioassay-An application in blood typing .....	I-23
I (4) Liquid marbles as micro-bioreactors for rapid blood typing.....	I-29

<b>Appendix II Published Co-Authored Papers Not Included in the Main Body of This Thesis .....</b>	<b>II-1</b>
--	-------------

III (1) Strategy to enhance the wettability of bioactive paper-based sensors .....	II-3
III (2) Charge transport between liquid marbles .....	II-9
III (3) Paper-based device for rapid typing of secondary human blood groups..	II-17
III (4) Red blood cell transport mechanisms in polyester thread-based blood typing devices.....	II-27

**This page is intentionally blank**



**Declaration for thesis based or partially based on conjointly published or unpublished work**

**General Declaration**

In accordance with Monash University Doctorate Regulation 17.2 Doctor of Philosophy and Research Master's regulations the following declarations are made:

I hereby declare that this thesis contains no material which has been accepted for the award of any other degree or diploma at any university or equivalent institution and that, to the best of my knowledge and belief, this thesis contains no material previously published or written by another person, except where due reference is made in the text of the thesis.

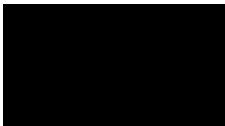
This thesis includes 4 original papers published in peer reviewed journals and 1 unpublished publications. The core theme of the thesis is to develop blood typing techniques based on bioactive paper devices and liquid micro reactors. The ideas, development and writing up of all the papers in the thesis were the principal responsibility of myself, the candidate, working within the Department of Chemical Engineering, Monash University under the supervision of Professor Wei Shen.

The inclusion of co-authors reflects the fact that the work came from active collaboration between researchers and acknowledges input into team-based research.

In the case of Chapters 2-6 my contribution to the work involved the following:

Thesis chapter	Publication title	Publication status*	Nature and extent of candidate's contribution
2	A study of the transport and immobilisation mechanisms of human red blood cells in a paper-based blood typing device studied using confocal microscopy	Published	Initiation, key ideas, experimental works, analysis of results, writing up
3	Revealing the transport behaviour of human red blood cells in paper using scanning electron microscopy combined with focused ion beam milling	To be submitted	Initiation, key ideas, experimental works, analysis of results, writing up
4	Control performance of paper-based blood analysis devices through paper structure design	Published	Initiation, key ideas, experimental works, analysis of results, writing up
5	Superhydrophobic surface supported bioassay – An application in blood typing	Published	Initiation, key ideas, experimental works, analysis of results, writing up
6	Liquid marbles as micro-bioreactors for rapid blood typing	Published	Initiation, key ideas, experimental works, analysis of results, writing up

I have / have not (circle that which applies) renumbered sections of submitted or published papers in order to generate a consistent presentation within the thesis.

**Signed:** .....  .....

**Date:** ..... **25-Sep-2015** .....

**This page is intentionally blank**

## ACKNOWLEDGEMENTS

PhD study is not easy. During the past four years, I suffered from difficulties, struggled, and get confused. But finally this study has been successfully completed. I am so pleased to have these research outcomes, because they make me feel I have made a little bit contribution to the development of science and technology for our world, though it is such tiny. I like a song of Kelly Clarkson, which says “what doesn’t kill you makes you stronger”. I think it is the same as for my PhD study. Here I would like to express my sincere appreciation to the people who cared, guided and helped me in my past life. Without them, I would not complete this research.

First of all, I would like to acknowledge respectfully, the help and support I have received from my dear supervisor, Professor Wei Shen, who has been an enduring mentor, a great teacher, an amazing scientist with particularly genius ideas and skills, and a patient friend at all stages of my PhD candidature. During my PhD candidature, he trained me to think critically and independently; encouraged me to try innovative ideas; taught me to improve my writing skills for publication in academic journals; supported me when I was in stress. Most importantly, I have learnt from him how to be a good researcher and a wise teacher, which will benefit me in my future career and my life.

I gratefully acknowledge Haemokinesis, ARC Linkage Grant, and Monash University for providing me the living allowance and tuition fee scholarship which have made my PhD work possible.

I would like to acknowledge Dr. Jing Fu, Dr. Boyin Liu in Department of Mechanical Engineering at Monash University, Dr. Siew Hoo in Department of Chemical Engineering at Monash University, Professor Yonghao Ni in Department of Chemical Engineering at University of New Brunswick, Dr. Wen Liu and Ms. Xiaolei Huang in China National Pulp and Paper Research Institute, for their collaborative work.

I would like to thank all the academic staff members at Bioresource Processing Research Institute of Australia (BioPRIA) and Department of Chemical Engineering at Monash University. Special thanks to Professor Gil Garnier and Dr. Warren Batchelor

for their kind support and suggestions. I also acknowledge the support of the administrative staff and the technical staff at BioPRIA and Department of Chemical Engineering, particularly Ms. Janette Anthony, Ms. Heather McIlesh, Ms. Lilyanne Price, Ms. Jill Crisfield, Ms. Kim Phu, Mr. Scott Sharman, Mr. Gamini Ganegoda, for their assistance throughout my study.

I would like to express many thanks to Dr. Junfei Tian for his help and suggestions throughout my project, especially for his innovative inspirations when I just started my candidature. I would like to thank Dr. Xu Li, Dr. David Ballerini, Dr. Tina Arbatan, Dr. Miaosi Li, Ms. Liyun Guan, Ms. Azadeh Nilghaz, for their support and help during the experimental work and paper writing. I will also thank Mr. Rong Cao, Ms. Windy Huang, Mr. Jielong Su, and all other students at BioPRIA for their friendship throughout my PhD study.

I would like to express my deep gratitude and thanks to my housemates. They are Dr. Kai Zhang, Mr. Le Song, Dr. Chengcheng Gao, Dr. Jie Zong, Ms. Yu Zhou, and Dr. Jie Zhang. I will always appreciate and cherish their help, support and friendship during my life.

Last but most importantly, I would like to thank my parents and every member in my family for their deep, unconditional and lifetime love, encouragement, and support. I love them forever.

## ABSTRACT

Blood typing is an important medical immunodiagnostic test for human blood transfusion and organ transplantation. Today, the global demand for accurate and rapid blood typing diagnosis is extremely large. However, highly sophisticated blood typing techniques are not appropriate for resource-limited regions, as they are either too expensive or require professional technicians to operate them. There is also an extensive demand for low-cost blood typing techniques with the capabilities of automation and high-throughput operation in blood bank laboratories and hospitals. To solve these problems, the research reported in this thesis focuses on the investigation and development of blood typing devices based on bioactive paper, and liquid micro reactors fabricated using superhydrophobic materials.

This thesis includes two parts, which present research work on blood typing techniques based on bioactive paper devices and liquid micro reactors. In the first part, research into the fundamental mechanisms of paper-based blood typing devices combines scientific information with microscopic techniques and expertise in papermaking. The agglutination and immobilization mechanisms of red blood cells (RBCs) in antibody-treated paper are explored using confocal microscopy. The transport pathways of RBCs within the fibre network of paper are studied using a combined dual beam system with scanning electron microscopy (SEM) and focused ion beam (FIB) technology. Both these microscopic methods developed are powerful techniques for providing the details of RBCs at cellular level inside paper. This part also demonstrates a potential application for controlling the performance of paper-based blood analysis devices through paper structure design, which can be achieved during the papermaking process. Clear understanding of the fundamental mechanisms is essential for the design and production of paper-based blood typing devices which meet the ASSURED criteria (affordable, sensitive, specific, user-friendly, rapid, equipment-free and deliverable to those who need them). It is also important for the development of other paper-based blood analysis devices, and will contribute to the improvement of public health situations in rural areas and developing countries.

The second part of this thesis presents innovations in the application of liquid micro reactors fabricated from superhydrophobic materials for blood typing devices. Two design concepts for the production of liquid micro reactors are demonstrated in this part: one is a superhydrophobic surface-supported liquid drop; the other is a liquid marble – a liquid drop wrapped in superhydrophobic powder. In both cases, the near-spherical shape of the liquid micro reactors enables the devices to provide clear and magnified side views to facilitate the observation of the detailed processes of RBC haemagglutination. Most importantly, by integrating these devices with advanced image capture and processing techniques, the automation of high-throughput blood typing, including rapid assay result interpretation, data storage, and transmission, can be achieved.

The author sincerely hopes that the findings presented in this thesis on the applications of bioactive paper and liquid micro reactors in blood typing will serve the community by providing high-performance, simple blood typing devices. The author also hopes that the findings will be extended to the development of other blood-based diagnostic devices.

## LIST OF PUBLICATIONS AND AWARDS

### Peer-Reviewed Journal Papers

The following published papers are included in the main body of this thesis as individual chapters. The sections of these published papers have been renumbered in order to generate a consistent presentation within the thesis. Papers in their published format are included as Appendix 1 in this thesis.

1. **Li, L.**; Tian, J.; Ballerini, D.; Li, M.; Shen, W., A study of the transport and immobilization mechanisms of human red blood cells in a paper-based blood typing device using confocal microscopy, *Analyst*, **2013**, 138 (17): 4933-4940.
2. **Li, L.**; Huang, L.; Liu, W.; Shen, W., Control performance of paper-based blood analysis devices through paper structure design, *ACS Applied Materials & Interfaces*, **2014**, 6 (23): 21624–21631.
3. **Li, L.**; Tian, J.; Li, M.; Shen, W., Superhydrophobic surface supported bioassay-An application in blood typing, *Colloids and Surfaces B: Biointerfaces*, **2013**, 106: 176-180.
4. Arbatan, T.; **Li, L.**; Tian, J.; Shen, W., Liquid marbles as micro-bioreactors for rapid blood typing, *Advanced Healthcare Materials*, **2011**, 1 (1): 80-83.

The following published papers are not included in the main body of this thesis and can be found in Appendix 2 in their published format.

1. Tian, J.; Jarujamrus, P.; **Li, L.**; Li, M.; Shen, W., Strategy to enhance the wettability of bioactive paper-based sensors, *ACS Applied Materials & Interfaces*, **2012**, 4 (12): 6573-6578.
2. Li, M.; Tian, J.; **Li, L.**; Liu, A.; Shen, W., Charge transport between liquid marbles, *Chemical Engineering Science*, **2013**, 97: 337-343.

3. Li, M.; Then, W. L.; **Li, L.**; Shen, W., Paper-based device for rapid typing of secondary human blood groups, *Analytical and Bioanalytical Chemistry*, **2014**, 406 (3): 669-677.
4. Nilghaz, A.; Ballerini, D.; Guan, L.; **Li, L.**; Shen, W., Red blood cell transport mechanisms in polyester thread-based blood typing devices, *Analytical and Bioanalytical Chemistry*, **2015**.

## Conference Papers

1. **Li, L.**; Huang, L.; Liu, W.; Shen, W., Improve blood typing performance within paper substrate through cellulosic network structure design, *The 249th ACS National Meeting & Exposition*, Denver, USA, **2015**.
2. **Li, L.**; Tian, J.; Li, M.; Shen, W., Superhydrophobic surface based bioassay for blood typing, *The 7th Biennial Australian Colloid & Interface Symposium*, Hobart, Australia, **2015**
3. **Li, L.**; Ballerini, D.; Tian, J.; Li, M.; Shen, W., Paper-Based Blood Grouping; Exploring the Mechanisms of Red Blood Cell Agglutination and Transportation in Antibody-Treated Paper, *The 15th Pulp and Paper Fundamental Research Symposium*, London, UK, **2013**.

## Awards

1. Excellence Award of the 8th “ChunHui” Start-up Competition for Overseas Chinese Students, Guangzhou, China, December 2013.
2. The Australian Museum Eureka Prize of “Innovative Use of Technology”, Group member, Sydney, Australia, September 2012.



3. IChemE award of “Dhirubhai Ambani Chemical Engineering Innovation for Resource-Poor People Award”, Group member, UK, November 2012.

**This page is intentionally blank**

## LIST OF FIGURES

### Chapter 1

- Figure 1:** A schematic of different types of blood group active proteins and glycoproteins based on their integration into the red cell surface membrane.. (With permission from ref. [3]. Copyright (2010) Geoff Daniels and Imelda Bromilo)
- Figure 2:** Example of ABO blood types. When an RBC possesses certain antigens on its surface, the corresponding antibody is absent in the blood plasma, and vice versa. (With permission from ref. [13]. Copyright (2007) McGraw-Hill Companies, Inc.)
- Figure 3:** The production of paper products from raw materials. (With permissions from ref. [68]. Copyright (2009) De Gruyter)
- Figure 4:** A simplified diagram of a Fourdrinier paper machine. (With permissions from ref. [68]. Copyright (2009) De Gruyter)
- Figure 5:** Schematic picture of the arrangement of cellulose, hemicelluloses and lignin in the secondary wall of wood fibres. (With permissions from ref.[67]. Copyright (2009) De Gruyter)
- Figure 6:** Examples of detection techniques for paper-based microfluidic devices. (a) Colourimetric detection of heavy metals. (b) Colourimetric detection of liver function. (c) Dual electrochemical/colourimetric determination of gold and iron. (d) Electrochemical detection of glucose, lactate and uric acid. (e) Antibody conjugated gold nanoparticle detection of immunoglobulin. (f) Antibody conjugated gold nanoparticle detection of *Pseudomonas aeruginosa* and *Staphylococcus aureus*. (g) ECL detection of a sample solution 2-(dibutylamino)-ethanol (DBAE). (h) Schematic of the construction of a CL sensor in paper-based microfluidics. (i) Fluorescent sensing for the growth of bacteria. (With permissions from ref.[82]. Copyright (2013) Royal Society of Chemistry)
- Figure 7:** Paper-based blood typing device using wicking of agglutinated RBCs from specific antigen/antibody interactions on dry paper strips. (With permissions from ref.[6]. Copyright (2010) American Chemical Society)
- Figure 8:** Paper-based blood typing assay using agglutinated blood fixations on papers and chromatographically eluted with 0.9% NaCl buffer for 10 min. (With permissions from ref. [8]. Copyright (2012) American Chemical Society)
- Figure 9:** Paper-based blood typing device for simultaneously determining Rh typing and forward and reverse ABO blood groups (With permissions from ref. [127]. Copyright (2015) Elsevier).
- Figure 10:** Blood typing results based on smartphone-based analysis. (a) Blood typing result (B+) is shown in bar channels, (b) reading the result using the Android

application, and c) acquiring the blood result with text on the screen. (With permissions from ref. [11]. Copyright (2014) American Chemical Society)

**Figure 11:** Schematic diagram of a simple protocol for blood typing using testing paper and inspection paper. (With permission from ref. [7] Copyright (2012) Royal Society of Chemistry)

**Figure 12:** Paper-based blood typing devices reporting results in written text. a) ABO and Rh groups; (With permissions from ref. [9]. Copyright (2012) WILEY-VCH Verlag GmbH & Co. KGaA) b) secondary blood groups. (With permissions from ref. [10]. Copyright (2014) Springer)

**Figure 13:** Protocol for semi-quantification of the desorbed antibody from testing papers by saline washing simulation. (With permission from ref. [7] Copyright (2012) Royal Society of Chemistry)

**Figure 14:** Basic structural units of a micro reactor system. (With permission from ref. [131] Copyright (2012) Elsevier)

**Figure 15:** Flow patterns: (a) parallel flow with longitudinal contact interface in a microchannel; (b) slug flow with transverse contact interface in a microchannel. (With permission from ref. [131] Copyright (2012) Elsevier)

**Figure 16:** Graphical demonstration of (a) normal surface and (b) superhydrophobic surface..

**Figure 17:** Behaviour of a liquid drop on a rough surface: (a) liquid penetrates into the spikes (Wenzel model); (b) liquid suspended on the spikes (Cassie–Baxter model).

**Figure 18:** A 50  $\mu\text{L}$  PVDF-coated water marble. (With permissions from ref.[156]. Copyright (2011) Royal Society of Chemistry)

**Figure 19:** Design concepts of liquid micro reactors for blood typing applications: (a) superhydrophobic surface-supported micro liquid drop; (b) liquid marble fabricated with hydrophobic powder.

## Chapter 2

**Figure 1:** An example of paper-based assay for rapid blood typing. (a) A schematic diagram of the anti-body treated paper. (b) An actual test result of blood A+. (With permissions from ref. [14]. Copyright (2012) American Chemical Society)

**Figure 2:** 2D (a) and 3D (b) confocal images of lignocellulosic fibres within paper captured by 20 $\times$  dry lens.

**Figure 3:** Confocal images of RBCs labelled with FITC within paper (a) and on slide glass (b) captured by 20 $\times$  dry lens.

**Figure 4:** Confocal images of non-agglutinated and agglutinated RBCs within paper. (a) 2D image of non-agglutinated RBCs captured by 20× dry lens. (b) 2D image of non-agglutinated RBCs captured by 60× oil lens. (c) 3D image of non-agglutinated RBCs captured by 60× oil lens; (d) 2D image of agglutinated RBCs captured by 20× dry lens. (e) 2D image of agglutinated RBCs captured by 60× oil lens. (f) 3D image of agglutinated RBCs captured by 60× oil lens. The separate (non-combined) images of paper and labelled RBCs can be found in the Supporting Information.

**Figure 5:** A schematic diagram of the observed elution bands of RBCs on antibody-treated paper.

**Figure 6:** Chromatographic elution patterns of A+ and B+ blood samples reacting with grouping antibodies anti-A, anti-B, and anti-D.

**Figure 7:** Confocal images of chromatographic elution patterns of non-agglutinated RBCs at elution distance of 0 cm (a), 5 cm (b), 8 cm (c) and agglutinated RBCs at elution distance of 0 cm (d), 5 cm (e), 8 cm (f).

**Figure 8:** Chromatographic elution patterns of haemolysed blood samples of A+ and O+.

**Figure 9:** Separated confocal signals of fibres and RBCs for Figure 4. a1 and a2 are fibre and RBC signals for Figure 4a respectively, and etc.

### Chapter 3

**Figure 1:** Water penetration in paper is dominantly via film flow. Water wicks along fibre-fibre overlaps.

**Figure 2:** Interference in human blood plasma proteins to observation of RBCs within fibre network of paper.

**Figure 3:** RBCs and cellulose fibres in a reconstructed 3D image can be distinguished by their sizes and internal structures.

**Figure 4:** 3D FIB-based SEM images of RBCs within paper network..

**Figure 5:** Cross-sectional view of paper substrate containing RBCs. (a) The position of cross- section on paper substrate. (b) The original SEM image of cross-section. (c) The image composed by Avizo of cross-section.

**Figure 6:** (a) An illustration of RBC pathways within paper based on SEM results. (b) and (c) are not realistic structural representations; rather they are simplified models to depict the RBC retention mechanisms in positions B and D of (a).

## Chapter 4

**Figure 1:** Apparent thickness (a) and apparent bulk (b) of hardwood and softwood handsheets of different basis weights.

**Figure 2:** Apparent thickness (a) and apparent bulk (b) of handsheets with different content of hardwood and softwood fibres (basis weight of all sheets were 20 g/m<sup>2</sup>).

**Figure 3:** Pore size distributions of (a) hardwood paper with different basis weights, (b) softwood paper with different basis weights, and (c) paper with different content of hardwood and softwood fibres (basis weight of 20 g/m<sup>2</sup>).

**Figure 4:** Lateral chromatographic elution blood typing tests using papers of different basis weights: (a) scanned images of testing results; (b) mean optical densities of positive (+) and negative (-) tests. H – hardwood fibres; S - softwood fibres. The numbers after H and S are the basis weights of papers in g/m<sup>2</sup>.

**Figure 5:** Lateral chromatographic elution blood typing tests using paper with different content of hardwood fibres: (a) scanned images of testing results; (b) Mean optical densities of positive (+) and negative (-) tests.

**Figure 6:** Vertical flow-through blood typing tests using paper of different basis weights: (a) scanned images of testing results; (b) Mean optical densities of positive (+) or negative (-) tests. H - hardwood fibres; S - softwood fibres. The numbers after H and S are basis weight of papers in g/m<sup>2</sup>.

**Figure 7:** Vertical flow-through blood typing tests using paper of different content of hardwood fibres: (a) scanned images of testing results; (b) Mean optical densities of positive (+) or negative (-) tests.

## Chapter 5

**Figure 1:** (a) scheme of the side-view profile of a water droplet on a (super-) hydrophobic surface ( $R$  and  $h$  are the radius and the height of the droplet, respectively;  $\theta$  is the contact angle); (b) A plot of the height of a 20  $\mu\text{L}$  droplet on a supporting surface with respect of its contact angle with the surface (gravity effect is not considered). The red line shows the difference of the heights of water droplets on a hydrophobic surface ( $\theta = 120^\circ$ ) and a superhydrophobic surface ( $\theta = 150^\circ$ ).

**Figure 2:** Photos of two 10  $\mu\text{L}$  blood droplets (A+ and B+) mixed with 10  $\mu\text{L}$  anti-B reagent. Haemagglutination was immediately observed inside the droplet of

B+ blood sample (second row), due to the specific interaction between anti-B and the B-antigen carried by RBCs of the B+ sample. There was, however, no haemagglutination in the droplet of A+ blood sample during the entire 180s standing time (first row), since anti-B is not a specific antibody to the antigen carried by the RBCs of the A+ sample..

**Figure 3:** Photos of the blood agglutination of the six blood samples (A+, A-, B+, AB+, O+ and O-) when they are respectively mixed with three antibodies (Anti-A, Anti-B and Anti-D) on superhydrophobic surface. The red star represents blood aggregation was found in that photo. The blood type can be determined by observing the aggregation of blood with different antibodies.

**Figure 4:** Illustration of the measurement of colour intensity (magenta channel). The blood aggregation can be detected by comparing the colour intensity of the standard area in the images of different drops. From the identified aggregation of blood caused by their corresponding antibodies, the type of blood can be determined.

**Figure 5:** The scheme of observation and record system.

## Chapter 6

**Figure 1:** The Schematic illustration of the steps of micro reactor preparation and blood type identification. (a) Ten microlitres of blood is placed on a hydrophobic PCC powder bed to form the blood marble, (b) Ten microlitres of an antibody solution (yellow circle) is injected inside the blood marble to complete the preparation of the micro reactor. (c) When the corresponding antigens are not present on the surface of RBCs, no separation is visible. d) When the corresponding antigens are present, RBC agglutination reaction will take place; this will result in the separation of marble colour into two distinct light (upper) and dark (lower) parts.

**Figure 2:** Summary of blood typing results after the corresponding antibodies are injected into the marble micro reactor. Green ticks are added to the photos where the separation of agglutinated RBC is observed. The cross signs are added to photos where agglutination caused colour separation is not observed. Overall volume of the micro reactor after the antibody injection is 20  $\mu\text{L}$ .

**Figure 3:** (a) A 100  $\mu\text{L}$  blood marble micro bio-reactor made of A+ blood and hydrophobic PCC powder after the injection of Anti-A solution. (b) A 100 $\mu\text{L}$  blood marble micro bio-reactor made of A+ blood and PTFE powder after the injection of Anti-A solution.

**This page is intentionally blank**



## LIST OF TABLES

### Chapter 1

**Table 1:** Some examples of forward blood typing. “Positive” means the presence of haemagglutination reaction; “negative” means the absence of haemagglutination reaction.

**Table 2:** Comparison of classical blood typing techniques.

**Table 3:** ASSURED criteria for an ideal POC test in low-resource settings.

**Table 4:** Factors influencing the use of microfluidic diagnostic technology (MDT) and the features of a successful MDT-based POC diagnostic device.

**Table 5:** The content of cellulose, hemicelluloses and lignin in softwoods and hardwoods

**Table 6:** Paper as substrate for microfluidic devices in comparison with traditional materials.

**Table 7:** Primary advantages and disadvantages of fabrication techniques for paper-based microfluidic devices.

### Chapter 4

**Table 1:** Basis weight, thickness and bulk of hardwood and softwood handsheets.

**Table 2:** Basis weight, thickness and bulk of handsheets made from different content of hardwood and softwood fibres.

**Table 3:** Mean optical density of positive or negative lateral chromatographic elution blood typing tests using paper with different basis weights. Standards deviation is from five measurements.

**Table 4:** Mean optical density of positive or negative lateral chromatographic elution blood typing tests using paper made from different content of hardwood fibres. Standards deviation is from five measurements.

**Table 5:** Mean optical density of positive or negative vertical washing blood typing tests using paper with different basis weights. Standards deviation is from six measurements.

**Table 6:** Mean optical density of positive or negative vertical washing blood typing tests using paper made from different content of hardwood fibres. Standards deviation is from five measurements.

## **Chapter 5**

**Table 1:** The magenta intensity of the standard area in each image of Figure 3.

## LIST OF ABBREVIATIONS

2D	Two dimension
3D	Three dimension
AKD	Alkyl ketene dimer
APPI	Australian Pulp and Paper Institute
ASA	Alkenyl succinic acid anhydride
ASSURED	Affordable, sensitive, specific, user-friendly, rapid and robust, equipment free, delivered
BioPRIA	Bioresource Processing Research Institute of Australia
BSE	Backscattered electron
CE	Capillary electrophoresis
CL	Chemiluminescence
CMC	Sodium carboxymethyl cellulose
DBAE	2-(dibutylamino)-ethanol
DMSO	Dimethyl sulphoxide
DNA	Deoxyribonucleic acid
EAPap	Electro-active paper
EC	Electrochemical
ECL	Electrochemiluminescence
EDTA	Ethylenediaminetetraacetic acid
FIB	Focused ion beam
FITC	Fluorescein isothiocyanate
HDFN	Haemolytic disease of the fetus and newborn
HIV	Human immunodeficiency virus
HTR	Haemolytic transfusion reactions
IC	Integrated circuits
IgG	Immunoglobulin G
IgM	Immunoglobulin M
ISBT	International Society of Blood Transfusion

LOC	Lab-on-a-chip
MDT	Microfluidic diagnostic technology
MG	Microgels
NIST	National Institute of Standards and Technology, USA
PAM	Polyacrylamide
PBS	Phosphate buffered saline
PCC	Precipitated calcium carbonate
PDADMAC	Poly diallyl dimethyl ammonium chloride
PDMS	Polydimethylsiloxane
PMMA	Polymethyl methacrylate
POC	Point of care
PVDF	Polyvinylidene difluoride
PSS	Physical saline solution
RBCs	Red blood cells
Rh	Rhesus
RH	Relative humidity
SE	Secondary electron
SEM	Scanning electron microscopy
SERS	Surface-enhanced Raman scattering
TAPPI	Technical Association of the Pulp and Paper Industry
TDR	Special Program for Research and Training in Tropical Diseases
DARPA	United States Defense Advanced Research Projects Agency
WHO	World Health Organization
μPADs	Microfluidic paper-based analytical devices
μTAS	Miniaturized total chemical analysis systems

## LIST OF NOMENCLATURE

cm	centimetre
dm	decimetre
g	gram
hPa	hundred Pascal
kV	kilovolt
L	liter
m	metre
mg	milligram
min	minute
mg	milligram
mL	milliliter
mm	millimetre
nA	nanoampere
nm	nanometre
Pa	Pascal
$h$	height of drop
$l$	liquid penetration distance
$r$	equivalent capillary pore radius
$R$	radius of drop
s	second
$t$	penetration time
$\gamma$	surface tension
$\gamma_{sv}$	interfacial tensions of the solid-vapour interface
$\gamma_{sl}$	interfacial tensions of the solid-liquid interface
$\gamma_{lv}$	interfacial tensions of the liquid-vapour interface
$\eta$	viscosity
$\theta$	contact angle

μL

microlitre

°C

degree Celsius

---

# Chapter 1

## *Introduction and Literature Review*

---

**This page is intentionally blank**



### 1.1 INTRODUCTION

Blood typing is the process of testing red blood cells (RBCs) to determine which antigens are present and which are absent [1]. Accurate and rapid determination of human blood groups is imperative for many medical procedures such as blood transfusion and organ transplantation [2]. The International Society of Blood Transfusion (ISBT) recognises 328 different antigens and 30 major blood group systems, among which the ABO and Rhesus systems are of the greatest clinical importance. Without ABO compatibility testing, around one third of unscreened blood transfusions would lead to potentially fatal haemolytic transfusion reactions [3, 4]. The red blood cell antigen D of the Rh system is considered to be the most common culprit, also causing haemolytic disease of the foetus and in newborns (HDFN) [5]. In our world today, the demand for blood typing diagnosis is extremely large. On the one hand, there is an urgent demand for low-cost point-of-care (POC) blood typing devices which could be used for bedside compatibility checks, fast blood typing in emergency situations, developing regions and remote locations without access to hospital and laboratory facilities. On another hand, novel low-cost blood typing devices with the capability of automation and high throughput operations need to be developed for blood bank laboratories where large numbers of blood samples need to be assayed.

To solve the first problem, our research group in Australian Pulp and Paper Institute (APPI) has made a great effort to explore and develop a series of paper-based blood typing devices [6-11]. These bio-functional devices are not only easy to use, but also disposable. Among them, a device designed by our group is able to report patient's blood type in unambiguous written text [9]. Once the production of these devices becomes industrialized, it will help to improve the public health conditions in both developed and developing countries significantly. However, the basic mechanisms including the agglutination, immobilization and transport behaviours of red blood cells within paper, as well as the effect of paper physical structure on these behaviours are still not clear. In my thesis, Chapter 2 will focus on understanding the mechanism of haemagglutination-induced immobilization of RBCs in antibody-treated bioactive paper by using confocal microscopy. In Chapter 3, the transport pathways of RBCs within fibre network of paper are studied by the combined dual beam system with

scanning electron microscopy (SEM) and focused ion beam (FIB) technology. Chapter 4 will investigate the influence of fibre type and the internal pore structures of paper sheet on the RBCs' transport behaviours in paper and the final blood typing performance. Comprehending these mechanisms is not only necessary for the future design of more sophisticated paper-based blood typing devices with high sensitivity and assaying speed, but also important for the development of other paper-based blood analysis devices.

In order to address the second challenge, we successfully converted the liquid bio-micro reactors fabricated by superhydrophobic materials into blood typing devices. By integrating these devices with the advanced image acquisition and processing system, blood typing can be done automatically, quickly and efficiently in large scale. At the same time, the results of blood typing, including the images and videos of the haemagglutination reactions, can be stored digitally to form a retrievable database. The data can be retrieved following medical protocols by doctors or patients anytime and anywhere via internet. Besides, the advantages of blood typing devices based on liquid micro reactors also include the requirement of a tiny amount of sample, disposability and reduced biohazards. In this thesis, two innovative studies on the practical applications of liquid micro reactors for blood typing are presented. These micro reactors are fabricated by two different methods respectively. In Chapter 5, the liquid micro reactor is formed by simply dropping reaction solution onto the superhydrophobic substrate due to its non-wettable property. In Chapter 6, the liquid micro reactor is constructed by forming liquid marble coated with hydrophobic powder of precipitated calcium carbonate (PCC).

The literature review chapter consists of four sections (Section 1.2, 1.3, 1.4 and 1.5). The first section is a brief introduction to the concept of blood groups and current existing blood typing techniques in our world. Also, this section outlines the urgent needs of exploring innovative low-cost POC blood typing devices as well as the blood typing devices with capability of automation and high throughput operations. The second section presents an overview of chemical and physical characteristics of paper; and identifies the advantages of using paper rather than other materials as substrate for microfluidic devices. The third section summarizes the current fabrication and detection methods of paper-based microfluidic devices. In the last section, the

phenomenon of superhydrophobicity, characteristics of superhydrophobic surface and several applications of superhydrophobic materials are reviewed. Subsequently, the ideas of designing liquid micro reactors based on superhydrophobic materials will be proposed.

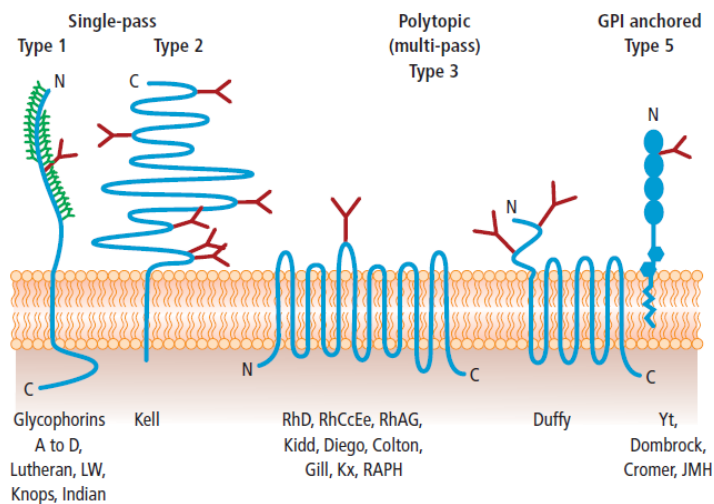
Section 1.6 presents the aims of the current research, and Section 1.7 outlines the structure of the thesis in detail.

## 1.2 BLOOD GROUPING TECHNIQUES

### 1.2.1 Blood Groups

#### 1.2.1.1 What is the blood group?

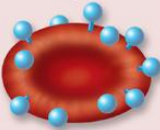
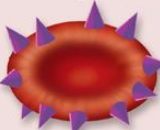
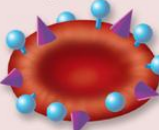
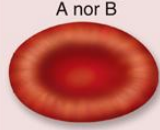



The blood group is classified based on inherited difference (polymorphisms) in antigens on the surface of the red blood cells. Blood group antigens could be proteins, glycoproteins, or glycolipids. The blood group proteins and glycoproteins are integral structures of the red cell membrane [3, 4]. Figure 1 shows the schematic representations of some blood group proteins and glycoproteins in the membrane [3]. The antibody existing in the blood plasma protects the body from any perceived threat caused by foreign antigens. Landsteiner's Law describes the relationship between antigens on the RBCs and the antibody in the blood serum for ABO system: when an RBC possesses certain antigens on its surface, the corresponding antibody is absent in the blood plasma and vice versa [12, 13], as shown in Figure 2.



**Figure 1.** A schematic of different types of blood group active proteins and glycoproteins based on their integration into the red cell surface membrane.

Since the discovery of the ABO blood group system in 1900, a multitude of blood group antigens have been identified. The International Society of Blood Transfusion (ISBT) recognises 328 different antigens and 30 blood group systems. Each blood group system stands for either a single gene or a cluster of two or three close genes of

the related sequence. Of these, the ABO and RhD groups are the most important systems in transfusion medicine. In addition, there are 28 minor systems of diverse clinical and biological relevance, such as Kell system, Duffy system, Kidd system and Diego system [3, 4].

ABO Blood Types				
	Antigen A	Antigen B	Antigens A and B	Neither antigen A nor B
Erythrocytes				
Plasma	Anti-B antibodies 	Anti-A antibodies 	Neither anti-A nor anti-B antibodies	Both anti-A and anti-B antibodies 
Blood type	<b>Type A</b> Erythrocytes with type A surface antigens and plasma with anti-B antibodies	<b>Type B</b> Erythrocytes with type B surface antigens and plasma with anti-A antibodies	<b>Type AB</b> Erythrocytes with both type A and type B surface antigens, and plasma with neither anti-A nor anti-B antibodies	<b>Type O</b> Erythrocytes with neither type A nor type B surface antigens, but plasma with both anti-A and anti-B antibodies

**Figure 2.** Example of ABO blood types. When an RBC possesses certain antigens on its surface, the corresponding antibody is absent in the blood plasma, and vice versa.

## 1.2.1.2 Medical and biological significance of blood groups

First of all, blood groups are of great clinical importance in blood transfusion and transplantation medicine. Many blood group antibodies are able to cause rapid destruction of transfused red blood cells possessing the corresponding antigen, leading to a haemolytic transfusion reaction (HTR) [2, 3, 14]. It could happen immediately or several days after the transfusion. At the worst, HTRs give rise to disseminated intravascular coagulation, renal failure, and death. At the mildest, they reduce the efficiency of the transfusion. Therefore blood typing is an indispensable step before blood transfusion and any transplantation process. Moreover, immunoglobulin G (IgG) blood group antibodies have the potential to cross the placenta and attack fetal red blood cells expressing the corresponding antigen during pregnancy and haemolyse. This could result in alloimmune fetal haemolytic anaemia, more commonly known as haemolytic disease of the fetus and newborn (HDFN). The most common antigens causing HDFN are D and c of the Rh system and K of the Kell system [5, 15].

The biological importance of many blood group antigens can be surmised from their structure [16]. The following functions have been attributed to blood group antigens: transporters of biologically important molecules across the red cell membrane; receptors of external stimuli and cell adhesion; regulators of autologous complement to prevent red cell destruction; enzymes; anchors of the red cell membrane to the cytoskeleton; and providers of an extracellular carbohydrate matrix to protect the cell from mechanical damage and microbial attack [3, 16]. Besides, there has been increasing evidence that the blood groups are associated with various diseases and cancers [17, 18].

### **1.2.2 Existing Blood Typing Techniques**

#### **1.2.2.1 Blood typing principles**

Blood typing is an assay of testing red blood cells to determine which antigens are present and which are absent. It is standard practice to perform tests for A, B, and D (Rh) antigens. Tests for other antigens are only performed in selected cases, although regulations may vary from region to region [1, 4].

Today, most of the techniques developed for blood typing are based on the principle of interaction between RBC antigens and antibodies [1]. Haemagglutination reactions happen when antibodies bond to the particular bonding sites on the antigens of RBCs, leading to the formation of blood lumps that cannot be stably suspended in the plasma. In contrast, the absence of agglutination indicates no haemagglutination reaction [19].

In forward blood typing, the presence or absence of certain antigens on the surface of red blood cells is determined. Usually, the commercial antibodies are used to test the presence of the corresponding antigens on RBCs. This is clinically performed by introducing antibody into a blood sample; the appearance of RBCs' agglutination indicates the presence of the corresponding antigens on RBCs, while the absence of agglutination indicates the absence of the antigen [3, 4]. Table 1 shows some examples of forward blood typing. On the other hand, reverse blood typing refers to the tests determining the antibodies in the serum by using the reagent RBCs with known

antigens. The type of antibodies in the serum also depends on whether haemagglutination reaction appears [20, 21].

**Table 1.** Some examples of forward blood typing. “Positive” means the presence of haemagglutination reaction; “negative” means the absence of haemagglutination reaction.

Antibody A	Antibody B	Antibody D	Results
Positive	negative	negative	A, Rh-
Negative	positive	positive	B, Rh+
Positive	positive	negative	AB, Rh-

## 1.2.2.2 Conventional laboratory blood typing techniques

In the pathological laboratory, the most common assays used for the identification of blood groups include slide test, tube test, microplate method, as well as the column agglutination system [1, 22-24]. Table 2 compares the major features of these techniques.

**Table 2.** Comparison of classical blood typing techniques.

Test	Technology	Assay time (min)	Assay cost	Comments
Slide	Manual	1-5	++	Insensitive, fast, labour-intensive
Tube	Manual	10-30	++	Sensitive, time-consuming, centrifugation needed
Microplate	Manual and automated	10-30	+++	Sensitive, fast, centrifugation usually not needed
Column agglutination	Manual and automated	10-45	+++	Sensitive, time-consuming, centrifugation needed, easy documentation

In the slide test method, a glass slide is usually used on which a drop of a specific antibody is mixed with blood from the patient. The presence and absence of agglutination of the red blood cells with different antibodies determines the blood type of the patient. The main advantage of this method is that it is a fast and inexpensive test that can be conducted without the need for specific equipment such as a centrifuge. However, the sensitivity of this method is not high [1, 25]. Therefore, this technique is not frequently used today, and its application is mainly found in a quick check of a known blood group.

Tube testing is a very common technique that has been used for many years and is still used in many laboratories. In a tube test, an antibody and the patient's blood are transferred into a glass or plastic test tube where they are allowed to react. After centrifugation, the RBCs in the tube are gently re-suspended and examined for agglutination to determine the blood type. The tube test method can also be used to conduct antibody screening, identification, and compatibility testing. The advantage of the tube test over the slide test is that it is more sensitive and relatively faster. Nevertheless, it requires a number of different manual steps to be performed by a technician. Moreover, it is very difficult to automate [1, 26].

In terms of the microplate technique, it can be considered as a matrix of 96 “short” test tubes. After the reagents and the blood or serum of the patient have been dispensed, the plate is incubated and centrifuged, after which RBCs in the wells are re-suspended and examined for agglutination. The microplate technique can be used for testing antigens on RBCs and for antibodies in plasma. The advantages of this method include enhanced sensitivity of reactions, savings in reagents and supplies, and the ability for the dispensing steps to be automated using pipetting devices [22, 23, 27, 28].

The column agglutination technique is in the form of the gel centrifugation assay. It is a solid phase testing method inspired by the principle of gel filtration for separation of red blood cells from human blood. This method standardizes RBC agglutination reactions by trapping the agglutinates and permits simple and reliable reading [24, 29]. The column agglutination technology has a number of advantages. In general, it is easy to use. Therefore, the demand for highly skilled laboratory technicians is reduced. In



addition, the sample volumes required for this test are also significantly reduced compared with those required for the tube test [1, 30].

Apart from the above classical blood typing techniques, advanced but highly technical assays for blood grouping have been reported recently, including gene sequencing of deoxyribonucleic acid (DNA) and flow cytometry-based assays [31, 32]. Nonetheless, the major disadvantages of these assays are the need for special laboratory instruments operated by trained laboratory personnel, the long time required for the procedure, and the high cost of these tests. Furthermore, these assays routinely require 6 mL of blood collected by syringe.

### **1.2.3 Demand for Low-cost POC Blood Typing Devices**

Blood typing is of significant importance for people's health and lives. Today, over 108 million units of blood are collected worldwide for blood banking, transfusion and treatment of multiple clinical conditions or for life-saving procedures every year [2]. One third of unscreened blood transfusions can lead to a haemolytic transfusion reaction that might be fatal [3]. As a result, determination of ABO and Rh blood groups for both blood recipients and donors is mandatory to ensure compatibility before the commencement of blood transfusions [33].

However, the blood typing tests that are a standard component of diagnostic systems in developed nations are often unavailable, unreliable or unaffordable in undeveloped and developing nations. Since low-infrastructure sites serve most of the global population, the lack of reliable blood typing tests at these sites will not ensure the compatibility of blood recipient and donor before the commencement of blood transfusion [8, 19]. In 2006, a study done by Yager's group [34] showed that, of the world's 6.1 billion population, 3 billion lack basic sanitation, 2 billion do not have access to electricity, and more than 1 billion lack basic healthcare services and clean drinking water. Among these human populations, access to blood typing tests which require a professional technician or advanced equipment could not be guaranteed. Consequently, the exploitation of new low-cost blood typing techniques that can be used in resource-

limited settings, and preferably, by non-professionals with little or no laboratory training, is indeed necessary and urgent.

Point-of-care tests are considered to be vanguard analytical systems in clinical analysis that provide onsite and reliable analytical results including qualitative and quantitative data in a rapid and easy way [35]. Compared with conventional diagnosis in a clinical laboratory, POC diagnostic tests are generally implemented near the patient (e.g. at home, emergency department of a hospital, bedside) in a remote and decentralized way. Their main purpose is to bring the clinical test results to the patient more conveniently and rapidly [34, 36].

In 2003, the World Health Organization Special Program for Research and Training in Tropical Diseases (WHO/TDR) proposed the well-accepted ASSURED guidelines (Table 3) which provide criteria for designing POC diagnostic devices with ideal characteristics that can be used at all levels of the healthcare system, including in undeveloped and developing countries [37-39].

**Table 3.** ASSURED criteria for an ideal POC test in low-resource settings.

Affordable
Sensitive (avoids false negative results)
Specific (avoids false positive results)
User-friendly (simple to perform in a few steps with minimal training, uses non-invasive specimens)
Rapid and robust (can be stored at room temperature and results available within 30 min)
Equipment-free or minimal equipment that can be solar-powered
Delivered (accessible to end-users)

In fact, the commercial development of diagnostic tests designed specifically for low-resource settings has long been hindered by perceptions of a low return on investment and concerns regarding the challenges of implementation in countries with less-developed healthcare systems. Commercial partners have shown limited willingness to engage in the development of new diagnostics for undeveloped and developing regions

[35, 40]. Therefore, in order to improve the health status of the economically disadvantaged human population of the world and attract interest and investment from commercial bodies, researchers in this field should explore the development of a variety of POC diagnostic innovations which are low-cost and easily manufactured. For this reason, the work reported in the Part I of this thesis explores the feasibility of using cheap materials (e.g. paper) to fabricate high-performance low-cost POC blood typing devices for undeveloped and developing regions.

### **1.2.4 Automation of Blood Typing Techniques**

Nowadays, automation is being steadily introduced into clinical laboratories. Fully automated equipment for diagnostic analyzers has become integral to nearly every laboratory. Nonetheless, it is a fact that blood bank laboratories have been much slower in adopting automation. There are some particular reasons for this situation. For instance, manual testing methods have been taken as the predominant blood banking technology for quite a long time. Blood bank laboratories have resisted change, especially in high-income countries where there has been an abundant supply of well-trained technologists. However, the most important reason is the difficulty of automation of the current classical blood typing methods [1].

There are a variety of advantages of introducing automated blood typing techniques into pathological laboratories and hospitals. First, the employment of automated blood typing techniques is able to increase the safety and security of the analytical process [41]. False-positive or false-negative results may be acquired, if inadequate attention is paid to careful collection and handling of blood samples, serum-to-RBC ratios, RBC concentrations, suspension media, incubation times and temperatures, as well as checking for agglutination [42-44]. Since there is no acceptable margin of error, each test result for blood typing must be correct. Automation can help to reduce the laboratory error rate by removing the variability that is typical for manual test methods performed by different technicians. If all steps of the testing process are standardized, the rate of error will decline [1].

The second advantage of automating blood typing techniques is that it can improve the efficiency of the test process [41]. In contemporary society, finding appropriately

qualified staff is becoming more and more difficult. Consequently, if automated blood typing equipment can take over the routine tasks of the testing process, such as dispensing reagents and samples, incubation, and reading, professional technicians will spend more time on other activities that add more value to the process. In this case, the laboratory is able to deliver a faster and better service to its customers (e.g. the physicians and patients).

Last but not least, we must also consider the financial advantages brought by the introduction of automated blood typing techniques. Since clinical laboratories and hospitals often face the pressure of limited or declining budgets, the introduction of automated blood typing equipment may appear to be expensive. However, there are many areas where significant savings can be obtained by the automation of blood typing techniques [1, 41]. Examples include the reduction of costly hands-on time that the professional laboratory technicians spend on repetitive routine activities such as dispensing samples and reagents. Another example is that an optimized test process with less variation is able to help avoid the waste of testing reagents and materials caused by human error.

Today, the demand for blood typing in larger batches is growing at an increasing rate. Accordingly, the development of novel low-cost blood typing devices with the capability of automation and high throughput operation is of significant importance for blood bank laboratories and hospitals where large numbers of blood samples need to be assayed. In order to address this challenge, the work reported in Part II of this thesis integrates blood typing devices based on liquid bio-microreactors with advanced image acquisition and processing system to develop novel blood typing systems. With these systems, the aim of identifying blood types automatically on a large scale can be achieved. In addition, the entire blood typing process, including images and videos of reactions, can be stored digitally to form a large database by taking the advantage of imaging technology. The data can also be retrieved by doctors or patients at any time or place via the internet.

## **1.3 PAPER AS SUBSTRATE FOR MICROFLUIDIC DEVICES**

### **1.3.1 Microfluidic Devices**

#### **1.3.1.1 Review of microfluidics**

Microfluidics refers to systems that use channels with dimensions of tens to hundreds of micrometers to process or manipulate minute amounts of fluids ranging from  $10^{-18}$  L to  $10^{-9}$  L [45]. From the perspective of engineering, microfluidics can be defined as the investigation of flows that circulate in artificial Microsystems [46]. The flows can be simple or complex, mono- or multi-phasic. Using microfluidic technology, processes like separation, isolation, and chemical/biological reactions that usually require laborious hours are able to be reduced to just a few minutes or even seconds. Moreover, since the sample volumes in microfluidic devices are in the range of pL to  $\mu$ L, microfluidic devices are ideal for handling precious, costly, toxic, or dangerous samples [47].

Microfluidic devices originated from the integrated circuits (IC) industry, the first IC having been invented by Kilby in 1958 [48]. However, the great boost in the research field of microfluidic devices started from the early 1990s with funding from the United States Defense Advanced Research Projects Agency (DARPA). At that time, there had always been a military need to practise medicine in challenging and resource-limited environments. Therefore, researchers have long been exploring robust medical technologies that can minimize the burden of military staff and the machines transporting them. Surprisingly, the microfluidic technologies developed with DARPA's support also show the characteristics needed for the delivery of appropriate medical diagnostics to the poorest people in our world [34]. Nowadays, the potential of microfluidic devices to enhance the decentralization of medical testing has been accepted as a critical element in the evolution of healthcare, especially for civilian healthcare in developing countries.

In the early stage of the development of microfluidic devices, the raw materials were typically chosen from silicon or glass, since the fabrication techniques using these materials were well-developed. However, these techniques are generally expensive and

time-consuming, and they require access to specialized facilities. Therefore, these devices are only marginally desirable in situations where rapid evaluation of prototypes is required [49, 50]. Polymers and elastomers are becoming more and more attractive for the fabrication of microfluidic devices, since microstructures can be inexpensively constructed in them using several high throughput methods, such as injection moulding, soft lithography, laser ablation, X-ray photolithography and hot embossing [51]. The most commonly used polymers include polydimethylsiloxane (PDMS) [49, 52, 53], polymethyl methacrylate (PMMA) [51, 54] and polystyrene (PS) [55, 56]. Of these, PDMS is by far the most preferred polymeric building material for microfluidic devices [57].

Recently, the integration of multiple microfluidic technologies has been increasingly recognized as a central technical challenge in the development of functional microfluidic devices. The ultimate goal of integration is to create all-in-one microchips that are able to perform all processes, including transport, separation, reaction and detection [58, 59]. The domain of integrated microfluidic analysis devices has been designated as miniaturized total chemical analysis systems ( $\mu$ TAS) or lab-on-a-chip (LOC) systems and the two terms are essentially synonymous.  $\mu$ TAS emphasizes the analytical function of a microfluidic chip [60], while LOC technologies include microfluidic chips as well as non-fluidic miniaturized systems such as sensors and arrays (the so-called biochips) [61]. Multi-functional microfluidic devices could be applied to biology research to streamline complex assay protocols, to substantially reduce the sample volume, to reduce the cost of reagents and maximize information gleaned from precious samples, to provide gains in scalability for screening applications and batch sample processing analogous to multi-well plates, and to provide the investigator with substantially more control and predictability of the spatio-temporal dynamics of the cell micro-environment. Due to the numerous advantages of microfluidics, an increasing number of large corporations have set up their own research and development divisions to explore commercialization opportunities in microfluidics [62].

Although there have been a number of great successes in microfluidics, researchers are continuing to explore new materials and fabrication methods for developing various innovative microfluidic devices that are desired for a large range of different

applications [19, 47]. One such application is POC diagnostic devices in developing countries [34, 36].

### **1.3.1.2 Microfluidic technologies for POC diagnostic devices**

In many ways, the natural features of microfluidic technologies make it possible for a POC diagnostic device to meet the ASSURED criteria established by the WHO. These features include low consumption of reagents and sample, miniaturization of the diagnostic device, integration of complex analysis functions, and short assay time. Therefore, it comes as no surprise that the research on microfluidic technologies for POC applications has increased significantly in recent years [34]. Many researchers believe there will be soon microfluidics-based POC and home-care devices that can perform assays at sensitivity, specificity and reproducibility levels similar to those of central laboratory analysers, but which require very little user input other than the insertion of the sample. Such devices are also expected to be able to work properly under the constraints of untrained workers, electricity shortages, limited laboratory supplies, and rough handling during transportation and storage [63].

In previous studies, there have been a variety of microfluidic devices showing potential for use in POC applications. These devices are fabricated using different materials (e.g. metal, plastic) and methods (e.g. photolithography, electrochemical anodization) [58]. For instance, Gervais et al. patterned PDMS by photolithography as a one-step POC chip for the detection of C-reactive protein by measuring fluorescent signals [64]. A self-powered microfluidic blood analysis system that integrates sample volume metering, whole-blood plasma separation, multiple immunoassays and flow propulsion was invented by Dimov et al. using PDMS and glass microscope slides [65].

For the future development of new microfluidic-based POC diagnostic devices, there are a number of key factors that will influence the introduction, acceptability and sustainability of these technologies. These factors are summarized in Table 4. One of the greatest challenges in deploying microfluidic-based POC diagnostic devices in the developing world will be bringing the cost down close to that of the most inexpensive of current tests, namely lateral flow immunoassays. These assays have been successfully used for pregnancy testing, drugs, cholesterol, and cardiac markers in

developing countries [64, 66]. Therefore, researchers must think in innovative ways and explore low-cost materials for the fabrication of microfluidic-based POC tools.

**Table 4.** Factors influencing the use of microfluidic diagnostic technology (MDT) and the features of a successful MDT-based POC diagnostic device.

<b>Key factors that will affect the introduction, acceptance and sustained use of an MDT</b>	<b>Corresponding features of a MDT-based POC device</b>
Cost of the technology	Low cost
Degree of accuracy	High degree of accuracy
Quality control	Reproducible chip performance
Level of training of users	User interface that requires little training
Length of time to obtain test result	Short time to obtain test result
Performance in a variety of settings	Stable ambient temperature storage and low power consumption
Performance under variable operating conditions (such as temperature or humidity) over time	Reproducible operation in variable environments, and ruggedness
Local education on health issues	A high perceived need for the test
Availability of successful therapies	Potential for significant health improvements

## 1.3.2 Overview of Paper

Paper is a thin sheet of material that is produced by pressing cellulosic fibres together. Originally intended purely for writing and printing purposes, paper is used for a variety of other purposes today [67]. Different kinds of paper products, such as newsprint, packaging paper board printing and writing paper, tissue and packaging paper, are widely manufactured on a large scale today.

The applications of paper and paper-based products are limitless. Novel paper-based specialty products are continually being explored. Recently paper has drawn much interest as a potential material for microfluidic devices in analytical and clinical



chemistry due to its versatility, high abundance and low cost. However, can paper overcome the limitations of all the solid phase materials currently used in lateral flow assays? Can an entire analytical assay be built upon a single paper material? Can paper meet the performance requirements and reduce costs for manufacturers? To address all these questions, it is essential to understand the papermaking process, the chemical and physical properties of paper and the advantages of paper as a substrate for microfluidic devices.

### 1.3.2.1 Production process of paper

Paper is the final product of a process of pulping and papermaking from raw materials containing cellulosic fibres, as shown in Figure 3 [68]. Pulp technology deals with the liberation of fibres fixed in the wood or plant matrix, while papermaking technology unifies the fibres to form the paper web [67, 69].

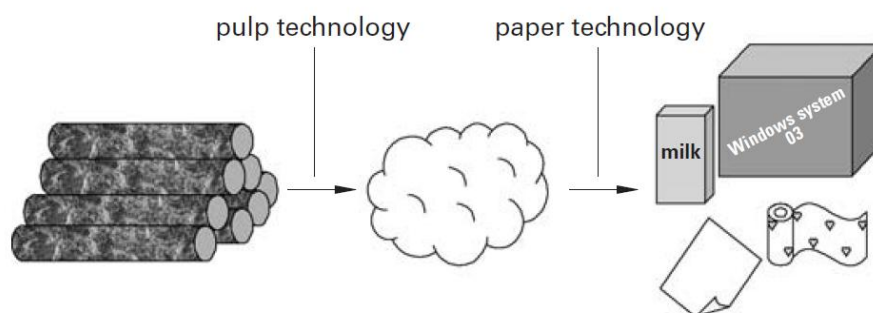


**Figure 3.** The production of paper products from raw materials.

The raw materials come from wood, recycled fibres and non-wood materials such as cotton, jute, flax (linen), hemp, bamboo, ramie, sisal, bagasse, grass and straw [68, 69]. The selection of raw materials is primarily determined by the quality requirements of the final paper product. For example, printing paper is mainly made from wood, while the major raw source of filter and chromatography papers is cotton. Today, wood constitutes 90% of the raw material in the industry due to the fact that processing of non-wood plants is more costly [70]. After wood, the second largest share of pulp produced worldwide is pulp made from recycled paper. Apart from good economic reasons, a major force in this drive to recycling is derived from public pressure to reduce the amount of used paper that is landfilled as waste [71].

In general, pulping can be achieved in two ways, either mechanically or chemically [68]. For mechanical pulping, fibres in the wood can be released by grinding the wood chips. In this process, some easily dissolved carbohydrates and extractives are lost, but the overall yield of pulp is little affected. The pulp yield for mechanical pulp is generally about 90 to almost 100 %, depending on the mechanical pulping method chosen. Groundwood pulp is produced by pressing round wood logs against a rotating cylinder made of sandstone. Another type of mechanical pulp is refiner pulp, which is acquired by feeding chips into the centre of two refining discs [69, 72]. For chemical pulping, most of the lignin is removed by delignification and the fibres are released. The delignification of wood is achieved by degrading the lignin molecules and introducing charged groups, keeping the lignin fragments in solution and eventually removing them by washing. The chemical pulping methods include mainly kraft cooking and sulfite cooking. After chemical pulping, only approximately half of the wood becomes pulp, the other half being dissolved. Chemical pulp fibres are more flexible than mechanical pulp fibres. They conform better to each other when forming the paper and offer good strength properties [68, 73]. After the pulping process, the pulp obtained is coloured, the degree of colouring depending on the pulping process. For certain paper products, the dark pulp has to be bleached. Bleaching leads to brighter paper, which gives better contrast between the print and the paper. Bleaching can also remove chemical structures in the pulp material that would make the paper yellow after a certain time [72, 74].

In the papermaking process, the dilute fibre slurry is sprayed on to a moving wire. Apart from fibres, fillers, retention aids and wet strength additives may also be added to the slurry. The wire is an endless woven wire cloth with a mesh size allowing the water to be drained, but retaining the fibres on the wire. From the wire, the paper web enters the pressing section of the paper machine, where water is pressed out by squeezing the paper web between steel rollers. To further increase the dryness of the paper, it is dried in the drying section, usually consisting of cylinders with steam within them. At the end of the paper machine, the web is reeled [68, 69, 75, 76]. The whole process is shown in Figure 4 [68].

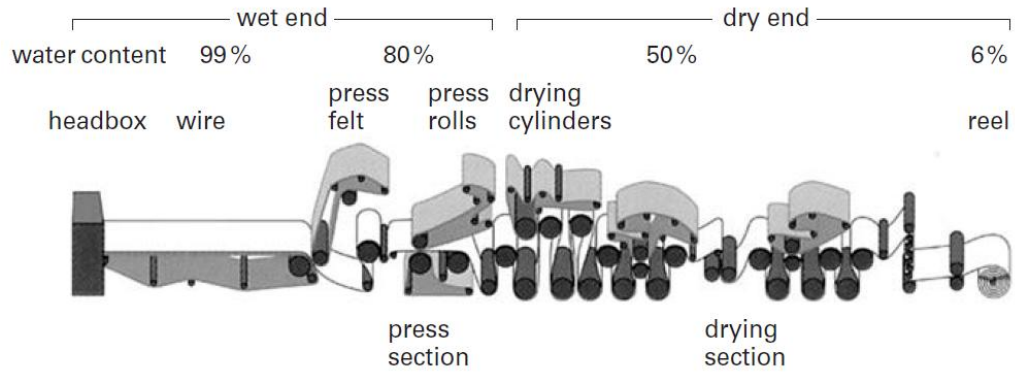


**Figure 4.** A simplified diagram of a Fourdrinier paper machine.

The properties of paper can be affected by every step of the production process, and further influence the performance of the microfluidic device fabricated using this paper product.

### 1.3.2.2 Paper chemistry

Wood is the main raw material for pulping and papermaking. The composition and structure of wood differ between species, locations of growth, and parts of the tree stem. Although the diversity of wood structure is high, it always consists mainly of cellulose, hemicelluloses, and lignin, together with small amounts of extractives, such as terpenoids, resin acids, fatty acids, pectin, proteins, and inorganic matter [69, 70, 77]. Figure 5 shows the chemical structures and distributions of cellulose, hemicelluloses and lignin in the secondary wall of wood fibres [67]. The content of cellulose, hemicelluloses and lignin in softwoods and hardwoods can be found in Table 5 [70]. Since the existence of lignin causes ageing and yellowing of paper, it is considered an undesirable component in papermaking. The main objective of pulping is to remove the lignin and try to preserve the polysaccharides [68].

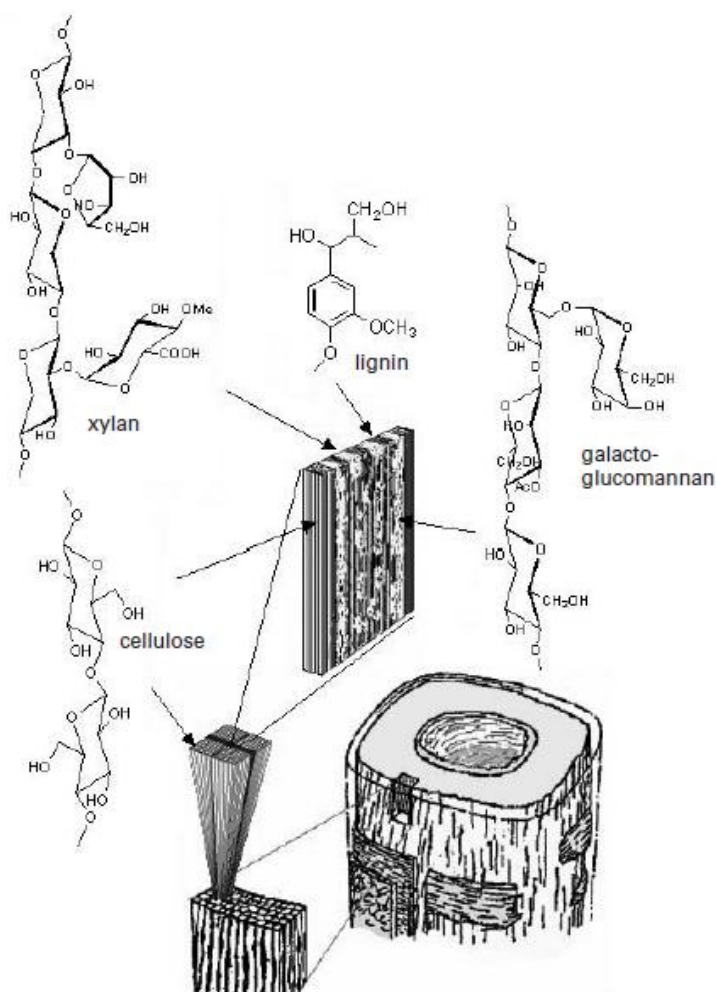


**Figure 5.** Schematic picture of the arrangement of cellulose, hemicelluloses and lignin in the secondary wall of wood fibres.

**Table 5.** The content of cellulose, hemicelluloses and lignin in softwoods and hardwoods.

	Softwoods	Hardwoods
Cellulose	40-44%	40-44%
Hemicelluloses	30-32%	25-35%
Lignin	25-30%	18-25%

Paper can be functionalized by modifying its chemical properties. For example, paper sheet is naturally hydrophilic, but it can be converted to hydrophobic by using sizing reagents, such as alkyl ketenedimer (AKD), alkenyl succinic acid anhydride (ASA) and rosin. In this way, paper acquires the ability of resisting the spreading and penetration of fluid. This capability is important when paper is used for printing and packaging [78,

79]. When paper is used for fabricating microfluidic devices, the modification of its surface chemistry is more important. This is discussed in detail in Section 1.3.3.

### 1.3.2.3 Paper physics

Paper is a three-dimensional network with a porous structure formed of multiple layers of cellulosic fibres. It is often considered to be an infinite network in two dimensions, while finite in the thickness direction [80, 81]. Attention should be given to the anisotropic properties of paper, since the paper-based microfluidic assays are carried out either parallel or perpendicularly to the paper surface. Some important physical characteristics of paper for microfluidic applications include surface area, capillary flow rate, pore size, porosity, thickness and colour.

The surface area of the paper is important because of its impact on reagent deposition, sensitivity, specificity and reproducibility. When other parameters are kept constant, the surface area drops nonlinearly with pore size, increases nonlinearly with porosity and increases linearly with thickness [81, 82]. The internal surface area of porous membranes is given as  $\text{m}^2 \text{g}^{-1}$  of polymer. By multiplying the internal surface area by the basis weight, the surface area ratio can be calculated. The surface area ratio is expressed as  $\text{m}^2$  internal surface area divided by  $\text{m}^2$  frontal area. The surface area ratios of current commercially available immunochromatographic assays range from 50 to 200 [82].

The Lucas-Washburn equation (Equation (1)) is used commonly to describe the water absorption process driven by capillary force [83]:

$$l = \sqrt{\frac{\gamma r \cos \theta}{2\eta}} t \quad (1)$$

where,  $l$  is the liquid penetration distance,  $r$  is the equivalent capillary pore radius of substrate,  $\gamma$  and  $\eta$  are the surface tension and viscosity of the liquid,  $\theta$  is the contact angle and  $t$  is the time of penetration.

However, this equation can only be used as a semi-quantitative model for describing the general behaviour of liquid penetration in paper, as paper is a more complicated medium than a single capillary tube [80, 81]. Capillary flow rate is important in the performance of paper-based microfluidic assays, as it is critical in achieving consistent sensitivity, depending on the location of the detection line/zone [47, 84]. Measuring capillary flow rate is usually not preferred since the speed decays exponentially when the fluid front travels along the substrate. Instead, capillary flow time is measured to inversely represent the flow rate [82].

Pore size and pore size distribution are important parameters in the selection of porous materials for the fabrication of microfluidic devices [82, 85]. The pore size (nominal or absolute) relates to the size of particles retained by the filter. Traditionally, membranes are characterised based on their nominal pore size. Nominal size is the diameter of the largest pore in the filtration direction. Experimental determination of pore size is accomplished by forcing hard particles through the membrane. The pore size distribution defines the range of pore sizes in the membrane and it determines the capillary flow rate as a function of the aggregate pore size [80, 81].

Porosity is another key physical property, which is defined as the volume of air in the 3D membrane structure [86]. Different from the pore size, porosity is an independent parameter. It is traditionally defined as the void volume of the membrane. Therefore, it can help to estimate the total volume of the sample required for wet-out of the paper [80, 85]. When pore size distribution and thickness are kept constant, the capillary flow rate increases linearly with the porosity of the paper [82].

The colour of the paper is important because it plays a role in image analysis [6, 8, 85]. The paper used for POC should be white, preferably with no tinge or hue. Paper tends to turn yellow to brown upon prolonged storage due to exposure to humidity, heat and light [74]. Acceptable limits of colour decay must be identified and compensated for during the readout.

### **1.3.2.4 Comparison of paper with other materials for microfluidic devices**

In comparison with other microfluidic substrates, paper is shown to be advantageous in many aspects, including production cost, portability, disposability, flexibility, biodegradability and biocompatibility. The price of paper is around 0.1 cents/dm<sup>2</sup>, which is 200 times less expensive than poly ethylene terephthalate and 1,000 times less expensive than glass [87]. Furthermore, the development and introduction to the market of paper-based systems requires only a relatively small investment. Therefore, the use of paper-based microfluidic devices has not only become very popular among the scientific community, but they are also easily applied in practical, real-life situations [23, 28], even in places without ready access to laboratory facilities, such as the developing world, in the military, and in emergency situations [15, 20]. Other properties of paper are compared with those of the traditional substrates for microfluidic devices and listed in Table 6. Because of these advantages, the interest in the development of paper-based microfluidic devices has been increasing significantly in the past few years, and there has been a number of successful examples for innovative analytical applications, such as bioactive paper [6, 88], electro-active paper (EAPap) [89, 90], and surface-enhanced Raman scattering (SERS)-active paper [91, 92].

**Table 6.** Paper as substrate for microfluidic devices in comparison with traditional materials.

Property	Material			
	Glass	Silicon	PDMS	Paper
Surface profile	Very low	Very low	Very low	Moderate
Flexibility	No	No	Yes	Yes
Structure	Solid	Solid	Solid, gas-permeable	Fibrous
Surface-to-volume ratio	Low	Low	Low	High
Fluid flow	Forced	Forced	Forced	Capillary action
Sensitive to moisture	No	No	No	Yes
Biocompatibility	Yes	Yes	Yes	Yes
Disposability	No	No	No	Yes
Biodegradability	No	No	To some extent	Yes
High-throughput fabrication	Yes	Yes	No	Yes
Fictionalization	Difficult	Moderate	Difficult	Easy
Spatial resolution	High	Very high	High	Low to moderate
Homogeneity of the material	Yes	Yes	Yes	No
Price	Moderate	High	Moderate	Low
Initial investment	Moderate	High	Moderate	Low

## 1.3.3 Development of Paper-Based Microfluidic Devices

Paper has been used as low-cost chromatographic substrates for analytical tests since 1850. The origins of the development of diagnostics and bio-detection based on paper strips can be traced back to the 1950s. From that time, paper strip tests of biologically relevant species, such as glucose in urine, were as simple as pH paper tests [47, 93]. In the 1980s, paper was widely used as substrate for POC diagnostics [94], but these paper strip tests are not sufficient to operate multiple and quantitative analyses. In 2007, a



new concept of fabricating  $\mu$ PADs to simultaneously detect multiple analytes in a liquid sample was introduced by the Whitesides Group [95]. To date, research on paper-based microfluidic devices has experienced a period of explosion; most published works focus on the invention of low-cost and simple fabrication techniques and the exploration of new applications for low-volume bio/chemical/medical/environmental analysis by incorporating efficient detection methods.

## 1.3.3.1 Fabrication techniques

The most popular fabrication techniques for paper-based microfluidic devices can be divided into seven general categories: (1) photolithography [95-97], (2) plotting [98], (3) printing [99-101], (4) etching [102, 103], (5) dipping [104], (6) cutting [105], and (7) drawing [106, 107]. The advantages and disadvantages of these fabrication techniques are summarized in Table 7. The fundamental principle underlying these fabrication techniques is to pattern barriers on a sheet of paper in order to create capillary channels of micron-scale diameter on paper. The barriers acquired can be subdivided into the three types: (1) hydrophobic walls created by modification of fibres with agents such as wax, photoresist, or AKD; (2) air-solid phase boundaries as in cutting; (3) physical barriers formed by blocking of the porous structure with polymer such as polydimethylsiloxane, polystyrene, or polyurethane [108]. Of these, hydrophobic barriers are the most commonly used for paper-based microfluidics. However, it should be noted that these are not suitable for oleophilic samples, such as those containing cholesterol.

**Table 7.** Primary advantages and disadvantages of fabrication techniques for paper-based microfluidic devices.

Technique	Advantages	Disadvantages
Photolithography	High resolution of microfluidic channels; can be adapted to use low-cost facilities	Requires multistep process; devices are vulnerable to bending; requires expensive equipment
Plotting	Patterning agent is cheap;	Deteriorated barrier

## Chapter 1

		can work with any surface; devices are flexible	definition; difficult to produce on a large scale
Printing	Wax printing	Simple and fast fabrication process; biodegradability of barriers	Requires an extra heating step
	Screen printing	Simple process; deposition of thick layers is possible	Low resolution of microfluidic channels; less applicable for prototyping
	Flexographic printing	Low ink usage; avoids heat treatment	Limited compatibility of solvents; requires different printing plates
	Ink-jet printing	Uses very cheap AKD; fast and simple; requires only a desktop printer	Nozzle clogging; requires an extra heating step
	Laser printing	High resolution; high availability	Only surface treatment; requires extra coating for liquid flow
	Transparency transfer printing	Wax pattern printed on transparency can be transferred to any substrate	Low resolution
Etching		Requires only a single printing apparatus	Slow; uses organic solvents; not suitable for mass fabrication
Dipping		Low-cost and widely available	Requires metal or polymer template, slow
Cutting	Manual	No contamination from chemicals; fabrication of 3D structures is possible; applicable in resource- limited locations	Low resolution
	Computer- controlled		
	Laser cutter		
	Mechanical drill		
Drawing		Extremely cheap and	Low resolution

	widely available; resources like ballpoint pens filled with polymer and wax pencils can be used	
--	---	--

### 1.3.3.2 Detection techniques

To date, a wide variety of detection techniques have been proposed for paper-based microfluidic devices. Applications for such detection methods include medical diagnostics, food pathogens and environmental testing [108, 109]. An ideal detection method for the paper-based microfluidic device should possess at least the following abilities: 1) delivery of clear and stable contrast results after sampling; 2) instantaneous response without complicated equipment; 3) accurate and reliable data analysis support tools; 4) detection limits and selectivity comparable with the standard methods [47, 108]. Currently the most popular fabrication techniques for paper-based microfluidic devices can be sub-divided into six general categories: (1) colourimetric detection, (2) electrochemical detection, (3) nanoparticle-based detection, (4) electrochemiluminescent detection, (5) chemiluminescent detection, and (6) fluorescent detection.

#### *Colourimetric detection*

Colourimetric detection is the most prevalent detection method, because the paper substrate offers a bright, high-contrast, colourless background for colour change reading [110]. Early examples of colorimetric detection in paper-based microfluidics were demonstrated using pH, glucose and protein assays in artificial urine [95, 103]. When samples are introduced to the paper-based microfluidic assay, they are distributed into the reaction zones. This process eventually yields a colour change and enables visual determination of analyte levels using a calibration chart. Currently, molecular and enzymatic dyes represent the simplest and most common method for colourimetric detection [82]. A disadvantage of colourimetric detection in lateral-flow and flow-through assays is the inhomogeneity of the colour distribution, which may lead to difficulty in judgment of the final colour by the naked eye [103]. However, by utilizing a calibration chart, a hand-held reader, a camera phone or more advanced image processing equipment, colourimetric detection is capable of providing qualitative

and semi-quantitative results [95, 111, 112]. Figures 6a and 6b show examples of colourimetric assays for applications of biomedical testing and environmental monitoring.

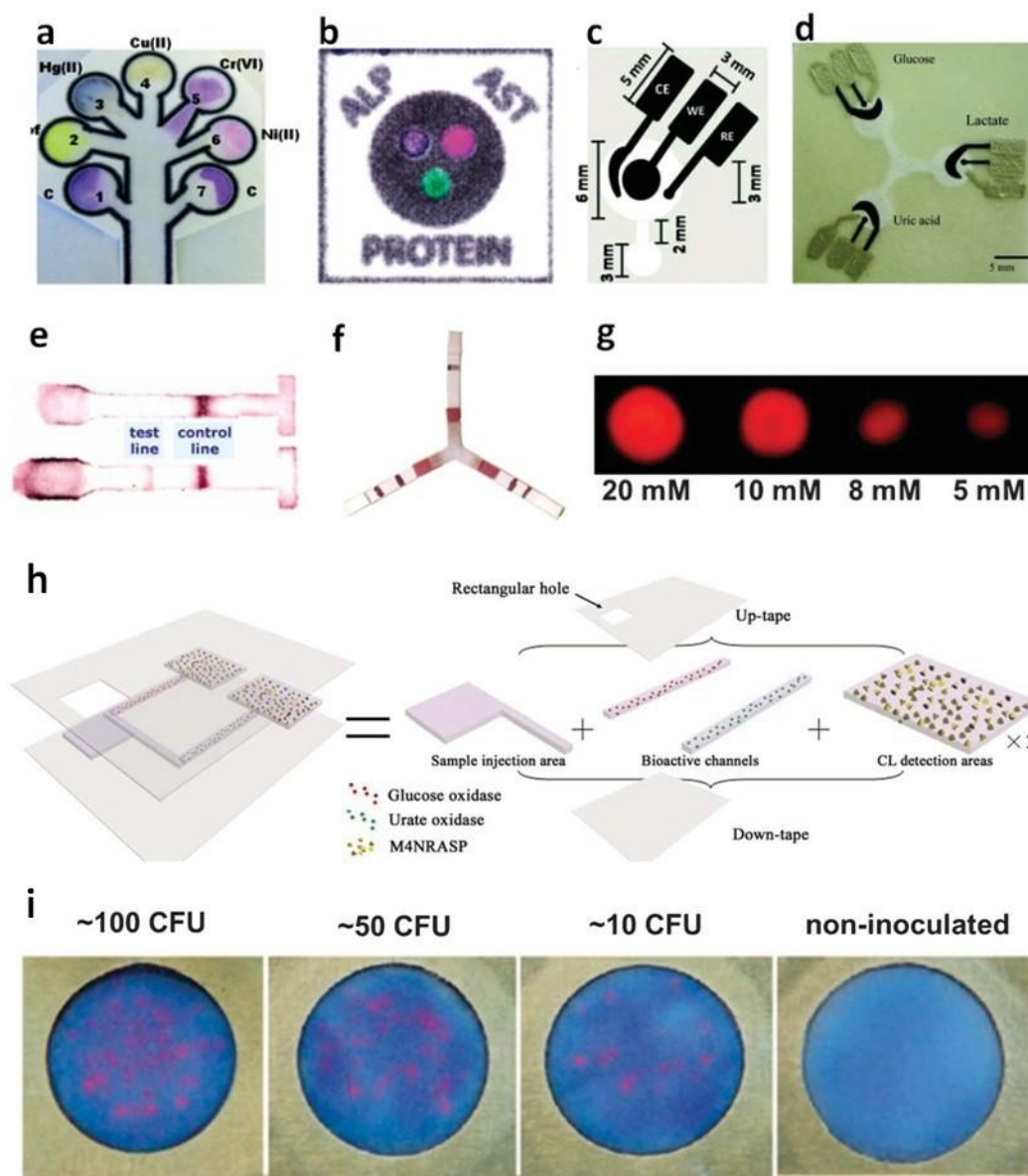


**Figure 6.** Examples of detection techniques for paper-based microfluidic devices [82]. (a) Colourimetric detection of heavy metals. (b) Colourimetric detection of liver function. (c) Dual electrochemical/colourimetric determination of gold and iron. (d) Electrochemical detection of glucose, lactate and uric acid. (e) Antibody conjugated gold nanoparticle detection of immunoglobulin. (f) Antibody conjugated gold nanoparticle detection of *Pseudomonas aeruginosa* and *Staphylococcus aureus*. (g) ECL detection of a sample solution 2-(dibutylamino)-ethanol (DBAE). (h) Schematic of the construction of a CL sensor in paper-based microfluidics. (i) Fluorescent sensing for the growth of bacteria.

### *Electrochemical detection*

Electrochemical (EC) detection is one of the most popular detection techniques, which is able to measure the electrical signals from solutions directly with minimal pre-treatment of analytes [47]. The EC detection technique has been applied to the biological determination of glucose, lactate, uric acid, cholesterol, tumours, markers, dopamine and drugs [89, 113-116]. There are also environmental monitoring applications such as the detection of heavy metals. Figure 6c illustrates an EC-based device for detection of gold and iron, for which carbon inks are used in the fabrication of the counter and working electrodes, whereas silver/silver chloride ink is used for the fabrication of reference electrodes [117]. In the paper-based assays shown in Figure 6d, reaction zones comprise the multiple-electrode mechanism [113]. The main advantage of using EC detection techniques for paper-based devices is that they are insensitive to light, dust, and insoluble compounds. However, the requirement for a detection instrument increases the complexity and the testing cost [82].

### *Nanoparticle-based detection*

In paper-based microfluidics, the feasibility of using nanoparticle-based detection has been demonstrated with metabolites [102], bacterial agents [118] in key disease diagnosis such as human immunodeficiency virus (HIV) [119], malaria [120] and tuberculosis [121] and in environmental monitoring applications [122]. The nanoparticle-based detection technique is able to greatly enhance the sensitivity and selectivity of the test. The first systematic study employing nanoparticle-based detection was in multi-analyte immunochemical detection on filter paper (Figure 6e) [102]. Figure 6f shows another example of antibody conjugated gold nanoparticle detection of *Pseudomonas aeruginosa* and *Staphylococcus aureus*, which adopts folding techniques and microplate paper platforms [118].

### *Electrochemiluminescent detection*

Electrochemiluminescent (ECL) detection is an attractive detection technique for paper-based microfluidic devices, because it has the advantages of both luminescence

and electrochemical methods [47]. This detection mechanism of the ECL method is based on the luminescence generated by electrochemical reactions. The exergonic reactions of electrochemically generated intermediates result in an electronically excited state. This state emits light upon relaxation to a lower level state and thus enables readouts, even without a photodetector. Since ECL detection is performed in the dark, the process is independent of ambient light [82]. At present, applications of the ECL detection technique include analytes, tumour markers and ions [90, 114, 123]. Figure 6g demonstrates an ECL-based device for the detection of 2-(dibutylamino)-ethanol (DBAE) [90]. This is the first application of the ECL detection technique on a paper-based analytical device.

### *Chemiluminescent (CL) detection*

The detection mechanism of the CL technique is based on measurement of the intensity of light emitted by a chemical reaction. In the presence of reactants and a catalyst or excited intermediate, light can be produced together along with other products. The CL detection methods are usually praised for their simplicity, high sensitivity, low cost, and compatibility with micromachining technologies, as well as the fact that measurement can be performed in the dark [82]. An example of a CL-based microfluidic device for determination of glucose and uric acid is shown in Figure 6h, which is based on oxidase reactions coupled with the chemiluminescence reactions of a rhodanine derivative with the hydrogen peroxide generated in an acid medium [124].

### *Fluorescent detection*

The fluorescent detection technique brings new capabilities to paper-based microfluidics. The first demonstration of fluorescent sensing methods for paper-based microfluidic device was completed on paper microzone plates [82]. These paper plates were relatively thin and low-cost. A later study adopted the fluorescent technique for the detection of DNA using paper strips containing DNA-conjugated microgels (MGs) [125]. In another study, a portable paper-based device was fabricated for determination of the growth of bacteria or the amplification of bacteriophages. In this case, a fluorescent mCherry reporter was employed to quantify the growth of bacteria and the concentration of arabinose (see Figure 6i) [126]. In terms of the drawbacks of this

detection method, it should be noted that there is a requirement for additional readers and some paper substrates containing fluorescent additives may produce high background signals.

### 1.4 PAPER-BASED BLOOD TYPING DEVICES

Based on the promising development of paper-based microfluidic devices and the demand for low-cost POC blood typing, numerous research studies have been conducted on exploiting paper-based blood typing devices in recent years. Most of these devices are low-cost, rapid, reliable, portable and disposable. They are of significant value for bedside compatibility checks and fast blood typing in emergency situations and in places where there is no access to laboratory equipment, such as rural areas and developing countries. In this section, we summarize the development of paper-based blood typing devices, and present the current challenges and future trends.

#### 1.4.1 Development of Paper-Based Blood Typing Devices

The design concepts of paper-based blood typing devices are mostly based on filtration and chromatographic separation principles. Based on the flow pattern of blood samples within paper substrates, the current paper-based blood typing devices can be divided into two categories: (1) lateral flow, and (2) vertical flow-through. For the lateral flow pattern, the direction of blood flow is parallel to the paper sheet. On the other hand, the direction of blood flow is perpendicular to the paper sheet for the vertical flow-through pattern.

##### *Lateral flow pattern*

Khan et al. [6] invented a paper-based diagnostic device for instantaneous blood typing in 2010 (see Figure 7). This is the first application of paper-based microfluidics for blood typing. The design concept of the device is based on the difference of the capillary wicking rates of agglutinated blood and non-agglutinated blood. Paper strips are soaked in anti-A, anti-B and anti-D solutions; then a blood sample is introduced at the centre of the paper strip, leading to different wicking behaviour. The agglutinated red cells show very little wicking, while the serum wicks for a much longer distance than the agglutinated red cells. Therefore, an agglutinated blood sample shows a chromatographic separation from the wicking serum.



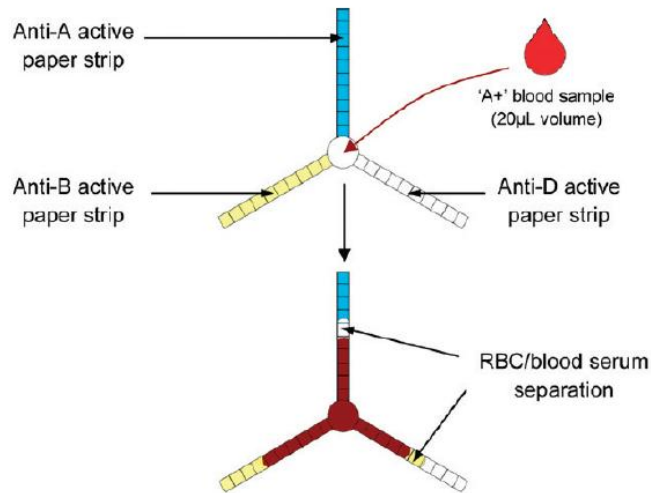


**Figure 7.** Paper-based blood typing device using wicking of agglutinated RBCs from specific antigen/antibody interactions on dry paper strips.

Al-Tamini et al. [8] developed and validated another paper-based assay for rapid blood typing. This method is based on the different behaviours of agglutinated and non-agglutinated red blood cells when they are eluted with a saline solution. Grouping antibodies are spotted and dried on the paper, followed by spotting blood onto the antibodies and laterally eluting them with 0.9% NaCl buffer for 10 min by capillary absorption. Agglutinated RBCs are fixed on the paper substrate, resulting in a high optical density of the spot, with no visual trace in the buffer wicking path. In contrast, non-agglutinated RBCs can easily be eluted by the buffer and show low optical density of the spot and clearly visible traces of RBCs in the buffer wicking path (refer to Figure 8). This assay shows that RBCs fixation on paper is able to detect blood groups (ABO and RhD) accurately with excellent reproducibility.

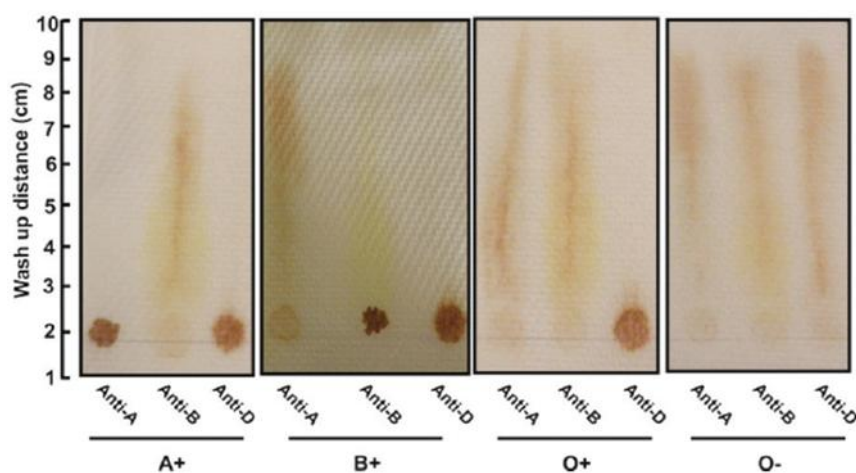


**Figure 8.** Paper-based blood typing assay using agglutinated blood fixations on papers and chromatographically eluted with 0.9% NaCl buffer for 10 min.

Noiphung et al. [127] reported a paper-based device that can perform three functions simultaneously, including Rh and forward and reverse ABO blood typing within 10 min. The paper device is fabricated using a combination of wax printing and dipping methods to generate a two-sided device for forward and reverse blood typing assays (see Figure 9). The blood sample is diluted to 50% for forward blood typing, whereas the whole blood sample can be used for reverse grouping. The ratio between the distance of red blood cell movement and plasma separation is the criterion for agglutination and indicates the presence of the corresponding antigen or antibody. The stability of antibodies that are absorbed to the paper-based device can be retained at 4°C for up to 21 days. Moreover, the test results can be kept for at least 7 days at room temperature, which is very useful for re- evaluation. However, the accuracy of this method is largely affected by the haematocrit of the blood sample.

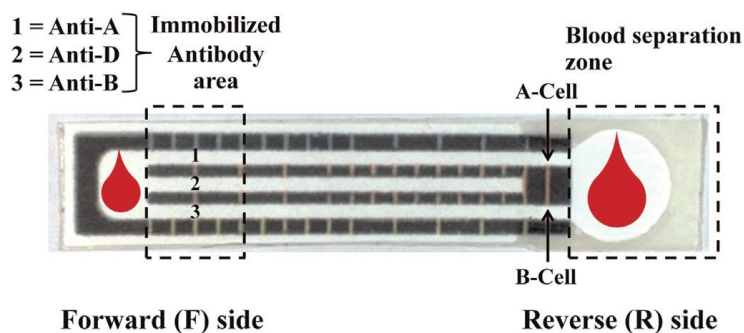


**Figure 9.** Paper-based blood typing device for simultaneously determining Rh typing and forward and reverse ABO blood groups.

More recently, Guan et al. [11] applied the barcode reading concept for the first time in the design of a paper-based blood typing device by adapting smartphone-based technology. The device is fabricated using a printing technique to define hydrophilic bar channels which are treated with Anti-A, -B, and -D antibodies, respectively. The blood sample is then introduced into these channels to perform blood typing assays. The blood type can be visually identified from the laterally eluting lengths in the bar channels. A smartphone-based analytical application is programmed to read the bar channels to interpret this barcode-like information for users. The entire process is shown in Figure 10. This innovation is a breakthrough in the development of paper-based blood typing devices, as the employment of smartphone technology increases the capability of paper-based diagnostics with rapid assay result interpretation, data storage, and transmission.

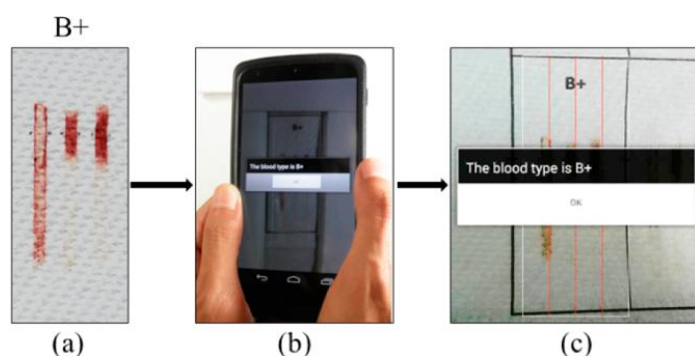


**Figure 10.** Blood typing results based on smartphone-based analysis. (a) Blood typing result (B+) is shown in bar channels, (b) reading the result using the Android application, and (c) acquiring the blood result with text on the screen.

## *Vertical flow-through pattern*

Jarujamrus et al. [7] developed a simple protocol for blood typing using testing paper and inspection paper (refer to Figure 11). The testing paper is treated by dosing commercial antibody solutions onto it. The blood sample is then delivered onto the testing paper and allowed to interact with the antibody for 30 seconds. Saline solution is then introduced vertically onto the blood sample-loaded testing paper; it penetrates the testing paper and wets the inspection paper. The inspection paper is then separated from the testing paper for visual inspection. A visible blood stain on the inspection paper indicates that the RBC agglutination has not occurred and the test is negative.

Conversely, the lack of a blood stain on the inspection paper indicates that the RBC agglutination occurred and the test is positive.

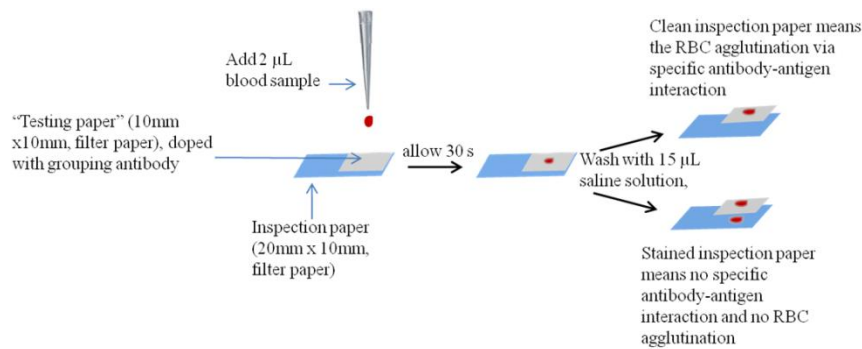


**Figure 11.** Schematic diagram of a simple protocol for blood typing using testing paper and inspection paper.

Recently, Li et al. [9] designed the first paper-based blood typing device with the capability of text-reporting. This invention presents a new concept of adding grouping antibodies onto paper which has printed patterns of text and symbols. For example, the anti-A solution is dosed into the printed text pattern “A”. If the RBCs of a blood sample undergo haemagglutination due to anti-A in the text pattern “A”, agglutination of RBCs occurs inside the patterned “A” zone; the deep red colour formed by the agglutinated RBCs cannot be vertically washed away using saline solution and the paper reports the blood type of this sample with the letter “A” formed by the colouring effect of the agglutinated RBCs. The actual blood type tests of eight blood types are presented in Figure 12a. This design concept has also been applied to the detection of various clinically important secondary blood types (see Figure 12b) [10]. This innovation enables non-professional users to identify blood types directly, which is of great significance for developing countries where trained medical professionals may not always be available. The text reporting blood typing concept using bioactive paper has been explored by the diagnostic industry as a new class of sensitive, rapid and user-friendly device.

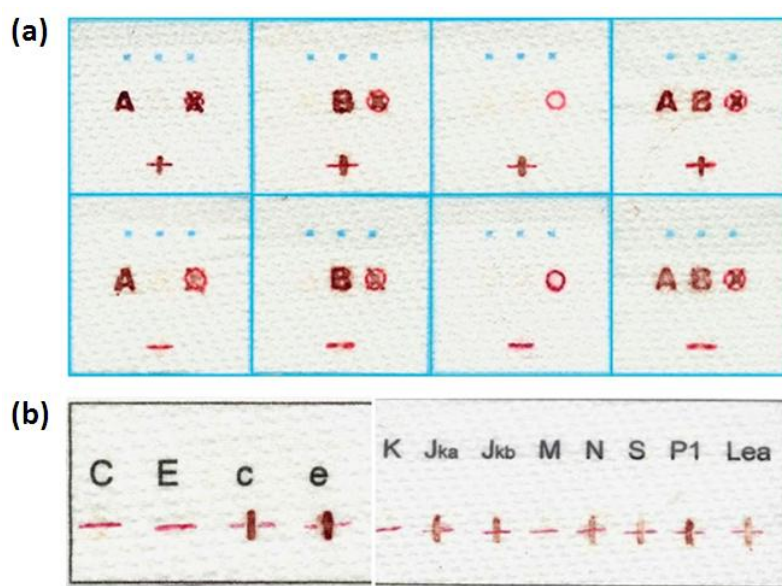


**Figure 12.** Paper-based blood typing devices reporting results in written text. (a) ABO and Rh groups; (b) secondary blood groups.

### 1.4.2 Previous Studies of Fundamentals for Paper-based Blood Typing Devices

Although there have been significant achievements in the development of paper-based blood typing devices, it is still important to understand the basic mechanisms in order to produce a more advanced device that fully meets the ASSURED criteria. Researchers have done some preliminary studies of the fundamentals for the design of paper-based blood typing devices.

Jarujamrus et al. [7] conducted a semi-quantitative study of the adsorption and desorption of antibody molecules in antibody-treated paper substrate. The researchers took a biochemical approach and analyzed the amount of antibody that could be washed off the antibody-treated paper (see Figure 13). Their hypothesis was that a blood sample introduced onto the paper could re-dissolve a fraction of antibody, which deposits and dries on the fibre surface. The re-dissolved antibody molecules could then work in specific interactions with the RBCs, leading to haemagglutination within the paper. Their results showed that around 34% to 42% of antibody molecules carried by the antibody-treated paper could be re-dissolved by saline solution or a blood sample. It was also suggested that the adsorbed antibody molecules alone on paper matrix were

not sufficient to immobilize RBCs into large agglutinated lumps. In contrast, paper containing both adsorbed and desorbed antibody molecules was able to agglutinate the corresponding RBCs more efficiently.

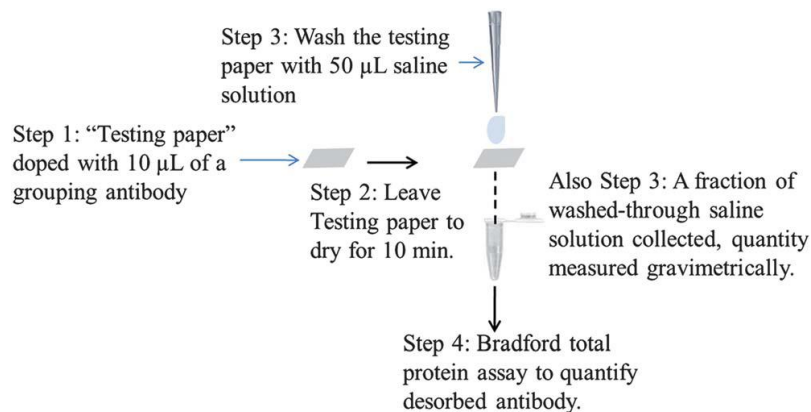


**Figure 13.** Protocol for semi-quantification of the desorbed antibody from testing papers by saline washing simulation.

Guan et al. [128] investigated the stability of the primary blood typing antibodies (Anti-A, Anti-B and Anti-D IgM) on paper. They discovered that the longevity of blood group antibodies sorbed into paper is improved by the mixing of additives such as glycerol, PVP and dextran. Of these, low molecular weight additives provide a lower level of protection to antibodies than high molecular weight polymers, because they are capable of penetrating the fibre walls. Moreover, freeze-drying was found to provide a much higher level of protection to antibodies than additives. The lack of antibody aggregations in freeze-dried paper lowered the intermolecular hydrogen bonding of antibody molecules, which helped retain their natural configuration and ability to interact with RBCs. The thermal stability of the non-aggregation of freeze-dried antibodies in paper substrate was also much higher than that of the unprotected antibodies. Therefore, they suggest that freeze-drying is a suitable method for providing long-term protection to antibodies in paper, whereas additives may be used for applications where shorter-term protection is required. The findings of this study are critical to the manufacture of a new type of paper-based blood typing device where blood group antibodies must be kept active on paper for extended periods.

Su et al. [129] qualified and analysed the commercial and experimental papers varying in different fibre composition, basis weight, density and porosity for their study of the

separation of agglutinated from non-agglutinated RBCs. The paper-based blood typing assay of the lateral elution pattern that was previously described by Al-Tamimi et al. [8] was adopted in this research. The results showed that the basis weight, density and porosity of paper significantly affect the separation of agglutinated and non-agglutinated RBCs, while the type of fibre plays a minor role in blood typing visualization. Thin and porous papers provide the best performance of blood typing, whereas thick and dense papers are inappropriate for blood typing, as they tend to retain indiscriminately both free RBCs and aggregated RBCs. Therefore, the researchers suggest that an ideal paper substrate for blood typing can be produced from low basis weight papers made from softwood fibres.

### 1.5 LIQUID MICRO REACTORS

Micro reactors are defined as miniaturized reaction systems fabricated by microtechnology and precision engineering [130]. The term “micro reactor” is generally used to describe a great number of devices that have small dimensions [131]. Micro reactors have shown striking advantages in heat and mass transfer rates. Moreover, the contact time, shape and size of the interface between fluids can be easily and precisely controlled [132]. These features make micro reactors ideal for fast reactions, highly exothermic reactions, and even explosive reactions [133-135]. The small volume capacity of micro reactors also allows the efficient development of more sophisticated flow reactions, since they greatly reduce the quantities of materials required for optimization of reaction conditions.

Studies of high throughput screening in microanalytical chemistry, biological analysis of cells and proteins, reaction kinetics and mechanisms are the initial uses of micro reactors [136-138]. The micro reactor technique has now become an interdisciplinary science connecting physics, chemistry, biology, and engineering arts for more applications, such as environmental monitoring, online process optimization, production of micro fuel cells, and especially for microorganic synthesis or production in the pharmaceutical industry, where the test-rig stage in the development of a drug does not require the production of large quantities of the chemical [139].

In this section, we review the micro reactor design principles and discuss how to fabricate liquid micro reactors for blood typing applications.

#### 1.5.1 Design Principles of Liquid Micro Reactors

A microchannel in the range of 10  $\mu\text{m}$  to 500  $\mu\text{m}$  is generally the simplest form of micro reactor (refer to Figure 14a) [131]. They can be fabricated from different materials such as ceramic, glass, plastic, silicon, quartz, metal and polymer. Of these, glass is the most commonly used material as it is chemically inert and transparent, which allows the visual inspection of microchannels. However, the selection of optimal material depends on their chemical compatibility with solvents and reagents, their cost,



and the detection methods used in process control. Different fabrication techniques are also included in microchannel production, including photolithography, powder moulding, powder blasting, injection molding, ultrasonic technologies, stamping and laser micro-formation [140]. It is also necessary to select an appropriate production technique, since it has a great impact on the flow in the micro reactor. The combination of microchannels and supporting base material forms a chip (see Figure 14b). The integration of a chip, supporting base material and connecting fluid lines form a unit (Figure 14c). Using a combination of other micro devices (mixers, heat exchangers, separators, absorbers etc.) and different element configurations, more complex micro reactor systems can be developed (Figure 14d) [131].

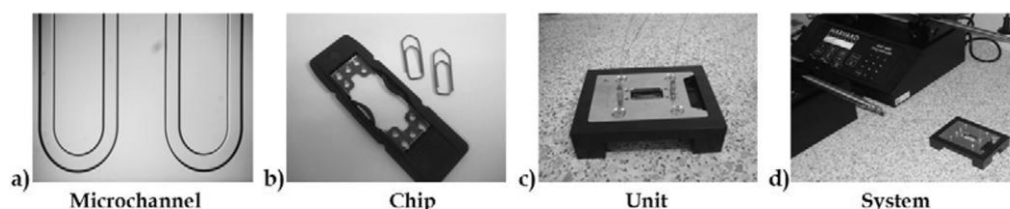


**Figure 14.** Basic structural units of a micro reactor system [131].

The requirement of increasing the throughput of micro reactors can be met by a numbering-up approach, rather than scaling-up [141]. In the numbering-up approach, the functional unit of a micro reactor is multiply repeated. Fluid connection between these units can be achieved by using distribution lines and flow equipartition zones [141, 142]. The most striking advantage of the numbering-up approach is that it is able to guarantee the desired features of a basic unit when increasing the total system size [131].

According to the type of reagent phases involved, micro reactors can be sub-divided into four categories: liquid-liquid, gas-liquid, gas-liquid-solid, and gas-gas-solid [143, 144]. For blood typing applications, both blood samples and antibody reagents are liquid phases. The most classical flow patterns for the liquid-liquid micro reactor system are parallel flow and slug or segmented flow (see Figure 15) [131]. In the case of parallel flow, phase contact, diffusion-based dispersion and reaction occur at the longitudinal interface. Given the small dimensions, the parallel flow is generally

laminar. This type of flow is easy for the control and modelling of the reaction and simultaneously provides high surface-to-volume ratios and interface areas, which is quite important, especially for multiphase systems. On the other hand, slug flow is a flow characterized by a series of liquid slugs of one phase separated by the other. Diffusion and reaction occur at the multiple transverse interfaces established. The flow pattern formation is determined by linear velocity, ratios of the phases, fluid properties, and the construction material of the micro reactor [143]. Therefore, all these parameters must be considered when controlling the flow pattern.

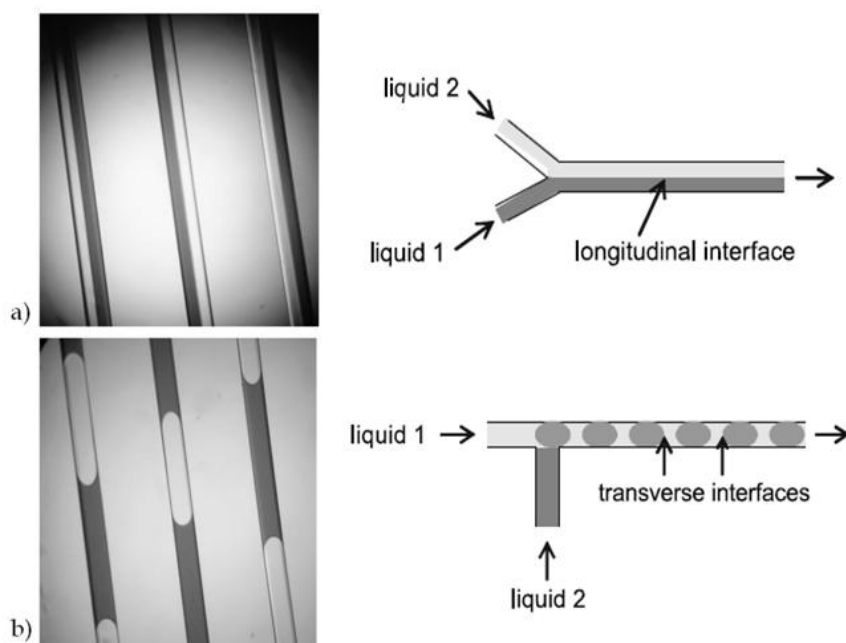


**Figure 15.** Flow patterns: (a) parallel flow with longitudinal contact interface in a microchannel; (b) slug flow with transverse contact interface in a microchannel.

However, the classical liquid-liquid micro reactors mentioned above are not suitable for blood typing applications, which have three basic requirements for the micro-device: 1) low cost; 2) easy observation of the RBCs agglutination reaction; 3) ability to observe the details in any reaction area. Therefore, a new type of liquid micro reactor must be developed for blood typing applications.

### 1.5.2 Superhydrophobicity for Liquid Micro Reactors for Blood Typing Applications

If a drop of liquid is placed on a solid surface, it will form a so-called contact angle ( $\theta$ ), as illustrated in Figure 16a. Young [145] first referred to the concept of contact angle in 1805. The contact angle of a liquid on a perfectly smooth and chemically homogeneous solid surface can be described by Young's equation (Equation 2):

$$\cos\theta = \frac{(\gamma_{sv} - \gamma_{sl})}{\gamma_{lv}} \quad (2)$$

where,  $\gamma_{sv}$ ,  $\gamma_{sl}$  and  $\gamma_{lv}$  are the interfacial tensions of the solid-vapour, solid-liquid and the liquid-vapour interface respectively. Young's contact angle is the result of thermodynamic equilibrium of the free energy at the solid–liquid–vapour interphases. According to the value of the contact angle, surface properties are determined to be hydrophobic ( $\theta > 90^\circ$ ) or hydrophilic ( $\theta < 90^\circ$ ) [146].

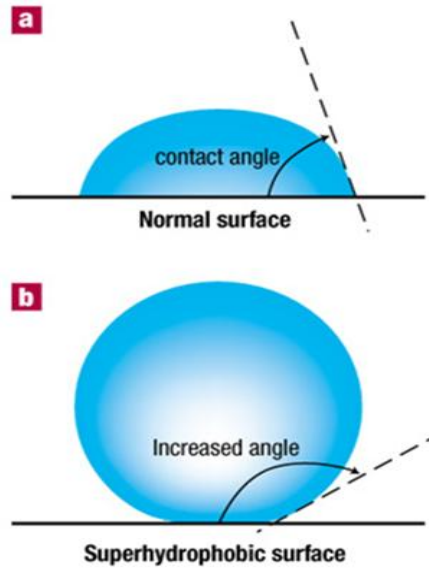


**Figure 16.** Graphical demonstration of (a) normal surface and (b) superhydrophobic surface.

Superhydrophobicity is an extreme state of hydrophobicity, with a contact angle greater than  $150^\circ$  and very little contact angle hysteresis [147, 148]. It is also known as super water repellence. On a superhydrophobic surface, the liquid droplet balls up on the surface and retains a pearl-like shape upon contact, as shown in Figure 17b. Such highly water-repellent surfaces are abundant in nature. Examples include, but are not limited to, lotus leaves, butterfly wings, mosquito eyes, red rose petals, gecko feet, desert beetles, spider silk, and fish scales [149].

The Wenzel [150] and Cassie-Baxter [151] models are the basic guidelines for the study of superhydrophobic surfaces, which describe the effect of surface morphology on wettability. As shown in Figure 17, when a water droplet is put on a rough surface, it can either penetrate or be suspended above the asperities. In either case, much higher contact angles are observed than that obtained for the corresponding smooth surface.

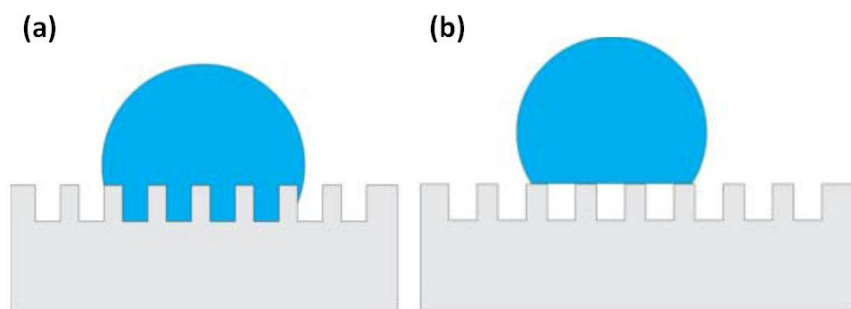


**Figure 17.** Behaviour of a liquid drop on a rough surface: (a) liquid penetrates into the spikes (Wenzel model); (b) liquid suspended on the spikes (Cassie-Baxter model).

Superhydrophobic powder refers to the phenomenon of superhydrophobicity associated with hydrophobic powders. Hydrophobic particles enwrapping liquid droplets allowed the manufacture of so-called "liquid marbles". This term was first introduced in the pioneering works of Qu à è [152] and Mahadevan [153]. Since then, intensive research has been done by various groups on the unusual physical and chemical properties of liquid marbles [152-155]. A typical liquid marble is depicted in Figure 18, which shows a polyvinylidene difluoride (PVDF) coated water marble [156].

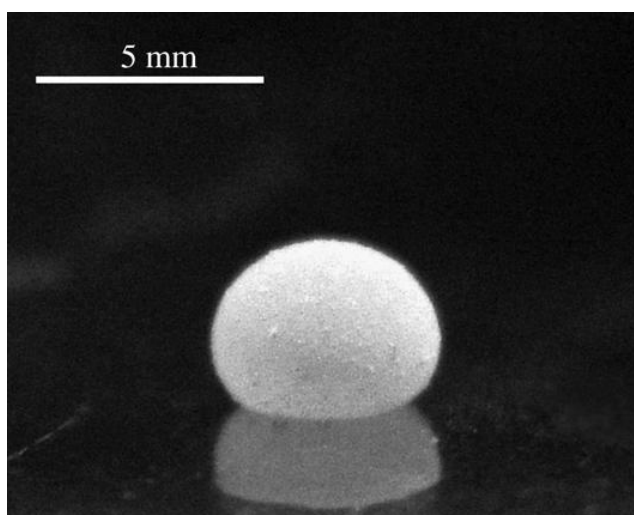


**Figure 18.** A 50  $\mu\text{L}$  PVDF-coated water marble.

Based on their unique structural characteristics, liquid marbles possess the following distinctive functionalities: (1) A porous shell partially covered by powder particles, which are loosely attached to the liquid surface, allowing gases or vapours to pass through; (2) An isolated liquid core that does not have any direct contact with the underlying supporting media, but is still accessible for manipulation due to the flexible powder shell; (3) It is very simple to actuate, transport, and manipulate liquid marbles using electric or magnetic fields, which is particularly useful in microfluidic applications; (4) Liquid marbles can be put either on a solid or a liquid surface. In either case, the direct contact between the liquid core and the underneath surface is prohibited by the non-wettable powder shell. The combination of these special structural properties provides liquid marbles great potential for a variety of applications, including gas sensing, synthesizing solid polyelectrolyte microspheres, water surface pollution detection and the manipulation of small quantities of liquids [157-161].

In order to meet the requirements of liquid micro reactors for blood typing, two design concepts based on superhydrophobicity are developed in this thesis (see Figure 19). One is a superhydrophobic surface-supported micro liquid drop; the other is a liquid marble fabricated using superhydrophobic powder. In either case, the near-spherical micro reactor fabricated based on superhydrophobicity is capable of providing an excellent side view, allowing the RBCs' haemagglutination reaction to be observed. Moreover, both the liquid droplet on a superhydrophobic surface and a liquid marble can easily roll off the testing substrate after blood typing assays, which prevents the testing substrate from being contaminated. Therefore, the assay substrate can be re-used unlimited times in the ideal state, so that the cost of performing blood typing assays in large volumes will be greatly reduced. Most importantly, by integrating these liquid micro reactor devices with advanced imaging capture and processing systems, the automation of high-throughput blood typing, including rapid assay result interpretation, data storage, and transmission can be achieved.

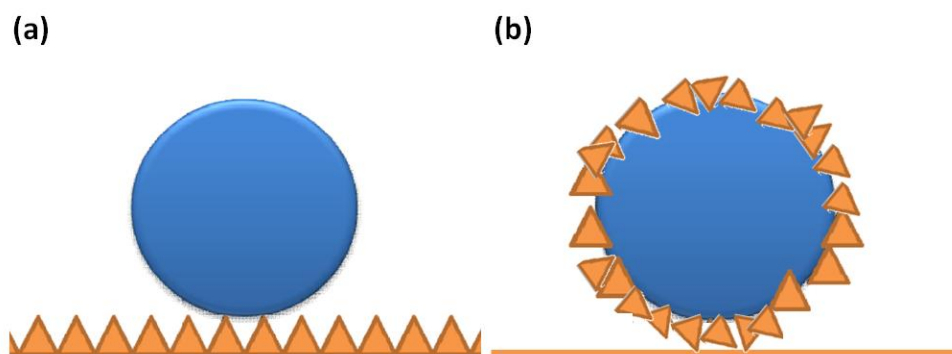


**Figure 19.** Design concepts of liquid micro reactors for blood typing applications: (a) superhydrophobic surface-supported micro liquid drop; (b) liquid marble fabricated with hydrophobic powder.

### 1.6 RESEARCH OBJECTIVES

The overall objective of this research is to investigate and develop blood typing devices based on bioactive paper and liquid micro reactors fabricated using superhydrophobic materials. The thesis includes two parts.

Part I studies the basic mechanisms of paper-based blood typing devices, which are essential for the future design of high-performance paper-based blood typing devices. The specific objectives of this part are:

- 1) To investigate the transport and immobilisation mechanisms of RBCs in antibody reagent-treated paper;
- 2) To study the transport pathways of RBCs in paper fibre networks;
- 3) To understand the effect of paper structure on blood typing performance.

The objective of Part II is to develop superhydrophobicity-based liquid micro reactor devices for high-throughput blood typing applications. The specific aims of this part include the following:

- 1) Develop superhydrophobic surface-supported micro liquid drops as liquid micro reactor devices.
- 2) Explore superhydrophobic powder-fabricated liquid marbles as liquid micro reactor devices.

### 1.7 THESIS OUTLINE

This thesis reports the investigation and development of blood typing devices based on bioactive paper and liquid micro reactors fabricated using superhydrophobic materials. It includes two parts. Part I, which is reported in Chapters 2-4, focuses on the investigation of the fundamental mechanisms of paper-based blood typing devices; and Part II, which is reported in Chapters 5-6, illustrates the development of superhydrophobicity-based liquid micro reactor devices for high-throughput blood typing.

This thesis is presented in the format of “Thesis by Publication” based on the Monash University Handbook for Doctoral and MPhil Degrees 2015 and the Thesis by Published and Unpublished papers (Monash Research Graduate School). Part I includes two published and one unpublished studies, with one publication presented in each chapter, while Part II includes two published studies, with one publication presented in each chapter. All published papers have been reformatted to comply with the requirements of the Thesis by Publication format. However, the content remains unchanged. The original publications are given in Appendix I.

#### **Part I Mechanisms of paper-based blood typing devices**

##### **Chapter 2: A study of the transport and immobilisation mechanisms of human red blood cells in a paper-based blood typing device using confocal microscopy**

(Published in *Analyst*)

In this chapter, a confocal microscopic method is reported for investigating the mechanism of RBC immobilization inside the paper which follows haemagglutination reactions. Confocal microscopy is shown to be a suitable technique for providing the details of RBC agglutination at the cellular level inside the fibre network of paper. The non-agglutinated RBCs do not undergo morphological change, distributing rather uniformly in the spaces of the fibre network and staying around the middle of the paper sheet. In contrast, the agglutinated RBCs are deformed, forming blood aggregates immobilized randomly at different positions on the fibre surface. Chromatographic



elution patterns of both agglutinated and non-agglutinated RBCs are also studied to gain insight into the transport behaviours of free RBCs and agglutinated aggregates.

### **Chapter 3: Revealing the transport behaviour of human red blood cells in paper using scanning electron microscopy combined with focused ion beam milling**

(Unpublished manuscript for submission)

This chapter reports an investigation of the transport mechanism of RBCs within paper substrate using scanning electron microscopy (SEM) and focused ion beam (FIB) technology. The liquid nitrogen slushing method and freeze drying technique enables the quick and accurate capture of RBCs' location within paper during the wetting process. Moreover, the employment of a combined dual beam system with FIB and SEM not only enables the 3D reconstruction of the whole paper network containing RBCs, but also makes it possible to study any specific RBC within the layer-by-layer paper fibre network. FIB-based cryo-SEM tomography is shown to be a suitable technique for providing the details of RBCs at the cellular level inside the fibre network of paper. The transport mechanism of RBCs within paper substrate will be a significant guide for the future design of paper-based blood diagnostic devices.

### **Chapter 4: Control performance of paper-based blood analysis devices through paper structure design**

(Published in *ACS Applied Materials & Interfaces*)

This chapter investigates the influence of paper structure on the performance of paper-based blood typing devices. In this study, paper substrates with different basis weights are prepared using different fibres. The effect of fibre type on paper structure is isolated from all other possible influencing factors by removing the fines from the pulps and not adding any chemical additives. The physical structures of paper sheet are characterized using apparent thickness and bulk measurements and with mercury intrusion porosimetry. RBC transport in paper carried by saline solution is studied in blood-typing assays by lateral chromatographic elution and vertical flow-through modes. The complexity of the paper's internal pore structure has a dominant influence on the transport of RBCs in paper. Hardwood fibre sheets with a low basis weight have a simple internal pore structure and allow for the easy transport of RBCs, while softwood

fibre papers are found to have a more complex pore structure, leading to blood-typing results of low clarity. This chapter provides the principles of paper substrate design for paper-based blood typing devices.

### **Part II Blood Typing Devices Based on Liquid Micro Reactors**

#### **Chapter 5: Superhydrophobic surface supported bioassay – An application in blood typing**

(Published in *Colloids and Surfaces B: Biointerfaces*)

This chapter describes a new application of superhydrophobic surfaces to form liquid micro reactors for the conduct of biological assays for human blood typing. The superhydrophobic substrate is fabricated using a simple printing technique with Teflon powder. The non-wettable property of the superhydrophobic surface by blood samples and antibody solutions causes the blood and antibody droplets to assume a near spherical shape, making it easy for haemagglutination reactions inside the droplet to be photographed or recorded by a digital camera and then analysed using image analysis software. The evaluation of assay results using image analysis techniques offers the potential to develop high throughput operations of rapid blood typing assays for pathological laboratories. With the capability of identifying detailed red blood cell agglutination patterns and intensities, this method is also useful for confirming blood samples that have weak RBC antigens.

#### **Chapter 6: Liquid marbles as micro-bioreactors for rapid blood typing**

(Published in *Advanced Healthcare Materials*)

This chapter reports the novel concept of using liquid marbles as bio-microreactors for rapid blood typing assays. Liquid marbles, made of low-cost hydrophobic precipitated calcium carbonate powder and a drop of blood, are introduced as miniature bio micro reactors capable of containing biological reactions. ABO and Rh blood typing is then carried out inside the liquid marbles. In the test, only a few seconds of gentle shaking of the blood marble is sufficient to initiate the haemagglutination reaction. Images of the micro reactors can be captured using a digital camera. The colour change caused by haemagglutination is clearly visible. The ability to use image analysis techniques offers

this method the potential to develop high-throughput rapid blood typing systems for pathological laboratories. It is also believed that the liquid marble bio-microreactor concept can be developed into more applications for chemical or biological assays.

### 1.8 REFERENCES

- [1] W. Malomgre, B. Neumeister, Recent and future trends in blood group typing, *Anal Bioanal Chem* 393 (2009) 1443-1451.
- [2] G. Daniels, M.E. Reid, Blood groups: the past 50 years, *Transfusion* 50 (2010) 281-289.
- [3] G. Daniels, I.M. Bromilow, *Essential Guide to Blood Groups*, Wiley-Blackwell: Chichester, West Sussex, UK, 2010.
- [4] G. Daniels, *Human blood groups*, Second Edition ed., Blackwell Science, Oxford, U. K., 2002.
- [5] C.M. Westhoff, The Rh blood group system in review: A new face for the next decade, *Transfusion* 44 (2004) 1663-1673.
- [6] M.S. Khan, G. Thouas, W. Shen, G. Whyte, G. Garnier, Paper diagnostic for instantaneous blood typing, *Analytical Chemistry* 82 (2010) 4158-4164.
- [7] P. Jarujamrus, J. Tian, X. Li, A. Siripinyanond, J. Shiowatana, W. Shen, Mechanisms of red blood cells agglutination in antibody-treated paper, *Analyst* 137 (2012) 2205-2210.
- [8] M. Al-Tamimi, W. Shen, R. Zeineddine, H. Tran, G. Garnier, Validation of paper-based assay for rapid blood typing, *Analytical Chemistry* 84 (2012) 1661-1668.
- [9] M. Li, J. Tian, M. Al-Tamimi, W. Shen, paper-based blood typing device that reports patient's blood type "in writing", *Angewandte Chemie International Edition* 51 (2012) 5497-5501.
- [10] M. Li, W. Then, L. Li, W. Shen, Paper-based device for rapid typing of secondary human blood groups, *Anal Bioanal Chem* 406 (2014) 669-677.
- [11] L. Guan, J. Tian, R. Cao, M. Li, Z. Cai, W. Shen, Barcode-like paper sensor for smartphone diagnostics: an application of blood typing, *Analytical Chemistry* 86 (2014) 11362-11367.
- [12] K. Landsteiner, *The Specificity of Serological Reactions*, Dover Publications, New York, U. S. A., 1962.
- [13] M. McKinley, V. O'Loughlin, *Human Anatomy*, McGraw-Hill Science/Engineering/Math, New York, U. S. A., 2007.
- [14] G. Daniels, J. Poole, M. De Silva, T. Callaghan, S. MacLennan, N. Smith, The clinical significance of blood group antibodies, *Transfusion Medicine* 12 (2002) 287-295.

- [15] N.D. Avent, M.E. Reid, The Rh blood group system: a review, *Blood* 95 (2000) 375-387.
- [16] E. Hosoi, Biological and clinical aspects of ABO blood group system, *The Journal of Medical Investigation* 55 (2008) 174-182.
- [17] G. Garratty, Relationship of blood groups to disease: do blood group antigens have a biological role?, *Revista Médica del Instituto Mexicano del Seguro Social* 53 (2005) S113-S121.
- [18] G. Garratty, *Immunobiology of transfusion medicine*, CRC Press, New York, U. S. A., 1993.
- [19] D. Ballerini, X. Li, W. Shen, An inexpensive thread-based system for simple and rapid blood grouping, *Anal Bioanal Chem* 399 (2011) 1869-1875.
- [20] M. Li, J. Tian, R. Cao, L. Guan, W. Shen, A low-cost forward and reverse blood typing device-a blood sample is all you need to perform an assay, *Analytical Methods* 7 (2015) 1186-1193.
- [21] J.H. Spindler, H. Klüter, M. Kerowgan, A novel microplate agglutination method for blood grouping and reverse typing without the need for centrifugation, *Transfusion* 41 (2001) 627-632.
- [22] F. Llopis, F. Carbonell-Uberos, M.C. Montero, S. Bonanad, M.D. Planelles, I. Plasencia, C. Riol, T. Planells, C. Carrillo, A. De Miguel, A new method for phenotyping red blood cells using microplates, *Vox Sanguinis* 77 (1999) 143-148.
- [23] J.H. Spindler, H. Kluter, M. Kerowgan, A novel microplate agglutination method for blood grouping and reverse typing without the need for centrifugation, *Transfusion* 41 (2001) 627-632.
- [24] Y. Lapierre, D. Rigal, J. Adam, D. Josef, F. Meyer, S. Greber, C. Drot, The gel test - a new way to detect red-cell antigen-antibody reactions, *Transfusion* 30 (1990) 109-113.
- [25] B.H. Estridge, A.P. Reynolds, N.J. Walters, *Basic medical laboratory techniques*, 4th ed., Cengage Learning, Albany, NY, USA, 2000.
- [26] J.-D. Tissot, C. Kiener, B. Burnand, P. Schneider, The direct antiglobulin test: still a place for the tube technique?, *Vox Sanguinis* 77 (1999) 223-226.
- [27] M.N. Crawford, F.E. Gottman, C.A. Gottman, Microplate system for routine use in blood bank laboratories, *Transfusion* 10 (1970) 258-263.

- [28] F. Llopis, F. Carbonell-Uberos, M.D. Planelles, M. Montero, N. Puig, T. Atienza, E. Alba, J.A. Montoro, A monolayer coagglutination microplate technique for typing red blood cells, *Vox Sanguinis* 72 (1997) 26-30.
- [29] M.M. Langston, J.L. Procter, K.M. Cipolone, D.F. Stroncek, Evaluation of the gel system for ABO grouping and D typing, *Transfusion* 39 (1999) 300-305
- [30] D. Harmening, *Modern blood banking and transfusion practices*, 4th ed., F.A. Davis, Philadelphia, PA, 1999.
- [31] D.J. Anstee, Red cell genotyping and the future of pretransfusion testing, *Blood* 114 (2009) 248-256.
- [32] J.D. Roback, S. Barclay, C.D. Hillyer, An automatable format for accurate immunohematology testing by flow cytometry, *Transfusion* 43 (2003) 918-927.
- [33] M.M. Strumia, W.H. Crosby, J.G. Gibson, T.G. Greenwalt, J.R. Krevans, General principles of blood transfusion, *Transfusion* 3 (1963) 303-346.
- [34] P. Yager, T. Edwards, E. Fu, K. Helton, K. Nelson, M. Tam, B. Weigl, Microfluidic diagnostic technologies for global public health, *Nature* 442 (2006) 412-418.
- [35] R.N. Peeling, D. Mabey, Point-of-care Tests for Diagnosing Infections in the Developing World, *European society of clinical microbiology and infectious Diseases* 16 (2010) 1062-1069.
- [36] P. Yager, G.J. Domingo, J. Gerdes, Point-of-care diagnostics for global health, *Annual Review of Biomedical Engineering* 10 (2008) 107-144.
- [37] H. Kettler, K. White, S. Hawkes, Mapping the landscape of diagnostics for sexually transmitted infections, 2004.
- [38] M. Urdea, S.S. Penny, M.Y. Olmsted, P. Giovanni, A. Kaspar, P. Shepherd, C.A. Wilson, S. Dahl, G. Buchsbaum, D.C. Moeller, H. Burgess, Requirements for high impact diagnostics in the developing world, *Nature* 444 S1 (2006) 73-79.
- [39] A.W. Martinez, S.T. Phillips, G.M. Whitesides, E. Carrilho, Diagnostics for the developing world: microfluidic paper-based analytical devices, *Analytical Chemistry* 82 (2010) 3-10.
- [40] C.D. Chin, T. Laksanasopin, Y.K. Cheung, D. Steinmiller, V. Linder, H. Parsa, J. Wang, H. Moore, R. Rouse, G. Umviligihozo, E. Karita, L. Mwambarangwe, S.L. Braunstein, J. van de Wijgert, R. Sahabo, J.E. Justman, W. El-Sadr, S.K. Sia, Microfluidics-based diagnostics of infectious diseases in the developing world, *Nat Med* 17 (2011) 1015-1019.

- [41] M. Bajpai, R. Kaur, E. Gupta, Automation in immunohematology, *Asian Journal of Transfusion Science* 6 (2012) 140-144.
- [42] B.A. Myhre, D. McRuer, Human error—a significant cause of transfusion mortality, *Transfusion* 40 (2000) 879-885.
- [43] B.R. Fastman, H.S. Kaplan, Errors in transfusion medicine: have we learned our lesson?, *Mount Sinai Journal of Medicine: A Journal of Translational and Personalized Medicine* 78 (2011) 854-864.
- [44] J.V. Linden, B. Paul, K.P. Dressler, A report of 104 transfusion errors in New York State, *Transfusion* 32 (1992) 601-606.
- [45] G.M. Whitesides, The origins and the future of microfluidics, *Nature* 442 (2006) 368-373.
- [46] P. Tabeling, *Introduction to Microfluidics*, Oxford University, New York, U.S.A., 2005.
- [47] X. Li, D.R. Ballerini, W. Shen, A perspective on paper-based microfluidics: current status and future trends, *Biomicrofluidics* 6 (2012) 11301-1130113.
- [48] J.S. Kilby, The integrated circuit's early history, *Proceedings of the IEEE* 88 (2000) 109-111.
- [49] J.C. McDonald, G.M. Whitesides, Poly(dimethylsiloxane) as a material for fabricating microfluidic devices, *Accounts of Chemical Research* 35 (2002) 491-499.
- [50] S. Vyawahare, A.D. Griffiths, C.A. Merten, Miniaturization and parallelization of biological and chemical assays in microfluidic devices, *Chemistry & Biology* 17 (2009) 1052-1065.
- [51] L. Brown, T. Koerner, J.H. Horton, R.D. Oleschuk, Fabrication and characterization of poly(methylmethacrylate) microfluidic devices bonded using surface modifications and solvents, *Lab on a Chip* 6 (2006) 66-73.
- [52] F. Zhou, M. Lu, W. Wang, Z.-P. Bian, J.-R. Zhang, J.-J. Zhu, Electrochemical immunosensor for simultaneous detection of dual cardiac markers based on a poly(dimethylsiloxane)-gold nanoparticles composite microfluidic chip: a proof of principle, *Clinical Chemistry* 56 (2010) 1701-1707.
- [53] M. Zhang, J. Wu, L. Wang, K. Xiao, W. Wen, A simple method for fabricating multi-layer PDMS structures for 3D microfluidic chips, *Lab on a Chip* 10 (2010) 1199-1203.

- [54] A. Piruska, I. Nikcevic, S.H. Lee, C. Ahn, W.R. Heineman, P.A. Limbach, C.J. Seliskar, The autofluorescence of plastic materials and chips measured under laser irradiation, *Lab on a Chip* 5 (2005) 1348-1354.
- [55] E.W.K. Young, E. Berthier, D.J. Guckenberger, E. Sackmann, C. Lamers, I. Meyvantsson, A. Huttenlocher, D.J. Beebe, Rapid Prototyping of Arrayed Microfluidic systems in polystyrene for cell-based assays, *Analytical Chemistry* 83 (2011) 1408-1417.
- [56] G. Mehta, J. Lee, W. Cha, Y.-C. Tung, J.J. Linderman, S. Takayama, Hard top soft bottom microfluidic devices for cell culture and chemical analysis, *Analytical Chemistry* 81 (2009) 3714-3722.
- [57] D.C. Duffy, J.C. McDonald, O.J.A. Schueller, G.M. Whitesides, Rapid prototyping of microfluidic systems in poly(dimethylsiloxane), *Analytical Chemistry* 70 (1998) 4974-4984.
- [58] J. West, M. Becker, S. Tombrink, A. Manz, Micro total analysis systems: Latest achievements, *Analytical Chemistry* 80 (2008) 4403-4419.
- [59] A. Arora, G. Simone, G.B. Salieb-Beugelaar, J.T. Kim, A. Manz, Latest Developments in micro total analysis systems, *Analytical Chemistry* 82 (2010) 4830-4847.
- [60] A. Manz, N. Graber, H.M. Widmer, Miniaturized total chemical analysis systems: A novel concept for chemical sensing, *Sensors and Actuators B: Chemical* 1 (1990) 244-248.
- [61] P.S. Dittrich, A. Manz, Lab-on-a-chip: microfluidics in drug discovery, *Nat Rev Drug Discov* 5 (2006) 210-218.
- [62] W.-C. Tian, E. Finehout, Current and future trends in microfluidics within biotechnology research, *Microfluidics for Biological Applications*, Springer US2009, pp. 385-411.
- [63] C.D. Chin, V. Linder, S.K. Sia, Lab-on-a-chip devices for global health: Past studies and future opportunities, *Lab on a Chip* 7 (2007) 41-57.
- [64] L. Gervais, E. Delamarche, Toward one-step point-of-care immunodiagnostics using capillary-driven microfluidics and PDMS substrates, *Lab on a Chip* 9 (2009) 3330-3337.
- [65] I.K. Dimov, L. Basabe-Desmonts, J.L. Garcia-Cordero, B.M. Ross, A.J. Ricco, L.P. Lee, Stand-alone self-powered integrated microfluidic blood analysis system (SIMBAS), *Lab on a Chip* 11 (2011) 845-850.



- [66] E. Aguilera-Herrador, M. Cruz-Vera, M. Valcárcel, Analytical connotations of point-of-care testing, *Analyst* 135 (2010) 2220-2232.
- [67] M. Ek, G. Gellerstedt, G. Henriksson, *Paper Chemistry and Technology*, Walter de Gruyter, Germany, 2009.
- [68] M. Ek, G. Gellerstedt, G. Henriksson, *Pulping Chemistry and Technology*, Walter de Gruyter, Berlin, Germany, 2009.
- [69] C.J. Biermann, *Handbook of Pulping and Papermaking*, Second Edition ed., Academic Press 1996.
- [70] M. Ek, G. Gellerstedt, G. Henriksson, *Wood Chemistry and Wood Biotechnology*, Walter de Gruyter, Berlin, Germany, 2009.
- [71] U. Höke, S. Schabel, *Recycled fibre and deinking*, WS Bookwell Oy, Porvoo, Finland, 2010.
- [72] B. Lönnberg, *Mechanical pulping*, WS Bookwell Oy, Porvoo, Finland 2010.
- [73] P. Fardim, *Chemical Pulping Part 1, Fibre Chemistry and Technology*, WS Bookwell Oy, Porvoo, Finland, 2010.
- [74] H.U. Seuss, *Pulp Bleaching Today*, Walter de Gruyter, Berlin, Germany, 2010.
- [75] H. Paulapuro, *Papermaking Part 1, Stock Preparation and Wet End*, WS Bookwell Oy, Porvoo, Finland, 2010.
- [76] M. Karlsson, *Papermaking Part 2, Drying*, WS Bookwell, Porvoo, Finland, 2010.
- [77] P. Stenius, *Forest Products Chemistry*, WS Bookwell, Porvoo, Finland, 2010.
- [78] R. Alén, *Papermaking Chemistry*, WS Bookwell, Porvoo, Finland, 2010.
- [79] J. Paltakari, *Pigment Coating and Surface Sizing of Paper*, WS Bookwell, Porvoo, Finland, 2010.
- [80] M. Ek, G. Gellerstedt, G. Henriksson, *Paper Products Physics and Technology*, Walter de Gruyter, Germany, 2009.
- [81] N. Kaarlo, *Paper Physics*, WS Bookwell Oy, Porvoo, Finland, 2010.
- [82] A.K. Yetisen, M.S. Akram, C.R. Lowe, Paper-based microfluidic point-of-care diagnostic devices, *Lab on a Chip* 13 (2013) 2210-2251.
- [83] E.W. Washburn, The dynamics of capillary flow, *Physical Review* 17 (1921) 273-283.
- [84] P. Lisowski, P.K. Zarzycki, Microfluidic paper-based analytical devices (mu PADs) and micro total analysis systems (mu TAS): Development, applications and future trends, *Chromatographia* 76 (2013) 1201-1214.

- [85] L. Li, X. Huang, W. Liu, W. Shen, Control performance of paper-based blood analysis devices through paper structure design, *ACS Applied Materials & Interfaces* 6 (2014) 21624-21631.
- [86] M.J. Moura, P.J. Ferreira, M.M. Figueiredo, The use of mercury intrusion porosimetry to the characterization of eucalyptus wood, pulp and paper, *Iberoamerican Congress on Pulp and Paper Research* São Paulo, Brasil, 2002.
- [87] S.-C. Tseng, C.-C. Yu, D. Wan, H.-L. Chen, L.A. Wang, M.-C. Wu, W.-F. Su, H.-C. Han, L.-C. Chen, Eco-friendly plasmonic sensors: Using the photothermal effect to prepare metal nanoparticle-containing test papers for highly sensitive colorimetric detection, *Analytical Chemistry* 84 (2012) 5140-5145.
- [88] S.M.Z. Hossain, C. Ozimok, C. Sicard, S. Aguirre, M.M. Ali, Y. Li, J. Brennan, Multiplexed paper test strip for quantitative bacterial detection, *Anal Bioanal Chem* 403 (2012) 1567-1576.
- [89] Z.H. Nie, F. Deiss, X.Y. Liu, O. Akbulut, G.M. Whitesides, Integration of paper-based microfluidic devices with commercial electrochemical readers, *Lab on a Chip* 10 (2010) 3163-3169.
- [90] J.L. Delaney, C.F. Hogan, J. Tian, W. Shen, Electrogenenerated chemiluminescence detection in paper-based microfluidic sensors, *Analytical Chemistry* 83 (2011) 1300-1306.
- [91] B. Li, W. Zhang, L. Chen, B. Lin, A fast and low-cost spray method for prototyping and depositing surface-enhanced Raman scattering arrays on microfluidic paper based device, *Electrophoresis* 34 (2013) 2162-2168.
- [92] W.W. Yu, I.M. White, Inkjet printed surface enhanced Raman spectroscopy array on cellulose paper, *Analytical Chemistry* 82 (2010) 9626-9630.
- [93] J.P. Comer, Semiquantitative specific test paper for glucose in urine, *Analytical Chemistry* 28 (1956) 1748-1750.
- [94] P. von Lode, Point-of-care Immunotesting: Approaching the Analytical performance of central laboratory methods, *Clinical Biochemistry* 38 (2005) 591-606.
- [95] A.W. Martinez, S.T. Phillips, M.J. Butte, G.M. Whitesides, Patterned paper as a platform for inexpensive, low-volume, portable bioassays, *Angewandte Chemie International Edition* 46 (2007) 1318-1320.

- [96] A.W. Martinez, S.T. Phillips, G.M. Whitesides, Three-dimensional microfluidic devices fabricated in layered paper and tape, *Proceedings of the National Academy of Sciences* 105 (2008) 19606-19611
- [97] S. Klasner, A. Price, K. Hoeman, R. Wilson, K. Bell, C. Culbertson, paper-based microfluidic devices for analysis of clinically relevant analytes present in Urine and Saliva *Anal Bioanal Chem* 397 (2010) 1821-1829.
- [98] D.A. Bruzewicz, M. Reches, G.M. Whitesides, Low-cost printing of poly(dimethylsiloxane) barriers to define microchannels in paper, *Analytical Chemistry* 80 (2008) 3387-3392.
- [99] Y. Lu, W. Shi, L. Jiang, J. Qin, B. Lin, Rapid prototyping of paper-based microfluidics with wax for low-cost, portable bioassay, *ELECTROPHORESIS* 30 (2009) 1497-1500.
- [100] X. Li, J. Tian, G. Garnier, W. Shen, Fabrication of paper-based microfluidic sensors by printing, *Colloids and Surfaces B: Biointerfaces* 76 (2010) 564-570.
- [101] J. Olkkonen, K. Lehtinen, T. Erho, Flexographically printed fluidic structures in paper, *Analytical Chemistry* 82 (2010) 10246-10250.
- [102] K. Abe, K. Kotera, K. Suzuki, D. Citterio, Inkjet-printed paper fluidic immuno-chemical Sensing Device, *Anal Bioanal Chem* 398 (2010) 885-893.
- [103] K. Abe, K. Suzuki, D. Citterio, Inkjet-printed microfluidic multianalyte chemical sensing paper, *Analytical Chemistry* 80 (2008) 6928-6934.
- [104] T. Songjaroen, W. Dungchai, O. Chailapakul, C.S. Henry, W. Laiwattanapaisal, Blood separation on microfluidic paper-based analytical devices, *Lab on a Chip* 12 (2012) 3392-3398.
- [105] P.J. Bracher, M. Gupta, E.T. Mack, G.M. Whitesides, Heterogeneous films of ionotropic hydrogels fabricated from delivery templates of patterned paper, *ACS Applied Materials & Interfaces* 1 (2009) 1807-1812.
- [106] H. Liu, R.M. Crooks, Paper-based electrochemical sensing platform with integral battery and electrochromic read-out, *Analytical Chemistry* 84 (2012) 2528-2532.
- [107] A. Russo, B.Y. Ahn, J.J. Adams, E.B. Duoss, J.T. Bernhard, J.A. Lewis, Pen-on-paper flexible electronics, *Advanced Materials* 23 (2011) 3426-3430.
- [108] E.W. Nery, L.T. Kubota, Sensing approaches on paper-based devices: a review, *Anal Bioanal Chem* 405 (2013) 7573-7595.
- [109] D.D. Liana, B. Raguse, J.J. Gooding, E. Chow, Recent advances in paper-based sensors, *Sensors* 12 (2012) 11505.

- [110] M. Xu, B.R. Bunes, L. Zang, Paper-based vapor detection of hydrogen peroxide: colorimetric sensing with tunable interface, *ACS Applied Materials & Interfaces* 3 (2011) 642-647.
- [111] A.K. Ellerbee, S.T. Phillips, A.C. Siegel, K.A. Mirica, A.W. Martinez, P. Striehl, N. Jain, M. Prentiss, G.M. Whitesides, Quantifying colorimetric assays in paper-based microfluidic devices by measuring the transmission of light through paper, *Analytical Chemistry* 81 (2009) 8447-8452.
- [112] D.-S. Lee, B.G. Jeon, C. Ihm, J.-K. Park, M.Y. Jung, A simple and smart telemedicine device for developing regions: a pocket-sized colorimetric reader, *Lab on a Chip* 11 (2011) 120-126.
- [113] W. Dungchai, O. Chailapakul, C.S. Henry, Electrochemical detection for paper-based microfluidics, *Analytical Chemistry* 81 (2009) 5821-5826.
- [114] S. Ge, L. Ge, M. Yan, X. Song, J. Yu, J. Huang, A disposable paper-based electrochemical sensor with an addressable electrode array for cancer screening, *Chemical Communications* 48 (2012) 9397-9399.
- [115] P. Rattanarat, W. Dungchai, D.M. Cate, W. Siangproh, J. Volckens, O. Chailapakul, C.S. Henry, A microfluidic paper-based analytical device for rapid quantification of particulate chromium, *Analytica Chimica Acta* 800 (2013) 50-55.
- [116] L.Y. Shiroma, M. Santhiago, A.L. Gobbi, L.T. Kubota, Separation and electrochemical detection of paracetamol and 4-aminophenol in a paper-based microfluidic device, *Analytica Chimica Acta* 725 (2012) 44-50.
- [117] A. Apilux, W. Dungchai, W. Siangproh, N. Praphairaksit, C.S. Henry, O. Chailapakul, Lab-on-paper with dual electrochemical/colorimetric detection for simultaneous determination of gold and iron, *Analytical Chemistry* 82 (2010) 1727-1732.
- [118] C.-z. Li, K. Vandenberg, S. Prabhulkar, X. Zhu, L. Schneper, K. Methee, C.J. Rosser, E. Almeida, Paper based point-of-care testing disc for multiplex whole cell bacteria analysis, *Biosensors and Bioelectronics* 26 (2011) 4342-4348.
- [119] B.A. Rohrman, R.R. Richards-Kortum, A paper and plastic device for performing recombinase polymerase amplification of HIV DNA, *Lab on a Chip* 12 (2012) 3082-3088.
- [120] E. Fu, T. Liang, P. Spicar-Mihalic, J. Houghtaling, S. Ramachandran, P. Yager, Two-dimensional paper network format that enables simple multistep assays for

- use in low-resource settings in the context of malaria antigen detection, *Analytical Chemistry* 84 (2012) 4574-4579.
- [121] B. Veigas, J.M. Jacob, M.N. Costa, D.S. Santos, M. Viveiros, J. Inacio, R. Martins, P. Barquinha, E. Fortunato, P.V. Baptista, Gold on paper-paper platform for Au-nanoprobe TB detection, *Lab on a Chip* 12 (2012) 4802-4808.
- [122] N. Ratnarathorn, O. Chailapakul, C.S. Henry, W. Dungchai, Simple silver nanoparticle colorimetric sensing for copper by paper-based devices, *Talanta* 99 (2012) 552-557.
- [123] M. Zhang, L. Ge, S. Ge, M. Yan, J. Yu, J. Huang, S. Liu, Three-dimensional paper-based electrochemiluminescence device for simultaneous detection of  $Pb^{2+}$  and  $Hg^{2+}$  based on potential-control technique, *Biosensors and Bioelectronics* 41 (2013) 544-550.
- [124] J. Yu, L. Ge, J. Huang, S. Wang, S. Ge, Microfluidic paper-based chemiluminescence biosensor for simultaneous determination of glucose and uric acid, *Lab on a Chip* 11 (2011) 1286-1291.
- [125] M.M. Ali, S.D. Aguirre, Y.Q. Xu, C.D.M. Filipe, R. Pelton, Y.F. Li, Detection of DNA using bioactive paper strips, *Chemical Communications* (2009) 6640-6642.
- [126] M. Funes-Huacca, A. Wu, E. Szepesvari, P. Rajendran, N. Kwan-Wong, A. Razgulin, Y. Shen, J. Kagira, R. Campbell, R. Derda, Portable self-contained cultures for phage and bacteria made of paper and tape, *Lab on a Chip* 12 (2012) 4269-4278.
- [127] J. Noiphung, K. Talalak, I. Hongwarittorn, N. Pupinyo, P. Thirabowonkitphithan, W. Laiwattanapaisal, A novel paper-based assay for the simultaneous determination of Rh typing and forward and reverse ABO blood groups, *Biosensors and Bioelectronics* 67 (2015) 485-489.
- [128] L. Guan, R. Cao, J. Tian, H. McLiesh, G. Garnier, W. Shen, A preliminary study on the stabilization of blood typing antibodies sorbed into paper, *Cellulose* 21 (2014) 717-727.
- [129] J. Su, M. Al-Tamimi, G. Garnier, Engineering paper as a substrate for blood typing bio-diagnostics, *Cellulose* 19 (2012) 1749-1758.
- [130] W. Ehrfeld, V. Hessel, H. Löwe, State of the Art of Microreaction Technology, *Microreactors*, Wiley-VCH Verlag GmbH & Co. KGaA2004, pp. 1-14.
- [131] A. Šalić, A. Tušek, B. Zelić, Application of microreactors in medicine and biomedicine, *Journal of Applied Biomedicine* 10 (2012) 137-153.

- [132] L. Licklider, W.G. Kuhr, Optimization of online peptide mapping by capillary zone electrophoresis, *Analytical Chemistry* 66 (1994) 4400-4407.
- [133] J.-i. Yoshida, A. Nagaki, T. Yamada, Flash chemistry: Fast chemical synthesis by using microreactors, *Chemistry – A European Journal* 14 (2008) 7450-7459.
- [134] J. Pelleter, F. Renaud, Facile, Fast and safe process development of nitration and bromination reactions using continuous flow reactors, *Organic Process Research & Development* 13 (2009) 698-705.
- [135] X. Zhang, S. Stefanick, F.J. Villani, Application of microreactor technology in process development, *Organic Process Research & Development* 8 (2004) 455-460.
- [136] P. Watts, S.J. Haswell, Microfluidic combinatorial chemistry, *Current Opinion in Chemical Biology* 7 (2003) 380-387.
- [137] J. El-Ali, P.K. Sorger, K.F. Jensen, Cells on chips, *Nature* 442 (2006) 403-411.
- [138] D. Gerber, S.J. Maerkl, S.R. Quake, An in vitro microfluidic approach to generating protein-interaction networks, *Nat Meth* 6 (2009) 71-74.
- [139] J.P. McMullen, K.F. Jensen, W. P, H. SJ, Integrated microreactors for reaction automation: New approaches to reaction development microfluidic combinatorial chemistry, *Annual Review of Analytical Chemistry* 3 (2010) 19-42.
- [140] T. McCreedy, Fabrication techniques and materials commonly used for the production of microreactors and micro total analytical systems, *TrAC Trends in Analytical Chemistry* 19 (2000) 396-401.
- [141] R. Schenk, V. Hessel, C. Hofmann, J. Kiss, H. Löwe, A. Ziogas, Numbering-up of micro devices: a first liquid-flow splitting unit, *Chemical Engineering Journal* 101 (2004) 421-429.
- [142] J.C. Charpentier, Process intensification by miniaturization, *Chemical Engineering & Technology* 28 (2005) 255-258.
- [143] G.N. Doku, W. Verboom, D.N. Reinhoudt, A. van den Berg, On-microchip multiphase chemistry—a review of microreactor design principles and reagent contacting modes, *Tetrahedron* 61 (2005) 2733-2742.
- [144] X. Yao, Y. Zhang, L. Du, J. Liu, J. Yao, Review of the applications of microreactors, *Renewable and Sustainable Energy Reviews* 47 (2015) 519-539.
- [145] T. Young, An essay on the cohesion of fluids, *Philosophical Transactions of the Royal Society of London* 95 (1805) 65-87.

- [146] H.Y. Erbil, Surface Chemistry of Solid and Liquid Interfaces, Blackwell Publishing, India, 2006.
- [147] X. Hong, X.F. Gao, L. Jiang, Application of superhydrophobic surface with high adhesive force in no lost transport of superparamagnetic microdroplet, Journal of the American Chemical Society 129 (2007) 1478-+.
- [148] X. Zhang, F. Shi, J. Niu, Y. Jiang, Z. Wang, Superhydrophobic surfaces: from structural control to functional application, Journal of Materials Chemistry 18 (2008) 621-633.
- [149] X. Yao, Y. Song, L. Jiang, Applications of bio-inspired special wettable surfaces, Advanced Materials 23 (2011) 719-734.
- [150] R.N. Wenzel, Surface roughness and contact angle, The Journal of Physical and Colloid Chemistry 53 (1949) 1466-1467.
- [151] A.B.D. Cassie, S. Baxter, Wettability of porous surfaces, Transactions of the Faraday Society 40 (1944) 546-551.
- [152] P. Aussillous, D. Quere, Liquid marbles, Nature 411 (2001) 924-927.
- [153] L. Mahadevan, Non-stick water, Nature 411 (2001) 895-896.
- [154] D. Quéré, P. Aussillous, Non-stick droplets, Chemical Engineering & Technology 25 (2002) 925-928.
- [155] A. Venkateswara Rao, M.M. Kulkarni, S.D. Bhagat, Transport of liquids using superhydrophobic aerogels, Journal of Colloid and Interface Science 285 (2005) 413-418.
- [156] E. Bormashenko, Liquid marbles: Properties and applications, Current Opinion in Colloid & Interface Science 16 (2011) 266-271.
- [157] J. Tian, T. Arbatan, X. Li, W. Shen, Liquid marble for gas sensing, Chemical Communications 46 (2010) 4734-4736.
- [158] Y. Zhao, J. Fang, H. Wang, X. Wang, T. Lin, Magnetic liquid marbles: Manipulation of liquid droplets using highly hydrophobic Fe<sub>3</sub>O<sub>4</sub> nanoparticles, Advanced Materials 22 (2010) 707-710.
- [159] P.S. Bhosale, M.V. Panchagnula, On synthesizing solid polyelectrolyte microspheres from evaporating liquid marbles, Langmuir 26 (2010) 10745-10749.
- [160] E. Bormashenko, R. Pogreb, Y. Bormashenko, A. Musin, T. Stein, New investigations on ferrofluidics: Ferrofluidic marbles and magnetic-field-driven drops on superhydrophobic surfaces, Langmuir 24 (2008) 12119-12122.

- [161] E. Bormashenko, A. Musin, Revealing of water surface pollution with liquid marbles, *Applied Surface Science* 255 (2009) 6429-6431.



---

## **Part I**

### ***Mechanisms of Paper-Based Blood Typing Devices***

---

In recent years, great efforts have been made in innovations in the use of bioactive paper to perform blood typing assays. These paper-based blood typing devices not only make blood typing more accessible in developing regions, but also provide people of developed countries with an easier and cheaper way to perform blood typing in circumstances where hospitals and pathological laboratories are not available. Nonetheless, many basic mechanisms of blood typing based on bioactive paper are still unclear, such as the agglutination, immobilization and transport of red blood cells within the fibre matrix in paper, as well as the effect of paper's physical structure on red blood cell behaviour in paper. A clear understanding of these fundamental mechanisms is critically important for bioactive paper design and the scaled-up production of paper-based blood typing devices that meet ASSURED criteria. Therefore, the first part of this thesis aims to provide a clear understanding of the behaviour of red blood cells inside paper.

In this part, novel microscopic methods, namely the confocal technique and the FIB-SEM technique, have been developed for the investigation of RBC agglutination, immobilization and transport mechanisms within paper. The confocal microscopic method is a relatively simple method, which is able to study the final state of RBC distribution within paper. The FIB-SEM technique is more advantageous for capturing the details of RBCs at any certain moment during the process of blood penetration into paper. The use of microscopic tools enables us to study the details of RBCs at the cellular level inside the fibre network of paper and obtain further scientific evidence to establish the agglutination, immobilization and transport mechanisms of RBCs within paper.

Furthermore, the research in this part has, for the first time, shown the possibility that we can control the performance of paper-based blood typing devices through paper structure design. This research has also investigated the mechanism of how paper structure affects the performance of paper-based blood typing devices. This mechanism specifically lays important foundations for the scaled-up production of paper-based blood typing devices.

The findings in this part are not only essential for the future design of more sophisticated paper-based blood typing devices with high sensitivity and assaying speed, but also important for the development of other paper-based blood analysis devices.

**This page is intentionally blank**

---

## **Chapter 2**

*A Study of the Transport and Immobilisation  
Mechanisms of Human Red Blood Cells in a  
Paper-Based Blood Typing Device Using Confocal  
Microscopy*

---

**This page is intentionally blank**

## Monash University

### Declaration for Thesis Chapter 2

#### Declaration by candidate

In the case of Chapter 2, the nature and extent of my contribution to the work was the following:

Nature of contribution	Extent of contribution (%)
Initiation, key ideas, experimental works, analysis of results, writing up	70

The following co-authors contributed to the work. If co-authors are students at Monash University, the extent of their contribution in percentage terms must be stated:

Name	Nature of contribution	Extent of contribution (%) for student co-authors only
Junfei Tian	Assisted in experimentation, paper reviewing and editing	10
David Ballerini	Assisted in experimentation, paper reviewing and editing	5
Miaosi Li	Assisted in experimentation	5
Wei Shen	Key ideas, reviewing and editing of the paper	Supervisor

The undersigned hereby certify that the above declaration correctly reflects the nature and extent of the candidate's and co-authors' contributions to this work\*.

**Candidate's  
Signature**

	<b>Date</b> 25-Sep-2015
--	----------------------------

**Main  
Supervisor's  
Signature**

	<b>Date</b> 25-Sep-2015
---	----------------------------

\*Note: Where the responsible author is not the candidate's main supervisor, the main supervisor should consult with the responsible author to agree on the respective contributions of the authors.

**This page is intentionally blank**



# **A Study of the Transport and Immobilisation Mechanisms of Human Red Blood Cells in a Paper- Based Blood Typing Device Using Confocal Microscopy**

*Lizi Li, Junfei Tian, David Ballerini, Miaosi Li and Wei Shen\**

Department of Chemical Engineering,  
Monash University, Clayton Campus, Vic. 3800, Australia

\*  


This paper has been published in *Analyst*

## **2.1 ABSTRACT**

Recent research on the use of bioactive paper for human blood typing has led to the discovery of a new method for identifying the haemagglutination of red blood cells (RBCs). When a blood sample is introduced onto paper treated with the grouping antibodies, RBCs undergo haemagglutination with the corresponding grouping antibodies, forming agglutinated cell aggregates in the paper. A subsequent washing of the paper with saline buffer could not remove these aggregates from the paper; this phenomenon provides a new method for rapid, visual identification of the antibody-specific haemagglutination reactions and thus the determination of the blood type. This study aims to understand the mechanism of RBC immobilization inside the paper which follows haemagglutination reactions. Confocal microscopy is used to observe the morphology of the free and agglutinated RBCs that are labelled with FITC. Chromatographic elution patterns of both agglutinated and non-agglutinated RBCs are studied to gain insight into the transport behaviour of free RBCs and agglutinated aggregates. This work provides new information about RBC haemagglutination inside the fibre network of paper on a microscopic level, which is important for the future design of paper-based blood typing devices with high sensitivity and assaying speed.

### 2.2 KEYWORDS

Paper-based diagnostic device, blood typing, immobilisation mechanisms, red blood cells, confocal microscopy

### 2.3 INTRODUCTION

Accurate and rapid determination of human blood groups is imperative for many medical procedures such as blood transfusion and organ transplantation [1]. Blood groups are classified based on inherited differences (polymorphisms) in antigens on the surface of the red blood cells (erythrocytes). The International Society of Blood Transfusion (ISBT) recognises 328 different antigens and 30 major blood group systems, among which the ABO and Rhesus systems are of the greatest clinical importance [2]. Without ABO compatibility testing, around one third of unscreened blood transfusions would lead to potentially fatal haemolytic transfusion reactions. The RBC antigen D of the Rh system is considered to be the most common culprit, also causing haemolytic disease of the foetus and in newborns (HDFN) [2].

The majority of techniques for determining ABO and Rh blood type are based on the principle of observing haemagglutination between RBC antigens and serum antibodies. Haemagglutination occurs when multi-armed antibodies bind to the particular binding sites on the antigens of RBCs, adhering cells together and leading to the formation of larger blood lumps that cannot be stably suspended in the plasma. Currently, the most common assays used for the identification of blood group include the slide test, tube test, micro plate and solid phase assays, as well as the column agglutination system [3-8]. Recently, advanced blood typing assays based on gene sequencing of DNA [9, 10] and flow cytometry [11] have been reported. Blood typing assays that are currently used in hospitals and pathological laboratories are capable of sensitively and specifically identify blood types; they are reliable and robust [12]. However, few point-of-care assays can be done without either dedicated laboratory instruments or the direct handling of the antibodies by the personnel who carry out the tests (such as the slide and tube tests) [13, 14]. In addition, the equipment-based assays usually take a long

time (10-30min), and the costs are high [7, 12]. A disadvantage common to all blood typing assays is that it is difficult for non-professionals and lay-users to interpret the assay result, since currently available blood typing devices require users to have some knowledge of blood typing and an understanding of device working principle. It follows that the availability of simple, rapid, cheap, and reliable methods for blood typing would be of significant benefit for point-of-care applications, such as bedside compatibility checks, fast blood typing in emergency scenarios, and in developing regions or remote locations where there may be no access to laboratory facilities [14].

Paper is a material fabricated by cellulosic fibre, which is easy-accessible, recyclable, environmental and low-cost [15]. The promising use of paper for environmental and diagnostic applications has been strongly highlighted [16-18]. Recently, innovations in the use of bioactive paper to perform blood typing assays have been reported in the literature [14, 19-21]; these innovations are based on a new mechanism for identifying haemagglutination. Khan et al. [19] found that agglutinated blood samples resulting from antibody-specific haemagglutination reactions transport differently in the porous structure of paper than stable blood samples with well dispersed red cells. They observed that agglutinated RBCs in paper could not be eluted chromatographically by the wicking of blood serum. This observation marked the discovery of a new blood typing method which relies on the visual identification of red cell transport behaviour in paper which led to a new concept for fabricating low-cost blood typing devices. Following work by Ballerini et al. [22] showed that the same principle could be used to fabricate inexpensive thread-based blood typing devices.

Jarujamrus et al. [20] investigated the separation of the agglutinated RBCs from the blood serum phase in filter paper. They took a biochemical approach and analysed the amount of antibody that could be washed off from an antibody-treated filter paper. Their hypothesis was that a blood sample introduced onto a piece of antibody-treated paper could re-dissolve a fraction of antibody deposited and dried on the fibre surface. The re-dissolved antibody molecules could then engage in specific interactions with the RBCs, leading to haemagglutination within paper. Jarujamrus et al. [20] showed that between 34 to 42% of antibody molecules carried by the antibody-treated paper could be re-dissolved by saline solution or a blood sample. Al-Tamimi et al. [14] reported a

chromatographic elution technique for blood typing. Their results showed that agglutinated RBCs in paper were immobilised within the paper structure and could not be eluted by saline solution, while non-agglutinated RBCs could be eluted easily. Their results again showed that agglutinated RBC lumps inside the paper have drastically different transport behaviour from non-agglutinated RBCs (Figure 1). Al-Tamimi et al. [14] and Su et al. [23] have also shown that the efficiency of chromatographic separation of agglutinated and non-agglutinated RBCs on paper could be increased by controlling the thickness and porosity of the paper.

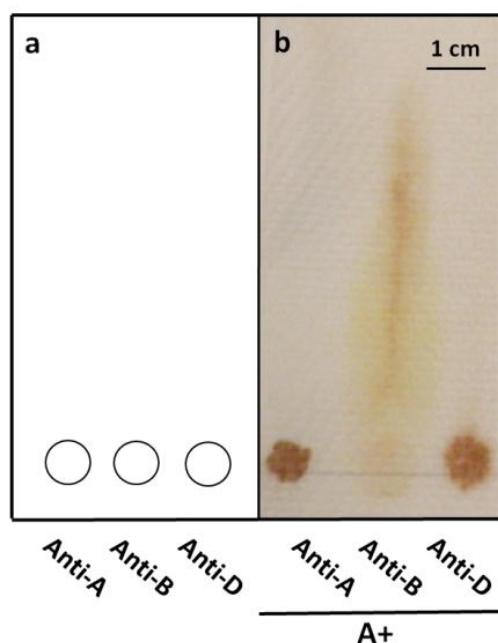


**Figure 1.** An example of paper-based assay for rapid blood typing. (a) A schematic diagram of the anti-body treated paper. (b) An actual test result of blood A+.[14]

More recently, Li et al. [21] applied this difference in transport behaviour between agglutinated and non-agglutinated RBCs in paper to design the first text-reporting blood typing device. This design presented a new concept of adding grouping antibodies onto paper which had printed patterns of text and symbols (i.e. to dose anti-A into the printed text pattern “A”). If the RBCs of a blood sample undergo haemagglutination reaction due to anti-A in the text pattern “A”, agglutination of RBCs would occur inside the patterned “A” zone; the deep crimson red colour formed by the agglutinated RBCs could not be washed away by saline solution and the paper will report the blood type of this sample with a letter “A” formed by the colouring effect of

the agglutinated RBCs. This design enables non-professional users who may not have the knowledge of blood typing to identify blood types; it is suitable for developing countries where trained medical professionals may not be always available. The text-reporting blood typing concept using bioactive paper has since been explored by the diagnostic industry as a new class of sensitive, rapid and user-friendly device.

In this study we focus on understanding the mechanism of haemagglutination-induced immobilization of RBCs in antibody-treated bioactive paper. Microscopic evidence will be sought to understand: (a) The morphology of the non-agglutinated RBCs in the fibre network of paper; (b) the morphology, size and distribution of agglutinated RBC aggregates formed after haemagglutination in the fibre network and (c) the transport behaviour of individual RBCs and large agglutinated RBC lumps driven by the wicking saline solution in paper. Confocal microscopy is used to observe RBC and agglutinated RBC lumps in the fibre network of paper. The results of this study revealed details of RBC agglutination inside the fibre network of paper with clarification on a cellular level. The immobilisation mechanism of the agglutinated RBC lumps inside the paper is established. Information obtained from this study will be used to guide future device designs, particularly the design of the paper structures suitable for the low-cost blood typing papers.

## **2.4 EXPERIMENTAL**

### **2.4.1 Materials**

Anti-coagulated blood samples were acquired from adult volunteers of known blood group by Dorevitch Pathology, Australia. All blood samples were stored in Vacutainer® tubes containing heparin, citrate and EDTA at 4 °C, and used within 5 days of collection. Epiclone™ anti-A, anti-B and anti-D monoclonal grouping reagents were sourced commercially from the Commonwealth Serum Laboratory, Australia. Anti-A and anti-B are transparent solutions, coloured cyan and yellow respectively, while anti-D is a clear colourless solution. Monoclonal grouping reagents were also kept at 4 °C. Kleenex paper towel with a basis weight of 34 g/m<sup>2</sup> and thickness of 140 µm was purchased from Kimberly-Clark, Australia. Analytical grades of NaCl, KCl,

$\text{Na}_2\text{HPO}_4$ , and  $\text{KH}_2\text{PO}_4$  were obtained from Sigma-Aldrich and used for preparation of physiological salt solution (PSS) and phosphate-buffered physiological salt solution (PBS, pH 7.4). Fluorescein isothiocyanate (FITC, isomer I, Product number: F7250) from Sigma-Aldrich was used for labelling RBCs. Anhydrous dimethyl sulphoxide (DMSO, from MERCK Chemicals Ltd, Australia) was employed to dissolve the FITC. Anhydrous D-glucose was provided by AJAX Chemicals Ltd., Australia. Microscope immersion oil was purchased from Sigma-Aldrich, Germany.

### 2.4.2 Methods

Red blood cells were labelled using the methods reported by Hauck et al. [24] and Hudetz et al. [25]. Firstly, whole blood was centrifuged at 800 r/min for 10 minutes and the plasma layer was removed. The red cells collected from the bottom of the centrifuge tube were then washed in PSS and incubated in PBS with D-glucose (0.5 mg/ml) and FITC (0.4 mg/ml) for 3 hours. The labelled cells were then washed in PSS twice and re-suspended at a hematocrit of 45%. The testing papers were prepared by adding 10  $\mu\text{L}$  of antibody solution onto 10 mm  $\times$  10 mm squares of Kleenex paper towel and allowing the antibody to penetrate and dry for 1 minute. In order to form the agglutinated blood lumps inside the paper sheet, 8  $\mu\text{L}$  of labelled and re-suspended blood sample was pipetted onto the paper from the opposite side to which the antibody was introduced. Thirty seconds were given for the interaction between RBCs and the antibody within paper. After that, the sample was placed onto a glass slide for confocal imaging. The microscopic images were recorded from the side which the blood was introduced into. A Nikon Ai1Rsi Confocal Microscope in the facilities at the Melbourne Centre for Nanofabrication was used for generating the confocal micrographs. The objective lenses employed for imaging were 20 $\times$  dry lens and 60 $\times$  oil immersion lens. Images of red blood cells within the antibody-treated paper were captured as x-y images or a series of x-y images with stepped variation in the z-direction for construction of 3D images (or z-stack images). The resolution of all images was 1024 $\times$ 1024 pixels and step width for the z-stack images was 0.125~0.250  $\mu\text{m}$ .

In order to gain a better understanding of the transport behaviour of agglutinated and

non-agglutinated RBCs on paper, an experiment of chromatographic elution by PSS was performed. Briefly, 10  $\mu\text{L}$  of antibody solution and 3  $\mu\text{L}$  of blood sample were dropped on a glass slide and allowed to react for 30 seconds. The mixture of blood and antibody was then transferred from the glass slide onto a piece of Kleenex paper around 2 cm from the lower edge of the paper, and allowed to be absorbed completely for 1 minute. The Kleenex paper was then suspended in PSS in a chromatography tank about 1 cm from its lower edge to ensure the blood spot remained above the buffer surface and the saline solution was allowed to elute up through the paper by capillary wicking for 10 minutes. The paper was then allowed to dry at room temperature on a blotting paper for another 10 minutes and the elution patterns of RBCs were characterized by observing the presence of RBCs at different points away from the original blood sample spot with the confocal microscope.

## **2.5 RESULTS AND DISCUSSION**

### **2.5.1 Observation of Red Blood Cells in Paper Using Confocal Microscopy**

In this confocal microscopy study a 405 nm laser was used to observe the fibre network of the Kleenex paper. The excitation wavelength of this laser beam is able to generate fluorescent emission in the blue spectral region from lignocellulosic fibres of the Kleenex paper; the fluorescent emission enabled clear images of the fibre network in the paper to be generated at a satisfactory resolution. Figure 2a shows a 2D image from a single confocal scan of Kleenex paper sample. Figure 2b shows a 3D reconstruction of a series of 2D scans from the same paper sample; all scans were obtained using a 20 $\times$  dry lens. These results clearly show that the distribution of fibres in the Kleenex paper is even but random. The width of the lignocellulosic fibres which form the Kleenex paper is around 20  $\mu\text{m}$  to 30  $\mu\text{m}$ ; the spaces between these fibres form the porous structure of paper.

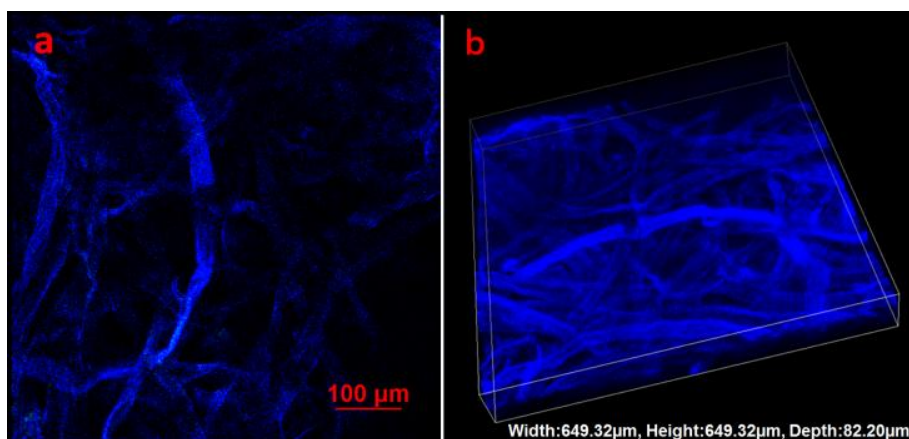


**Figure 2.** 2D (a) and 3D (b) confocal images of lignocellulosic fibres within paper captured by 20 $\times$  dry lens.

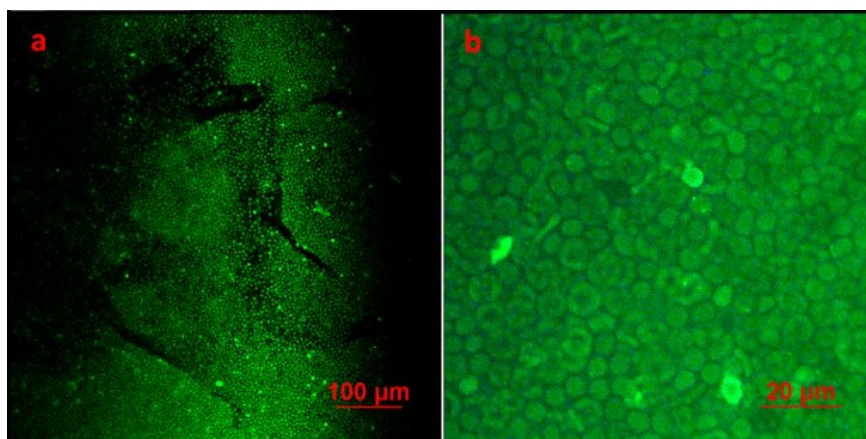


**Figure 3.** Confocal images of RBCs labelled with FITC within paper (a) and on slide glass (b) captured by 20 $\times$  dry lens.

Figures 3a and 3b show the FITC-labelled RBCs in the Kleenex paper and on top of a glass slide, respectively. FITC is widely used to attach a fluorescent label to proteins via the amine group. The isothiocyanate group in FITC reacts with amino terminals and primary amines in proteins. Isomer I of FITC was used in this study; it has the thiocyanate group on the fourth carbon of the benzene ring. This isomer has been reported to be suitable for labelling red blood cells [24, 25]. Our results in Figures 3a and 3b are in good agreement with those reports. Fluorescent emission spectrum is generated from the FITC-labelled red blood cells with a 488 nm laser line by the multiline argon-ion laser of the Nikon Ai1Rsi Confocal Microscope; this excitation wavelength is close to the absorption peak of FITC. As a result, the distribution of FITC-labelled RBCs in the porous structure of the paper can be clearly imaged by



confocal microscopy (Figure 3, by 20 $\times$  dry lens). Fortunately, the 488 nm laser line cannot excite fluorescent emission from the lignocellulosic fibres, therefore the fibre network of the paper appears in Figure 3a as dark spaces. Figure 3b shows enlarged confocal image of FITC-labelled RBCs observed using a 20 $\times$  dry lens on glass slide; it shows the morphology of RBCs after the FITC labelling. The RBCs retain the shape of centrally depressed disks, with diameters of 6-8  $\mu\text{m}$  and thickness of 2  $\mu\text{m}$ . These figures demonstrate that FITC-labelling of the RBCs does not change the morphology of the RBCs and that confocal microscopy is a suitable technique for obtaining detailed, cellular level information of RBC behaviour in paper made of lignocellulosic fibres. It is expected that, by combining the blue fluorescent emission signal from the fibre with the green fluorescent signal from the FITC-labelled red blood cells, a full picture of the RBCs in paper can be obtained.

### **2.5.2 The Activity of the Red Blood Cell Antigen after FITC Labelling**

The FITC labelling of the red blood cells does not have any noticeable effect on the activity of the RBC antigens on the surface of the red cells. This was confirmed by comparing the reactions of whole blood and FITC-labelled RBCs drawn from the same source with the corresponding antibodies on glass slides (results are not shown). Under the same assaying conditions, FITC labelling does not cause discernable differences in the sizes of the agglutinated RBC aggregates nor in the time required for the RBCs to agglutinate after contacting their corresponding antibodies.

### **2.5.3 Mechanisms of Red Blood Cell Immobilisation in Antibody-Treated Paper**

Figures 4a and 4b show the two-dimensional confocal micrographs of RBCs of type O+ introduced into a paper sample treated with anti-A reagent with 20 $\times$  dry lens and 60 $\times$  oil immersion lens respectively. These figures combine the signals from the lignocellulosic fibres in paper (blue) and the FITC-labelled RBCs (green), and provide a much clearer visual identification of positions of the RBCs within the fibre network. Since O+ red blood cells do not carry the A antigen, no haemagglutination is expected

to occur. Results in Figures 4a and 4b reveal the O+ RBCs distribute rather uniformly in the spaces of the fibre network of the paper treated with anti-A. Figure 4c shows a 3D confocal image of type O+ RBCs in paper treated with anti-A; it shows that red blood cells have penetrated through the fibre network and reached around the middle of the paper sheet. However, the RBCs remain free of any morphological change.

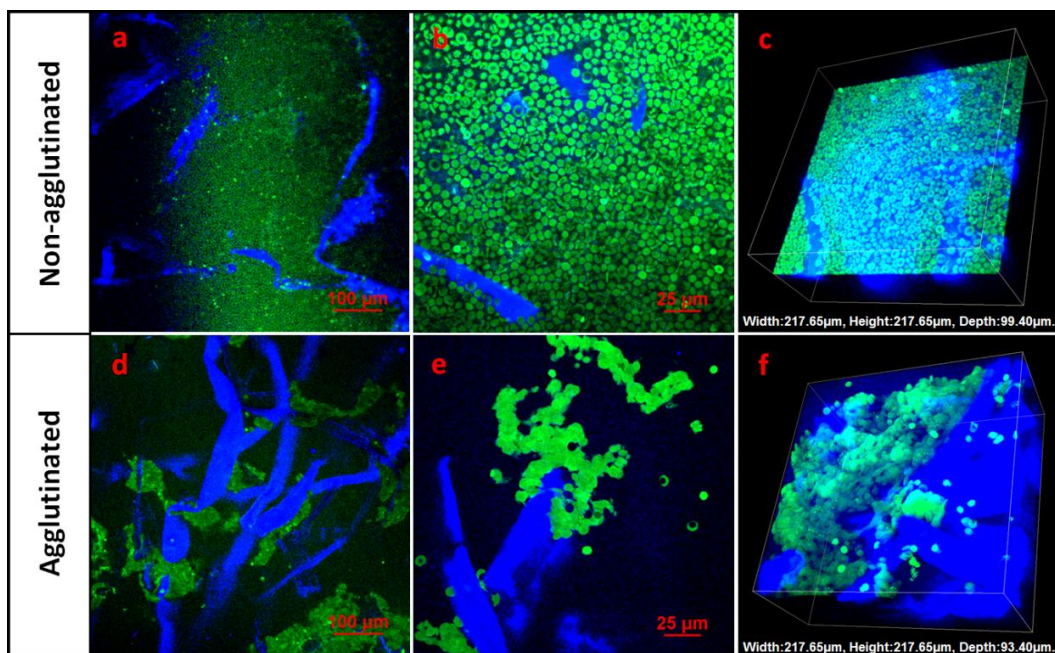


**Figure 4.** Confocal images of non-agglutinated and agglutinated RBCs within paper. (a) 2D image of non-agglutinated RBCs captured by 20 $\times$  dry lens. (b) 2D image of non-agglutinated RBCs captured by 60 $\times$  oil lens. (c) 3D image of non-agglutinated RBCs captured by 60 $\times$  oil lens; (d) 2D image of agglutinated RBCs captured by 20 $\times$  dry lens. (e) 2D image of agglutinated RBCs captured by 60 $\times$  oil lens. (f) 3D image of agglutinated RBCs captured by 60 $\times$  oil lens. The separate (non-combined) images of paper and labelled RBCs can be found in the Supporting Information.

Figures 4d and 4e show two examples of 2D confocal images acquired using 20 $\times$  dry and 60 $\times$  oil immersion lenses of type O+ RBCs in anti-D treated papers. Strong changes in both the RBC distributions in the fibre network and in cell morphology show the occurrence of haemagglutination of type O+ RBCs with anti-D.

Several observations may be made regarding the mechanisms of RBC haemagglutination inside paper. First, the sizes of agglutinated RBC lumps vary

significantly. Most lumps contain hundreds of RBCs, while others contain only a few. The bonding of antibody molecules with the RBCs appears to be strong, since some RBCs appear to have lost their natural disk-like shape when they become agglutinated. However, haemagglutination of RBCs does not cause massive haemolysis of the cells; this is supported by the observation that although cells formed aggregates, the profiles of cells can still be identified.

Second, many RBCs have moved toward one another during haemagglutination to form large lumps. The movement of red cells freed large areas of the fibre surface from cell coverage (Figures 4d and 4e). Figure 4f also shows that there are a few single red blood cells that apparently adhere to the fibre surface. This raises the possibility that some individual red cells could undergo interactions directly with the antibody molecules adsorbed on the fibre surface and become immobilised there. While this possibility does exist, the fibre surface coverage by such individual cells is small; these adsorbed, individual cells make negligible visual contribution to the assay result. These observations support the conclusion of a previous study by Jarujamrus et al. [20], who found that a significant fraction of antibody molecules introduced into an antibody-treated paper could be washed off from the fibre surface by saline solution or by the serum phase of a blood sample. Therefore the dominant mechanism of RBC agglutination inside an antibody-treated paper is through the haemagglutination caused by the released antibody molecules from the fibre surface.

Thirdly, the confocal results show that the major mechanism for the immobilisation of the agglutinated RBC lumps inside the fibre network is the strong adhesion of the lumps to the fibres and mechanical entrapment. Figures 4d, 4e and 4f show that large agglutinated RBC lumps of the dimension similar to those of the interfibre pores were formed inside the paper and the entrapment and adhesion of those lumps occurred mostly at the gaps and pores between fibres. These factors make the chromatographic elution of the lumps practically impossible. The confocal results are in full agreement with the conclusion by Al-Tamimi et al. [14]; they provide detailed microscopic evidence of the working mechanism of this new blood typing method using bioactive paper.

### **2.5.4 An Application Study of Blood Elution Patterns in Paper Using the Confocal Method**

One design of bioactive paper-based blood typing devices for identification of haemagglutination in paper is based on paper chromatography [14]. Grouping antibodies (anti-A, anti-B and anti-D) are first spotted at 2 cm above the bottom edge of a piece of Kleenex paper, then a blood sample is introduced onto the grouping antibody spot; the spot containing antibody and the blood sample is referred to as the “antibody & blood sample zone”. The Kleenex paper is then dipped into a chromatographic tank, with the bottom edge slightly submerged into the saline solution. The saline solution penetrates through the interfibre pores of the paper towel, wicking across spots of grouping antibodies and the blood samples within the spots. If haemagglutination occurs in the antibody spots, the agglutinated blood sample will not be eluted up by the rising saline solution. If haemagglutination does not occur, the blood sample will be eluted out of the grouping antibody spot, forming an elongated, visible chromatographic track of blood. The difference in the elution behaviours of the blood sample provides an easy and accurate method for the identification of the blood type [14].

In practice, however, two elution bands may be observed. The first band can be observed close to the wicking front of saline solution and the second band can be observed behind the first band. In some assays, these two bands could be observed simultaneously; in other assays only one could be observed. Figure 5 shows a schematic description of this phenomenon. Confocal microscopy was used to investigate the two bands to gain an understanding of this phenomenon.

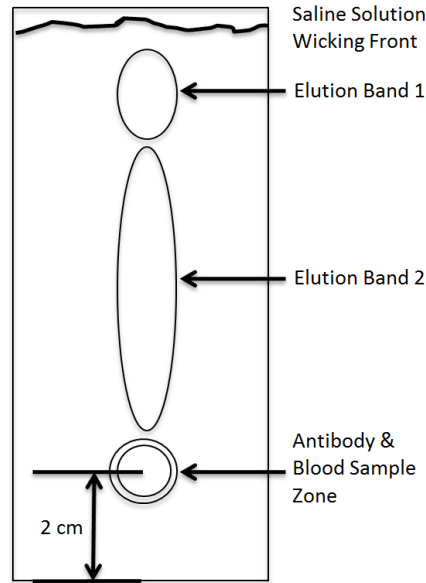


**Figure 5.** A schematic diagram of the observed elution bands of RBCs on antibody-treated paper.

In this study, FITC-labelled RBCs were used to perform the chromatographic elution blood typing assays. The FITC-labelled RBCs were first mixed with each of the grouping antibodies on separate glass slides to ensure complete reaction; the mixture of blood and antibody reagent was then spotted onto the Kleenex paper and chromatographic elution was begun. This procedure was adopted in this investigation because the two bands could be reproducibly observed in all assays. The chromatographic elution patterns of the A+ blood sample with anti-A, anti-B and anti-D, as well as the patterns of the B+ blood sample with the three antibodies are presented in Figure 6. In all negative assays two bands can be observed simultaneously; whereas in all positive assays only the first band can be observed.

For confocal microscopy investigation, samples of blood of type A+ and B+ reacting with anti-B reagent were adopted to represent non-agglutinated and agglutinated groups for chromatographic elution experiments by saline solution. The confocal image taken from the antibody & blood sample zone of the positive assay is shown in Figure 7d. Large lumps of agglutinated red blood cells are observed inside pores surrounded by fibres; this observation is consistent with the findings in Figure 4. Another confocal

image taken from the second band of the negative assay shows sparsely populated single red cells and small clusters formed by a few red cells on the fibre surface (Figure 7b). This band therefore consists of the eluted, non-agglutinated RBCs. Further confocal images taken from the position of the second band of a positive assay failed to identify any RBCs (Figure 7e). This is because most of RBCs have been agglutinated in the spotting point in the antibody & blood sample zone; only a very small number of free RBCs are available in this zone for chromatographic elution. Therefore it is very difficult to find free RBCs from the position of the second band. The confocal result is in good agreement with the elution pattern of positive assays observed in Figure 6.

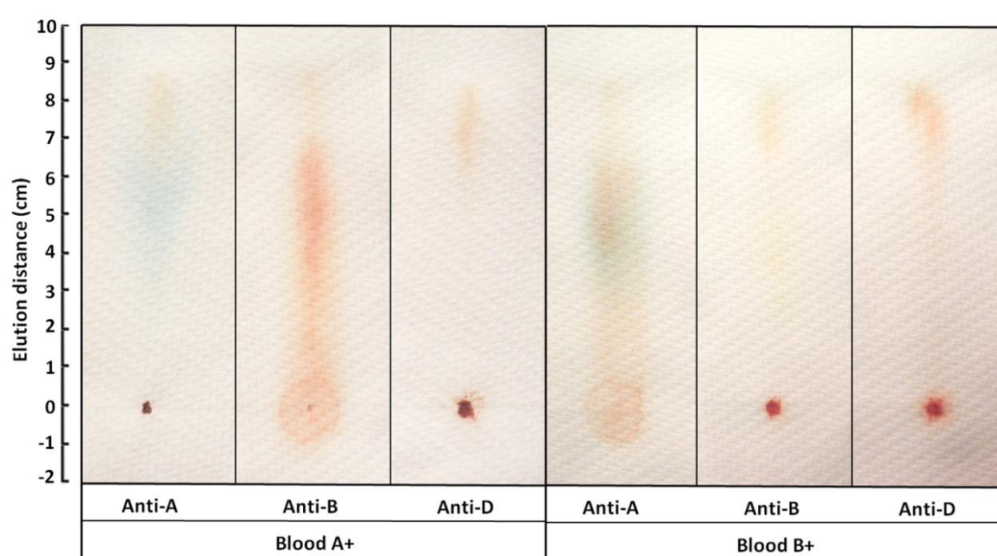


**Figure 6.** Chromatographic elution patterns of A+ and B+ blood samples reacting with grouping antibodies anti-A, anti-B, and anti-D.

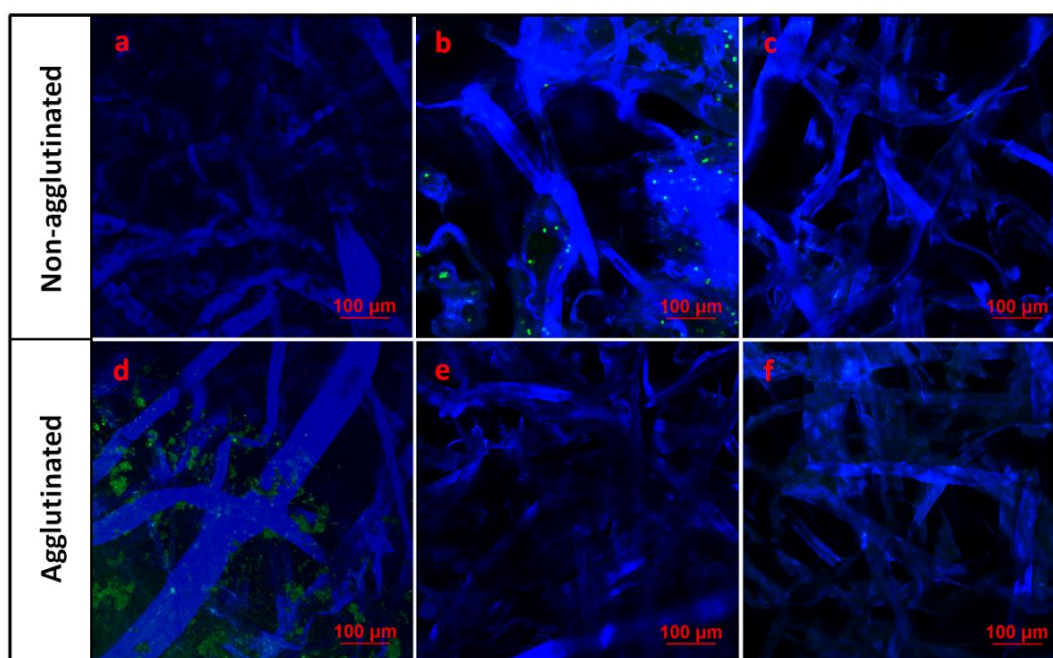


**Figure 7.** Confocal images of chromatographic elution patterns of non-agglutinated RBCs at elution distance of 0 cm (a), 5 cm (b), 8 cm (c) and agglutinated RBCs at elution distance of 0 cm (d), 5 cm (e), 8 cm (f).

Confocal images of the first bands of all negative and positive assays did not show any cells, despite Figure 6 showing that the first bands of all assays have a weak blood colour. An explanation is that the first band is the elution band of haemoglobin from the internal fluid of ruptured RBCs; this band has the deep red colour of blood but not due to the presence of non-ruptured RBCs. To support this explanation, chromatographic elution of two haemolysed blood samples of type A+ and O+ were conducted under the same conditions. The haemolysed blood samples were obtained by mixing 3  $\mu\text{L}$  of blood and 10  $\mu\text{L}$  of distilled water for 5 minutes. The activity of haemolysed blood samples were evaluated by adding their corresponding grouping antibodies. The absence of haemagglutination reactions proved that the haemolysis of the RBCs had occurred. The chromatographic elution patterns of haemolysed blood samples of type A+ and O+ are shown in Figure 8. The presence of only the first band confirms that it is indeed caused by the haemoglobin released after haemolysis of RBCs.



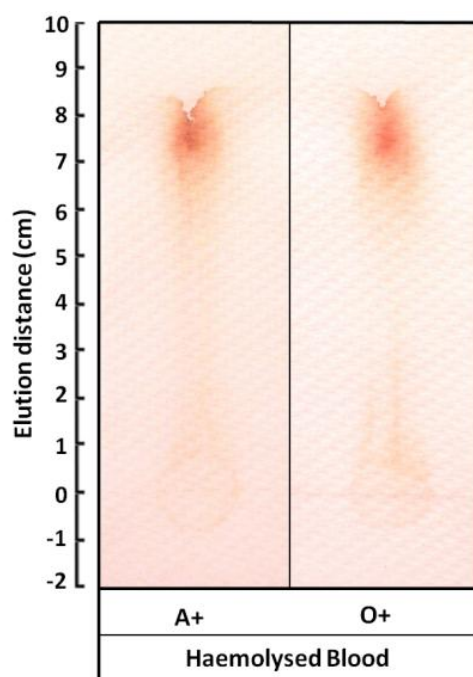


**Figure 8.** Chromatographic elution patterns of haemolysed blood samples of A+ and O+.

In this application study, the confocal microscopy method was used to investigate the two chromatographic elution bands and the spotting zone of blood typing assays on paper for the details of their composition. Confocal micrographs reveal that the rupture of RBCs occurred in the spotting zone. Haemoglobin released by the ruptured cells was eluted by the saline solution faster than the free RBCs and small cell clusters resulting in the first band close to the elution front, while free RBCs form the second elution band.

## 2.6 CONCLUSIONS

A confocal microscopy method was developed to study the mechanism of the agglutination of RBCs in a paper-based blood typing device. This work shows that confocal microscopy is a suitable technique for providing the details of RBC agglutination at the cellular level inside the fibre network of paper. Human RBCs can be labelled by FITC without the antigens on the surface of the red cells losing their activity. Two laser beams of differing wavelength were used to excite fluorescent signals with two different emission wavelengths in lignocellulosic fibres and FITC-



labelled red cells. These confocal signals were collected by different channels and formed into 2D and 3D confocal images for investigation of the fibre network, RBCs, and the different distributions of free RBCs and agglutinated blood lumps inside the fibre network. The non-agglutinated RBCs do not undergo morphological change, distributing rather uniformly in the spaces of the fibre network and staying around middle of paper sheet. On the other hand, the agglutinated RBCs are deformed, forming blood aggregates immobilised randomly at different positions on the fibre surface.

Kleenex paper towel was used as the substrate to prepare the paper-based blood typing device. The size of the interfibre pores of the Kleenex paper was shown by confocal micrographs to be much larger than the RBCs; the RBCs can thus be eluted by saline solution either vertically or laterally through the interfibre pores. RBCs undergo haemagglutination inside paper that was treated with the corresponding antibody. It has been confirmed by the confocal study that the release of antibody molecules from the fibre surface by dissolution is the main mechanism that causes haemagglutination. Haemagglutination of RBCs in the fibre network results in the formation of large lumps of aggregated cells, which become immobilised by mechanical entrapment within the interfibre pores. These aggregates could not be eluted by saline solution and thus result in the visual effect of the blood colouring becoming fixed on the paper. The non-agglutinated RBCs can be eluted by saline solution, therefore leaving no colour on paper after elution.

The confocal method was used to understand the chromatographic bands formed when blood samples are eluted in paper. This confocal method will be a powerful tool for understanding antibody and RBC interaction and for designing more sensitive bioactive paper-based blood typing devices in the future.

## **2.7 SUPPORTING INFORMATION**

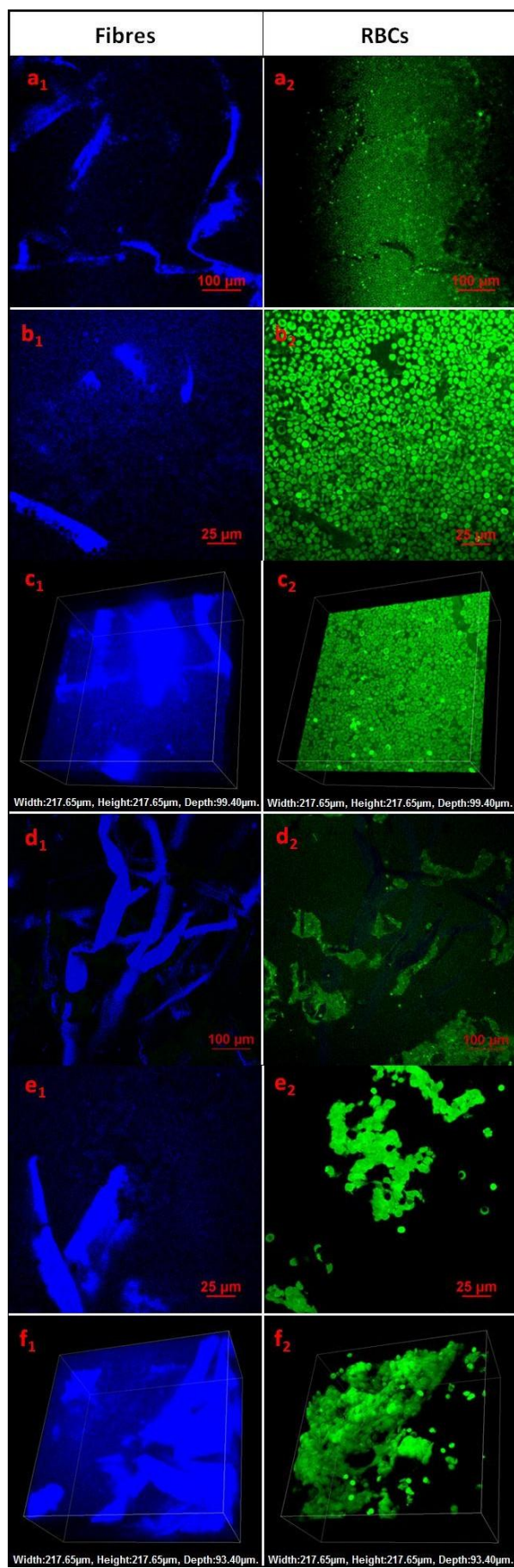


**Figure 9.** Separated confocal signals of fibres and RBCs for Figure 4. a1 and a2 are fibre and RBC signals for Figure 4a respectively, and etc.

## 2.8 ACKNOWLEDGEMENT

This work is supported by Australian Research Council Grants (ARC DP1094179 and LP110200973). Authors thank Haemokinesis for its support through an ARC Linkage Project. Authors also thank staff of MCN for Confocal training and usage and Dr M. Al-Tamini of Department of Chemical Engineering for information on red cell tagging. Ms Lizi Li, Ms Miaosi Li and Mr. David Ballerini thank the Monash University Research and Graduate School and the Faculty of Engineering for postgraduate research scholarships.

## 2.9 REFERENCES

- [1] G. Daniels, M.E. Reid, Blood groups: the past 50 years, *Transfusion* 50 (2010) 281-289.
- [2] G. Daniels, I. Bromilow, *Essential Guide to Blood Groups*, 2nd ed., Wiley-Blackwell: Chichester, West Sussex, UK, 2010.
- [3] D. Pramanik, *Principles of Physiology*, 3rd ed., Academic Publishers, Kolkata, India, 2010.
- [4] B.H. Estridge, A.P. Reynolds, N.J. Walters, *Basic Medical Laboratory Techniques*, 4th ed., Cengage Learning, Albany, NY, USA, 2000.
- [5] F. Llopis, F. Carbonell-Uberos, M.C. Montero, S. Bonanad, M.D. Planelles, I. Plasencia, C. Riol, T. Planells, C. Carrillo, A. De Miguel, A New Method for phenotyping red blood cells using microplates, *Vox Sanguinis* 77 (1999) 143-148.
- [6] J.H. Spindler, H. Kluter, M. Kerowgan, A novel microplate agglutination method for blood grouping and reverse typing without the need for centrifugation, *Transfusion* 41 (2001) 627-632.
- [7] Y. Lapierre, D. Rigal, J. Adam, D. Josef, F. Meyer, S. Greber, C. Drot, The gel test - a new way to detect red-cell antigen-antibody reactions, *Transfusion* 30 (1990) 109-113.

- [8] M.M. Langston, J.L. Procter, K.M. Cipolone, D.F. Stroncek, Evaluation of the gel system for ABO grouping and D typing, *Transfusion* 39 (1999) 300-305
- [9] D.J. Anstee, Red cell genotyping and the future of pretransfusion testing, *Blood* 114 (2009) 248-256.
- [10] J. Petrik, Microarray technology: the future of blood testing?, *Vox Sanguinis* 80 (2001) 1-11.
- [11] J.D. Roback, S. Barclay, C.D. Hillyer, An automatable format for accurate immunohematology testing by flow cytometry, *Transfusion* 43 (2003) 918-927.
- [12] D. Harmening, *Modern blood banking and transfusion practices*, 4th ed., F.A. Davis, Philadelphia, PA, 1999.
- [13] F. Giebel, S.M. Picker, B.S. Gathof, Evaluation of four bedside test systems for card performance, handling and safety, *Transfusion Medicine and Hemotherapy* 35 (2008) 33-36.
- [14] M. Al-Tamimi, W. Shen, R. Zeineddine, H. Tran, G. Garnier, Validation of paper-based assay for rapid blood typing, *Analytical chemistry* 84 (2012) 1661-1668.
- [15] L. Neimo, *Papermaking Chemistry*, Fapet Oy, Helsinki, Finland, 1999.
- [16] X. Li, J. Tian, T. Nguyen, W. Shen, Paper-based microfluidic devices by plasma treatment, *Anal Chem* 80 (2008) 9131-9134.
- [17] X. Li, J. Tian, G. Garnier, W. Shen, Fabrication of paper-based microfluidic sensors by printing, *Colloids and Surfaces B: Biointerfaces* 76 (2010) 564-570.
- [18] Z.H. Nie, F. Deiss, X.Y. Liu, O. Akbulut, G.M. Whitesides, Integration of paper-based microfluidic devices with commercial electrochemical readers, *Lab on a Chip* 10 (2010) 3163-3169.
- [19] M.S. Khan, G. Thouas, W. Shen, G. Whyte, G. Garnier, Paper diagnostic for instantaneous blood typing, *Analytical chemistry* 82 (2010) 4158-4164.
- [20] P. Jarujamrus, J. Tian, X. Li, A. Siripinyanond, J. Shiowatana, W. Shen, Mechanisms of red blood cells agglutination in antibody-treated paper, *Analyst* 137 (2012) 2205-2210.
- [21] M.S. Li, J.F. Tian, M. Al-Tamimi, W. Shen, Paper-based blood typing device that reports patient's blood type "in writing", *Angewandte Chemie-International Edition* 51 (2012) 5497-5501.

- [22] D.R. Ballerini, X. Li, W. Shen, An inexpensive thread-based system for simple and rapid blood grouping, *Analytical and bioanalytical chemistry* 399 (2011) 1869-1875.
- [23] J.L. Su, M. Al-Tamimi, G. Garnier, Engineering paper as a substrate for blood typing bio-diagnostics, *Cellulose* 19 (2012) 1749-1758.
- [24] E.F. Hauck, S. Apostel, J.F. Hoffmann, A. Heimann, O. Kempfski, Capillary flow and diameter changes during reperfusion after global cerebral ischemia studied by intravital video microscopy, *J Cereb Blood Flow Metab* 24 (2004) 383-391.
- [25] A.G. Hudetz, G. Feher, C.G.M. Weigle, D.E. Knuese, J.P. Kampine, Video microscopy of cerebrocortical capillary flow: response to hypotension and intracranial hypertension, *American Journal of Physiology: Heart and Circulatory Physiology* 268 (1995) H2202-H2210.

**This page is intentionally blank**

---

## Chapter 3

*Revealing the Transport Behaviour of Human Red  
Blood Cells in Paper Using Scanning Electron  
Microscopy Combined with Focused Ion Beam  
Milling*

---

**This page is intentionally blank**



## Monash University

### Declaration for Thesis Chapter 3

#### Declaration by candidate

In the case of Chapter 3, the nature and extent of my contribution to the work was the following:

Nature of contribution	Extent of contribution (%)
Initiation, key ideas, experimental works, analysis of results, writing up	55

The following co-authors contributed to the work. If co-authors are students at Monash University, the extent of their contribution in percentage terms must be stated:

Name	Nature of contribution	Extent of contribution (%) for student co-authors only
Boyin Liu	Experimental works, writing up	20
Siew Hoo	Experimental works	5
Jing Fu	Reviewing of the paper	
Yonghao Ni	Reviewing of the paper	
Wei Shen	Key ideas, reviewing and editing of the paper	Supervisor

The undersigned hereby certify that the above declaration correctly reflects the nature and extent of the candidate's and co-authors' contributions to this work\*.

Candidate's Signature		Date 25-Sep-2015
-----------------------	--	---------------------

Main Supervisor's Signature		Date 25-Sep-2015
-----------------------------	--	---------------------


\*Note: Where the responsible author is not the candidate's main supervisor, the main supervisor should consult with the responsible author to agree on the respective contributions of the authors.

**This page is intentionally blank**

# **Revealing the Transport Behaviour of Human Red Blood Cells in Paper Using Scanning Electron Microscopy Combined with Focused Ion Beam Milling**

*Lizi Li, Boyin Liu, Siew Hoo, Jing Fu, Yonghao Ni and Wei Shen\**

BioPRIA, Department of Chemical Engineering,  
Monash University, Clayton Campus, Vic. 3800, Australia



This paper has been prepared for submission to *ACS Applied Materials and Interfaces*

## **3.1 ABSTRACT**

In this work we report an investigation of the transport mechanism of red blood cells (RBCs) inside the fibre network of paper using a combined dual beam system with scanning electron microscopy (SEM) and focused ion beam (FIB) technology. Our motivation is to explore a new microscopic method to study the transport behaviour of RBCs in paper sensors designed for blood analysis. Cryogenically treated paper samples with isotonic citrate phosphate buffer suspended RBCs were freeze dried to preserve the integrity of RBCs inside the fibre network structure. This provided the opportunity to observe the distribution of RBCs inside the fibre network using the FIB-SEM technique and to analyze the RBC transport pathways. We show that the transport of human blood is driven by capillary wicking of blood plasma along channels formed by fibre-fibre overlaps. The main structural features of the fibre network that slow the transport of RBCs in paper are the blocked inter-fibre pores between two different layers of fibres, as well as the blocking of fibre-fibre overlaps by crossing fibres. This work establishes an important experimental method to view RBCs inside the fibre network in paper, which is a powerful method to aid the future design of paper-based blood analysis devices.

### 3.2 KEYWORDS

Paper-based diagnostic device, blood typing, transport behaviour, red blood cells, SEM, FIB

### 3.3 INTRODUCTION

The laboratory-scale development of paper-based blood analysis devices has attracted much attention in recent years [1-4]. These innovations provide the foundations for the future development of clinical diagnostic techniques for blood analysis. Paper is a low-cost material made from cellulosic fibres; the fibre network is porous and formed by multi-layers of fibres stacked in a 3D structure [5, 6]. The pore structures of fibre networks can be controlled in the papermaking process, enabling us to design papers with different functions to perform analytical and pathological tests. The rise of paper-based microfluidic platforms makes it possible for many affordable, portable and disposable point-of-care (POC) diagnostic devices to be fabricated [3, 7, 8]. These paper-based blood diagnostic devices are not only able to detect diseases like anaemia, malaria and human immunodeficiency virus (HIV) [9, 10], but are also able to do blood typing tests [11-15], as well as semi-quantitative analysis of compounds such as glucose, cholesterol, and lactate [16, 17]. Low-cost paper-based sensors have the potential to substantially improve the health of people in rural areas and developing countries through early diagnosis and screening of diseases, and are also important for military medicine and emergency situations.

Whole blood contains about 45.0% red blood cells (RBCs), 54.3% plasma and 0.7% white blood cells [18]. The recently-reported paper-based blood diagnostic devices generally take either RBCs or plasma as analytes for biochemical tests. Controlled separation of RBCs from plasma is therefore required for these tests. Yang et al. [9] have developed a simple paper-based test for measuring the concentration of haemoglobin, which is in the red blood cells. Noiphung et al. [17] report a paper-based glucose detection method which is able to complete the separation of RBCs from whole blood within 4 min. Liu [10] has invented a paper-based integrated diagnostic device for nucleic acid detection of HIV from blood which also has the capability of fast RBC

separation by the paper-based device itself. Our research group at Monash has invented a series of paper-based devices for blood typing [11-15]. These devices are made by depositing antibody molecules on paper substrates to detect the different but specific antigens present on the surface of red blood cells to determine blood type. Since blood typing assays rely on the identification of the haemagglutination of RBCs between antigens on RBCs and their corresponding antibodies, these assay require the paper to have the ability to discriminate agglutinated RBC lumps from free RBCs. Understanding the transport behaviour of RBCs within the fibre network in paper is therefore important for the design of paper-based devices for different blood analyses. This understanding will enable us to engineer the fibre network structure of paper to increase the efficiency of blood analyses and to facilitate the scaled-up production of this paper for the commercialization of paper-based blood analysis technologies.

In order to identify the RBC transport pathways, it is necessary to obtain the microscopic information about RBCs in the fibre network of the paper. Our hypothesis is that microscopic information on the positions and aggregation patterns of RBCs in paper during blood transport will help us to establish the RBC transport mechanism in the paper. This hypothesis is based on research indicating that capillary flow in paper is via film flow [19], and our recent macroscopic characterization of the sheet structures of paper made for blood typing applications.

In order to identify the RBC transport pathways, microscopic information on the positions and aggregation patterns of RBCs in paper must be obtained. In the study reported here we investigated the use of scanning electron microscopy (SEM) together with focused ion beam milling (FIB) as a new method to collect a series of cross-sectional images of the fibre network of paper. Images collected by this method can clearly identify and distinguish fibres from RBCs, allowing the positions of RBCs in the fibre network to be determined. These images can be recombined using software to form a 3D image of the fibre network containing the transport channels of RBCs. The FIB technology, which is widely used in the field of semiconductor materials, is a unique tool for the fabrication of micro- and nano-scale features [20]. The combined dual beam system with FIB and SEM has been used for revealing in 3D the construction of cell-material interfaces [21, 22]. By analyzing the distribution of RBCs

within fibre networks in paper, the pathways of blood sample flow in paper can be revealed. The FIB-SEM technique provides critical information that will aid the design of high-performance paper-based blood analysis devices for diagnostic purposes.

### **3.4 EXPERIMENTAL SECTION**

#### **3.4.1 Materials**

Eucalyptus hardwood bleached kraft pulp was obtained from the National Institute of Standards and Technology (NIST), USA. The properties of this pulp were retrieved from the official investigation reports of NIST standard reference material 8495. Standard blotting paper with a basis weight of 280 g/m<sup>2</sup> was obtained from Fibrosystem AB, Sweden, and was used as the absorbent paper to make handsheets. Reagent red blood cells (Revercell™, 15%) were purchased from bioCSL Pty. Ltd., Australia and stored at 4 °C. Whole blood samples from adult volunteers with known blood groups were obtained from Red Cross Australia. The blood was stabilized with anticoagulant additives and stored in Vacutainer® test tubes containing heparin, citrate and ethylenediaminetetraacetic acid (EDTA) at 4 °C, and used within 7 days of collection. Liquid nitrogen was provided by the Department of Chemical Engineering, Monash University.

#### **3.4.2 Methods**

##### **3.4.2.1 Handsheet making**

Hardwood fibres were obtained from disintegrating bleached kraft pulp of eucalyptus using a Messmer® standard pulp disintegrator. The revolution of the disintegrator was set at 7500. The Technical Association of the Pulp and Paper Industry (TAPPI) standard method T205 was followed for making the hardwood fibres into handsheets with a British Handsheet Former (Mavis Engineering LTD., London, UK). The basis weight of the handsheets was 20 g/m<sup>2</sup>. All handsheets were conditioned at 23 °C and 50% RH (relative humidity) for 24 hours before specimen preparation for microscopic observation.

### 3.4.2.2 Specimen preparation and SEM observation

For SEM sample preparation, handsheets were cut into 10 mm × 10 mm paper squares. The suspension of reagent red blood cells was centrifuged at 1500 r/min for 5 minutes to reach a haematocrit of 45% before using. A paper square was fixed using nipper horizontally; one micro-litre of concentrated blood reagent was introduced onto the paper surface and allowed to penetrate the paper network for 30 s. The samples were then dipped into liquid nitrogen for quick freezing. The frozen samples were sent for lyophilisation for 24 hours using a freeze dryer (-59.4°C, 0.081hPa) (HETO PowerDry PL6000, Thermo Scientific, USA). The paper squares were then mounted on metallic stubs using conductive tapes for SEM and FIB tomography respectively. Since both paper and RBCs are non-conductive materials, the specimens need to be coated with a layer of non-oxidising metal to reduce charging effects. Each specimen was sputter-coated with gold (SC7620 sputter coater, Quorum Technologies Ltd., Lewes, UK) for 30 seconds for SEM observation. The specimen was then observed with a scanning electron microscope (Phenom G2 Pro desktop SEM, Eindhoven, Netherlands).

### 3.4.2.3 FIB tomography setup

For sample preparation for FIB tomography, sputter coating was performed with a sputter coater (Emitech K550X; Quorum Technologies Ltd., Lewes, UK) to coat the sample with ~ 20 nm of gold. The samples were then transferred to an FIB/SEM instrument (Helios Nanolab 600; FEI Company, Hillsboro, USA). The vacuum in the analyzing chamber was below  $10^{-3}$  Pa and the sample stage was tilted and maintained at the eucentric point, where both the electron and ion beams can focus on the same selected area on the sample for milling and imaging. A cross-section 150 µm long was milled first by the ion beam at a high current of 6.5 nA. Sufficient milling time was allowed to cut through the paper. A thin platinum layer ~1 µm thick was deposited by FIB deposition on the top surface to further enhance the imaging quality by reducing charging. Before performing FIB tomography, cleaning using a 2.8 nA ion beam at the cross-section was carried out. For high resolution SEM acquisition, a low accelerating voltage of 3 kV was selected, and electron signals were acquired using a secondary electron (SE) detector, or a mixed mode of SE and backscattered electron (BSE) signals.

### 3.4.2.4 Data collection and 3D reconstruction

Auto Slice and View software (FEI Company, Hillsboro, USA) was used for data collection. It acquires high-resolution 3D images by milling a serial of cross-sections (or slides) and imaging each slice of the defined volume of sample. The total number of tomograms collected was 250. With the pixel size set to 38 nm, 250 tomograms were acquired, each being approximately 740 nm thick. The serial tomograms were saved automatically for further processing. Image alignment was performed in Avizo (FEI Visualization Sciences Group, Hillsboro, USA) to correct the deviations with cross-correlation alignment. Segmentation and 3D surface reconstruction were then processed using the same software with the final output in triangular meshes. Finally, 3D images of RBCs in the paper were constructed to enable visualization of the distribution of RBCs in the paper fibre network.

## 3.5 RESULTS AND DISCUSSION

### 3.5.1 Theoretical Background of Aqueous Fluid Transportation in Paper Network

The Lucas-Washburn equation is often used as an approximation for fluid penetration in paper. It assumes that the pores in paper are cylindrical and have the equivalent radii; fluid penetration through pores in paper is driven by capillary force, and fluid surface tension and fluid wetting conditions in the fibre wall dominate the rate of fluid transportation, while fluid viscosity contributes to the drag force of fluid flow in the pore [23]. However, since pores in paper are formed with cellulose fibres that have large aspect ratios of length vs. width, pores of fibre networks cannot be assumed to be cylindrical. It has therefore been recognized that the Lucas-Washburn equation is an oversimplification of fibre networks in paper, which is a more complex porous material made up of multi layers of cellulosic fibres. In 2003, Roberts et al. [19] conducted cryo-scanning electron microscopy experiments to visualize the penetration pathways of a wetting fluid into paper. Their results indicated that the fluid movement is due primarily to the advancement of the wetting fluid in the form of a film along channels formed by fibre-fibre overlaps, instead of the piston-style filling of pores by the



advancing fluid. Figure 1 is a typical example of fluid distribution in the paper network. The channels formed by fibre-fibre overlaps are shown to form a highly interconnected dense network of fluid flow pathways, which efficiently transport the fluid. Roberts et al. [19] showed that the frontal meniscus cannot advance through a pore that transverses the paper sheet, and the wetting fluid flows as a film along the edges of the pore and moves down the pores. In addition, the fluid also flows along the crevices formed by indentations and fibre surface roughness.

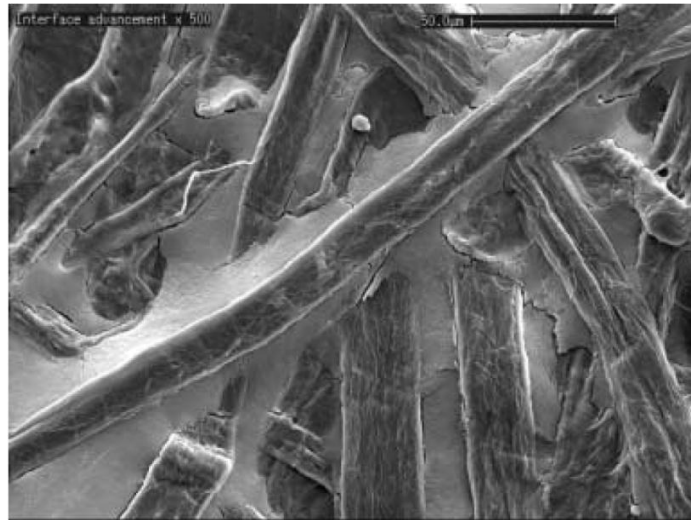


**Figure 1.** Water penetration in paper is dominantly via film flow [19]. Water wicks along fibre-fibre overlaps.

Human blood is a heterogeneous fluid containing red blood cells, white blood cells and plasma [18]. Cells in blood can be seen as suspended particles in the plasma phase; they do not provide driving force for the capillary flow of blood in paper. The plasma phase possesses the fluid properties which drives the capillary transport of blood within paper. It is expected that blood transport in paper is also via film flow through the channels formed by fibre-fibre overlaps. While the plasma phase provides the capillary driving force, RBCs in a blood sample are only transported with the movement of the plasma phase following the wicking pathways of plasma in the fibre network.

### **3.5.2 Capturing the Moment that Blood Penetrates the Fibre Network in Paper**

In a previous study, we presented the mechanism of RBC immobilization in fibre networks caused by antibody-specific haemagglutination using confocal microscopy [24]. This study showed that confocal microscopy is a good tool for observing RBCs within paper network. However, two major shortcomings remain. First, the image resolution deteriorates when the thickness of the paper sample becomes greater. Secondly, confocal microscopy is unable to capture the moment when blood just penetrates the fibre network in a paper, because the transport of RBCs within paper is a kinetic process. Confocal microscopy is only able to capture the final state of RBC distribution within the fibre network of paper.

In our study, we captured the moment that an RBC suspension penetrates the paper network by using flash-freezing in liquid nitrogen (at  $-196^{\circ}\text{C}$ ). This allows the actual distribution of RBCs during sample transportation within paper to be preserved. During freeze drying, all the liquid materials, including the liquid component inside RBCs, are lyophilized completely. On the other hand, the solid-phase substances, such as the cellulosic fibres and the external membranes of RBCs, are preserved in the original state for later SEM study.

Isotonic citrate phosphate buffer suspended reagent red blood cells, instead of human whole blood, were used in this work. The reason for this was to avoid the interference of proteins in human blood plasma in the observation of RBCs within the fibre network of paper. The normal total human blood plasma protein level is 63-83 g/L; it includes mainly albumins, globulins, and fibrinogen [25]. Water comprises around 90-93% of blood plasma by volume [26]. During the freeze drying process, water is lyophilized completely. Nonetheless, the freeze dried proteins may fill the interfibre channels of the paper network, interfering with the observation of RBCs (Figure 2). Instead, the isotonic citrate phosphate buffer suspended Revercell<sup>TM</sup> red blood cells contains no protein; freeze drying of such samples provides a clean fibre network, enabling RBCs to be observed clearly.

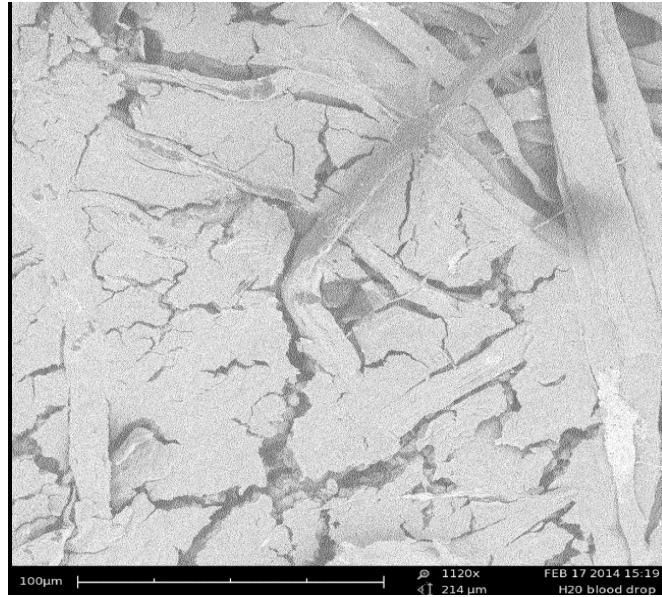


**Figure 2.** Interference in human blood plasma proteins to observation of RBCs within fibre network of paper.

### 3.5.3 Construction of 3D FIB-Based SEM Images of RBCs in Paper Network

FIB-based SEM technology is a good tool for the 3D reconstruction of cell-material interfaces [21, 22]. It was employed in our research for the construction of 3D models of RBCs in paper network. During the process of FIB tomography, 250 tomograms were collected within each 740 nm thickness approximately. The serial tomograms were automatically aligned, segmented and saved. In our study, FIB-based SEM technology has been shown to be a robust method for reconstructing 3D model paper structure from 2D SEM images, despite there being milling marks on each of the 2D images. Moreover, it provides an easy way to investigate the distribution of RBCs in paper network in detail. Firstly, the rebuilt 3D model can be manipulated using the Avizo 3D visualization software so that the 3D fibre network structure can be studied from any angle. Secondly, each of the 2D images contains details of the actual geometries of fibre-fibre junctions, RBC positions in the fibre network and the shapes of RBCs while flowing along channels of the fibre network.

We can clearly see from our results that, first, RBCs are much smaller than fibres (hardwood); second, RBCs can be clearly distinguished from the fibres via their

different textures; the cross-section of RBC is porous due to water loss in the freeze drying process. In contrast, the cross-sections of fibres are much wider, and no such porous structures can be observed. In addition, the lumens of large fibres can also be observed (see Figure 3 for a lumen of a dried fibre). However, lumens in fibres are not expressed in 3D reconstructed models. In this way, the positions of RBCs in fibre networks can be established in each 2D image to provide an overview of RBC transport in paper. It should be noted that the curtaining effect (i.e. the ion beam milling marks in the vertical direction of the sample) is inevitable under large ion current milling; it does not, however, affect the quality of reconstructed 3D model of fibre network. Therefore, the FIB-SEM method is able to provide microscopic information on the RBC transport pathways.

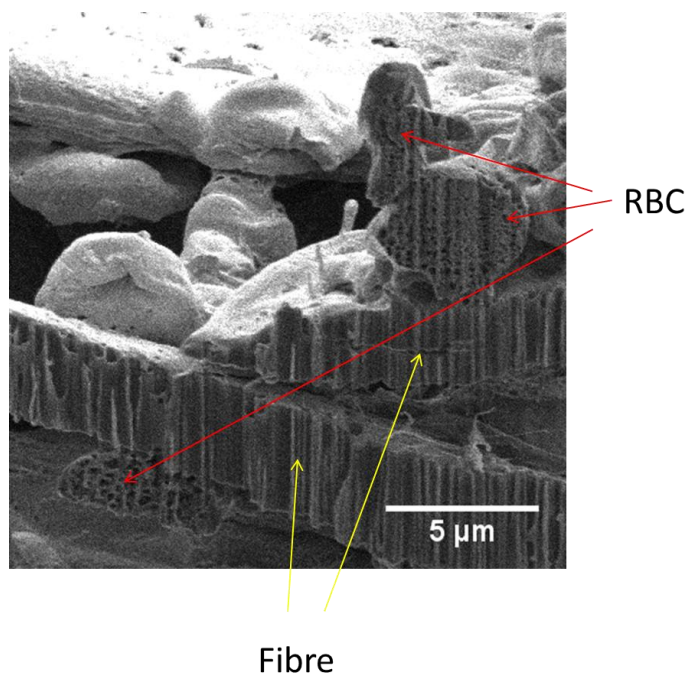


**Figure 3.** RBCs and cellulose fibres in a reconstructed 3D image can be distinguished by their sizes and internal structures.

It should be noted that there is an undesirable, though expected, shape change in a reconstructed RBC, since the biconcave disk shape of an RBC cannot be completely restored through software reconstruction. This is because the milling thickness of each tomogram was chosen as 740 nm. With this thickness, considering the size of human RBCs, each RBC can only be reconstructed with 2 to 10 serial tomograms, depending

on the orientation of the cells. Therefore, there will be a loss of topographic detail of an RBC in 3D reconstruction, due to the limited number of tomograms. This is a compromise that is necessary in order to acquire a larger volume of the paper sample with a limited number of laser cuts to study the distribution of RBCs in paper fibres. However, since our research focus is the distribution and pathways of RBCs in paper network, the undesirable shape change of the reconstructed RBCs does not affect our study, provided the position of the RBCs can be confirmed.

### **3.5.4 The Pathways of Human Red Blood Cells in Paper Networks**

Since blood contains 54.3% plasma [18], its transportation behaviour in paper should be similar to that of water, which has been studied by Roberts et al. [19] This is supported by the reconstructed 3D image obtained by FIB-SEM showing that RBCs are located along fibre overlaps or trapped in positions intercepted or surrounded by two or more fibres (Figure 4). This indicates that RBCs are transported along with the wicking plasma phase. The highly interconnected network of cellulosic fibres generates a large number of overlaps which are continuous capillary grooves that facilitate the transportation of blood. Blood also wicks along the capillary structures of fibre surface cracks and grooves. When a continuous fibre overlap is disrupted by a crossing fibre (Figures 4, 5 and 6), the wicking direction of blood changes direction and advance in the fibre overlap involving the crossing fibre. Such change in the blood transport pathway may result in trapping of RBCs in the fibre junctions (Figures 4 and 6). Since paper is formed of multiple layers of fibres, the wicking front of blood follows the fibre overlaps and transports from the top layer to the next layer below. Upon reaching the next layer below, blood may meet resistance, as there may be fibres in the next layer blocking the wicking pathway (Figures 4, 5, 6). Such blockage will not stop the plasma from wicking further down, but will stop RBCs from wicking further down, if the cross-section of the blocked wicking pathway is smaller than the minimum cross-section of an RBC. In this circumstance, many RBCs may be entrapped in the above-described locations (Figures 4, 5 and 6).

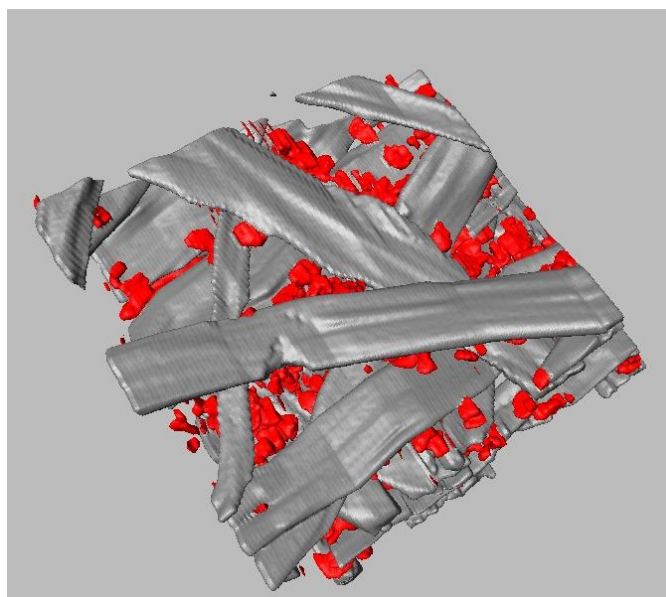


**Figure 4.** 3D FIB-based SEM images of RBCs within paper network.

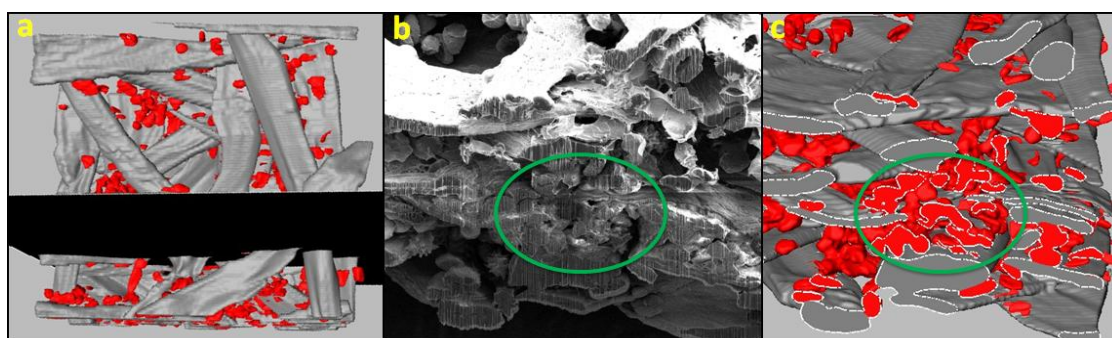


**Figure 5.** Cross-sectional view of paper substrate containing RBCs. (a) The position of cross-section on paper substrate. (b) The original SEM image of cross-section. (c) The image composed by Avizo of cross-section.

The use of the combined dual beam system with scanning electron microscopy and focused ion beam technology not only shows the 3D reconstruction of paper network containing RBCs, but also makes it possible to study any specific RBC within different layers of fibres inside the paper via cross-sectional analysis. As shown in Figure 5, an original SEM view of the cross-section in paper (Figure 5b) was made at the position of the dark plane (Figure 5a), while Figure 5c shows the colour image composed by the Avizo software of the same cross-section. From Figures 5b and 5c, it can be observed from the area inside the green circles that many RBCs are trapped between layers of fibres. These RBCs were driven by the buffer, wicking down the channel from the top

right of the green circle through an inter-fibre pore. We can also observe that a fibre at the bottom of the green circle partially blocks the pathway of RBCs, trapping them. This result is consistent with the observations reported in our previous paper [27], where we found paper made from softwood fibres presents higher resistance to RBC transport than papers made from hardwood fibres. The reason is that softwood fibres are wider than hardwood fibres and can block the pores more thoroughly than hardwood fibres. This kind of cross-sectional view provides critical information about the transport behaviour of blood in paper. The major structural features that slow down the transport of RBCs in paper network are fibres immediately underneath the pores in the above fibre layer. The FIB-SEM technique therefore enables researchers to design high performance papers for blood analysis by minimizing such fibre network structures.

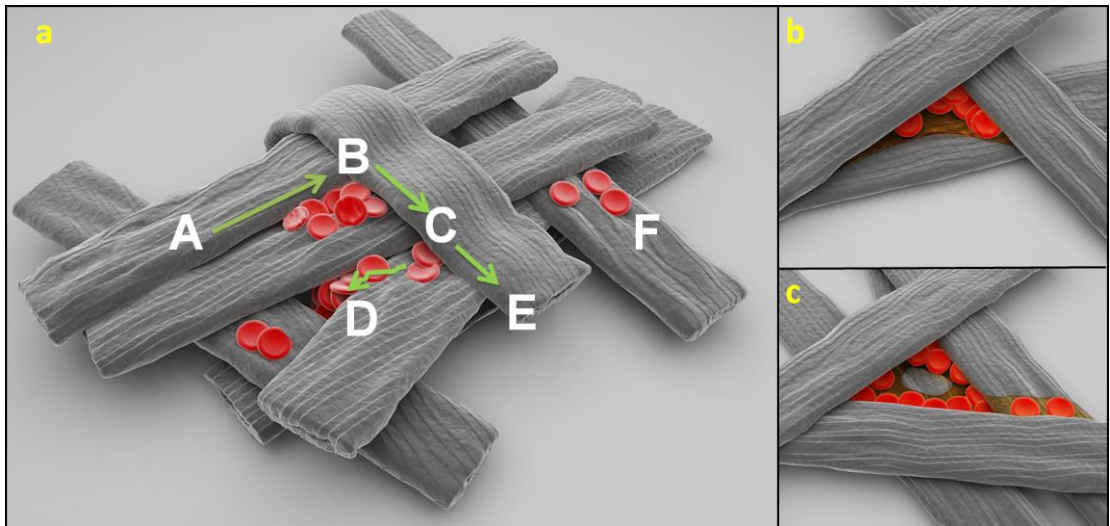


**Figure 6.** (a) An illustration of RBC pathways within paper based on SEM results. (b) and (c) are not realistic structural representations; rather they are simplified models to depict the RBC retention mechanisms in positions B and D of (a).

In Figure 6a, we illustrate a typical RBC pathway in paper with a model fibre network. Here the blood enters the network from the fibre-fibre overlap A-B; as it hits the crossing fibre (B-C), the blood flow changes direction and follows a new fibre-fibre overlap B-C. Upon the change of blood flow direction, some RBCs are left in corner  $\angle ABC$ . Such transport behaviour is consistently observed in Figure 4. This is likely to be caused by the sudden change of the blood flow velocity forced by the crossing fibre,



and also by the thickening of the flowing blood film at the corner forced by the Laplace pressure (Figure 6b) [19]. As the blood continues to flow in the direction of BC, the width of the flowing film is narrower than that in the corner of  $\angle ABC$ ; Figure 6a further illustrates the flow pattern. When the blood flow passes point C, it may split into two directions, CD and CE. In the CD direction, the blood flow comes to a vertical pore, which takes it to the next layer of fibres in the network (Figure 6a). In this process the blood wicking front still follows the fibre-fibre overlap between the fibre layers (Figure 6c); this fluid flow pattern has been demonstrated by Roberts et al. using water on paper [19]. The fibre underneath the vertical pore (e.g., the pores described in location D in Figure 6) can significantly influence the movement of free RBCs, as shown in Figure 4. This is because the fibre immediately underneath the pore may partially or completely cover the pore and block the transport of free RBCs. Therefore, RBCs may be retained in locations where the vertical pores are blocked. In locations where vertical pores are not completely blocked, blood will continue to penetrate the next layer of the fibre network, and by following the same film flow pattern, go further down the network. The cross-sectional FIB-SEM data show inhomogeneous distribution of RBC pathways in different layers of the fibre network; the connectivity of the vertical pores with channels of fibre-fibre overlaps in the next layer of fibres forms the transport pathways for the blood sample. Partial or total blockage of the pathway by a structural feature at point D in Figure 6 is the dominant factor affecting the transport of RBCs in paper.

Figures 4 and 5 show that a small number of RBCs remain on top of the fibres, instead of in the fibre-fibre overlaps. We also illustrated this feature in Figure 6. There are two possible contributing factors for RBCs remaining on top of fibres. First, when blood is introduced onto paper, it saturates the top layer of the paper and RBCs can be found in any location on the paper surface, including on the top of fibres. As the blood sample rapidly penetrates the paper structure, there is a rapid loss of the fluidic component of the blood. The RBCs on top of the fibre cannot be carried by the penetrating fluid and are therefore left on the top of the fibre. Second, this feature may have been created by our sample preparation technique. Since the paper samples were flash-frozen in liquid nitrogen, the position of each RBC was fixed instantly.



Our results suggest that, in a real assay, it is likely that RBCs may be immobilized via the first mechanism; in this case fibre surface roughness may also enhance RBC retention via this mechanism. However, the RBC population on fibre tops is small; although FIB-SEM can clearly identify these RBCs, this mechanism is not the main contributing factor to the clarity of the blood typing assays. Instead, RBC retention by fibre-fibre overlaps and, in particular, the blocked vertical pores in paper sheet are the main contributing factors to the low clarity of the blood typing assays.

### **3.6 CONCLUSIONS**

A scanning electron microscopy method, combined with the focused ion beam technique, has been developed to investigate the transport mechanism of RBCs within paper substrate. This work shows that the FIB-SEM approach is a suitable method to study the details of human red blood cells inside the fibre network of paper at the cellular level. Pre-treatments of liquid nitrogen and freeze drying make it possible to rapidly freeze the kinetic process of RBC transport carried by the suspension fluid. In this way, the purpose of characterizing the transport behaviour of RBCs at any certain moment during their transportation inside paper substrate can be achieved. Moreover, this combined dual beam system not only enables the 3D reconstruction of whole paper network containing RBCs, but also makes it possible to study any specific location in the fibre network by analyzing each cross-section for RBC distribution within paper.

The microscopic results obtained from this study show that the transport of an RBC suspension in paper is driven by the capillary force; fibre-fibre overlap is an effective form of capillaries for fluid (i.e., RBC suspension or blood) transport. Our results show that some RBCs may be trapped in locations where channels of fibre-fibre overlaps are blocked by crossing fibres, or by blocked transverse pores between different layers of fibres in the paper. These preliminary findings can be used for the future design of paper-based blood analysis devices.

### **3.7 ACKNOWLEDGEMENTS**

This work is supported by Australian Research Council Grants (ARC DP1094179 and LP110200973). The authors thank Haemokinesis for its support through an ARC

Linkage Project. Ms Lizi Li thanks the Monash University Research and Graduate School and the Faculty of Engineering for her postgraduate research scholarships.

### 3.8 REFERENCES

- [1] W.K.T. Coltro, C.M. Cheng, E. Carrilho, D.P. de Jesus, Recent advances in low-cost microfluidic platforms for diagnostic applications, *Electrophoresis* 35 (2014) 2309-2324.
- [2] P. Lisowski, P.K. Zarzycki, Microfluidic paper-based analytical devices (mu PADs) and micro total analysis systems (mu TAS): Development, applications and future trends, *Chromatographia* 76 (2013) 1201-1214.
- [3] X. Li, D.R. Ballerini, W. Shen, A Perspective on Paper-based Microfluidics: Current Status and Future Trends, *Biomicrofluidics* 6 (2012) 11301-1130113.
- [4] A.K. Yetisen, M.S. Akram, C.R. Lowe, Paper-based microfluidic point-of-care diagnostic devices, *Lab on a Chip* 13 (2013) 2210-2251.
- [5] K.J. Niskanen, Paper physics, Fapet Oy, Helsinki, Finland, 1999.
- [6] M. Ek, G. Gellerstedt, G. Henriksson, Paper Products Physics and Technology, Walter de Gruyter, Germany, 2009.
- [7] E.W. Nery, L.T. Kubota, Sensing approaches on paper-based devices: a review, *Anal Bioanal Chem* 405 (2013) 7573-7595.
- [8] M. Santhiago, E.W. Nery, G.P. Santos, L.T. Kubota, Microfluidic paper-based devices for bioanalytical applications, *Bioanalysis* 6 (2014) 89-106.
- [9] X.X. Yang, N.Z. Piety, S.M. Vignes, M.S. Benton, J. Kanter, S.S. Shevkoplyas, Simple paper-based test for measuring blood hemoglobin concentration in resource-limited settings, *Clinical Chemistry* 59 (2013) 1506-1513.
- [10] F. Liu, Paper-based integrated diagnostic device for nucleic acid detection of HIV from Blood, *Biophysical Journal* 106 (2014) 417A-417A.
- [11] M.S. Khan, G. Thouas, W. Shen, G. Whyte, G. Garnier, Paper diagnostic for instantaneous blood typing, *Analytical Chemistry* 82 (2010) 4158-4164.
- [12] D. Ballerini, X. Li, W. Shen, Patterned paper and alternative materials as substrates for low-cost microfluidic diagnostics, *Microfluidics and Nanofluidics* 13 (2012) 769-787.

- [13] M. Al-Tamimi, W. Shen, R. Zeineddine, H. Tran, G. Garnier, Validation of paper-based assay for rapid blood typing, *Analytical Chemistry* 84 (2012) 1661-1668.
- [14] M.S. Li, J.F. Tian, M. Al-Tamimi, W. Shen, Paper-based blood typing device that reports patient's blood type "in writing", *Angewandte Chemie-International Edition* 51 (2012) 5497-5501.
- [15] P. Jarujamrus, J.F. Tian, X. Li, A. Siripinyanond, J. Shiowatana, W. Shen, Mechanisms of red blood cells agglutination in antibody-treated paper, *Analyst* 137 (2012) 2205-2210.
- [16] Z.H. Nie, F. Deiss, X.Y. Liu, O. Akbulut, G.M. Whitesides, Integration of paper-based microfluidic devices with commercial electrochemical readers, *Lab on a Chip* 10 (2010) 3163-3169.
- [17] J. Noiphung, T. Songjaroen, W. Dungchai, C.S. Henry, O. Chailapakul, W. Laiwattanapaisal, Electrochemical detection of glucose from whole blood using paper-based microfluidic devices, *Analytica Chimica Acta* 788 (2013) 39-45.
- [18] G. Daniels, I.M. Bromilow, *Essential Guide to Blood Groups*, Wiley-Blackwell: Chichester, West Sussex, UK, 2010.
- [19] R.J. Roberts, T.J. Senden, M.A. Knackstedt, M.B. Lyne, Spreading of aqueous liquids in unsized papers is by film flow, *Journal of Pulp and Paper Science* 29 (2003) 123-131.
- [20] A.A. Tseng, Recent developments in nanofabrication using focused ion beams, *Small* 1 (2005) 924-939.
- [21] A. Al-Abboodi, J. Fu, P.M. Doran, P.P.Y. Chan, Three-dimensional nanocharacterization of porous hydrogel with ion and electron beams, *Biotechnology and Bioengineering* 110 (2013) 318-326.
- [22] B. Liu, H.H. Yu, T.W. Ng, D.L. Paterson, T. Velkov, J. Li, J. Fu, Nanoscale focused ion beam tomography of single bacterial cells for assessment of antibiotic effects, *Microscopy and Microanalysis* 20 (2014) 537-547.
- [23] E.W. Washburn, The dynamics of capillary flow, *Physical Review* 17 (1921) 273-283.
- [24] L.Z. Li, J.F. Tian, D. Ballerini, M.S. Li, W. Shen, A study of the transport and immobilisation mechanisms of human red blood cells in a paper-based blood typing device using confocal microscopy, *Analyst* 138 (2013) 4933-4940.

- [25] J. Schaller, S. Gerber, U. Kämpfer, S. Lejon, C. Trachsel, Blood Plasma Proteins, Human Blood Plasma Proteins, John Wiley & Sons, Ltd2008, pp. 17-20.
- [26] D.J. Bell, The distribution of glucose between the plasma water and the erythrocyte water in hens' blood, Quarterly Journal of Experimental Physiology and Cognate Medical Sciences 42 (1957) 410-416.
- [27] L. Li, X. Huang, W. Liu, W. Shen, Control performance of paper-based blood analysis devices through paper structure design, ACS Applied Materials & Interfaces 6 (2014) 21624-21631.

---

## Chapter 4

*Control Performance of Paper-based Blood  
Analysis Devices through Paper Structure Design*

---

**This page is intentionally blank**

**Monash University**

**Declaration for Thesis Chapter 4**

**Declaration by candidate**

In the case of Chapter 4, the nature and extent of my contribution to the work was the following:

<b>Nature of contribution</b>	<b>Extent of contribution (%)</b>
Initiation, key ideas, experimental works, analysis of results, writing up	75

The following co-authors contributed to the work. If co-authors are students at Monash University, the extent of their contribution in percentage terms must be stated:

<b>Name</b>	<b>Nature of contribution</b>	<b>Extent of contribution (%) for student co-authors only</b>
<b>Xiaolei Huang</b>	Experimental works	10
<b>Wen Liu</b>	Assisted in experimentation	5
<b>Wei Shen</b>	Key ideas, reviewing and editing of the paper	Supervisor

The undersigned hereby certify that the above declaration correctly reflects the nature and extent of the candidate's and co-authors' contributions to this work\*.

<b>Candidate's Signature</b>		<b>Date</b> 25-Sep-2015
------------------------------	---	----------------------------

<b>Main Supervisor's Signature</b>		<b>Date</b> 25-Sep-2015
------------------------------------	--	----------------------------

\*Note: Where the responsible author is not the candidate's main supervisor, the main supervisor should consult with the responsible author to agree on the respective contributions of the authors.

**This page is intentionally blank**



# Control Performance of Paper-based Blood Analysis Devices through Paper Structure Design

*Lizi Li, Xiaolei Huang, Wen Liu and Wei Shen\**

Department of Chemical Engineering,  
Monash University, Clayton Campus, Vic. 3800, Australia

\* 

This paper has been published in *ACS Applied Materials and Interfaces*

## 4.1 ABSTRACT

In this work, we investigated the influence of paper structure on the performance of paper-based analytical devices that are used for blood analysis. The question that we aimed to answer is how the fibre type (i.e., softwood and hardwood fibres) influences the fibre network structure of the paper, which affects the transport of red blood cells (RBCs) in paper. In the experimental design, we isolated the influence of fibre types on the paper structure from all other possible influencing factors by removing the fines from the pulps and not using any additives. Mercury porosimetry was employed to characterize the pore structures of the paper sheets. The results show that papers with a low basis weight that are made with short hardwood fibres have a higher porosity (i.e., void fraction) and simpler pore structures compared with papers made with long softwood fibres. RBC transport in paper carried by saline solution was investigated in two modes: lateral chromatographic elution and vertical flow-through. The results showed that the complexity of the paper's internal pore structure has dominant influence on the transport of RBCs in paper. Hardwood fibre sheets with a low basis weight have a simple internal pore structure and allow for the easy transport of RBCs. Blood typing sensors built with low basis weight hardwood fibres deliver high-clarity assays. Softwood fibre papers are found to have a more complex pore structure, which makes RBC transport more difficult, leading to blood typing results of low clarity. This

study provides the principle of paper sheet design for paper-based blood analysis sensors.

### 4.2 KEYWORDS

Paper-based diagnostic sensors, paper structure, hardwood fibre, softwood fibre, blood typing, mercury porosimetry

### 4.3 INTRODUCTION

Paper-based microfluidic devices and paper-based sensors have attracted a lot of attention because of their potential applications in point-of-care, immunoassays, food quality testing, environmental monitoring, and disease screening in resource-limited areas [1-10]. Paper made of cellulose fibres demonstrates significant advantages over other substrates such as silicon and glass when used in the manufacturing of low-cost, disposable and flexible diagnostic devices [1, 2, 11-13]. Paper-based sensors use the hydrophilic nature of the cellulose fibre network to transport homogeneous aqueous liquids by capillary wicking. To control the direction of liquid wicking on paper, previous publications reported a variety of methods to pattern the paper [1, 14-17]. By physically and chemically functionalizing paper and patterned paper devices, many routine chemical and biological assays can be performed using paper-based devices without the need for sophisticated analytical equipment [1, 9-11]. More recently, paper-based microfluidic diagnostics has evolved from analyzing samples of very simple matrices to analyzing samples of more complex matrices, such as animal and human blood samples [18-20]. Paper-based device design has increasingly involved the use of a colloid suspension, such as metal nanoparticles and encapsulated functional nanoparticles, as the reaction media or indicator system [21, 22]. Although several methods of using paper to separate and analyze heterogeneous samples have been demonstrated, the physicochemical properties of paper that are best suited for analyzing a heterogeneous sample are not yet fully understood [1]. Paper is a material with a three-dimensional porous structure that is formed by multiple layers of cellulosic fibres [23, 24]. It has been used for a long time as a filtration medium for separating solid and

colloidal particles from heterogeneous fluids. To better utilize the filtration property of the paper to design high-performance paper sensors for complex sample analysis, a detailed understanding of the fibre network structure and particle transport behaviour in paper is necessary.

Our group has developed a series of paper-based fluidic devices for blood typing; these devices work based on filtration and chromatographic separation principles [8, 18, 19, 25]. Whole human blood is composed of a continuous plasma phase with red blood cells (RBCs) in a suspension state. The blood group is classified based on the inherited differences (polymorphisms) in the antigens on the surface of the RBCs [26-28]. Whereas the biochemical basis of a paper-based blood typing assay is the hemagglutination of RBCs by their corresponding grouping antibodies, the mechanism of interpreting the assay result relies on the transport behaviours of agglutinated RBC lumps and non-agglutinated free RBCs within the porous fibre network of the paper. Paper-based blood typing devices are fabricated by simply imbibing blood group antibody solutions into the fibre network of a paper. In a blood typing assay, a blood sample is allowed to imbibe into the paper that has been treated with the antibodies. This design concept allows the hemagglutination to occur inside the fibre network of the paper. For a positive assay, hemagglutination makes RBCs agglutinate via the inter-cellular cross-linking by their corresponding antibody molecules. The agglutinated RBC lumps are then immobilized primarily by mechanical entrapment in the porous structure of paper. In contrast, no hemagglutination occurs in a negative assay; non-agglutinated RBCs remain stably dispersed in the plasma phase and can move through porous fibre network of paper, with plasma occurring as a single suspension phase [18, 25, 29]. To display the blood typing result, the assay is subjected to either a buffer elution in a chromatographic tank or a buffer rinsing step to allow a small volume of buffer to penetrate the paper. Buffer elution or buffer rinsing is intended to flush out free RBCs from the fibre network. Because only non-agglutinated RBCs are free in the fibre network and agglutinated RBC lumps are not, a chromatographic elution or buffer rinsing can provide visual evidence of the occurrence of hemagglutination: a negative assay should show no blood color on the paper, whereas a positive result should show a strong blood color [18, 19].

A successful blood typing assay on paper must differentiate a positive assay from a negative one with high clarity. In our investigation, we observed that blood typing assay clarity is dependent on the type of paper selected. Visually, low clarity means that a negative assay may carry a faint to moderate blood color, whereas a positive assay occasionally gives a low density of the blood color; these observations may lead to an ambiguous assay result. To improve the clarity of the paper-based blood typing assays, paper structures must be characterized and their influence on the movements of RBCs must be understood. This understanding will provide key information not only for selecting the right papers to fabricate blood typing devices but also for fabricating paper-based devices for other blood analyses.

A paper sheet is often considered as an infinite network in its lateral dimensions but finite in the vertical (or z-) direction [24]. Because paper-based blood typing devices typically adopt two different designs, i.e., the lateral chromatographic flow design [8, 18] and the vertical flow-through design [19, 25], the paper structure may influence the sample flow and the RBC separation of these flow modes differently, due to the anisotropic structural characteristics of paper.

In an actual papermaking process, a variety of chemical additives are used to improve the paper sheet properties, which include the wet and dry strength and printability additives. These additives include cationic starch, sodium carboxymethyl cellulose (CMC) and cationic polymers, such as polyacrylamide (PAM) and poly diallyl dimethyl ammonium chloride (PDADMAC) [13, 30, 31]. Wood pulps also contain a fraction of fine fibrous and granular particles known as fines. However, for the papers that are used for blood typing, the charges carried by additives may affect the transport behaviour of RBCs in fibre networks because RBCs are negatively charged in the plasma environment [28]. Fines may also interact with fibres and RBCs. Because of the above factors, no commercial paper possesses the optimized properties for blood typing assays.

In this work, we investigate the effect of paper structure on the performance of paper-based blood typing devices. Papers with different basis weights were made using different fibres. To clearly identify the influence of paper's physical structures on its

blood typing performance, no chemical additives were used and the fine particles in the pulp were removed in this study. The paper sheet properties were characterized with apparent thickness and apparent bulk measurements and with mercury intrusion porosimetry. Blood typing assays by lateral chromatographic elution and vertical flow-through modes were investigated to study the red blood cell transport behaviour in the papers' internal porous structure and the paper-based sensor performance.

### **4.4 EXPERIMENTAL SECTION**

#### **4.4.1 Materials**

Eucalyptus hardwood bleached kraft pulp and northern softwood bleached kraft pulp were obtained from the National Institute of Standards and Technology, USA. The properties of these pulps were retrieved from the reports of NIST standard reference materials 8495 and 8496. Standard blotting paper with a basis weight of 280 g/m<sup>2</sup> was obtained from Fibrosystem AB, Sweden, and used as the absorbent paper for making handsheets. Blood samples were collected from adult volunteers with known blood groups through Red Cross Australia. All blood samples were stabilized with anticoagulant additives, stored in Vacutainer® test tubes containing heparin, citrate and EDTA at 4 °C and used within 7 days of collection. ALBAclone® Anti-A (Z001), anti-B (Z011) and anti-D (Z039) monoclonal grouping reagents were sourced commercially from Alba Bioscience Ltd., UK. Anti-A and anti-B are a transparent cyan and a transparent yellow solution, respectively, whereas anti-D is a colorless solution. Monoclonal grouping reagents were also kept at 4 °C. Analytical grade NaCl from Sigma-Aldrich was used to prepare the physiological saline solution.

#### **4.4.2 Methods**

Hardwood and softwood fibres were obtained by disintegrating hardwood and softwood pulps using Messmer® standard pulp disintegrator for 7500 revolutions. The fibres were then thoroughly washed with a 150-mesh to remove the fines. Handsheets with basis weights of 20 g/m<sup>2</sup>, 35 g/m<sup>2</sup> and 50 g/m<sup>2</sup> were made with hardwood and

softwood fibres. Handsheets ( $20 \text{ g/m}^2$ ) with different contents of hardwood and softwood fibres were also made. TAPPI (The Technical Association of the Pulp and Paper Industry) standard method T205 was followed for making the handsheets. All handsheets were conditioned at  $23^\circ\text{C}$  and 50% RH for 24 hours before measuring their physical properties. The sheet basis weight, apparent thickness and apparent bulk were measured following the TAPPI standard method T220. The terms “thickness” and “bulk” used below indicate the “apparent thickness” and “apparent bulk”. The mercury intrusion measurements were performed using an AutoPore IV 9500 instrument (Micromeritics, USA).

For the lateral chromatographic elution test, paper handsheets were cut into  $100 \text{ mm} \times 30 \text{ mm}$  strips. Ten microliters of antibody solution was spotted 2 cm from the shorter side of the paper strip and allowed to be absorbed completely over 30 seconds. An aliquot of  $1 \text{ }\mu\text{L}$  of whole blood sample was dropped onto the center of the antibody spot and allowed to react with the antibody reagent for 30 seconds. Then, the paper strip was suspended in a physical saline solution in a chromatographic tank to allow elution for 90 seconds; the distance between the blood spot and the level elution buffer was kept at 10 mm. The paper strip was then removed from the chromatographic tank and suspended in a fume cupboard to be dried in air at room temperature for 10 minutes. The dried paper strip was then scanned using a scanner (Epson Perfection 2450) for image analysis.

For the vertical flow-through saline-rinsing blood typing test, handsheets were cut into  $10 \text{ mm} \times 10 \text{ mm}$  paper squares. The testing paper was prepared by adding  $10 \text{ }\mu\text{L}$  of antibody solution to the paper surface and allowing it to dry in air for 3 minutes. One microliter of whole blood sample was introduced onto the paper and allowed to react with the antibody reagent for 30 seconds. The testing paper was then transferred onto a sheet of blotting paper to perform the saline rinsing. Rinsing was performed by introducing a total of  $30 \text{ }\mu\text{L}$  of saline solution onto the center of the blood spot for two applications; the absorbing power of the blotting paper assisted the rinsing buffer to penetrate through the testing paper. The rinsed blood testing paper was allowed to dry in the fume cupboard for 10 minutes. A scan of the dried testing paper was then obtained.

The optical density values of blood spots of the positive and negative assays were assessed and reported as the mean  $\pm$  SD (standard deviation). Unpaired two-tailed t-tests were used to compare the mean optical density values for the analysis of different blood samples with different testing modes. One-way analysis of variance (ANOVA) was applied to compare the mean red color optical density in more than two groups. The statistical analysis was performed using the GraphPad Prism (version 6) software with  $P < 0.05$  considered significant.

## 4.5 RESULTS AND DISCUSSION

### 4.5.1 Isolation of the Paper Physical Structure from the Influence of Chemical Additives and Fines

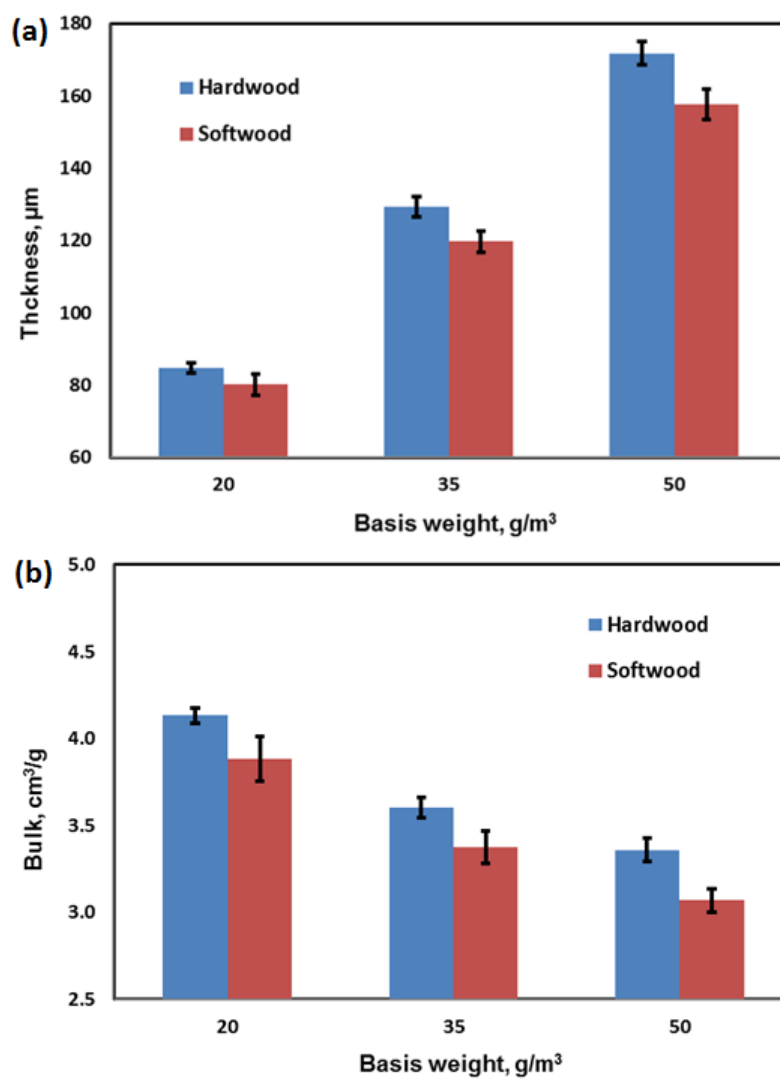
To gain a precise understanding of the influence that the paper sheet physical structure has on its blood typing performance, we formed handsheets using well-characterized softwood and hardwood pulps, but without using any additives. Fines were also removed because their contribution to RBC transport should be investigated separately.

Handsheets with basis weights of 20 g/m<sup>2</sup>, 35 g/m<sup>2</sup> and 50 g/m<sup>2</sup> were made with hardwood and softwood fibres respectively. Figure 1a shows that the apparent thickness of the handsheets increased substantially with the increase in sheet basis weight. For hardwood handsheets, when the basis weight was doubled from 25 g/m<sup>2</sup> to 50 g/m<sup>2</sup>, the thickness increased from 84.9  $\mu$ m to 171.9  $\mu$ m, representing an increase of 102.5%. For handsheets made from softwood fibres, a similar trend can be observed. This trend is intuitively appreciable because the number of fibre layers increases proportionally to the basis weights of handsheets. Figure 1a also shows that all of the hardwood handsheets have greater apparent thickness compared with the softwood handsheets of the same basis weight. Figure 1b shows that for each basis weight, hardwood sheets have a higher bulk value than do the softwood sheets. The bulk of a paper is defined as the reciprocal of the sheet density and has an unit of cm<sup>3</sup>/g [32]. Additionally, the bulk of the hardwood and softwood handsheets decreased from 4.13 cm<sup>3</sup>/g to 3.36 cm<sup>3</sup>/g and from 3.88 cm<sup>3</sup>/g to 3.07 cm<sup>3</sup>/g, respectively, as the sheet basis

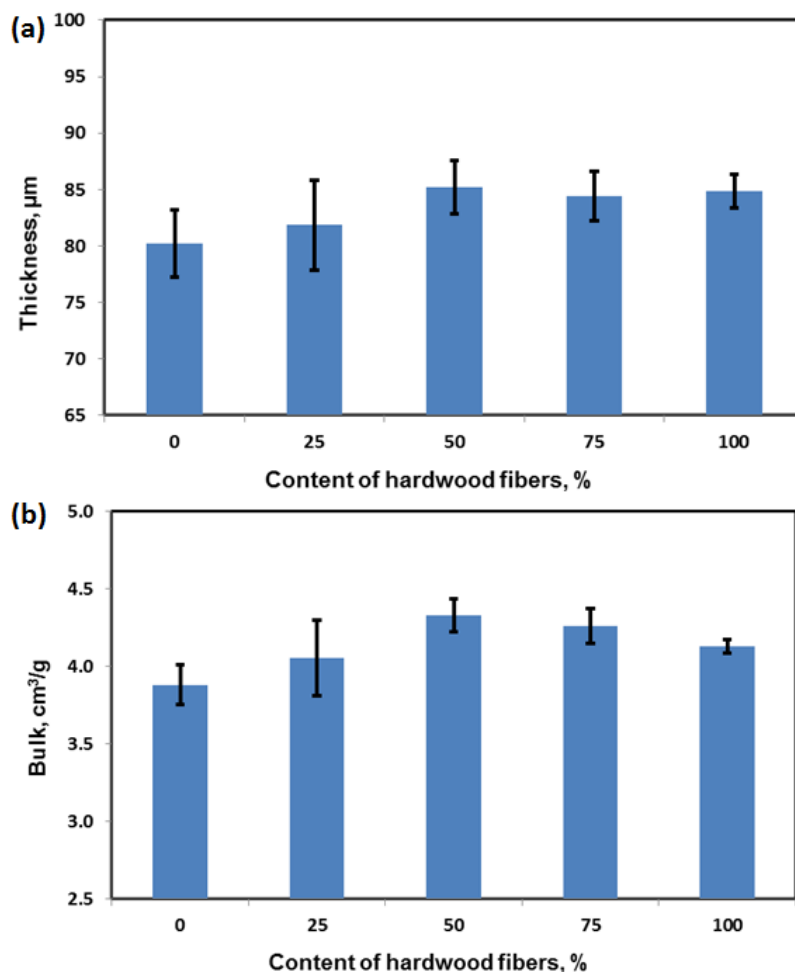
weights doubled from 25 g/m<sup>2</sup> to 50 g/m<sup>2</sup>. The data in Figure 1b indicate that the volume of voids in a hardwood sheet was higher than that in a softwood sheet of the same basis weight. This finding also indicates that the fibre network became denser as the sheet basis weight increased.

Figure 2 shows the thickness and bulk of handsheets made of different blends of hardwood and softwood fibres, all with a basis weight of 20 g/m<sup>2</sup>. The thickness of the handsheets increases with the content of hardwood fibres to 50% at first and then levels off. This trend, however, is only suggested because the error bars of some data sets are large. Detailed handsheet data can be found in Table 2 in the Supporting Information. By varying the sheet thickness and bulk through controlling the content of different fibres, the structure of the paper network can be varied in a controlled manner. This provides the possibility to investigate the influence of the paper's physical structure on the transportation and immobilization of RBCs, without any interference from chemical additives.





**Figure 1.** Apparent thickness (a) and apparent bulk (b) of hardwood and softwood handsheets of different basis weights.



**Figure 2.** Apparent thickness (a) and apparent bulk (b) of handsheets with different content of hardwood and softwood fibres (basis weight of all sheets were  $20 \text{ g/m}^2$ ).

#### 4.5.2 Characterization of Pore Size Distribution of Paper

Mercury porosimetry was used to characterize the pore size distribution of handsheet samples. Figure 3a shows the pore size distributions of hardwood handsheets of different basis weights. The data show similar bimodal patterns. Such a pattern has been reported previously [33]. Silvy et al. [33] attributed the low-intensity peak of larger pore diameters to the pores located on the surface of the paper and the high-intensity peak of smaller pore diameters (between 10 and 30  $\mu\text{m}$ ) to pores inside the sheets. Our results show that both peaks for hardwood  $20 \text{ g/m}^2$  paper are higher than those of papers with higher basis weights; this finding indicates that papers with lower

basis weight have a more porous surface and internal structures. This finding is in agreement with the sheet bulk results shown in Figure 1b.

The sizes of the surface pores of hardwood paper are centered at approximately 100  $\mu\text{m}$  and range from 45  $\mu\text{m}$  to 200  $\mu\text{m}$ . Because RBCs have the shape of biconcave disks, with a diameter of 6-8  $\mu\text{m}$  and a thickness of 2  $\mu\text{m}$  [29], they can easily pass through the surface pores of hardwood paper. Furthermore, the integral of the Log differential intrusion plot over a certain pore size range gives the cumulative mercury intrusion volume; it reflects the pore volume corresponding to the pore size range of the material being tested [34]. Because the 20  $\text{g}/\text{m}^2$  hardwood handsheet has the highest volume of surface pores, it could therefore be hypothesized to have a greater capability to allow for the lateral transportation of free RBCs via chromatographic elution.

Figure 3a also shows that the internal pores of hardwood handsheets with basis weights of 20  $\text{g}/\text{m}^2$ , 35  $\text{g}/\text{m}^2$  and 50  $\text{g}/\text{m}^2$  are centered at 20  $\mu\text{m}$ , 18  $\mu\text{m}$  and 10  $\mu\text{m}$ , respectively. Among these handsheets, the 20  $\text{g}/\text{m}^2$  one has an internal volume of 8.4 ml/g, while the internal volumes of the 35  $\text{g}/\text{m}^2$  and 50  $\text{g}/\text{m}^2$  sheets are much lower, being 4.7 ml/g and 4.2 ml/g, respectively. In addition, the high-intensity peak of the 20  $\text{g}/\text{m}^2$  hardwood handsheet is narrower than those of higher basis weights. These findings suggest that low basis weight handsheets have more uniform internal pore size distribution, which is a desirable sheet property for separation. It is noted, however, that the internal pore size distribution of the 50  $\text{g}/\text{m}^2$  hardwood sheet has a shoulder, suggesting that the internal structure is formed by pores of two sizes. We hypothesized that the internal pore structure of the 50  $\text{g}/\text{m}^2$  hardwood sheet was less uniform and more complex. One explanation of this observation is that sheets of high basis weight contain more fibres, which contribute to more fibre-fibre bonding; this leads to a more complex internal pore structure of the sheet. We hypothesize that RBC transport in complex pore structures would be more difficult. This effect is discussed in more detail below.

Internal pores with diameters smaller than 8  $\mu\text{m}$  would not provide easy transport pathways to free RBCs. Although it is known that red cells can pass through veins with smaller diameters than those of RBCs under pressure through cell deformation [35, 36],

no report has shown that this would also occur for RBCs travelling in a porous network under no external pressure.

In summary, hardwood handsheets of lower basis weights could have the potential to transport free RBCs more efficiently via both chromatographic elution and flow-through modes because of their large surface volume and internal pores that have uniform sizes.

The pore size distributions of softwood papers are illustrated in Figure 3b. The first (left) peak corresponds to surface pores; the second peak with more than one shoulder corresponds to the internal pores. The pore volume of softwood handsheets decreases as the basis weight increases; this trend is similar to that observed for hardwood sheets. This trend indicates that sheets of higher basis weights contain more fibres and therefore more fibre-fibre bondings, which leads to denser sheets (see also Figure 1b). This finding is in agreement with the sheet bulk data in Figure 1b.

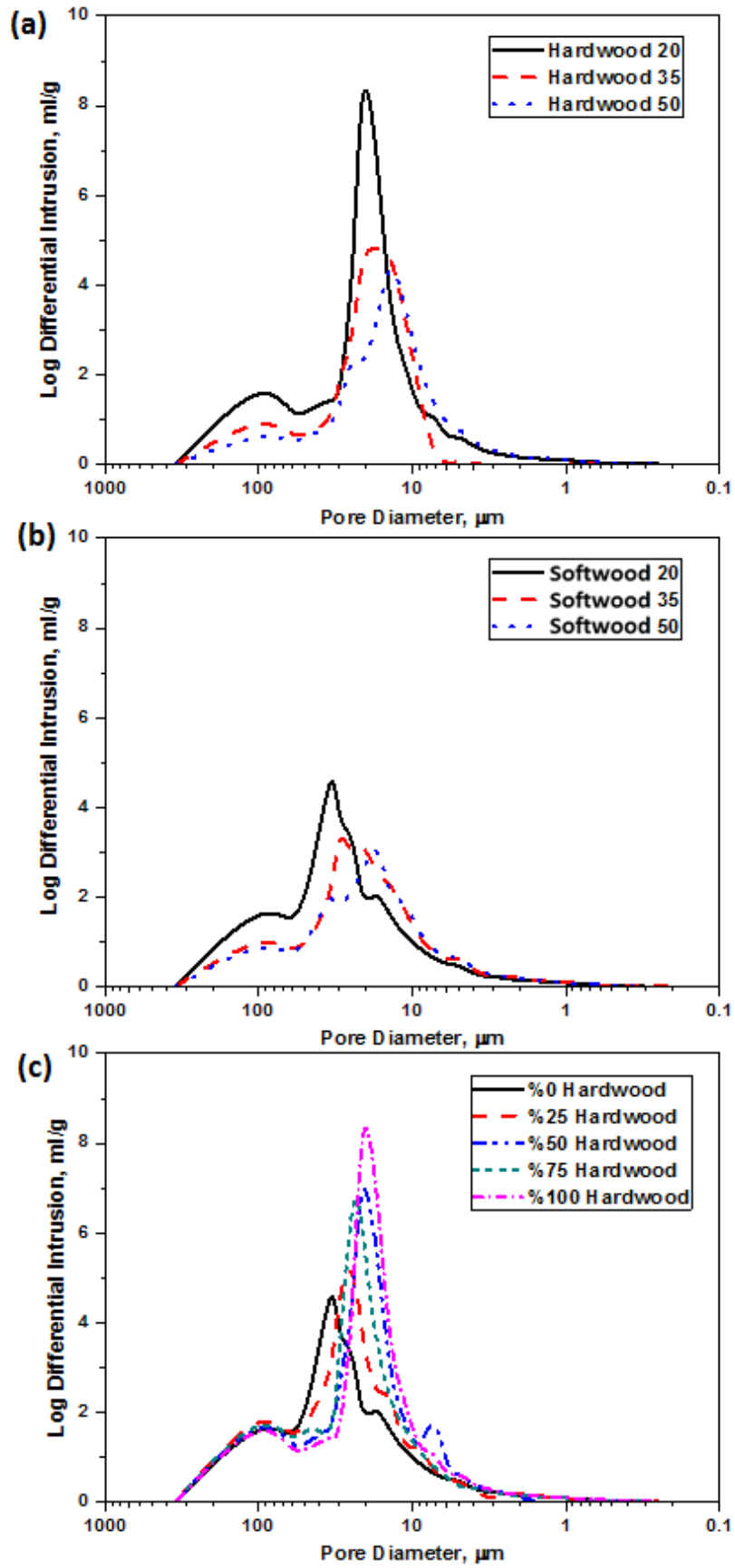


**Figure 3.** Pore size distributions of (a) hardwood paper with different basis weights, (b) softwood paper with different basis weights, and (c) paper with different content of hardwood and softwood fibres (basis weight of 20 g/m<sup>2</sup>).

The first peak of surface pores of softwood paper is also centered at approximately 100  $\mu\text{m}$ , similar to that of the hardwood paper. The most interesting information in Figure 3b, however, is that the mercury intrusion results show more than one peak in the region of internal pores, indicating that the internal pore structures of the softwood sheets are more complicated than those of hardwood sheets and that mercury intrusion into the softwood handsheets has met a hierarchical internal structure. This can be clearly observed from the four peaks (shoulders) of the intrusion curve for the internal pore region of the 20 g/m<sup>2</sup> softwood sheet. At the end of each step of the hierarchical structure, the rate of mercury intrusion slowed down, but the rate increased again when mercury intruded into the pores of the next hierarchical step. Such a hierarchical structure implies that channels for liquid transport are more complex for softwood sheets than for hardwood sheets of the same basis weight. This could make the transport of RBC in softwood sheets more difficult. The mercury intrusion results are discussed with respect to the RBC elution results below.

The pore size distributions of papers made by blending hardwood and softwood fibres in different proportions were also analyzed using mercury porosimetry, and the results are presented in Figure 3c. The basis weight of all of the sheets made with mixed fibres was 20 g/m<sup>2</sup>. The results show that mixing short and long fibres in different proportions does not change the size or volume of the surface pores. Thus, the surface pores are dominantly determined by the basis weight of the sheets and sheet-forming conditions, but not by the fibres. Figure 3c also shows three expected trends. First, as the percentage of long softwood fibres in the handsheets increases, the overall pore volume of the sheets decreases. This trend is supported by the conclusion of the previous section that long softwood fibres form denser sheets. Second, the pore size of handsheets increases with an increase in the percentage of softwood fibres. This trend can be explained as follows: the pore size of a network structure formed with larger fibres (both in length and in width) is larger than that formed with smaller fibres. Third, the internal sheet structure becomes increasingly complex as the percentage of long

fibres is increased to above 50%. This trend is supported by the increased fibre network hierarchical structure with the increase of long fibres in the network.

With the above insights into the handsheet surface and internal structures, we have made hypotheses concerning RBC transport behaviour in different sheets. Tests of these hypotheses are presented below.

### **4.5.3 Effect of Paper's Physical Structure on Lateral Elution Blood Typing Performance**

In the lateral chromatographic elution blood typing test, blood was spotted onto a handsheet treated with grouping antibody reagents; the spotted sheet was then chromatographically eluted by physical saline solution in a chromatographic tank for 90 seconds. A blood sample spotted on its corresponding antibody will agglutinate and become immobilized on the same spot in paper and resisting saline elution; this signifies a positive test result. Conversely, a blood sample spotted onto non-corresponding antibodies will not agglutinate; RBCs remain free and can be eluted away by the saline buffer, leaving behind no, or a very faint, blood spot. Such an assay signifies the negative result. The critical criterion of a high-performance blood typing device is the ability to distinguish a positive result from a negative result with high clarity. Both surface and internal pores of paper affect the fixation and transport of agglutinated and free RBCs.

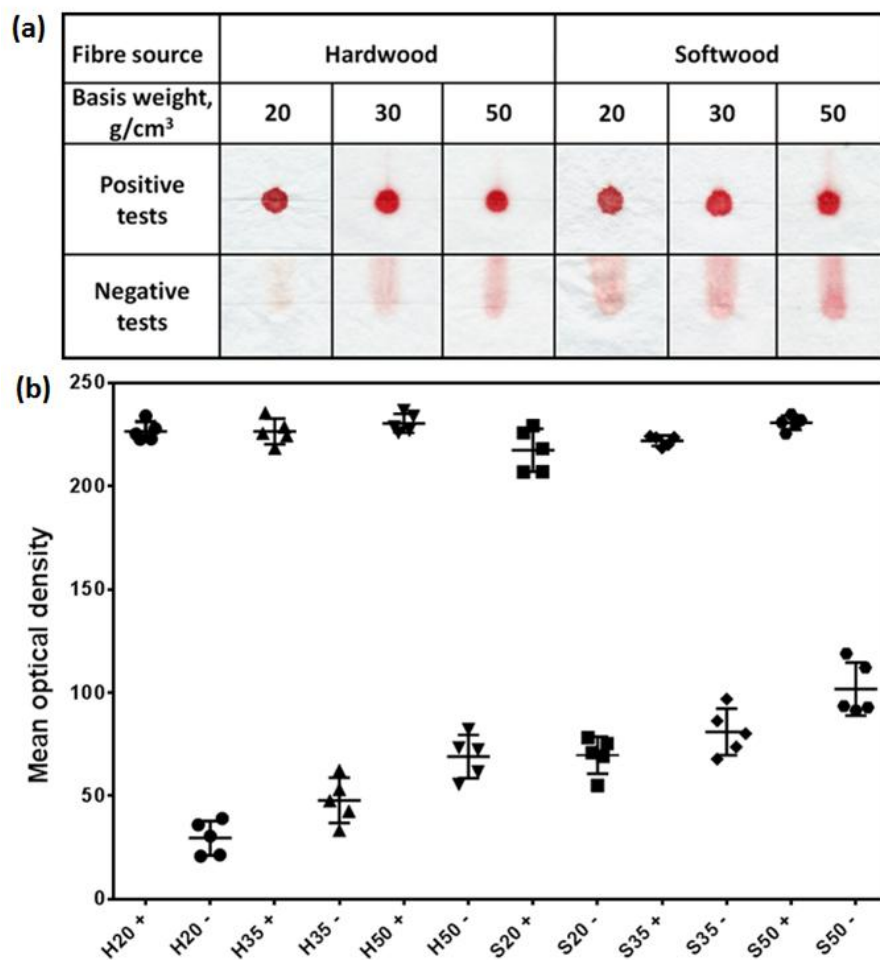


**Figure 4.** Lateral chromatographic elution blood typing tests using papers of different basis weights: (a) scanned images of testing results; (b) mean optical densities of positive (+) and negative (-) tests. H – hardwood fibres; S - softwood fibres. The numbers after H and S are the basis weights of papers in g/m<sup>2</sup>.



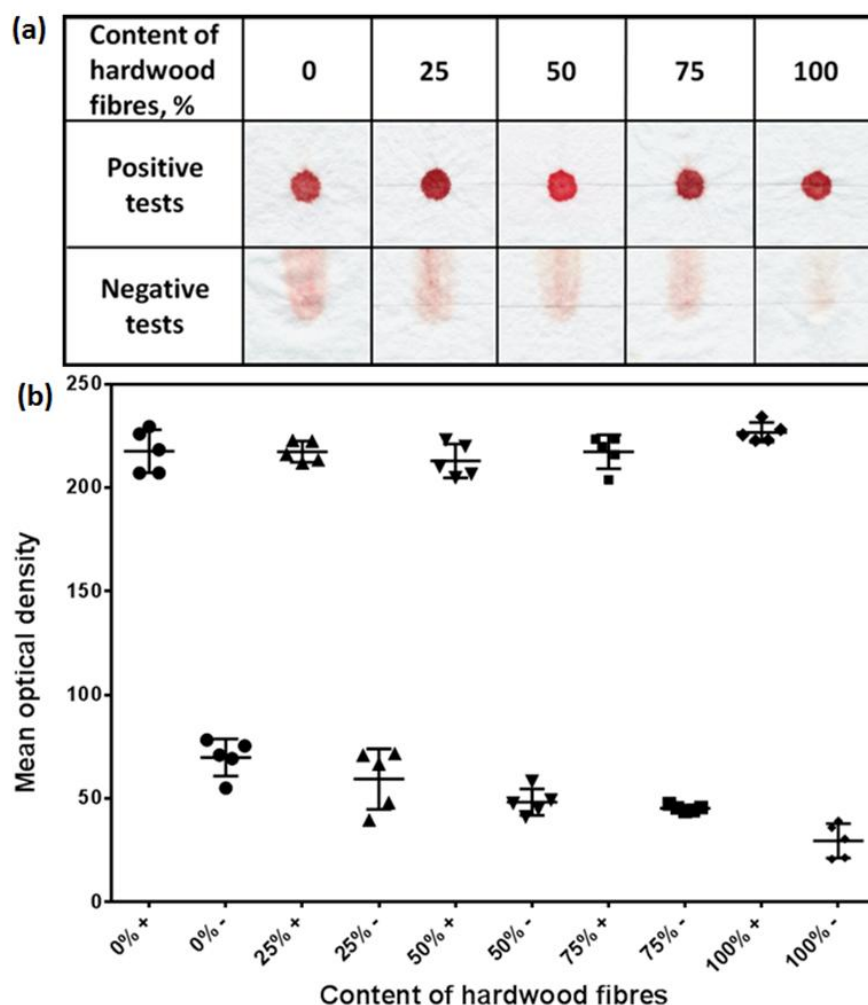


**Figure 5.** Lateral chromatographic elution blood typing tests using paper with different content of hardwood fibres: (a) scanned images of testing results; (b) Mean optical densities of positive (+) and negative (-) tests.

From Figure 4a, the positive and negative results for the 20 g/m<sup>2</sup> hardwood paper had the highest clarity judged by naked eye, whereas the results for the 50 g/m<sup>2</sup> softwood sheet had the lowest clarity. Quantitative analysis of optical density of the blood spotting area is given in Figure 4b and Table 3 in the Supporting Information. The optical densities of all positive tests were high and not significantly affected by either sheet basis weight or fibre type. However, the optical density of all negative tests increased substantially with an increase in sheet basis weight. In addition, the scanned images of chromatographic elution blood spots on handsheets containing different percentages of softwood fibres (Figure 5a) show that although the positive tests on all sheets have high optical density (Table 4), the optical density of negative results

increases with the increase in softwood fibre content; this reduces the clarity of the negative tests. Therefore, for sheets of the same basis weight, their chromatographic elution performance reduces as the content of the softwood fibre in the sheet increases.

To interpret the above results, the following points are considered. First, the reason why positive tests are less affected by the physical structure of paper sheets is because the RBC reacted with the corresponding antibody and agglutinated into large aggregates. Our previous confocal microscopy study revealed that agglutinated RBC aggregates were immobilized inside the fibre network through entrapment in inter-fibre gaps and adhesion to the fibre surface [29, 37]. Those immobilized RBC aggregates could not be moved by capillary-driven buffer elution. Therefore, the physical properties of paper sheets have a weak influence on the clarity of positive tests performed using the chromatographic elution method.

Second, the physical structure of the paper substrate plays a significant role in the elution of non-agglutinated RBCs in a negative test using the chromatographic elution method. Mercury intrusion results of handsheets made with different fibres and mixed fibres showed that most internal pores of all sheets are sufficiently large for free RBCs to pass through. However, the internal pore structures became more complicated as the content of softwood fibres increased (Figure 3c and Figure 5) and as the sheet basis weight increased (Figure 3a, b and Figure 4). Because the movement of RBCs in the fibre network is driven by the capillary flow of the plasma phase, it will be slowed down when the network becomes more complex.

Roberts et al [38]. showed that the penetration of aqueous liquid in paper was by film flow. V-shaped micro-grooves formed by the inter-fibre gaps constitute a major group of channels for liquid transport in paper. Their model shows that liquid wicking along a fibre gap is interrupted or stopped when the liquid wicking front hits the discontinuity of a V-groove channel. Roberts et al. showed that fibre-fibre crossing points could be points of discontinuity, which could cause the liquid wicking front to stop and then change to another channel to continue the wicking [38]. In our study of blood wicking in paper, RBCs are likely to be caught at the fibre-fibre crossing points where the buffer wicking front hits points of discontinuity. This will increase the chance for more

and more RBCs to be left behind the buffer wicking front, reducing the clarity of a negative blood typing assay by chromatographic elution.

Softwood fibres are approximately three times longer and are thicker than hardwood fibres [39]. In a paper sheet, a single softwood fibre may have more fibre-fibre crossing points than a single hardwood fibre because of the greater length of the former. He et al. and Batchelor et al. proposed a new analytical model that links the paper sheet cross-sectional properties of the fibres in the sheet to the number of fibre-fibre crossing points per unit length of fibre; their modeling work concluded that the number of fibre-fibre crossing points along a single softwood fibre in a sheet is greater than that along a hardwood fibre [37, 40]. This greater number leads to a larger number of liquid flow discontinuities along a single softwood fibre than a single hardwood fibre. Because of the greater width of a softwood fibre compared with a hardwood fibre, the fibre-fibre contact area of two crossing softwood fibres is greater than those of two crossing hardwood fibres. Therefore, fibre-fibre crossings formed by softwood fibres present more substantial discontinuities to the liquid flow and RBC migration. In this study, the observed more complex internal pore structures of softwood fibre sheets agree with the above analysis. Therefore, buffer wicking in paper sheets with higher softwood fibre content will meet a greater number of discontinuities. This creates more obstacles to the elution of free RBCs, resulting in negative elution blood typing with low clarity. Increasing the sheet basis weight has a similar effect.

In summary, paper's physical structure affects the clarity of positive tests of chromatographic elution blood typing relatively weakly, but affects the clarity of negative tests significantly. Our investigation shows that paper sheets of low basis weight and high hardwood fibre content provide greater assay clarity for chromatographic elution blood typing. The results from this study provide a guide for the future investigation of paper chemical effects on elution blood typing.

#### **4.5.4 Effect of Paper Physical Structure on Vertical Flow-Through Blood Typing Performance**

An advantage of the flow-through test over the lateral elution test in practical blood typing application is its rapidness; test results can be read immediately after rinsing. The mechanism of buffer rinsing and buffer elution is different, and the influence of paper properties on the clarity of flow-through rinsing results is thus different.

For the buffer rinsing method, the buffer does not just enter the pores in a paper sheet by capillary wicking. Instead, when a drop of buffer is added to the blood spot on paper surface, it floods the blood spot. Because the agglutination of RBCs by their corresponding antibodies is a reversible process, some large lumps of agglutinated RBCs may dissociate into smaller ones or even to free RBCs when flooded by buffer, and flushed away by the rinsing buffer. Figure 6a shows that the color densities of positive assays obtained using the rinsing method are weaker than those obtained using the elution method for the same handsheets, whereas the clarity of negative assays was improved.

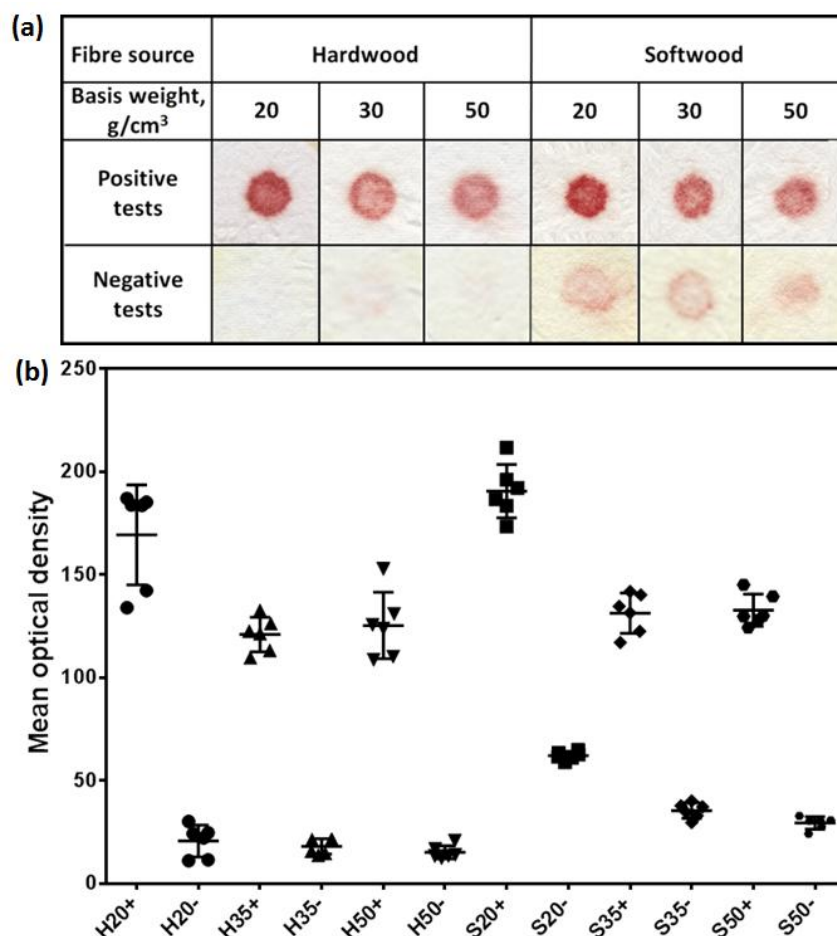


**Figure 6.** Vertical flow-through blood typing tests using paper of different basis weights: (a) scanned images of testing results; (b) Mean optical densities of positive (+) or negative (-) tests. H - hardwood fibres; S - softwood fibres. The numbers after H and S are basis weight of papers in g/m<sup>2</sup>.

The antibody concentration in the paper sheet is likely to be the major factor affecting the color density of positive assays. Because buffer rinsing can cause the dissociation of agglutinated RBCs, a higher antibody concentration in the sheet will resist such dissociation by shifting the equilibrium toward the RBC agglutination. In the antibody treatment of the sheets, the same quantity of antibody solutions were added to sheets of different basis weights, which have different thickness (Figure 1a). Our experimental observation showed no significant difference in sizes of antibody-wetted areas on sheets of different basis weights. Considering that low basis weight sheets have low thickness, the antibody would be distributed in a smaller volume; the antibody concentration in low basis weight sheets is likely to be higher than that in high basis weight sheets. Because the RBC agglutination is controlled by the equilibrium involving the antibody concentration, it is expected that the RBC agglutination on the 20 g/m<sup>2</sup> sheets would be the strongest. The results of optical density for positive tests in Figure 6 and Table 5 (in Supporting Information) support this analysis. For the rinsing method, the blood spot color densities of positive assays on sheets of different basis weights are different. This trend is different from that observed for the elution method. The slightly higher optical density of positive result on 20 g/m<sup>2</sup> softwood than on 20 g/m<sup>2</sup> hardwood sheets can be attributed to the higher complexity of the internal pore structure in the softwood sheet compared with the hardwood sheet; complex pore structures make the movement of agglutinated RBCs in fibre network difficult.

For negative assays, hardwood fibre sheets show higher clarity than do softwood fibre sheets. This result can also be attributed to the structures of the fibre network. The less complex pore structures of hardwood fibres allow easy movement of RBCs with the rinsing buffer to travel through the sheets. Again, the more complex pore structure of the softwood fibre sheets makes RBC movement more difficult.

The blood typing assay performances of all 20 g/m<sup>2</sup> mixed fibre sheets are shown in Figure 7. According to the above analysis, it can be understood that color density of all

positive assays is not significantly dependent on fibre mixing. However, the color density of negative assays is affected by the content of softwood fibres because of the increasing complexity in the sheet pore structure as the softwood fibre content increases.

In summary, the future design of paper sheets for buffer rinsing or flow-through blood typing sensors will need to follow the principle using low basis weight sheet with low softwood fibres.

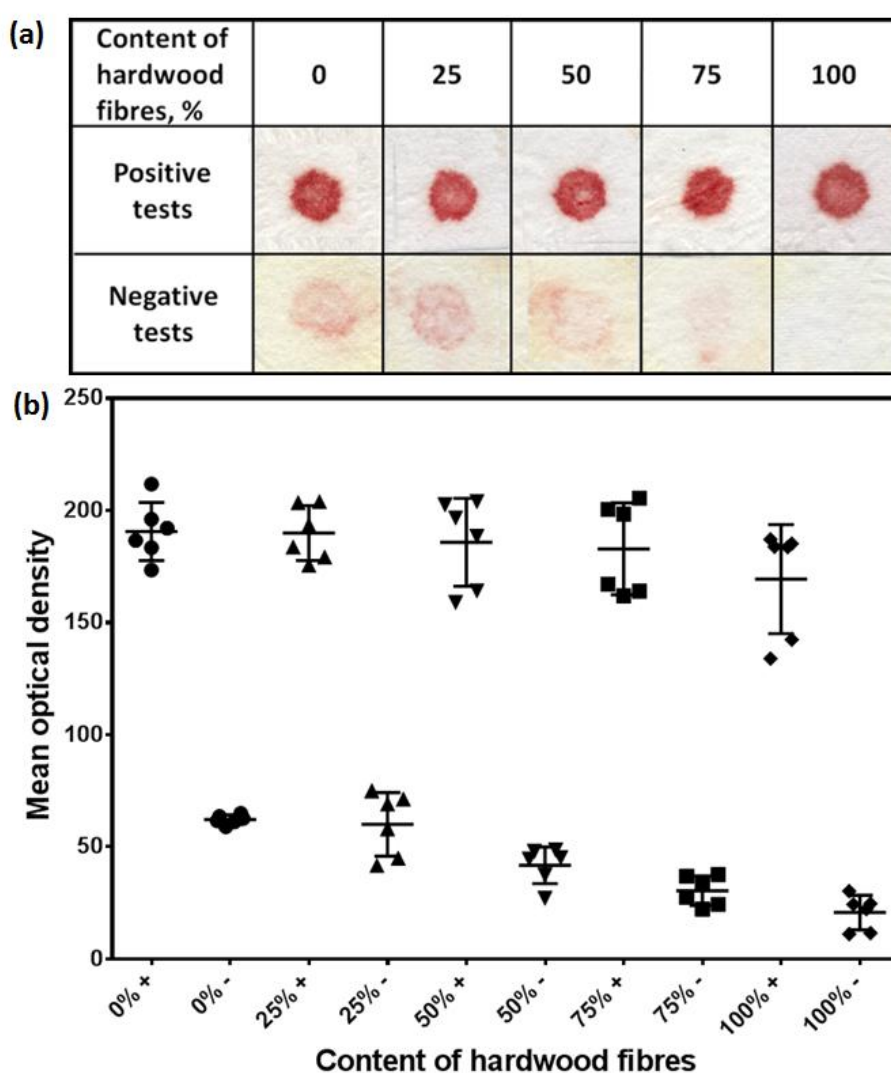


**Figure 7.** Vertical flow-through blood typing tests using paper of different content of hardwood fibres: (a) scanned images of testing results; (b) Mean optical densities of positive (+) or negative (-) tests.

### 4.6 CONCLUSIONS

In this study, we identified two important paper sheet physical properties that significantly influence the RBC transport behaviour in paper: the fibre type and the sheet's internal pore structures. These properties must be controlled in paper sheet design for blood analysis applications. Low basis weight papers made with hardwood fibres have high porosities (i.e., the void fraction) and a simple internal pore structure. These properties, particularly the simple internal pore structure, allow the easy transport of RBCs in paper. Sensors made with such paper deliver high-clarity assay results. However, papers made with softwood fibres have lower porosity, and mercury porosimetry data revealed more complex sheet internal pore structures. Complex pore structures do not allow the easy transport of RBCs; thus, paper sheets made of softwood fibres have an inferior blood typing performance compared with sheets made of hardwood fibres. Our analysis suggests that the number of fibre-fibre contacts along a single fibre in a sheet is likely to be a significant factor that affects the RBC transport. This analysis is made based on the aqueous liquid flow pattern in paper that was previously reported. The liquid penetration front in a fibre network may be slowed down when it hits a discontinuity in its flow path, and fibre-fibre contacts in paper were identified by Roberts et al. as discontinuities for liquid penetration. Softwood fibres are much longer and thicker than hardwood fibres; the number of fibre-fibre contacts on a single softwood fibre is therefore greater than those on a single hardwood fibre in a paper sheet. RBC transport in softwood paper is therefore more difficult. The finding of this work will be used as a guide for future paper sheet design for paper-based blood analysis sensors.

For future work, more pulping and papermaking parameters including refining and addition of papermaking chemicals could be investigated.

### 4.7 SUPPORTING INFORMATION

**Table 1.** Basis weight, thickness and bulk of hardwood and softwood handsheets.

Type of paper	Basis weight (g/m <sup>2</sup> )	Thickness (μm)	Bulk (cm <sup>3</sup> /g)
<b>H20</b>	20.5	84.85 ± 1.46	4.13 ± 0.04
<b>H35</b>	35.4	129.40 ± 2.77	3.60 ± 0.06
<b>H50</b>	51.2	171.88 ± 3.19	3.36 ± 0.07
<b>S20</b>	20.5	80.20 ± 2.99	3.88 ± 0.13
<b>S35</b>	35.6	119.8 ± 2.91	3.37 ± 0.09
<b>S50</b>	51.4	157.8 ± 4.15	3.07 ± 0.07

**Table 2.** Basis weight, thickness and bulk of handsheets made from different content of hardwood and softwood fibres.

Content of hardwood fibres	Basis weight (g/m <sup>2</sup> )	Thickness (μm)	Bulk (cm <sup>3</sup> /g)
<b>0%</b>	20.5	80.20 ± 2.99	3.88 ± 0.13
<b>25%</b>	20.2	81.84 ± 4.00	4.06 ± 0.24
<b>50%</b>	19.7	85.20 ± 2.38	4.33 ± 0.11
<b>75%</b>	19.8	84.40 ± 2.16	4.26 ± 0.11
<b>100%</b>	20.5	84.85 ± 1.46	4.13 ± 0.04

**Table 3.** Mean optical density of positive or negative lateral chromatographic elution blood typing tests using paper with different basis weights. Standards deviation is from five measurements.

Type of paper	Positive test	Negative test	Difference	P value <sup>1</sup>
<b>H20</b>	226.7 ± 2.1	29.5 ± 3.7	197.2 ± 4.3	< 0.0001
<b>H35</b>	226.7 ± 2.8	47.8 ± 4.9	178.8 ± 5.6	< 0.0001
<b>H50</b>	230.5 ± 2.1	69.0 ± 4.7	161.5 ± 5.1	< 0.0001
<b>S20</b>	217.5 ± 4.6	69.7 ± 4.0	147.8 ± 6.1	< 0.0001
<b>S35</b>	222.1 ± 1.1	81.0 ± 5.0	141.1 ± 5.2	< 0.0001



<b>S50</b>	230.9 ± 1.5	101.8 ± 5.8	129.1 ± 6.0	< 0.0001
<b>P value<sup>2</sup> = 0.0116    P value<sup>2</sup> &lt; 0.0001</b>				

P value<sup>1</sup> is from unpaired two-tailed t test. P value<sup>2</sup> is from one way ANOVA. P value < 0.05 considered significant.

**Table 4.** Mean optical density of positive or negative lateral chromatographic elution blood typing tests using paper made from different content of hardwood fibres.

Standards deviation is from five measurements.

<b>Content of hardwood fibres</b>	<b>Positive test</b>	<b>Negative test</b>	<b>Difference</b>	<b>P value<sup>1</sup></b>
<b>0%</b>	217.5 ± 4.6	69.7 ± 4.0	147.8 ± 6.1	< 0.0001
<b>25%</b>	217.3 ± 2.3	59.3 ± 6.5	158.0 ± 6.9	< 0.0001
<b>50%</b>	212.9 ± 3.7	48.2 ± 2.8	164.6 ± 4.6	< 0.0001
<b>75%</b>	217.3 ± 3.6	45.2 ± 0.7	172.0 ± 3.7	< 0.0001
<b>100%</b>	226.7 ± 2.1	29.5 ± 3.7	197.2 ± 4.3	< 0.0001
<b>P value<sup>2</sup> = 0.1040    P value<sup>2</sup> &lt; 0.0001</b>				

P value<sup>1</sup> is from unpaired two-tailed t test. P value<sup>2</sup> is from one way ANOVA. P value < 0.05 considered significant

**Table 5.** Mean optical density of positive or negative vertical washing blood typing tests using paper with different basis weights. Standards deviation is from six measurements.

<b>Type of paper</b>	<b>Positive test</b>	<b>Negative test</b>	<b>Difference</b>	<b>P value<sup>1</sup></b>
<b>H20</b>	169.4 ± 9.9	20.6 ± 3.1	148.7 ± 10.4	< 0.0001
<b>H35</b>	121.0 ± 3.4	18.1 ± 1.5	102.9 ± 3.8	< 0.0001
<b>H50</b>	125.3 ± 6.6	15.1 ± 1.3	110.2 ± 6.7	< 0.0001
<b>S20</b>	190.6 ± 5.3	62.1 ± 0.8	128.5 ± 5.4	< 0.0001
<b>S35</b>	131.3 ± 4.0	35.4 ± 1.5	95.9 ± 4.3	< 0.0001
<b>S50</b>	132.8 ± 3.2	29.4 ± 1.2	103.4 ± 3.4	< 0.0001
<b>P value<sup>2</sup> &lt; 0.0001</b>		<b>P value<sup>2</sup> &lt; 0.0001</b>		

P value<sup>1</sup> is from unpaired two-tailed t test. P value<sup>2</sup> is from one way ANOVA. P value<0.05 considered significant

**Table 6.** Mean optical density of positive or negative vertical washing blood typing tests using paper made from different content of hardwood fibres. Standards deviation is from five measurements.

Content of hardwood fibres	Positive test	Negative test	Difference	P value <sup>1</sup>
0%	190.6 ± 5.3	62.1 ± 0.8	128.5 ± 5.4	< 0.0001
25%	189.9 ± 5.0	60.0 ± 5.8	129.9 ± 7.6	< 0.0001
50%	185.8 ± 8.0	41.8 ± 3.4	144.1 ± 8.7	< 0.0001
75%	182.9 ± 8.4	30.3 ± 2.7	152.6 ± 8.8	< 0.0001
100%	169.4 ± 9.9	20.6 ± 3.1	148.7 ± 10.4	< 0.0001
<b>P value<sup>2</sup>= 0.2995    P value<sup>2</sup>&lt; 0.0001</b>				

P value<sup>1</sup> is from unpaired two-tailed t test. P value<sup>2</sup> is from one way ANOVA. P value<0.05 considered significant

## 4.8 ACKNOWLEDGEMENTS

This work is supported by Australian Research Council Grants (ARC DP1094179 and LP110200973). Authors thank Haemokinesis for its support through an ARC Linkage Project. Ms Lizi Li thanks the Monash University Research and Graduate School and the Faculty of Engineering for postgraduate research scholarships.

## 4.9 REFERENCES

- [1] X. Li, D.R. Ballerini, W. Shen, A perspective on paper-based microfluidics: current status and future trends, *Biomicrofluidics* 6 (2012) 11301-1130113.
- [2] K. Abe, K. Kotera, K. Suzuki, D. Citterio, Inkjet-printed paper fluidic immuno-chemical sensing device, *Anal Bioanal Chem* 398 (2010) 885-893.

- [3] J.L. Delaney, C.F. Hogan, J. Tian, W. Shen, Electrogenerated chemiluminescence detection in paper-based microfluidic sensors, *Analytical Chemistry* 83 (2011) 1300-1306.
- [4] J.L. Delaney, E.H. Doeven, A.J. Harsant, C.F. Hogan, Use of a mobile phone for potentiostatic control with low cost paper-based microfluidic sensors, *Analytica Chimica Acta* 790 (2013) 56-60.
- [5] Y. Zhu, X. Xu, N.D. Brault, A.J. Keefe, X. Han, Y. Deng, J. Xu, Q. Yu, S. Jiang, Cellulose paper sensors modified with zwitterionic poly(carboxybetaine) for sensing and detection in complex media, *Analytical Chemistry* 86 (2014) 2871-2875.
- [6] K. Joo-Hyung, M. Seongcheol, U.K. Hyun, Y. Gyu-Young, K. Jaehwan, Disposable chemical sensors and biosensors made on cellulose paper, *Nanotechnology* 25 (2014) 092001.
- [7] T.-K. Kang, Tunable piezoresistive sensors based on pencil-on-paper, *Applied Physics Letters* 104 (2014) 073117-073117-073113.
- [8] M.S. Khan, G. Thouas, W. Shen, G. Whyte, G. Garnier, Paper Diagnostic for instantaneous blood typing, *Analytical Chemistry* 82 (2010) 4158-4164.
- [9] E.W. Nery, L.T. Kubota, Sensing approaches on paper-based devices: a review, *Anal Bioanal Chem* 405 (2013) 7573-7595.
- [10] M. Santhiago, E.W. Nery, G.P. Santos, L.T. Kubota, Microfluidic paper-based devices for bioanalytical applications, *Bioanalysis* 6 (2014) 89-106.
- [11] R. Pelton, Bioactive paper provides a low-cost platform for diagnostics, *Trends in Analytical Chemistry* 28 (2009) 925-942.
- [12] C.J. Biermann, *Handbook of Pulping and Papermaking*, Second Edition ed., Academic Press 1996.
- [13] M. Ek, G. Gellerstedt, G. Henriksson, *Paper Chemistry and Technology*, Walter de Gruyter, Germany, 2009.
- [14] X. Li, J. Tian, T. Nguyen, W. Shen, Paper-based microfluidic devices by plasma treatment, *Analytical Chemistry* 80 (2008) 9131-9134.
- [15] X. Li, J. Tian, G. Garnier, W. Shen, Fabrication of paper-based microfluidic sensors by printing, *Colloids and Surfaces B: Biointerfaces* 76 (2010) 564-570.

- [16] A.W. Martinez, S.T. Phillips, M.J. Butte, G.M. Whitesides, Patterned paper as a platform for inexpensive, low-volume, portable bioassays, *Angewandte Chemie* 119 (2007) 1340-1342.
- [17] D. Ballerini, X. Li, W. Shen, Patterned paper and alternative materials as substrates for low-cost microfluidic diagnostics, *Microfluidics and Nanofluidics* 13 (2012) 769-787.
- [18] M. Al-Tamimi, W. Shen, R. Zeineddine, H. Tran, G. Garnier, Validation of paper-based assay for rapid blood typing, *Anal Chem* 84 (2012) 1661-1668.
- [19] M.S. Li, J.F. Tian, M. Al-Tamimi, W. Shen, Paper-based blood typing device that reports patient's blood type "in writing", *Angewandte Chemie-International Edition* 51 (2012) 5497-5501.
- [20] H. Li, D. Han, G.M. Pauletti, A.J. Steckl, Blood coagulation screening using a paper-based microfluidic lateral flow device, *Lab on a Chip* 14 (2014) 4035-4041.
- [21] C.H. Lee, L. Tian, S. Singamaneni, Paper-based SERS swab for rapid trace detection on real-world surfaces, *ACS Applied Materials & Interfaces* 2 (2010) 3429-3435.
- [22] M.O. Noor, U.J. Krull, Paper-based solid-phase multiplexed nucleic acid hybridization assay with tunable dynamic range using immobilized quantum dots as donors in fluorescence resonance energy transfer, *Analytical Chemistry* 85 (2013) 7502-7511.
- [23] M. Ek, G. Gellerstedt, G. Henriksson, *Paper Products Physics and Technology*, Walter de Gruyter, Germany, 2009.
- [24] K.J. Niskanen, *Paper physics*, Fapet Oy, Helsinki, Finland, 1999.
- [25] P. Jarujamrus, J.F. Tian, X. Li, A. Siripinyanond, J. Shiowatana, W. Shen, Mechanisms of red blood cells agglutination in antibody-treated paper, *Analyst* 137 (2012) 2205-2210.
- [26] G. Daniels, M.E. Reid, Blood groups: the past 50 years, *Transfusion* 50 (2010) 281-289.
- [27] J.K.M. Duguid, I.M. Bromilow, New technology in hospital blood technology in hospital blood banking, *Journal of Clinical Pathology* 46 (1993) 585-588.
- [28] G. Daniels, I.M. Bromilow, *Essential Guide to Blood Groups*, Wiley-Blackwell: Chichester, West Sussex, UK, 2010.

- [29] L. Li, J. Tian, D. Ballerini, M. Li, W. Shen, A study of the transport and immobilisation mechanisms of human red blood cells in a paper-based blood typing device using confocal microscopy, *Analyst* 138 (2013) 4933-4940.
- [30] H. Paulapuro, *Papermaking Part 1, Stock Preparation and Wet End*, 2nd Edition ed., Fapet, Helsinki, Finland, 2008.
- [31] R. Alén, *Papermaking Chemistry*, Fapet, Helsinki, Finland, 2007.
- [32] J. Levlin, L. Soderhjelm, *Pulp and Paper Testing*, Fapet, Helsinki, Finland, 1999.
- [33] J. Silvy, C. Pannier, J. Veyre, 16th Eucepa Conference Proceedings Pairs, 1976.
- [34] P.A. Webb, C. Orr, *Analytical Methods in Fine Particle Technology*, 1997.
- [35] W.H. Reinhart, S. Chien, Roles of cell geometry and cellular-viscosity in red-cell passage through narrow pores, *American Journal of Physiology* 248 (1985) C473-C479.
- [36] X. Gong, K. Sugiyama, S. Takagi, Y. Matsumoto, The deformation behaviour of multiple red blood cells in a capillary vessel, *Journal of Biomechanical Engineering* 131 (2009) 074504-074504.
- [37] W.J. Batchelor, J. He, W.W. Sampson, Inter-fibre contacts in random fibrous materials: experimental verification of theoretical dependence on porosity and fibre width, *Journal of Materials Science* 41 (2006) 8377-8381.
- [38] R.J. Roberts, T.J. Senden, M.A. Knackstedt, M.B. Lyne, Spreading of Aqueous Liquids in Unsized Papers is by Film Flow, *Journal of Pulp and Paper Science* 29 (2003) 123-131.
- [39] P. Fardim, *Chemical Pulping*, Fapet, Helsinki, Finland, 1999.
- [40] J. He, W. Batchelor, R. Johnston, An analytical model for number of fibre–fibre contacts in paper and expressions for relative bonded area (RBA), *Journal of Materials Science* 42 (2007) 522-528.

**This page is intentionally blank**

---

## **Part II**

### ***Blood Typing Devices Based on Liquid Micro Reactors***

---

The second part of this thesis presents investigations of the use of liquid micro reactors fabricated from superhydrophobic materials to build low-cost blood typing devices. The reactors are based on the concept of a miniaturized reaction system. These investigations were motivated by our pursuit of the development of novel low-cost blood typing devices with the potential of automation and high throughput operation. This research can potentially benefit blood bank laboratories and hospitals, where large numbers of blood samples need to be grouped.

The most challenging sections of this research were to design and fabricate liquid micro reactors, and to provide the liquid micro reactors with the capability of high-throughput blood typing. The first difficulty has been successfully overcome in two ways: one is a superhydrophobic surface-supported liquid; the other is a liquid marble wrapped in superhydrophobic powder. These approaches are presented in Chapters 6 and 7, respectively. To overcome the second challenge, we combined the liquid micro reactor with image capture and processing techniques to analyse the RBC haemagglutination reaction inside the liquid micro reactor. Since the near-spherical liquid micro reactor is able to provide an excellent side view, it is much easier to obtain and analyze the magnified images of RBC haemagglutination.

Our blood typing devices based on liquid micro reactors fabricated from superhydrophobic materials have the following two main features. First, blood typing devices based on liquid micro reactors have advantages over paper-based blood typing devices. For example, as they are especially designed for high-throughput blood typing, their processes are more easily automated for assay result interpretation, data storage, and transmission. Second, we believe that the concept of the superhydrophobicity-based liquid micro reactor can also be applied to chemical and biological assays.



---

## **Chapter 5**

***Superhydrophobic Surface Supported Bioassay –  
An Application in blood Typing***

---

**This page is intentionally blank**

**Monash University**

**Declaration for Thesis Chapter 5**

**Declaration by candidate**

In the case of Chapter 5, the nature and extent of my contribution to the work was the following:

<b>Nature of contribution</b>	<b>Extent of contribution (%)</b>
Initiation, key ideas, experimental works, analysis of results, writing up	43

The following co-authors contributed to the work. If co-authors are students at Monash University, the extent of their contribution in percentage terms must be stated:

<b>Name</b>	<b>Nature of contribution</b>	<b>Extent of contribution (%) for student co-authors only</b>
<b>Junfei Tian</b>	Initiation, key ideas, experimental works, analysis of results, writing up	43
<b>Miaosi Li</b>	Assisted in experimentation	5
<b>Wei Shen</b>	Key ideas, reviewing and editing of the paper	Supervisor

The undersigned hereby certify that the above declaration correctly reflects the nature and extent of the candidate's and co-authors' contributions to this work\*.

<b>Candidate's Signature</b>		<b>Date</b> <b>25-Sep-2015</b>
------------------------------	---	-----------------------------------

<b>Main Supervisor's Signature</b>		<b>Date</b> <b>25-Sep-2015</b>
------------------------------------	--	-----------------------------------

\*Note: Where the responsible author is not the candidate's main supervisor, the main supervisor should consult with the responsible author to agree on the respective contributions of the authors.

**This page is intentionally blank**

# **Superhydrophobic Surface Supported Bioassay – An Application in Blood Typing**

*Lizi Li, Junfei Tian, Miaosi Li and Wei Shen\**

Department of Chemical Engineering,  
Monash University, Clayton Campus, Vic. 3800, Australia

\*

This paper has been published in *Colloids and Surfaces B: Biointerfaces*

## **5.1 ABSTRACT**

This study presents a new application of superhydrophobic surfaces in conducting biological assays for human blood typing using a liquid drop micro reactor. The superhydrophobic substrate was fabricated by a simple printing technique with Teflon powder. The non-wetting and weak hysteresis characteristics of superhydrophobic surfaces enable the blood and antibody droplets to have a near-spherical shape, making it easy for the haemagglutination reaction inside the droplet to be photographed or recorded by a digital camera and then analysed by image analysis software. This novel blood typing method requires only a small amount of blood sample. The evaluation of assay results using image analysis techniques offers potential to develop high throughput operations of rapid blood typing assays for pathological laboratories. With the capability of identifying detailed red blood cell agglutination patterns and intensities, this method is also useful for confirming blood samples that have weak red blood cell antigens.

## **5.2 KEYWORDS**

Superhydrophobic surface; liquid drop micro reactor; bioassay; blood typing; digital image analysis

### 5.3 INTRODUCTION

The superhydrophobic phenomenon and fabrication of artificial superhydrophobic surfaces have attracted intense research in recent years. The strong water-repellent property of superhydrophobic surfaces forces water droplets to assume large contact angles ( $>150^\circ$ ) and can be designed to have very weak hysteresis on those surfaces [1-4]. Superhydrophobic surfaces have many practical applications such as self-cleaning [5, 6], anti-wetting [7], water-repellence [8, 9], oil-water separation [10], anti-freezing [4] and fluid-drag reduction [11].

While numerous studies have been directed towards the fabrication and applications of superhydrophobic surfaces for water-repellence, anti-wetting and oil-water separation, some research works have focused on utilizing the water droplet supported by superhydrophobic surfaces for practical applications. The non-wetting and weak hysteresis characteristics of superhydrophobic surfaces enables a lab-on-chip analytical sensor to be designed; aqueous droplets containing analytes can be manipulated for analytical purposes, such as sample storage, transport, mixing and splitting on a lab-on-chip device [12]. More recently, several researchers explored the use of aqueous droplets on superhydrophobic pedestals as a micro-scale reactor to perform chemical reactions and the growth of crystals [13, 14].

The near-spherical shape of an aqueous droplet on a superhydrophobic surface allows for a sufficient elevation of its centre of gravity so that a micro-scale physical transformation or biochemical reaction occurring inside the droplet can be clearly observed and recorded from the side view. The superhydrophobic surface supported micro-scale analytical or diagnostic reactors require materials of low-cost and are easy to be transformed into an automated high volume biochemical assays. To date, however, there is little information about superhydrophobic surface supported biochemical assays in literature.

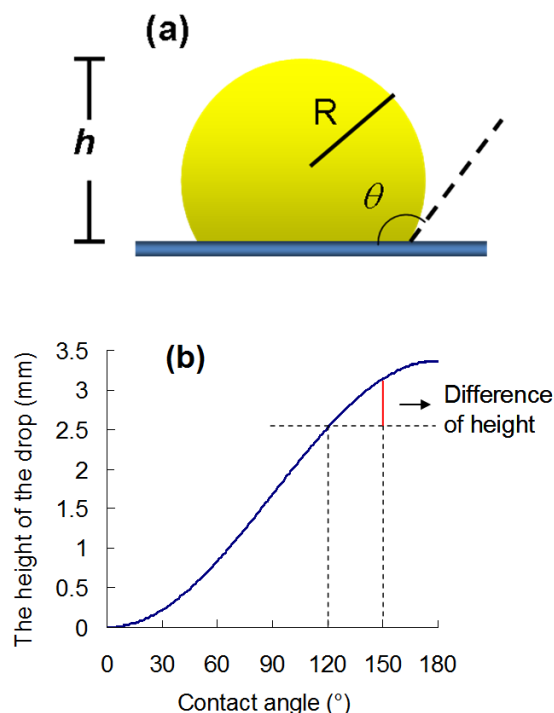


**Figure 1.** (a) scheme of the side-view profile of a water droplet on a (super-) hydrophobic surface ( $R$  and  $h$  are the radius and the height of the droplet, respectively;  $\theta$  is the contact angle); (b) A plot of the height of a 20  $\mu\text{L}$  droplet on a supporting surface with respect of its contact angle with the surface (gravity effect is not considered). The red line shows the difference of the heights of water droplets on a hydrophobic surface ( $\theta = 120^\circ$ ) and a superhydrophobic surface ( $\theta = 150^\circ$ ).

To clearly observe a living reaction inside an aqueous droplet from the side view, the droplet needs to have a sufficient height on the supporting surface; for this reason a hydrophobic surface or a superhydrophobic surface is required. Eq. (1) and Figure 1a describe the height of a droplet and its contact angle with the supporting surface.

$$h = R [1 + \sin (\theta - 90^\circ)] \quad (1)$$

where  $h$  is the height of the drop,  $R$  is the radius of the drop and  $\theta$  is the contact angle of the drop on the surface. If the gravity effect is neglected, the height of a drop on a surface can be calculated by Eq. (1). Figure 1b shows the plot of the droplet height and its contact angle with the supporting surface. For a droplet having a radius of 1.68 mm ( $\sim 20 \mu\text{L}$ ) on a hydrophobic surface ( $\theta = 120^\circ$ ), the height is 2.52 mm. For the same droplet on a superhydrophobic surface ( $\theta = 150^\circ$ ), the height of the droplet increases

3.13 mm. The difference in droplet height on superhydrophobic and hydrophobic surfaces is moderate, and further increase in contact angle beyond  $150^\circ$  results in only a very small increase in droplet height. Therefore, for the purpose of only acquiring side views of a droplet, a highly hydrophobic surface would be sufficient. However, a significant advantage of using superhydrophobic surface for biochemical assay is that the liquid sample can easily roll off the surface after test; this prevents the surface from being contaminated. For some assays, this advantage may be important, since the superhydrophobic supporting surface may be reused. This highly useful function of superhydrophobic surfaces needs to be further explored to enable chemical and biological reactions, and biochemical assays to be conducted in a high throughput capacity and at low cost.

In this study, we demonstrate the use of superhydrophobic surfaces for biological assays through making observations of the haemagglutination reaction of human red blood cells (RBC) and blood typing assay. Accurate and rapid typing of human blood is not only of great importance for blood transfusion and transplantation medicine [15], but also critically important for blood banking, and for screening or cross-checking donors' blood samples. For the later, in particular, high throughput methods are required to process large number of samples rapidly. Although the lateral flow and the Gel Card technologies are the mainstream technologies currently in use in hospitals and pathological laboratories, diagnostic industry has never stopped exploring new technologies [17,19-22,25-27]. In this work superhydrophobic substrate was fabricated by using a simple contact printing method developed in our laboratory [16]; the substrate is inexpensive and disposable, suitable for use as a laboratory consumable item. In a blood typing application, the haemagglutination reaction inside the blood sample droplet can be imaged by using a digital camera and suitable software can be used for the blood type identification. The use of digital camera allows photos of an assay to be kept for retrieval and analysis, and it has the potential to reveal detailed agglutination process if camera with high magnification is used. Further automation in assay result evaluation will provide a new potential method for rapid blood typing assays of high throughput operation, with the capability of providing magnified photo and video footage of the agglutination reaction, which will be of a significant diagnostic aid to the identifying of blood samples whose RBCs carry weak antigens.



### 5.4 MATERIALS AND METHODS

Teflon powder with an average particle size of 35  $\mu\text{m}$  was obtained from Sigma-Aldrich. The polymer film used in this study was a commercial overhead transparency (Xerox). A UV curable flexographic post-print varnish (UV 412) was received as a gift from Flint Inks (Flint Group Australia). Six blood samples (type A+, A-, B+, AB+, O+ and O-) were received from a pathological laboratory, following the ethical protocols. All blood samples were stored in Vacutainer<sup>®</sup> test tubes containing lithium-heparin anticoagulant at 4  $^{\circ}\text{C}$  and used within 5 days of collection. Epiclone<sup>™</sup> anti-A, anti-B and anti-D monoclonal grouping reagents were sourced commercially from the Commonwealth Serum Laboratory, Australia. Anti-A and anti-B are colour-coded cyan and yellow solutions respectively, while anti-D is a clear colourless solution. All monoclonal grouping reagents were also stored at 4  $^{\circ}\text{C}$ .

#### 5.4.1 Fabrication of Superhydrophobic Teflon Powder Surface on Polymer Film

The superhydrophobic surface on polymer film was fabricated by a contact printing method developed in our laboratory [16]. A thin layer of UV curable flexographic post-print varnish was uniformly transferred onto the transparency film with a roller. Teflon powder was then dusted onto the film and adhered to the uncured varnish. The film was then passed through a UV curing station. Upon curing, the UV varnish tightly glued the Teflon powder particles on the film. The micron-scale roughness of Teflon particles on the film formed the required superhydrophobic surface.

#### 5.4.2 Observation of Haemagglutination Reaction inside the Blood Sample Drop

Blood samples of two types, A+ and B+, were chosen to demonstrate the time dependency of haemagglutination reaction with anti-B solution inside near-spherical blood droplets supported by the superhydrophobic surface. 10  $\mu\text{L}$  of each blood sample

was placed on the superhydrophobic surface using a micropipette (Eppendorf research®). The same volume of anti-B solution was then injected into the blood droplet with a micropipette, and gently stirred with the micropipette-head. The droplets were then monitored for haemagglutination reaction for 180 seconds with a digital microscopy camera (Moticam 2500); photographs were taken at 30 second intervals from the beginning of the blood sample and antibody mixing.

### **5.4.3 Blood Typing Assay on Superhydrophobic Surfaces**

The experimental procedure of performing a blood typing assay is similar to observing the haemagglutination reaction except that three droplets of each blood sample were taken and mixed with three different antibody reagents; anti-A, anti-B and anti-D. The sample blood type can be identified from the pattern of the haemagglutination reaction(s) with the three antibodies. Photos of the sample droplets taken by the camera provide clear identification of the occurrence of a haemagglutination reaction.

A simple colour density measurement method is presented in this study to digitally determine the changes of colour intensities of the blood sample droplets after being mixed with antibody solutions. This method can potentially be used to automate this blood typing assay for high throughput applications.

## **5.5 RESULTS AND DISCUSSION**

### **5.5.1 Contact Angle Characterization of the Superhydrophic Teflon Powder Surface**

Contact angle measurements were used to characterize the printed Teflon powder surface. Water, a blood sample and antibody solutions were used as liquids for contact angle measurements. Contact angles for water, blood (A+), anti-A, anti-B and anti-D with the Teflon powder surface were determined to be  $158.6^{\circ} \pm 1.0^{\circ}$ ,  $153.1^{\circ} \pm 2.2^{\circ}$ ,  $154.1^{\circ} \pm 3.2^{\circ}$ ,  $155.8^{\circ} \pm 1.3^{\circ}$  and  $148.5^{\circ} \pm 0.2^{\circ}$ , respectively. This data is the average of 5 measurements and the standard deviations are also given.

From the contact angle data of water with the surface it can be seen that the printed Teflon powder surface was superhydrophobic since the water contact angle was significantly higher than  $150^\circ$ . The blood and antibody solutions also showed contact angles greater than or close to  $150^\circ$ . The only liquid that has the lower than  $150^\circ$  contact angle was the anti-D solution. The slightly lower contact angle of anti-D solution compared to that of the other antibody solutions may be related to its formulation being different from other antibody solutions. However, it can be found that such a small difference in contact angle between the blood sample and the antibody solutions means that there is a negligible difference in the practical application of observing haemagglutination reactions inside the sample droplets.

### 5.5.2 Observation of Haemagglutination inside the Blood Sample Droplet

To observe the haemagglutination reaction inside blood sample droplets, anti-B was introduced into two blood samples of A+ and B+ types. As anti-B was introduced into the drop of blood sample type B+, the specific antibody-antigen interaction resulted in an immediate haemagglutination of RBCs - a clear separation of agglutinated RBC lumps from the plasma phase can be observed inside the blood sample drop immediately after the anti-B introduction (Figure 2).

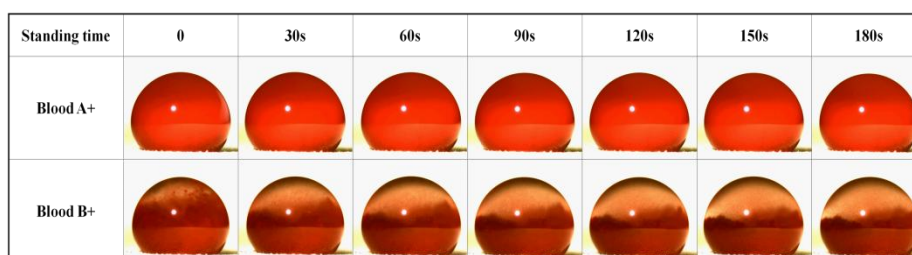


**Figure 2.** Photos of two 10  $\mu\text{L}$  blood droplets (A+ and B+) mixed with 10  $\mu\text{L}$  anti-B reagent. Haemagglutination was immediately observed inside the droplet of B+ blood sample (second row), due to the specific interaction between anti-B and the B-antigen carried by RBCs of the B+ sample. There was, however, no haemagglutination in the droplet of A+ blood sample during the entire 180s standing time (first row), since anti-B is not a specific antibody to the antigen carried by the RBCs of the A+ sample.

As time progressed to 90 seconds, the agglutination reaction led to the clearing of the top part of B+ sample droplet. Further standing of the sample to 180 seconds showed little further change in RBC separation. In contrast to the reaction of B+ blood sample with anti-B, the mixing of A+ blood sample with anti-B (a non-specific antibody) resulted in no haemagglutination reaction and therefore no separation of the RBCs inside the sample droplet (Figure 2). Haemagglutination of RBCs is the indication of the occurrence of specific interactions between the antigen present on the surface of the red blood cells and the corresponding antibody present or added in the plasma phase. Therefore haemagglutination of RBCs in the presence of blood typing antibodies provides identification of the blood type of the sample. Results in Figure 2 provide rapid and clear identification of the blood types of the samples. With the use of a digital camera, it is also possible for the captured images to be digitally analyzed to identify the blood types of the samples in an automated way for high throughput blood typing service application. Depending on the assay, the superhydrophobic substrate may be disposed of after use, or reused after allowing the sample drop to roll off the surface.

### **5.5.3 Blood Typing Using Superhydrophobic Surfaces as a Low-Cost Supporting Substrate**

The clear observation of haemagglutination reaction inside a blood sample droplet shows that a superhydrophobic substrate in general can be used to support micro reactors for biochemical assays. We further demonstrate the use of superhydrophobic surface for ABO and RhD blood typing assays. The use of superhydrophobic surfaces for blood typing may offer significant economic advantage, since the cost of such a surface is low.

Recently, low-cost paper- and thread-based blood typing platforms have been reported [15, 17-19]. Paper- and thread-based blood typing devices greatly reduce the cost and the time required for performing blood typing assays; they are particularly suitable for making user-operated devices for developing countries. As an alternative platform, superhydrophobic surface-based blood typing assays offer the following advantages: (1) Superhydrophobic surfaces combined with an imaging system allow automated high

throughput equipment to be built at a moderate to low cost. (2) Such equipment provides detailed visual haemagglutination patterns of samples, which may be further used for evaluation of haemagglutination reaction through image analysis. (3) Haemagglutination reactions inside the sample drop provide the possibility of extracting the plasma phase from the samples for other assays.

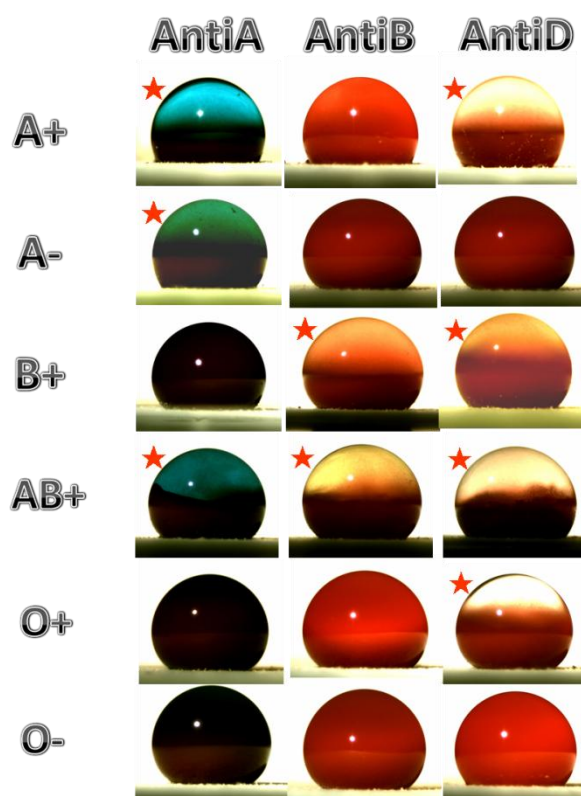


**Figure 3.** Photos of the blood agglutination of the six blood samples (A+, A-, B+, AB+, O+ and O-) when they are respectively mixed with three antibodies (Anti-A, Anti-B and Anti-D) on superhydrophobic surface. The red star represents blood aggregation was found in that photo. The blood type can be determined by observing the aggregation of blood with different antibodies.

Six blood samples were assayed using the superhydrophobic surface supported blood typing assay. For each blood sample, three sample droplets were placed on the superhydrophobic surface; these droplets were respectively mixed with anti-A, anti-B and anti-D following the protocol described in the experimental section. The samples droplets were then observed for haemagglutination reactions. Figure 3 shows images of the assaying results of the six blood samples; haemagglutination reaction can be easily identified from the photos taken from the side view of the droplets. Based on the

pattern of haemagglutination reactions in Figure 3, blood types of the samples were identified as being A+, A-, B+, AB+, O+ and O-. These results were in total agreement with the blood typing results obtained by the pathological laboratory using the Gel Card technology.

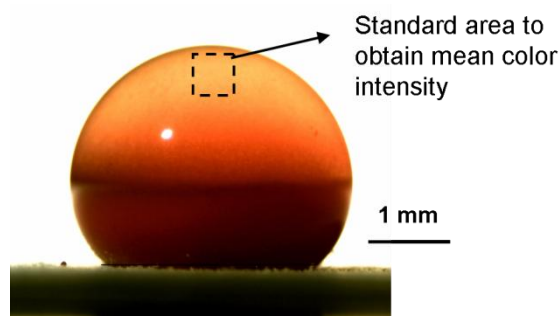


**Figure 4.** Illustration of the measurement of colour intensity (magenta channel). The blood aggregation can be detected by comparing the colour intensity of the standard area in the images of different drops. From the identified aggregation of blood caused by their corresponding antibodies, the type of blood can be determined.

**Table 1** The magenta intensity of the standard area in each image of Figure 3.

	<i>Anti-A</i>	<i>Anti-B</i>	<i>Anti-D</i>
<b>A+</b>	7.18±0.75	219.52±0.13	0.06±0.04
<b>A-</b>	70.22±2.93	253.04±0.53	253.23±0.26
<b>B+</b>	225.36±0.28	101.52±1.98	94.81±0.76
<b>AB+</b>	147.52±1.63	61.63±1.89	6.38±1.89
<b>O+</b>	219.65±0.57	253.79±0.41	0.23±0.15
<b>O-</b>	220.10±1.60	252.39±0.67	252.80±0.04

To explore the possible automation of using the superhydrophobic surface supported bioassay for high throughput blood typing assays, images in Figure 4 were digitally processed and identification of haemagglutination via image analysis was pursued by using Adobe Photoshop. The image analysis was performed on a standard square of 5 mm × 5 mm in the top part of the droplet image; the average colour intensity of the magenta channel was measured from the square. The choice of measuring the magenta channel is based on its large dynamic range [20], which is capable of providing more accurate measurement of the sample. Table 1 shows the magenta intensity of the

analyzed area of each image. The magenta colour intensity measured from the images of the sample drops shows strong contrast; samples with haemagglutination correspond to colour intensity values much lower than saturation, whereas samples with no haemagglutination show magenta colour intensity close to saturation.

In order for the haemagglutination status to be evaluated digitally, a colour intensity threshold of 180 was introduced to differentiate haemagglutination from non-haemagglutination. This threshold level was chosen as it is numerically around 40 above the highest colour intensity of the non-agglutinated sample and around 40 below the lowest colour intensity of the agglutinated sample. With this threshold level it is possible to digitally identify the haemagglutination reaction in a blood sample drop after the addition of antibody solution. The combination of the superhydrophobic supporting surface, the simple camera system and the software system presents a design concept of an automated blood typing device capable of high throughput analysis of blood samples. The digitized results obtained using this system can deliver direct blood typing result and also can be transmitted by mobile phone [21] or other electronic devices to a remote facility should it be necessary.

### 5.6 CONCLUSION

In this study we investigated a new application of using superhydrophobic surfaces to conduct biological assays. By using a superhydrophobic surface as a supporting surface for liquid droplets, a human blood typing assay was conducted. The non-wettable property of the superhydrophobic surface by blood samples and antibody solutions makes the blood and antibody droplets assume a near spherical shape, providing an excellent side view for the haemagglutination reaction to be observed inside the droplet. By observing the presence or absence of the haemagglutination reaction, specific antibody-RBC interactions can be identified; this method can be used for rapid blood typing. By using a camera and a simple image analysis system, haemagglutination inside the blood sample droplets can be digitally identified. This capability potentially makes the superhydrophobic surface supported blood typing assay suitable for high throughput assay applications. We believe that the superhydrophobic surface supported micro reactor concept can be developed into more applications for chemical or

biological assays.

### 5.7 SUPPORTING INFORMATION

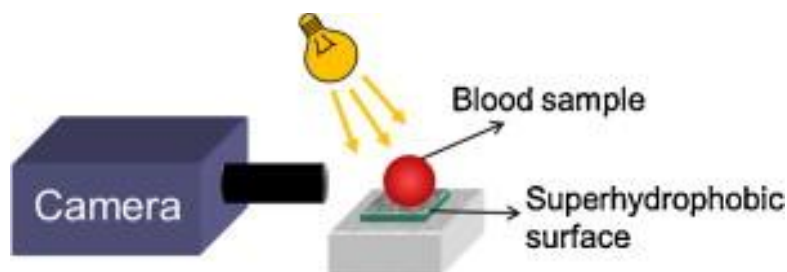


**Figure 5.** The scheme of observation and record system.

### 5.8 ACKNOWLEDGEMENTS

This work is supported by Australian Research Council Grants (ARC LP0990526 and LP110200973). Authors thank Haemokinesis for its support through an ARC Linkage Project. The authors would like to specially thank Dr. Emily Perkins, Department of Chemical Engineering and Mr Hansen Shen, student of the Faculty of Law of Monash University for proof reading the manuscript. Lizi Li, Junfei Tian and Miaosi Li thank Monash University Research and Graduate School and the Faculty of Engineering for their postgraduate research scholarships.

### 5.9 REFERENCES

- [1] X. Hong, X.F. Gao, L. Jiang, Application of superhydrophobic surface with high adhesive force in no lost transport of superparamagnetic microdroplet, *Journal of the American Chemical Society* 129 (2007) 1478-1479.
- [2] X. Zhang, F. Shi, J. Niu, Y. Jiang, Z. Wang, Superhydrophobic surfaces: from structural control to functional application, *Journal of Materials Chemistry* 18 (2008) 621-633.



- [3] A. Tuteja, W. Choi, M. Ma, J.M. Mabry, S.A. Mazzella, G.C. Rutledge, G.H. McKinley, R.E. Cohen, Designing superoleophobic surfaces, *Science* 318 (2007) 1618-1622.
- [4] X. Yao, Y. Song, L. Jiang, Applications of bio-inspired special wettable surfaces, *advanced materials* 23 (2011) 719-734.
- [5] R. Blossey, Self-cleaning surfaces - virtual realities, *Nature Materials* 2 (2003) 301-306.
- [6] V.A. Ganesh, H.K. Raut, A.S. Nair, S. Ramakrishna, A review on self-cleaning coatings, *Journal of Materials Chemistry* 21 (2011) 16304-16322.
- [7] T.L. Sun, L. Feng, X.F. Gao, L. Jiang, Bioinspired surfaces with special wettability, *Accounts of Chemical Research* 38 (2005) 644-652.
- [8] X.M. Li, D. Reinhoudt, M. Crego-Calama, What do we need for a superhydrophobic surface? A review on the recent progress in the preparation of superhydrophobic surfaces, *Chemical Society Reviews* 36 (2007) 1350-1368.
- [9] P. Roach, N.J. Shirtcliffe, M.I. Newton, Progress in superhydrophobic surface development, *Soft Matter* 4 (2008) 224-240.
- [10] L. Feng, Z. Zhang, Z. Mai, Y. Ma, B. Liu, L. Jiang, D. Zhu, A super-hydrophobic and super-oleophilic coating mesh film for the separation of oil and water, *Angewandte Chemie* 116 (2004) 2046-2048.
- [11] H. Mertaniemi, V. Jokinen, L. Sainiemi, S. Franssila, A. Marmur, O. Ikkala, R.H.A. Ras, Superhydrophobic tracks for low-friction, Guided Transport of Water Droplets, *Advanced Materials* 23 (2011) 2911-2914.
- [12] B. Balu, A.D. Berry, D.W. Hess, V. Breedveld, Patterning of superhydrophobic paper to control the mobility of micro-liter drops for two-dimensional lab-on-paper applications, *Lab on a Chip* 9 (2009) 3066-3075.
- [13] B. Su, S. Wang, Y. Song, L. Jiang, A miniature droplet reactor built on nanoparticle-derived superhydrophobic pedestals, *Nano Research* 4 (2011) 266-273.
- [14] B. Su, S. Wang, J. Ma, Y. Song, L. Jiang, "Clinging-microdroplet" patterning upon high-adhesion, pillar-structured silicon substrates, *Advanced Functional Materials* 21 (2011) 3297-3307.
- [15] M.S. Khan, G. Thouas, W. Shen, G. Whyte, G. Garnier, Paper diagnostic for instantaneous blood typing, *Analytical Chemistry* 82 (2010) 4158-4164.

- [16] J. Tian, X. Li, W. Shen, Printed two-dimensional micro-zone plates for chemical analysis and ELISA, *Lab on a Chip* 11 (2011) 2869-2875.
- [17] M. Al-Tamimi, W. Shen, R. Zeineddine, H. Tran, G. Garnier, Validation of paper-based assay for rapid blood typing, *Analytical Chemistry* 84 (2012) 1661-1668.
- [18] D.R. Ballerini, X. Li, W. Shen, An inexpensive thread-based system for simple and rapid blood grouping, *Anal Bioanal Chem* 399 (2011) 1869-1875.
- [19] T. Arbatan, L. Li, J. Tian, W. Shen, Liquid marbles as micro-bioreactors for rapid blood typing, *Advanced Healthcare Materials* 1 (2012) 80-83.
- [20] A.W. Martinez, S.T. Phillips, E. Carrilho, S.W. Thomas, H. Sindi, G.M. Whitesides, Simple telemedicine for developing regions: Camera phones and paper-based microfluidic devices for real-time, off-site diagnosis, *Analytical Chemistry* 80 (2008) 3699-3707.
- [21] J.L. Delaney, C.F. Hogan, J. Tian, W. Shen, Electrogenated chemiluminescence detection in paper-based microfluidic sensors, *Analytical Chemistry* 83 (2011) 1300-1306.

---

## **Chapter 6**

### ***Liquid Marbles as Micro Bio-Reactors for Rapid Blood Typing***

---

**This page is intentionally blank**

**Monash University**

**Declaration for Thesis Chapter 6**

**Declaration by candidate**

In the case of Chapter 6, the nature and extent of my contribution to the work was the following:

<b>Nature of contribution</b>	<b>Extent of contribution (%)</b>
Initiation, key ideas, experimental works, analysis of results, writing up	35

The following co-authors contributed to the work. If co-authors are students at Monash University, the extent of their contribution in percentage terms must be stated:

<b>Name</b>	<b>Nature of contribution</b>	<b>Extent of contribution (%) for student co-authors only</b>
<b>Tina Arbatan</b>	Initiation, key ideas, experimental works, analysis of results, writing up	45
<b>Junfei Tian</b>	Assisted in experimentation	10
<b>Wei Shen</b>	Key ideas, reviewing and editing of the paper	Supervisor

The undersigned hereby certify that the above declaration correctly reflects the nature and extent of the candidate's and co-authors' contributions to this work\*.

**Candidate's Signature**

	<b>Date</b> <b>25-Sep-2015</b>
---	-----------------------------------

**Main Supervisor's Signature**

	<b>Date</b> <b>25-Sep-2015</b>
--	-----------------------------------

\*Note: Where the responsible author is not the candidate's main supervisor, the main supervisor should consult with the responsible author to agree on the respective contributions of the authors.

**This page is intentionally blank**

# Liquid Marbles as Micro Bio-Reactors for Rapid Blood Typing

*Tina Arbatan, Lizi Li, Junfei Tian and Wei Shen\*,*

Australian Pulp and Paper Institute, Department of Chemical Engineering,  
Monash University, Clayton Campus, Vic. 3800, Australia

---

This paper has been published in *Advanced Healthcare Materials*

## 6.1 KEYWORDS

Liquid marble, micro bio-reactor, diagnostic assay, superhydrophobicity, blood typing

## 6.2 INTRODUCTION

Due to their unique properties, liquid marbles have been the subject of a collection of studies in the past decade, centered on fundamental research on their properties, as well as their practical applications [1-37]. These liquid droplets enwrapped with solid powder while having no direct contact with the supporting substrate may be exploited for a wide range of applications ranging from but not limited to, the displacement of a small volume of liquid without any leak left behind [2], water surface pollution detection [13], gas detection and gas-liquid reactions [8, 30, 31], and last but not the least, preparation of micro reactors [7, 30, 31, 34]. With numerous powder types available, the fabrication options of liquid marbles seem to be infinite. This enables the design of tailor-made liquid marble based systems for intended applications.

To our knowledge, fabrication of micro reactors by forming liquid marbles for the purpose of containing chemical reactions of microscales has been proposed by only a limited number of studies. For instance, Xue et. al. [34] have shown that a liquid marble coated with magnetic powder can be used as a miniature chemical reactor to

either encapsulate the reagents in a single marble, or in two separate marbles which could coalesced afterwards to trigger the reaction. These authors used fluorinated decyl polyhedral oligomeric silsesquioxane and magnetic powder aggregates to generate stable liquid marbles capable of encapsulating liquids of either high or low surface tension. They also demonstrated a chemiluminescence reaction between hydrogen peroxide and bis (2,4,6-trichlorophenyl) oxalate and a dye to prove the concept of the controllable liquid marble micro-reactors.

Tian et al. [30, 31] showed that the porous nature of the liquid marble shell could be used to allow gases to transport through the marble shell. They demonstrated the use of liquid marbles formed with gas-reactive indicator solutions to detect gases. Bormashenko et. al have also reported the use of polyvinylidene fluorid particles of micron size for fabrication of a liquid marble micro-reactor containing ammonia acetate, acetic acid and acetylacetone, which is then exposed to formaldehyde vapor to trigger the reaction.

### 6.3 EXPERIMENTAL

Four blood samples of known types were acquired and stored in Vacutainer® test tubes containing lithium-heparin anticoagulant from a pathological laboratory. Precipitated calcium carbonate powder (Precarb 100, BASF, which was then treated in-house with stearic acid) was used as the coating powder [38]. To prepare a blood marble, a drop of blood was placed on the hydrophobic PCC powder bed inside a Petri dish using a micropipette. The Petri dish was then shaken gently to allow the PCC particles to cover the blood drop uniformly. The same method was used to prepare PTFE coated marbles; a contact angle measurement system (Dataphysics OCA230, Germany) was used to take images of both marbles after haemagglutination inside the marbles has occurred. Epiclone™ Anti-A (colour-coded blue), Anti-B (colour-coded yellow) and Anti-D (colourless) monoclonal grouping reagents were acquired commercially from Commonwealth Serum Laboratory, Australia. The same volume of an as-received antibody was then injected into a blood marble using the micropipette, which finally constructed the micro bio-reactor for the RBC agglutination reaction to take place. This procedure was repeated three times to prepare three micro reactors containing the same



blood sample, but different antibodies. The blood type was then determined based on the method described above. Photos were taken using a Mju 9010 Olympus digital camera. A spatula was used to transfer the micro reactor onto a microscope glass slide and a suitable lighting condition was provided with a light source (Microlight 150, Fibreoptic lightguides, Australia).

### 6.4 RESULTS AND DISCUSSION

In this study we present the use of liquid marble as micro bio-reactors for biological reactions and diagnostic assays. We choose human blood grouping (ABO and Rh) as the biological system to demonstrate the use of liquid marble as a micro bio-reactor in practical diagnosis involving human blood, which is the most biologically informative human body fluid. The significant advantages of liquid marble micro bio-reactor are: First, it requires relatively small amount of samples and reagents. Second, it reduces bio hazards, since the power-wrapped biological sample makes no contact to the surface of the supporting substrate. Third, the control of the bio-reactions can be made by either coalescing marbles containing different reagents or by injecting into the marble of different reagents. Fourth, marbles are low-cost and therefore disposable. The construction of the micro bio reactors for this work is simple; in each blood grouping test three drops ( $3 \times 10 \mu\text{L}$ ) of a blood sample were used to prepare three “blood marbles”. Three antibody solutions (Anti-A, Anti-B and Anti-D) were injected into the three blood marble to initiate the test. Subsequently, ABO and Rh blood grouping is studied by monitoring whether or not haemagglutination reaction occurs inside each of the blood marble micro bio-reactor.

The presence or absence of certain antigens on the surface of a red blood cell (RBC) is an intrinsic biological property which determines a person’s blood group. On the other hand, antibodies existing in the blood plasma are available to protect the body when threatened by hostile antigens. According to Landsteiner’s Law, when an RBC possesses certain antigens on its surface, the corresponding antibody is absent in the blood plasma and vice versa [39]. Blood grouping is a basic yet essential test to be performed prior to a blood transfusion to avoid the consequences of incompatibility, which may lead to a fatal haemolytic reaction. A few examples of the current

techniques of blood grouping include dry instant blood typing plate [40]. Micro plate based techniques [41-43], and integrated microfluidic biochips are among other options of blood grouping [44]. Recently, interesting progress has been made in the fabrication of low-cost, disposable and easy to use paper-based [45] and thread-based [46] blood typing devices. The liquid marble micro bio-reactor method we report herein has the same advantages in terms of, low-cost, disposability, not relying on any medical facilities.

The micro reactors in this work were made by coating blood drops with hydrophobic powder of precipitated calcium carbonate (PCC). An antibody solution was subsequently injected into the micro bio-reactor to test for haemagglutination. (Figure 1) portrays the schematic illustration of the steps of the experiment. Before the antibody injection, all blood marbles were in a homogeneous red colour. Immediately after the injection of antibody solution into the blood marbles, strong darkening of the marbles injected with Anti-A was observed. This is because that commercial Anti-A solution is colour-coded with a blue dye for identification purpose (Figure 2). If haemagglutination reaction occurs, the initial uniform red colour of the blood marble separates into two clearly discernible parts of light- and dark-red colours due to the precipitation of the agglutinated RBCs to the bottom of the marble. The appearance of such colour separation of a blood marble signals the agglutination reaction, indicating the presence of the corresponding antigen on the surface of RBCs. On the other hand, if colour separation of the blood marble does not occur, it indicates that the corresponding antigens are absent. The blood grouping results of A+, B+, O+ and O- samples can be seen in (Figure 2). It is worth noting that due to the strong red colour of the blood samples, if the haemagglutination does not occur, even by providing a strong backlighting, the blood marble micro bio-reactor will still remains uniformly dark-red in colour and opaque. On the other hand, if haemagglutination reaction occurs, a lighter-coloured upper part develops when agglutinated RBCs settles to the lower part of the marble.

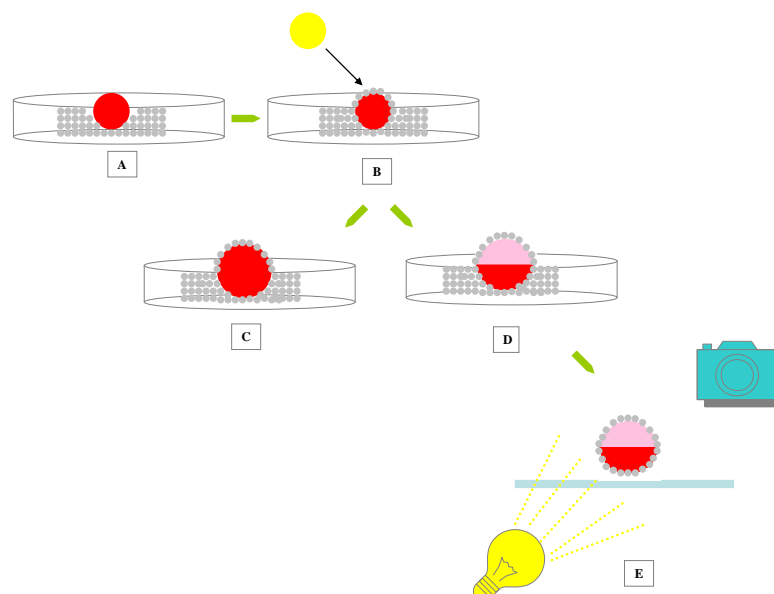


**Figure 1.** The Schematic illustration of the steps of micro reactor preparation and blood type identification. (a) Ten microlitres of blood is placed on a hydrophobic PCC powder bed to form the blood marble, (b) Ten microlitres of an antibody solution (yellow circle) is injected inside the blood marble to complete the preparation of the micro reactor. (c) When the corresponding antigens are not present on the surface of RBCs, no separation is visible. (d) When the corresponding antigens are present, RBC agglutination reaction will take place; this will result in the separation of marble colour into two distinct light (upper) and dark (lower) parts.

This method requires three blood marble micro bio-reactors to determine the blood group (ABO RhD) of a blood sample. The interpretation of the blood grouping test result can be made following this example: For a blood marble made of a B+ sample, injections of Anti-B and Anti-D solutions will cause the separation of uniformly red-coloured marbles into a light-red (top) and dark-red (bottom) parts. However, the injection of Anti-A will not change the colour uniformity of the marble, as no haemagglutination will occur between a B+ sample and anti-A (Figure 2).

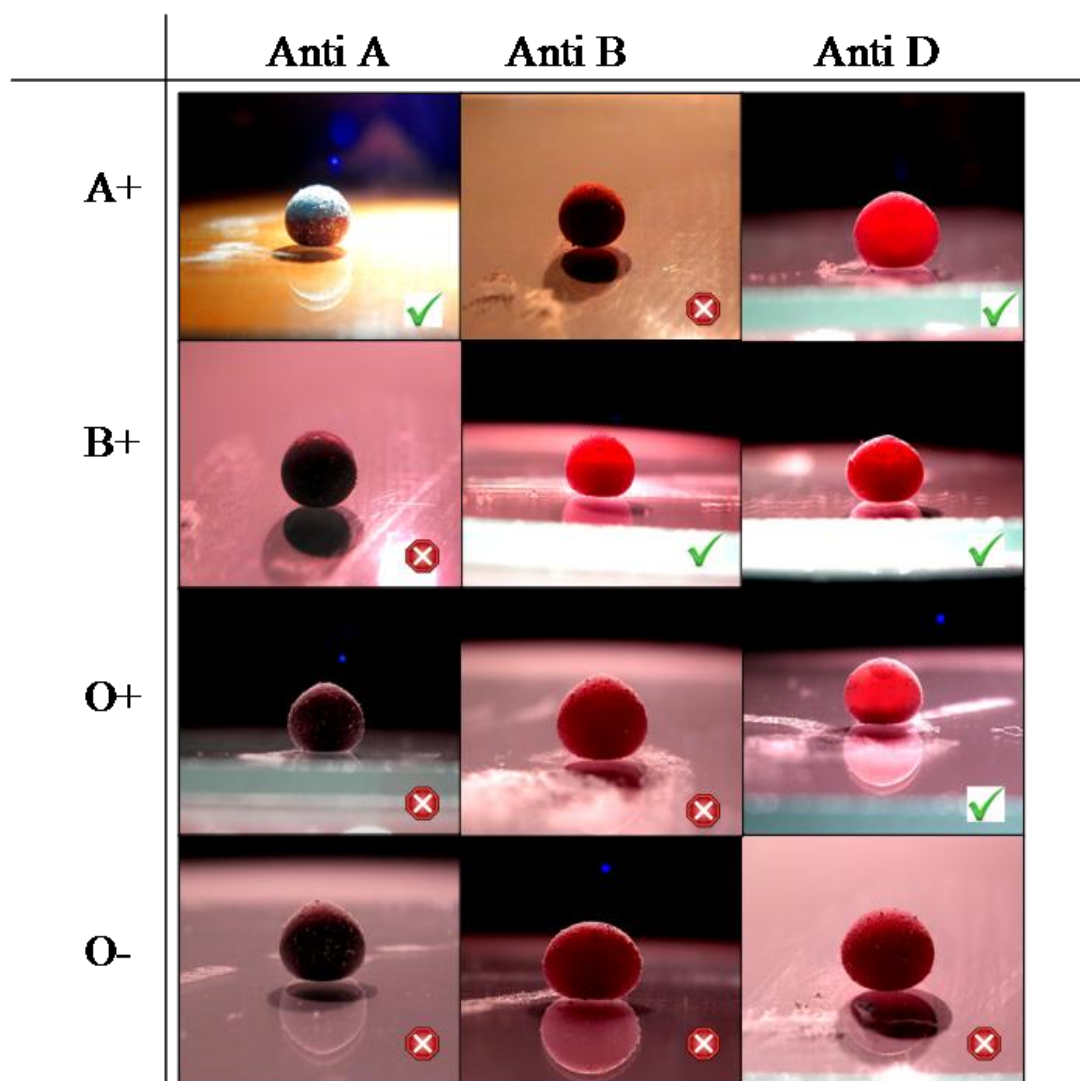


**Figure 2.** Summary of blood typing results after the corresponding antibodies are injected into the marble micro reactor. Green ticks are added to the photos where the separation of agglutinated RBC is observed. The cross signs are added to photos where agglutination caused colour separation is not observed. Overall volume of the micro reactor after the antibody injection is 20  $\mu\text{L}$ .

According to the literature, blood surface tension is lower than that of water [38]. This might explain the higher than usual deformation of the blood marbles, compared with the pure water marble. Further study of the physical properties of blood marbles can be done in our future investigations. Nevertheless, based on our observations, blood marble micro bio-reactor has the potential to be used rapid blood typing tests. Only a few seconds of gentle shaking of the marble containing the blood and antibody mixture is enough to initiate the haemagglutination reaction. Whilst the main powder used for

this study was PCC treated with stearic acid [47], we have also used PTFE powder of 100  $\mu\text{m}$  particle size (Figure 3) just to demonstrate the feasibility of using other powders for the same application. The two powders used in this work are just examples of the numerous powder type options that can be used for the same purpose.

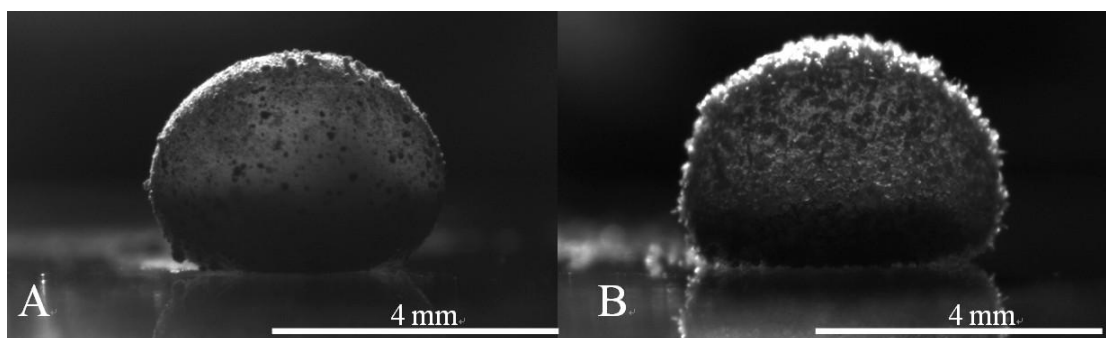


**Figure 3.** (a) A 100  $\mu\text{L}$  blood marble micro bio-reactor made of A+ blood and hydrophobic PCC powder after the injection of Anti-A solution. (b) A 100 $\mu\text{L}$  blood marble micro bio-reactor made of A+ blood and PTFE powder after the injection of Anti-A solution.

The choice of PCC was made mainly because of its low cost, availability, environmental compatibility, and ease of hydrophobization. PCC crystallites are about 1  $\mu\text{m}$  in length but clusters containing a few crystallites can have large sizes of several micrometers. Further aggregations of the clusters can be seen on the surface of the blood marble. However, the colour change caused by haemagglutination is clearly visible. Since only a minute amount of powder is needed to form a marble, and considering the low-cost of the PCC powder, this method can be regarded as one of the most inexpensive methods suitable for ABO and Rh blood typing. Furthermore, after the blood typing test, the used marble micro reactor can be burnt to eliminate any potential bio hazards. We believe that this study may open a new door for the further biological applications of using liquid marble as micro bio-reactors.

## 6.5 ACKNOWLEDGEMENTS

The authors would like to acknowledge Dr Mohammad al-Tamimi for kindly providing the blood samples. Monash University postgraduate scholarships, as well as funding received from ARC LP0989823, are gratefully acknowledged.

### 6.6 REFERENCES

- [1] T. Arbatan, W. Shen, Measurement of the surface tension of liquid marbles, *Langmuir* 27 (2011) 12923-12929.
- [2] P. Aussillous, D. Quere, Liquid marbles, *Nature* 411 (2001) 924-927.
- [3] P. Aussillous, D. Quéré, Properties of liquid marbles, *Proceedings of the Royal Society A: Mathematical, Physical and Engineering Sciences* 462 (2006) 973-999.
- [4] U.K.H. Bangi, S.L. Dhere, A.V. Rao, Influence of various processing parameters on water-glass-based atmospheric pressure dried aerogels for liquid marble purpose, *Journal of Materials Science* 45 (2010) 2944-2951.
- [5] P.S. Bhosale, M.V. Panchagnula, On Synthesizing Solid Polyelectrolyte Microspheres from Evaporating Liquid Marbles, *Langmuir* 26 (2010) 10745-10749.
- [6] P.S. Bhosale, M.V. Panchagnula, H.A. Stretz, Mechanically robust nanoparticle stabilized transparent liquid marbles, *Applied Physics Letters* 93 (2008).
- [7] E. Bormashenko, R. Balter, D. Aurbach, Micropump based on liquid marbles, *Applied Physics Letters* 97 (2010).
- [8] E. Bormashenko, R. Balter, D. Aurbach, Use of liquid marbles as micro-reactors, *International Journal of Chemical Reactor Engineering* 9 (2011) 1542-6580.
- [9] E. Bormashenko, Y. Bormashenko, A. Musin, Water rolling and floating upon water: Marbles supported by a water/marble interface, *Journal of Colloid and Interface Science* 333 (2009) 419-421.
- [10] E. Bormashenko, Y. Bormashenko, A. Musin, Z. Barkay, On the mechanism of floating and sliding of liquid marbles, *ChemPhysChem* 10 (2009) 654-656.
- [11] E. Bormashenko, Y. Bormashenko, G. Oleg, On the nature of the friction between nonstick droplets and solid substrates, *Langmuir* 26 (2010) 12479-12482.
- [12] E. Bormashenko, Y. Bormashenko, R. Pogreb, O. Gendelman, Janus Droplets: Liquid Marbles Coated with Dielectric/Semiconductor Particles, *Langmuir* 27 (2011) 7-10.
- [13] E. Bormashenko, A. Musin, Revealing of water surface pollution with liquid marbles, *Applied Surface Science* 255 (2009) 6429-6431.

- [14] E. Bormashenko, R. Pogreb, A. Musin, R. Balter, G. Whyman, D. Aurbach, Interfacial and conductive properties of liquid marbles coated with carbon black, *Powder Technology* 203 (2010) 529-533.
- [15] E. Bormashenko, R. Pogreb, G. Whyman, A. Musin, Y. Bormashenko, Z. Barkay, Shape, vibrations, and effective surface tension of water marbles, *Langmuir* 25 (2009) 1893-1896.
- [16] E. Bormashenko, T. Stein, R. Pogreb, D. Aurbach, "Petal effect" on surfaces based on lycopodium: High-stick surfaces demonstrating high apparent contact angles, *Journal of Physical Chemistry C* 113 (2009) 5568-5572.
- [17] M. Dandan, H.Y. Erbil, Evaporation rate of graphite liquid marbles: Comparison with water droplets, *Langmuir* 25 (2009) 8362-8367.
- [18] D. Dupin, S.P. Armes, S. Fujii, Stimulus-responsive liquid marbles, *Journal of the American Chemical Society* 131 (2009) 5386-5387.
- [19] E. Bormashenko, Liquid marbles: Properties and applications, *Current Opinion in Colloid & Interface Science* 16 (2011) 266-271.
- [20] N. Eshtiaghi, J.J.S. Liu, K.P. Hapgood, Formation of hollow granules from liquid marbles: Small scale experiments, *Powder Technology* 197 (2010) 184-195.
- [21] N. Eshtiaghi, J.S. Liu, W. Shen, K.P. Hapgood, Liquid marble formation: Spreading coefficients or kinetic energy?, *Powder Technology* 196 (2009) 126-132.
- [22] S. Fujii, S. Kameyama, S.P. Armes, D. Dupin, M. Suzuki, Y. Nakamura, PH-responsive liquid marbles stabilized with poly(2-vinylpyridine) particles, *Soft Matter* 6 (2010) 635-640.
- [23] L. Gao, T.J. McCarthy, Ionic liquid marbles, *Langmuir* 23 (2007) 10445-10447.
- [24] S.H. Kim, S.Y. Lee, S.M. Yang, Janus microspheres for a highly flexible and impregnable waterrepelling interface, *Angewandte Chemie - International Edition* 49 (2010) 2535-2538.
- [25] P. McEleney, G.M. Walker, I.A. Larmour, S.E.J. Bell, Liquid marble formation using hydrophobic powders, *Chemical Engineering Journal* 147 (2009) 373-382.
- [26] G. McHale, S.J. Elliott, M.I. Newton, D.L. Herbertson, K. Esmer, Levitation-free vibrated droplets: Resonant oscillations of liquid marbles, *Langmuir* 25 (2009) 529-533.

- [27] G. McHale, M.I. Newton, Liquid marbles: Principles and applications, *Soft Matter* 7 (2011) 5473-5481.
- [28] T.H. Nguyen, K. Hapgood, W. Shen, Observation of the liquid marble morphology using confocal microscopy, *Chemical Engineering Journal* 162 (2010) 396-405.
- [29] D. Quéré Non-sticking drops, *Reports on Progress in Physics* 68 (2005) 2495-2532.
- [30] J. Tian, T. Arbatan, X. Li, W. Shen, Liquid marble for gas sensing, *Chemical Communications* 46 (2010) 4734-4736.
- [31] J. Tian, T. Arbatan, X. Li, W. Shen, Porous liquid marble shell offers possibilities for gas detection and gas reactions, *Chemical Engineering Journal* 165 (2010) 347-353.
- [32] A. Tosun, H.Y. Erbil, Evaporation rate of PTFE liquid marbles, *Applied Surface Science* 256 (2009) 1278-1283.
- [33] A.V. Rao, M.M. Kulkarni, S.D. Bhagat, Transport of liquids using superhydrophobic aerogels, *Journal of Colloid and Interface Science* 285 (2005) 413-418.
- [34] Y. Xue, H. Wang, Y. Zhao, L. Dai, L. Feng, X. Wang, T. Lin, Magnetic liquid marbles: A “precise” miniature reactor, *Advanced Materials* 22 (2010) 4814-4818.
- [35] H. Zeng, Y. Zhao, Dynamic behavior of a liquid marble based accelerometer, *Applied Physics Letters* 96 (2010).
- [36] N. Zhao, X.Y. Zhang, Y.F. Li, X.Y. Lu, S.L. Sheng, X.L. Zhang, J. Xu, Self-organized polymer aggregates with a biomimetic hierarchical structure and its superhydrophobic effect, *Cell Biochemistry and Biophysics* 49 (2007) 91-97.
- [37] Y. Zhao, J. Fang, H. Wang, X. Wang, T. Lin, Magnetic liquid marbles: manipulation of liquid droplets using highly hydrophobic  $\text{Fe}_3\text{O}_4$  nanoparticles, *Advanced Materials* 22 (2010) 707-710.
- [38] E. Hrnčič, J. Rosina, Surface tension of blood, *Physiological Research* 46 (1997) 319-321.
- [39] K. Landsteiner, On agglutination of normal human blood, *Transfusion* 1 (1961) 5-8.
- [40] D. Blakeley, B. Roser, B. Tolliday, C. Colaco, Dry instant blood typing plate for bedside use, *The Lancet* 336 (1990) 854-855.



- [41] F. Llopis, F. Carbonell-Uberos, M.C. Montero, S. Bonanad, M.D. Planelles, I. Plasencia, C. Riol, T. Planells, C. Carrillo, A. De Miguel, A new method for phenotyping red blood cells using microplates, *Vox Sanguinis* 77 (1999) 143-148.
- [42] F. Llopis, F. Carbonell-Uberos, M.D. Planelles, M. Montera, I. Plasencia, C. Carrillo, A new microplate red blood cell monolayer technique for screening and identifying red blood cell antibodies, *Vox Sanguinis* 70 (1996) 152-156.
- [43] J.H. Spindler, H. Kluter, M. Kerowgan, A novel microplate agglutination method for blood grouping and reverse typing without the need for centrifugation, *Transfusion* 41 (2001) 627-632.
- [44] D.S. Kim, S.H. Lee, C.H. Ahn, J.Y. Lee, T.H. Kwon, Disposable integrated microfluidic biochip for blood typing by plastic microinjection moulding, *Lab on a Chip - Miniaturisation for Chemistry and Biology* 6 (2006) 794-802.
- [45] M.S. Khan, G. Thouas, W. Shen, G. Whyte, G. Garnier, Paper Diagnostic for Instantaneous Blood Typing, *Analytical Chemistry* 82 (2010) 4158-4164.
- [46] D. Ballerini, X. Li, W. Shen, An inexpensive thread-based system for simple and rapid blood grouping, *Analitical Bioanalitical Chemistry* 399 (2011) 1869-1875.
- [47] T. Arbatan, X. Fang, W. Shen, Superhydrophobic and oleophilic calcium carbonate powder as a selective oil sorbent with potential use in oil spill clean-ups, *Chemical Engineering Journal* 166 (2011) 787-791.

**This page is intentionally blank**

---

## **Chapter 7**

### ***Conclusions and Future Work***

---

**This page is intentionally blank**

This thesis has reported a series of investigations and developments of blood typing devices based on bioactive paper and liquid micro reactors fabricated from superhydrophobic materials. Work published based on this research encompasses novel microscopic methods of studying RBC agglutination, immobilization and transport mechanisms within paper. The mechanism of how paper structure affects the performance of paper-based blood typing devices has been established. Two fabrication methods for liquid micro reactors for blood typing devices have also been developed.

Paper is a three-dimensional network of cellulosic fibres. In the present research, paper is regarded as a functional substrate for fabricating blood typing devices, rather than simply a normal substrate without the capability of changing properties. A core aim of this thesis was to understand the fundamental mechanisms of RBC agglutination, immobilization and transport behaviours within the 3D fibre network of paper, as well as the relationship between paper structure and these behaviours. Based on the outcomes of this study, we can further design and produce paper substrates with the most suitable structures to meet the requirements for fabricating blood typing devices with the best performance. In addition, this concept can be applied to the development of other paper-based blood analysis devices.

In this thesis, we have developed two new microscopic methods for studying the details of free RBCs and RBC agglutinates at the cellular level within the paper network: the confocal technique and the FIB-SEM technique. The confocal microscopic method was explored to study the final state of RBC distribution within the paper network, while the FIB-SEM technique was developed to capture the details of RBCs at any particular moment during the process of blood penetration into paper. The use of microscopic tools enables us to obtain scientific evidence to establish the agglutination, immobilization and transport mechanisms of RBCs within paper. Results from the confocal microscopic study show that the release of antibody molecules from the fibre surface by dissolution is the main mechanism causing haemagglutination. Haemagglutination of RBCs within the fibre network leads to the formation of large blood lumps, which can be immobilized by mechanical entrapment within the interfibre pores. The FIB-SEM microscopic study shows that fibre-fibre overlap is an effective form of capillaries for blood transport. Some RBCs may be trapped in locations where

channels of fibre-fibre overlaps are blocked by crossing fibres, or by blocked transverse pores between different layers of fibre in paper.

RBC immobilization and transport behaviours are closely affected by the physical structure of the paper network. We therefore propose that the performance of paper-based blood typing devices can be controlled through paper structure design. The desired paper structure can be acquired by controlling certain parameters of the papermaking process, such as type of pulp and pressure of the press. The study based on mercury intrusion porosimetry shows that RBCs are transported much more easily in papers with simple structures, which are uniform-sized pores without too much pore size variation. Paper made of hardwood fibres with low basis weights can provide such structures, whilst paper with softwood has a more complex internal pore structure. This may be because softwood fibres are thicker and may efficiently block the pores between different fibre layers. The complex pore structure makes RBC transport more difficult, leading to inferior blood-typing performance. Based on the above mechanism, we can design and produce paper with specialized structures, according to the requirement of future paper-based blood analysis devices, and avoid the production of undesirable paper structures.

Blood typing devices based on liquid micro reactors fabricated using superhydrophobic materials have been developed in this thesis to provide a potential method of low-cost, high-throughput blood typing. The design concept was to establish bio micro reactors capable of presenting the details of RBC haemagglutination reactions for image capture and analysis. A superhydrophobic surface-supported liquid drop and a liquid marble wrapped in superhydrophobic powder were fabricated as liquid micro reactors for the conduct of blood typing assays. The near-spherical shape of liquid micro reactors enables the camera to easily capture the details of RBC haemagglutination reactions for further analysis. Blood typing devices based on liquid micro reactors would be very useful for confirming blood samples that have weak RBC antigens, as detailed RBC agglutination patterns and intensities can be identified clearly. In addition, they have many other advantages, such as the small amount of blood required, the short assaying time and the ability of anti-bio contamination. We believe that the application of superhydrophobicity-based liquid micro reactors should not only be limited to blood

typing, but also expand into other chemical and biological assays, including other blood-based diagnostic assays.

Although the research outcomes reported in this thesis lay a solid foundation and make a significant contribution to the development of blood typing devices based on bioactive paper and liquid micro reactors, future work needs to be undertaken in the following directions:

- a) Establish a computer modelling system to simulate RBC transportation behaviours within paper fibre networks, which is able to predict the possible pathways of RBCs penetrating the paper from any direction.
- b) Investigate the influence of chemical additives in papermaking on the transportation and immobilization of RBCs within paper fibre networks. These chemical additives include a range of polymers which are added to the pulp stock during the papermaking process for the improvement of paper's dry strength, wet strength, and retention and drainage abilities.
- c) Integrate the paper-based blood typing platforms with advanced telemedicine techniques, such as smart phones, smart watches, tablets and other portable or wearable devices. This will increase the capability of paper-based diagnostics with rapid assay result interpretation, remote diagnosis, data storage and transmission.
- d) Apply the findings on the mechanisms of paper-based blood typing techniques in this thesis to the development and investigation of other paper-based biochemical, biomedical and chemical diagnostic devices.
- e) Extend the design concept of soft liquid micro reactors to other chemical, biological and medical assays.
- f) Improve the characteristics of the blood typing devices based on bioactive paper and liquid micro reactors, including their durability, strength, stability, temperature resistance, and humidity resistance.

- g) Realize the mass production of low-cost blood typing devices based on bioactive paper and liquid micro reactors. This will enable, all the difficulties which prevent large-scale production to be solved.

It is hoped that the research outcomes of this thesis can help to improve public health conditions in developing countries, and benefit people in developed countries in terms of home-based diagnosis and more efficient blood typing in large batches. However, we acknowledge that much remains to be done before these benefits can be applied in people's daily life. Intensive collaboration between scientists with different research backgrounds is required for this great transformation.



---

## **Appendix I**

***Published First and Co-Authored Papers Included  
in the Main Body of This Thesis***

---

**This page is intentionally blank**

# A study of the transport and immobilisation mechanisms of human red blood cells in a paper-based blood typing device using confocal microscopy†

Cite this: DOI: 10.1039/c3an00810j

Lizi Li, Junfei Tian, David Ballerini, Miaosi Li and Wei Shen\*

Recent research on the use of bioactive paper for human blood typing has led to the discovery of a new method for identifying the haemagglutination of red blood cells (RBCs). When a blood sample is introduced onto paper treated with the grouping antibodies, RBCs undergo haemagglutination with the corresponding grouping antibodies, forming agglutinated cell aggregates in the paper. A subsequent washing of the paper with saline buffer could not remove these aggregates from the paper; this phenomenon provides a new method for rapid, visual identification of the antibody-specific haemagglutination reactions and thus the determination of the blood type. This study aims to understand the mechanism of RBC immobilization inside the paper which follows haemagglutination reactions. Confocal microscopy is used to observe the morphology of the free and agglutinated RBCs that are labelled with FITC. Chromatographic elution patterns of both agglutinated and non-agglutinated RBCs are studied to gain insight into the transport behaviour of free RBCs and agglutinated aggregates. This work provides new information about RBC haemagglutination inside the fibre network of paper on a microscopic level, which is important for the future design of paper-based blood typing devices with high sensitivity and assaying speed.

Received 22nd April 2013

Accepted 3rd June 2013

DOI: 10.1039/c3an00810j

[www.rsc.org/analyst](http://www.rsc.org/analyst)

## Introduction

Accurate and rapid determination of human blood groups is imperative for many medical procedures such as blood transfusion and organ transplantation.<sup>1</sup> Blood groups are classified based on inherited differences (polymorphisms) in antigens on the surface of the red blood cells (erythrocytes). The International Society of Blood Transfusion (ISBT) recognises 328 different antigens and 30 major blood group systems, among which the ABO and Rhesus systems are of the greatest clinical importance.<sup>2</sup> Without ABO compatibility testing, around one third of unscreened blood transfusions would lead to potentially fatal haemolytic transfusion reactions. The RBC antigen D of the Rh system is considered to be the most common culprit, also causing haemolytic disease of the foetus and in newborns (HDFN).<sup>2</sup>

The majority of techniques for determining the ABO and Rh blood type are based on the principle of observing haemagglutination between RBC antigens and serum antibodies. Haemagglutination occurs when multi-armed antibodies bind to the particular binding sites on the antigens of RBCs, adhering cells together and leading to the formation of larger blood

lumps that cannot be stably suspended in the plasma. Currently, the most common assays used for the identification of blood groups include the slide test, tube test, micro plate and solid phase assays, as well as the column agglutination system.<sup>3–8</sup> Recently, advanced blood typing assays based on gene sequencing of DNA<sup>9,10</sup> and flow cytometry<sup>11</sup> have been reported. Blood typing assays that are currently used in hospitals and pathological laboratories are capable of sensitively and specifically identifying blood types; they are reliable and robust.<sup>12</sup> However, few point-of-care assays can be done without either dedicated laboratory instruments or the direct handling of the antibodies by the personnel who carry out the tests (such as the slide and tube tests).<sup>13,14</sup> In addition, the equipment-based assays usually take a long time (10–30 min), and the costs are high.<sup>7,12</sup> A disadvantage common to all blood typing assays is that it is difficult for non-professionals and lay-users to interpret the assay result, since currently available blood typing devices require users to have some knowledge of blood typing and an understanding of the device working principle. It follows that the availability of simple, rapid, cheap, and reliable methods for blood typing would be of significant benefit for point-of-care applications, such as bedside compatibility checks, fast blood typing in emergency scenarios, and in developing regions or remote locations where there may be no access to laboratory facilities.<sup>14</sup>

Paper is a material fabricated from cellulosic fibres, which are easy-accessible, recyclable, environment-friendly and of

Department of Chemical Engineering, Monash University, Wellington Rd, Clayton, Vic. 3800, Australia.

† Electronic supplementary information (ESI) available: Separated confocal signals of fibres and RBCs for Fig. 4. See DOI: 10.1039/c3an00810j

low-cost.<sup>15</sup> The promising use of paper for environmental and diagnostic applications has been strongly highlighted.<sup>16–18</sup> Recently, innovations in the use of bioactive paper to perform blood typing assays have been reported in the literature;<sup>14,19–21</sup> these innovations are based on a new mechanism for identifying haemagglutination. Khan *et al.*<sup>19</sup> found that agglutinated blood samples resulting from antibody-specific haemagglutination reactions transport differently in the porous structure of paper than stable blood samples with well dispersed red cells. They observed that agglutinated RBCs in paper could not be eluted chromatographically by the wicking of blood serum. This observation marked the discovery of a new blood typing method which relies on the visual identification of red cell transport behaviour in paper which led to a new concept for fabricating low-cost blood typing devices. Following work by Ballerini *et al.*<sup>22</sup> showed that the same principle could be used to fabricate inexpensive thread-based blood typing devices.

Jarujamrus *et al.*<sup>20</sup> investigated the separation of the agglutinated RBCs from the blood serum phase in filter paper. They took a biochemical approach and analysed the amount of antibody that could be washed off from an antibody-treated filter paper. Their hypothesis was that a blood sample introduced onto a piece of antibody-treated paper could re-dissolve a fraction of antibody deposited and dried on the fibre surface. The re-dissolved antibody molecules could then engage in specific interactions with the RBCs, leading to haemagglutination within paper. Jarujamrus *et al.*<sup>20</sup> showed that between 34 and 42% of antibody molecules carried by the antibody-treated paper could be re-dissolved by saline solution or a blood sample. Al-Tamimi *et al.*<sup>14</sup> reported a chromatographic elution technique for blood typing. Their results showed that agglutinated RBCs in paper were immobilised within the paper structure and could not be eluted by saline solution, while non-agglutinated RBCs could be eluted easily. Their results again showed that agglutinated RBC lumps inside the paper have drastically different transport behaviour from non-agglutinated RBCs (Fig. 1). Al-Tamimi *et al.*<sup>14</sup> and Su *et al.*<sup>23</sup> have also

shown that the efficiency of chromatographic separation of agglutinated and non-agglutinated RBCs on paper could be increased by controlling the thickness and porosity of the paper.

More recently, Li *et al.*<sup>21</sup> applied this difference in transport behaviour between agglutinated and non-agglutinated RBCs in paper to design the first text-reporting blood typing device. This design presented a new concept of adding grouping antibodies onto paper which had printed patterns of text and symbols (*i.e.* to dose anti-A into the printed text pattern “A”). If the RBCs of a blood sample undergo haemagglutination reaction due to anti-A in the text pattern “A”, agglutination of RBCs would occur inside the patterned “A” zone; the deep crimson red colour formed by the agglutinated RBCs could not be washed away by saline solution and the paper will report the blood type of this sample with a letter “A” formed by the colouring effect of the agglutinated RBCs. This design enables non-professional users who may not have the knowledge of blood typing to identify blood types; it is suitable for developing countries where trained medical professionals may not be always available. The text-reporting blood typing concept using bioactive paper has since been explored by the diagnostic industry as a new class of sensitive, rapid and user-friendly device.

In this study we focus on understanding the mechanism of haemagglutination-induced immobilization of RBCs in antibody-treated bioactive paper. Microscopic evidence will be sought to understand (a) the morphology of the non-agglutinated RBCs in the fibre network of paper, (b) the morphology, size and distribution of agglutinated RBC aggregates formed after haemagglutination in the fibre network and (c) the transport behaviour of individual RBCs and large agglutinated RBC lumps driven by the wicking saline solution in paper. Confocal microscopy is used to observe RBCs and agglutinated RBC lumps in the fibre network of paper. The results of this study revealed details of RBC agglutination inside the fibre network of paper with clarification on a cellular level. The immobilisation mechanism of the agglutinated RBC lumps inside the paper is established. Information obtained from this study will be used to guide future device designs, particularly the design of the paper structures suitable for the low-cost blood typing papers.

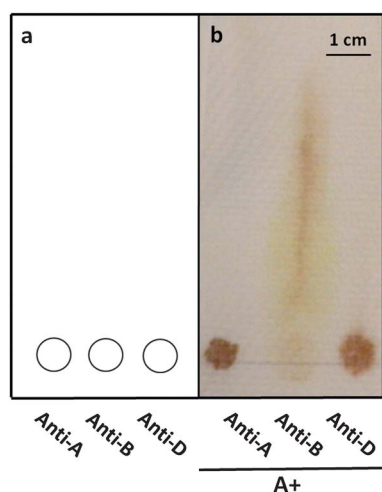


**Fig. 1** An example of paper-based assay for rapid blood typing. (a) A schematic diagram of the anti-body treated paper. (b) An actual test result of blood A+.<sup>14</sup>

## Experimental

### Materials

Anti-coagulated blood samples were acquired from adult volunteers of known blood group by Dorevitch Pathology, Australia. All blood samples were stored in Vacutainer® tubes containing heparin, citrate and EDTA at 4 °C, and used within 5 days of collection. Epiclone™ anti-A, anti-B and anti-D monoclonal grouping reagents were sourced commercially from the Commonwealth Serum Laboratory, Australia. Anti-A and anti-B are transparent solutions, coloured cyan and yellow respectively, while anti-D is a clear colourless solution. Monoclonal grouping reagents were also kept at 4 °C. Kleenex paper towel with a basis weight of 34 g m<sup>-2</sup> and a thickness of 140 μm was purchased from Kimberly-Clark, Australia. Analytical grades of NaCl, KCl, Na<sub>2</sub>HPO<sub>4</sub>, and KH<sub>2</sub>PO<sub>4</sub> were obtained from Sigma-Aldrich and used for preparation of physiological salt

solution (PSS) and phosphate-buffered physiological salt solution (PBS, pH 7.4). Fluorescein isothiocyanate (FITC, isomer I, product number: F7250) from Sigma-Aldrich was used for labelling RBCs. Anhydrous dimethyl sulphoxide (DMSO, from MERCK Chemicals Ltd, Australia) was employed to dissolve the FITC. Anhydrous D-glucose was provided by AJAX Chemicals Ltd., Australia. Microscope immersion oil was purchased from Sigma-Aldrich, Germany.

## Methods

Red blood cells were labelled using the methods reported by Hauck *et al.*<sup>24</sup> and Hudetz *et al.*<sup>25</sup> Firstly, whole blood was centrifuged at  $800\text{ r min}^{-1}$  for 10 minutes and the plasma layer was removed. The red cells collected from the bottom of the centrifuge tube were then washed with PSS and incubated in PBS with D-glucose ( $0.5\text{ mg ml}^{-1}$ ) and FITC ( $0.4\text{ mg ml}^{-1}$ ) for 3 hours. The labelled cells were then washed with PSS twice and re-suspended at a hematocrit of 45%. The testing papers were prepared by introducing  $10\text{ }\mu\text{L}$  of antibody solution onto  $10\text{ mm} \times 10\text{ mm}$  squares of Kleenex paper towel and allowing the antibody to penetrate and dry for 1 minute. In order to form the agglutinated blood lumps inside the paper sheet,  $8\text{ }\mu\text{L}$  of labelled and re-suspended blood sample was pipetted onto the paper from the opposite side to which the antibody was introduced. Thirty seconds were given for the interaction between RBCs and the antibody within paper. After that, the sample was placed onto a glass slide for confocal imaging. The microscopic images were recorded from the side which the blood was introduced into. A Nikon Ai1Rsi Confocal Microscope in the facilities at the Melbourne Centre for Nanofabrication was used for generating the confocal micrographs. The objective lenses employed for imaging were  $20\times$  dry lens and  $60\times$  oil immersion lens. Images of red blood cells within the antibody-treated paper were captured as x-y images or a series of x-y images with stepped variation in the z-direction for construction of 3D images (or z-stack images). The resolution of all images was  $1024 \times 1024$  pixels and the step width for the z-stack images was  $0.125\text{--}0.250\text{ }\mu\text{m}$ .

In order to gain a better understanding of the transport behaviour of agglutinated and non-agglutinated RBCs on paper, an experiment of chromatographic elution with PSS was performed. Briefly,  $10\text{ }\mu\text{L}$  of antibody solution and  $3\text{ }\mu\text{L}$  of blood sample were dropped on a glass slide and allowed to react for 30 seconds. The mixture of blood and antibody was then transferred from the glass slide onto a piece of Kleenex paper around  $2\text{ cm}$  from the lower edge of the paper, and allowed to absorb completely for 1 minute. The Kleenex paper was then suspended in PSS in a chromatography tank about  $1\text{ cm}$  from its lower edge to ensure the blood spot remained above the buffer surface and the saline solution was allowed to elute up through the paper by capillary wicking for 10 minutes. The paper was then allowed to dry at room temperature on a blotting paper for another 10 minutes and the elution patterns of RBCs were characterized by observing the presence of RBCs at different points away from the original blood sample spot with the confocal microscope.

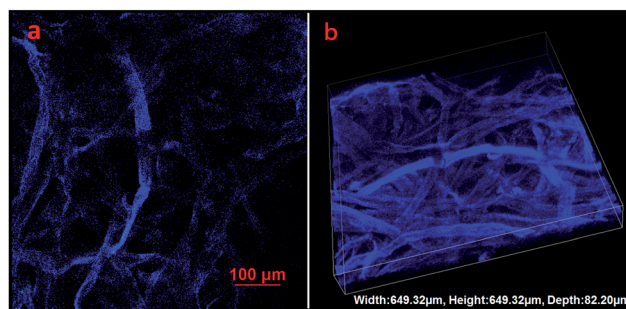


**Fig. 2** 2D (a) and 3D (b) confocal images of lignocellulosic fibers within paper captured by  $20\times$  dry lens.

## Results and discussion

### Observation of red blood cells in paper by confocal microscopy

In this confocal microscopy study a  $405\text{ nm}$  laser was used to observe the fibre network of the Kleenex paper. The excitation wavelength of this laser beam is able to generate fluorescent emission in the blue spectral region from lignocellulosic fibres of the Kleenex paper; the fluorescent emission enabled clear images of the fibre network in the paper to be generated at a satisfactory resolution. Fig. 2a shows a 2D image from a single confocal scan of the Kleenex paper sample. Fig. 2b shows a 3D reconstruction of a series of 2D scans from the same paper sample; all scans were obtained using a  $20\times$  dry lens. These results clearly show that the distribution of fibres in the Kleenex paper is even but random. The width of the lignocellulosic fibres that form the Kleenex paper is around  $20\text{ }\mu\text{m}$  to  $30\text{ }\mu\text{m}$ ; the spaces between these fibres form the porous structure of paper.

Fig. 3a and b show the FITC-labelled RBCs in the Kleenex paper and on top of a glass slide, respectively. FITC is widely used to attach a fluorescent label to proteins *via* the amine group. The isothiocyanate group in FITC reacts with amino terminals and primary amines in proteins. Isomer I of FITC was used in this study; it has the thiocyanate group on the fourth carbon of the benzene ring. This isomer has been reported to be suitable for labelling red blood cells.<sup>24,25</sup> Our results as shown in Fig. 3a and b are in good agreement with those reports. A

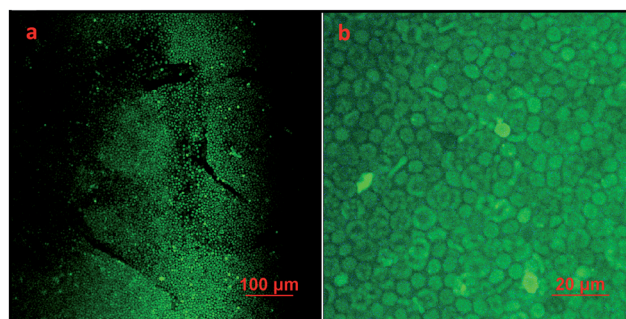


**Fig. 3** Confocal images of RBCs labelled with FITC within paper (a) and on a slide glass (b) captured by  $20\times$  dry lens.



fluorescent emission spectrum is generated from the FITC-labelled red blood cells with a 488 nm laser line by the multiline argon-ion laser of the Nikon Ai1Rsi Confocal Microscope; this excitation wavelength is close to the absorption peak of FITC. As a result, the distribution of FITC-labelled RBCs in the porous structure of the paper can be clearly imaged by confocal microscopy (Fig. 3, by 20 $\times$  dry lens). Fortunately, the 488 nm laser line cannot excite fluorescent emission from the lignocellulosic fibres, therefore the fibre network of the paper appears as dark spaces as shown in Fig. 3a. Fig. 3b shows an enlarged confocal image of FITC-labelled RBCs observed using a 20 $\times$  dry lens on a glass slide; it shows the morphology of RBCs after the FITC labelling. The RBCs retain the shape of centrally depressed disks, with diameters of 6–8  $\mu\text{m}$  and a thickness of 2  $\mu\text{m}$ . These figures demonstrate that FITC-labelling of the RBCs does not change the morphology of the RBCs and that confocal microscopy is a suitable technique for obtaining detailed, cellular level information of RBC behaviour in paper made of lignocellulosic fibres. It is expected that, by combining the blue fluorescent emission signal from the fibre with the green fluorescent signal from the FITC-labelled red blood cells, a full picture of the RBCs in paper can be obtained.

#### The activity of the red blood cell antigen after FITC labelling

The FITC labelling of the red blood cells does not have any noticeable effect on the activity of the RBC antigens on the surface of the red cells. This was confirmed by comparing the reactions of whole blood and FITC-labelled RBCs drawn from the same source with the corresponding antibodies on glass

slides (results are not shown). Under the same assaying conditions, FITC labelling does not cause discernible differences in the sizes of the agglutinated RBC aggregates nor in the time required for the RBCs to agglutinate after coming into contact with their corresponding antibodies.

#### Mechanisms of red blood cell immobilisation in antibody-treated paper

Fig. 4a and b show the two-dimensional confocal micrographs of RBCs of type O+ introduced into a paper sample treated with anti-A reagent acquired using a 20 $\times$  dry lens and a 60 $\times$  oil immersion lens respectively. These figures combine the signals from the lignocellulosic fibres in paper (blue) and the FITC-labelled RBCs (green), and provide a much clearer visual identification of positions of the RBCs within the fibre network. Since O+ red blood cells do not carry the A antigen, no haemagglutination is expected to occur. Results shown in Fig. 4a and b reveal that the O+ RBCs distribute rather uniformly in the spaces of the fibre network of the paper treated with anti-A. Fig. 4c shows a 3D confocal image of type O+ RBCs in paper treated with anti-A; it shows that red blood cells have penetrated through the fibre network and reached around the middle of the paper sheet. However, the RBCs remain free of any morphological change.

Fig. 4d and e show two examples of 2D confocal images of type O+ RBCs in anti-D treated papers acquired using 20 $\times$  dry and 60 $\times$  oil immersion lenses. Strong changes in both the RBC distributions in the fibre network and cell morphology show the occurrence of haemagglutination of type O+ RBCs with anti-D.

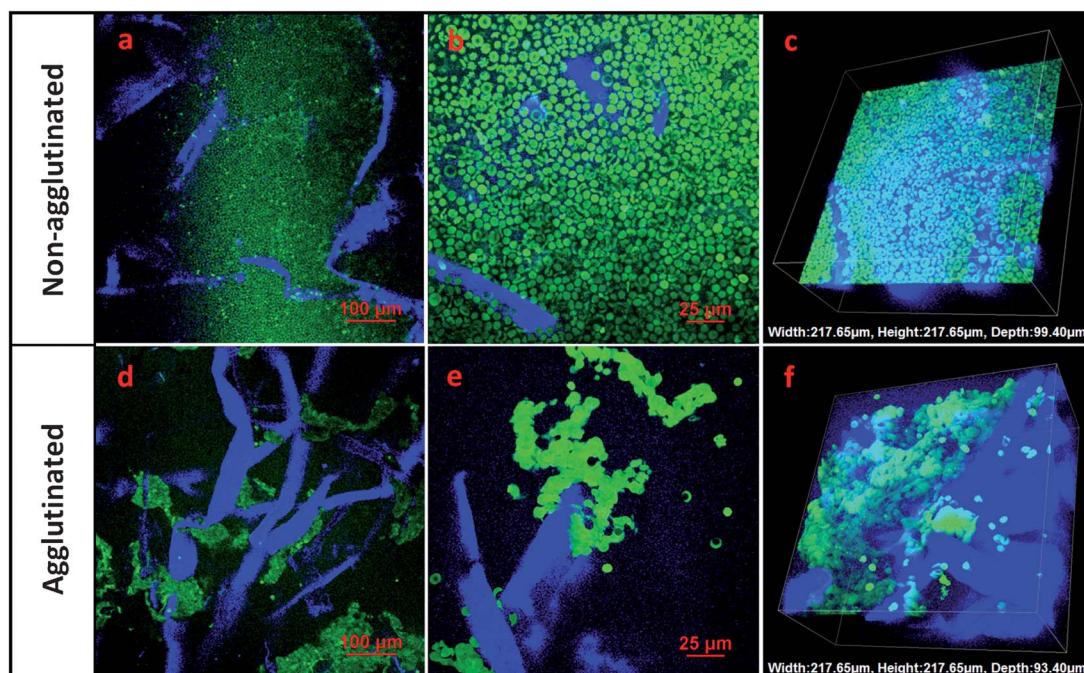


**Fig. 4** Confocal images of non-agglutinated and agglutinated RBCs within paper. (a) 2D image of non-agglutinated RBCs captured by 20 $\times$  dry lens. (b) 2D image of non-agglutinated RBCs captured by 60 $\times$  oil lens. (c) 3D image of non-agglutinated RBCs captured by 60 $\times$  oil lens; (d) 2D image of agglutinated RBCs captured by 20 $\times$  dry lens. (e) 2D image of agglutinated RBCs captured by 60 $\times$  oil lens. (f) 3D image of agglutinated RBCs captured by 60 $\times$  oil lens. The separate (non-combined) images of paper and labelled RBCs can be found in the ESI.†

Several observations may be made regarding the mechanism of RBC haemagglutination inside paper. First, the sizes of agglutinated RBC lumps vary significantly. Most lumps contain hundreds of RBCs, while others contain only a few. The bonding of antibody molecules with the RBCs appears to be strong, since some RBCs appear to have lost their natural disk-like shape when they become agglutinated. However, haemagglutination of RBCs does not cause massive haemolysis of the cells; this is supported by the observation that although cells formed aggregates, the profiles of cells can still be identified.

Secondly, many RBCs have moved toward one another during haemagglutination to form large lumps. The movement of red cells freed large areas of the fibre surface from cell coverage (Fig. 4d and e). Fig. 4f also shows that there are a few single red blood cells that apparently adhere to the fibre surface. This raises the possibility that some individual red cells could undergo interactions directly with the antibody molecules adsorbed on the fibre surface and become immobilised there. While this possibility does exist, the fibre surface coverage by such individual cells is small; these adsorbed, individual cells make negligible visual contribution to the assay result. These observations support the conclusion of a previous study by Jarujamrus *et al.*,<sup>20</sup> who found that a significant fraction of antibody molecules introduced into an antibody-treated paper could be washed off from the fibre surface by saline solution or by the serum phase of a blood sample. Therefore the dominant mechanism of RBC agglutination inside an antibody-treated paper is through the haemagglutination caused by the released antibody molecules from the fibre surface.

Thirdly, the confocal results show that the major mechanism for the immobilisation of the agglutinated RBC lumps inside the fibre network is the strong adhesion of the lumps to the fibres and mechanical entrapment. Fig. 4d–f show that large agglutinated RBC lumps of the dimension similar to those of the interfibre pores were formed inside the paper and the entrapment and adhesion of those lumps occurred mostly at the gaps and pores between fibres. These factors make the chromatographic elution of the lumps practically impossible. The confocal results are in full agreement with the conclusion by Al-Tamimi *et al.*,<sup>14</sup> they provide detailed microscopic evidence of the working mechanism of this new blood typing method using bioactive paper.

### An application study of blood elution patterns in paper using the confocal method

One design of bioactive paper-based blood typing devices for identification of haemagglutination in paper is based on paper chromatography.<sup>14</sup> Grouping antibodies (anti-A, anti-B and anti-D) are first spotted at 2 cm above the bottom edge of a piece of Kleenex paper, then a blood sample is introduced onto the grouping antibody spot; the spot containing antibody and the blood sample is referred to as the “antibody and blood sample zone”. The Kleenex paper is then dipped into a chromatographic tank, with the bottom edge slightly submerged into the saline solution. The saline solution penetrates through the interfibre pores of the paper towel, wicking across spots of

grouping antibodies and the blood samples within the spots. If haemagglutination occurs in the antibody spots, the agglutinated blood sample will not be eluted up by the rising saline solution. If haemagglutination does not occur, the blood sample will be eluted out of the grouping antibody spot, forming an elongated, visible chromatographic track of blood. The difference in the elution behaviours of the blood sample provides an easy and accurate method for the identification of the blood type.<sup>14</sup>

In practice, however, two elution bands may be observed. The first band can be observed close to the elution front of saline solution and the second band can be observed behind the first band. In some assays, these two bands could be observed simultaneously; in other assays only one could be observed. Fig. 5 shows a schematic description of this phenomenon. Confocal microscopy was used to investigate the two bands to gain an understanding of this phenomenon.

In this study, FITC-labelled RBCs were used to perform the chromatographic elution blood typing assays. The FITC-labelled RBCs were first mixed with each of the grouping antibodies on separate glass slides to ensure complete reaction; the mixture of blood and antibody reagent was then spotted onto the Kleenex paper and chromatographic elution was begun. This procedure was adopted in this investigation because the two bands could be reproducibly observed in all assays. The chromatographic elution patterns of the A+ blood sample with anti-A, anti-B and anti-D, as well as the patterns of the B+ blood sample with the three antibodies, are presented in Fig. 6. In all negative assays two bands can be observed simultaneously, whereas in all positive assays only the first band can be observed.

For confocal microscopy investigation, samples of blood of type A+ and B+ reacting with anti-B reagent were adopted to represent non-agglutinated and agglutinated groups for chromatographic elution experiments by saline solution. The confocal image taken from the antibody and blood sample zone

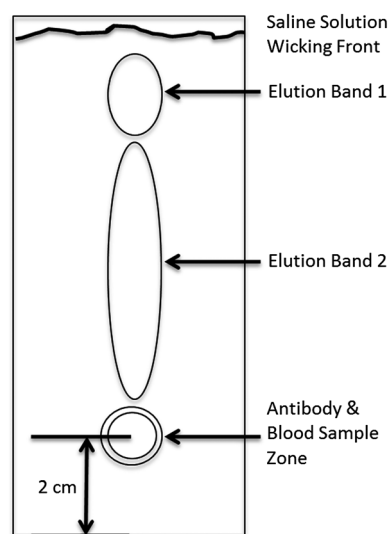


**Fig. 5** A schematic diagram of the observed elution bands of RBCs on antibody-treated paper.



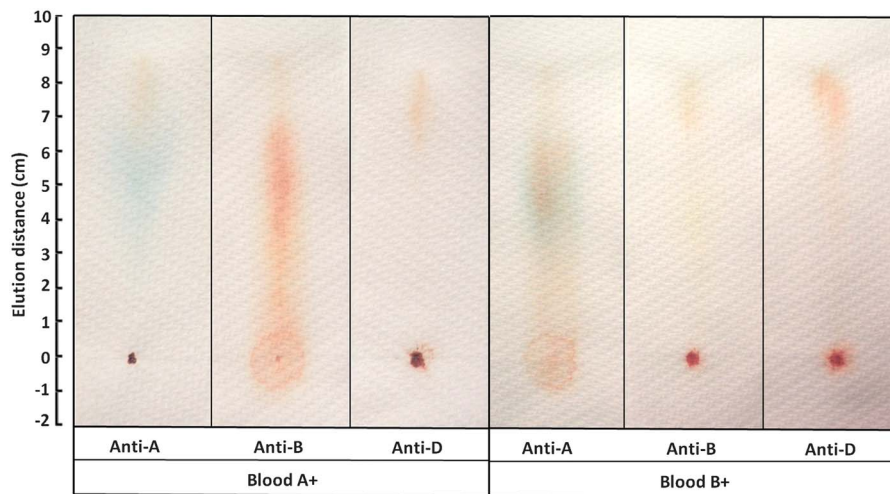


**Fig. 6** Chromatographic elution patterns of A+ and B+ blood samples reacting with grouping antibodies anti-A, anti-B, and anti-D.

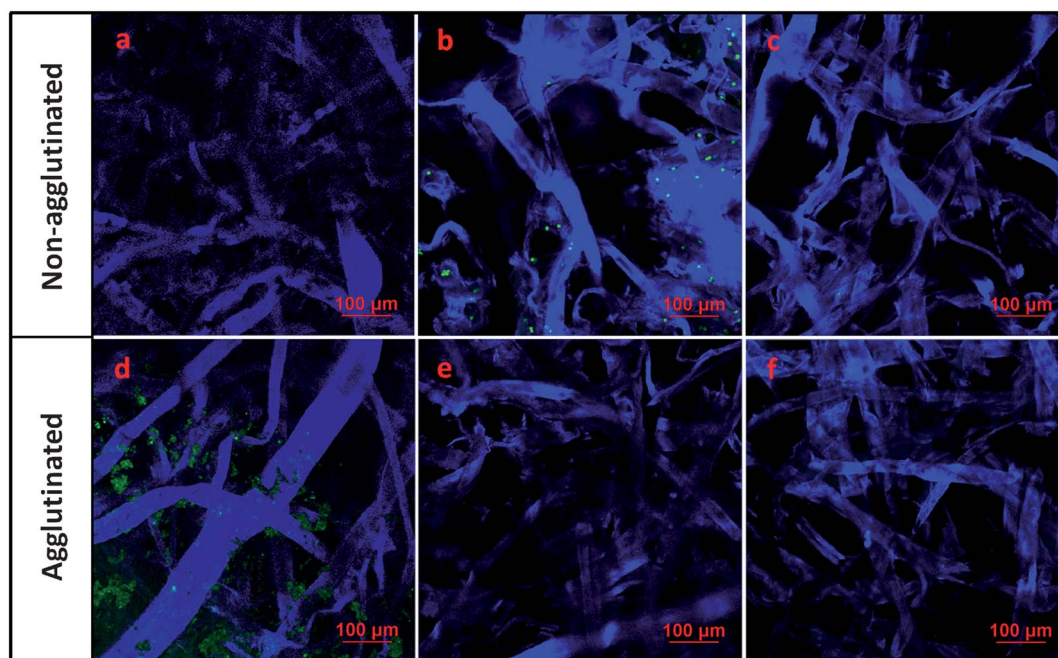


**Fig. 7** Confocal images of chromatographic elution patterns of non-agglutinated RBCs at an elution distance of 0 cm (a), 5 cm (b), and 8 cm (c) and agglutinated RBCs at an elution distance of 0 cm (d), 5 cm (e) and 8 cm (f).

of the positive assay is shown in Fig. 7d. Large lumps of agglutinated red blood cells are observed inside pores surrounded by fibres; this observation is consistent with the findings in Fig. 4. Another confocal image taken from the second band of the negative assay shows sparsely populated single red cells and small clusters formed by a few red cells on the fibre surface (Fig. 7b). This band therefore consists of the eluted, non-agglutinated RBCs. Further confocal images taken from the position of the second band of a positive assay failed to identify any RBCs (Fig. 7e). This is because most of the RBCs have been agglutinated in the spotting point in the antibody and blood sample zone; only a very small number of free RBCs are

available in this zone for chromatographic elution. Therefore it is very difficult to find free RBCs from the position of the second band. The confocal result is in good agreement with the elution pattern of positive assays observed in Fig. 6.

Confocal images of the first bands of all negative and positive assays did not show any cells, despite Fig. 6 showing that the first bands of all assays have a weak blood colour. An explanation is that the first band is the elution band of haemoglobin from the internal fluid of ruptured RBCs; this band has the deep red colour of blood but not due to the presence of non-ruptured RBCs. To support this explanation, chromatographic elution of two haemolysed blood samples of type A+ and



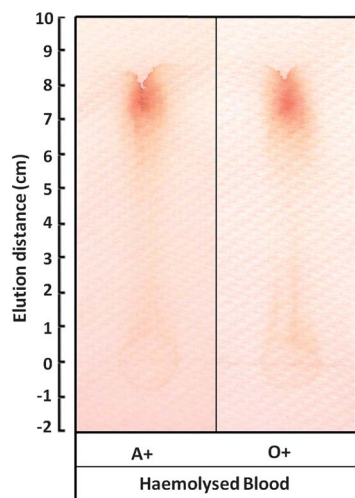


**Fig. 8** Chromatographic elution patterns of haemolysed blood samples of A+ and O+.

O+ was conducted under the same conditions. The haemolysed blood samples were obtained by mixing 3  $\mu$ L of blood and 10  $\mu$ L of distilled water for 5 minutes. The activity of haemolysed blood samples was evaluated by adding their corresponding grouping antibodies. The absence of haemagglutination reactions proved that the haemolysis of the RBCs had occurred. The chromatographic elution patterns of haemolysed blood samples of type A+ and O+ are shown in Fig. 8. The presence of only the first band confirms that it is indeed caused by the haemoglobin released after haemolysis of RBCs.

In this application study, the confocal microscopy method was used to investigate the two chromatographic elution bands and the spotting zone of blood typing assays on paper for the details of their composition. Confocal micrographs reveal that the rupture of RBCs occurred in the spotting zone. Haemoglobin released by the ruptured cells was eluted by the saline solution faster than the free RBCs and small cell clusters resulting in the first band close to the elution front, while free RBCs form the second elution band.

## Conclusions

A confocal microscopy method was developed to study the mechanism of the agglutination of RBCs in a paper-based blood typing device. This work shows that confocal microscopy is a suitable technique for providing the details of RBC agglutination at the cellular level inside the fibre network of paper. Human RBCs can be labelled with FITC without the antigens on the surface of the red cells losing their activity. Two laser beams of differing wavelength were used to excite fluorescent signals with two different emission wavelengths in lignocellulosic fibres and FITC-labelled red cells. These confocal signals were collected by different channels and converted into 2D and 3D confocal images for investigation of the fibre network, RBCs, and the different distributions of free RBCs and agglutinated blood lumps inside the fibre network. The non-agglutinated RBCs do not undergo morphological change, distributing rather

uniformly in the spaces of the fibre network and staying around the middle of the paper sheet. On the other hand, the agglutinated RBCs are deformed, forming blood aggregates immobilised randomly at different positions on the fibre surface.

A Kleenex paper towel was used as the substrate to prepare the paper-based blood typing device. The size of the interfibre pores of the Kleenex paper was shown by confocal micrographs to be much larger than the RBCs; the RBCs can thus be eluted by saline solution either vertically or laterally through the interfibre pores. RBCs undergo haemagglutination inside paper that was treated with the corresponding antibody. It has been confirmed by the confocal study that the release of antibody molecules from the fibre surface by dissolution is the main mechanism that causes haemagglutination. Haemagglutination of RBCs in the fibre network results in the formation of large lumps of aggregated cells, which become immobilised by mechanical entrapment within the interfibre pores. These aggregates could not be eluted by saline solution and thus result in the visual effect of the blood colouring becoming fixed on the paper. The non-agglutinated RBCs can be eluted by saline solution, therefore leaving no colour on paper after elution.

The confocal method was used to understand the chromatographic bands formed when blood samples are eluted in paper. This confocal method will be a powerful tool for understanding antibody and RBC interaction and for designing more sensitive bioactive paper-based blood typing devices in the future.

## Acknowledgements

This work is supported by Australian Research Council Grants (ARC DP1094179 and LP110200973). Authors thank Haemokinesis for its support through an ARC Linkage Project. Authors also thank staff of MCN for Confocal training and usage and Dr M. Al-Tamini of the Department of Chemical Engineering for information on red cell tagging. Ms Lizi Li, Ms Miaosi Li and Mr David Ballerini acknowledge the Monash University Research and Graduate School and the Faculty of Engineering for post-graduate research scholarships.

## Notes and references

- 1 G. Daniels and M. E. Reid, *Transfusion*, 2010, **50**, 281–289.
- 2 G. Daniels and I. Bromilow, *Essential Guide to Blood Groups*, Wiley-Blackwell, Chichester, West Sussex, UK, 2010.
- 3 D. Pramanik, *Principles of Physiology*, Academic Publishers, Kolkata, India, 2010.
- 4 B. H. Estridge, A. P. Reynolds and N. J. Walters, *Basic Medical Laboratory Techniques*, Cengage Learning, Albany, NY, USA, 2000.
- 5 F. Llopis, F. Carbonell-Uberos, M. C. Montero, S. Bonanad, M. D. Planelles, I. Plasencia, C. Riols, T. Planells, C. Carrillo and A. De Miguel, *Vox Sang.*, 1999, **77**, 143–148.
- 6 J. H. Spindler, H. Kluter and M. Kerowgan, *Transfusion*, 2001, **41**, 627–632.
- 7 Y. Lapierre, D. Rigal, J. Adam, D. Josef, F. Meyer, S. Greber and C. Drot, *Transfusion*, 1990, **30**, 109–113.

- 8 M. M. Langston, J. L. Procter, K. M. Cipolone and D. F. Stroncek, *Transfusion*, 1999, **39**, 300–305.
- 9 D. J. Anstee, *Blood*, 2009, **114**, 248–256.
- 10 J. Petrik, *Vox Sang.*, 2001, **80**, 1–11.
- 11 J. D. Roback, S. Barclay and C. D. Hillyer, *Transfusion*, 2003, **43**, 918–927.
- 12 D. Harmening, *Modern blood banking and transfusion practices*, F.A. Davis, Philadelphia, PA, 1999.
- 13 F. Giebel, S. M. Picker and B. S. Gathof, *Transfus. Med. Hemother.*, 2008, **35**, 33–36.
- 14 M. Al-Tamimi, W. Shen, R. Zeineddine, H. Tran and G. Garnier, *Anal. Chem.*, 2012, **84**, 1661–1668.
- 15 L. Neimo, *Papermaking Chemistry*, Fapet Oy, Helsinki, Finland, 1999.
- 16 X. Li, J. Tian, T. Nguyen and W. Shen, *Anal. Chem.*, 2008, **80**, 9131–9134.
- 17 X. Li, J. Tian, G. Garnier and W. Shen, *Colloids Surf., B*, 2010, **76**, 564–570.
- 18 Z. H. Nie, F. Deiss, X. Y. Liu, O. Akbulut and G. M. Whitesides, *Lab Chip*, 2010, **10**, 3163–3169.
- 19 M. S. Khan, G. Thouas, W. Shen, G. Whyte and G. Garnier, *Anal. Chem.*, 2010, **82**, 4158–4164.
- 20 P. Jarujamrus, J. Tian, X. Li, A. Siripinyanond, J. Shiowatana and W. Shen, *Analyst*, 2012, **137**, 2205–2210.
- 21 M. S. Li, J. F. Tian, M. Al-Tamimi and W. Shen, *Angew. Chem., Int. Ed.*, 2012, **51**, 5497–5501.
- 22 D. R. Ballerini, X. Li and W. Shen, *Anal. Bioanal. Chem.*, 2011, **399**, 1869–1875.
- 23 J. L. Su, M. Al-Tamimi and G. Garnier, *Cellulose*, 2012, **19**, 1749–1758.
- 24 E. F. Hauck, S. Apostel, J. F. Hoffmann, A. Heimann and O. Kempfski, *J. Cereb. Blood Flow Metab.*, 2004, **24**, 383–391.
- 25 A. G. Hudetz, G. Feher, C. G. M. Weigle, D. E. Knuese and J. P. Kampine, *Am. J. Physiol.: Heart Circ. Physiol.*, 1995, **268**, H2202–H2210.

# Control Performance of Paper-Based Blood Analysis Devices through Paper Structure Design

Lizi Li,<sup>†</sup> Xiaolei Huang,<sup>‡</sup> Wen Liu,<sup>‡</sup> and Wei Shen<sup>\*,†</sup>

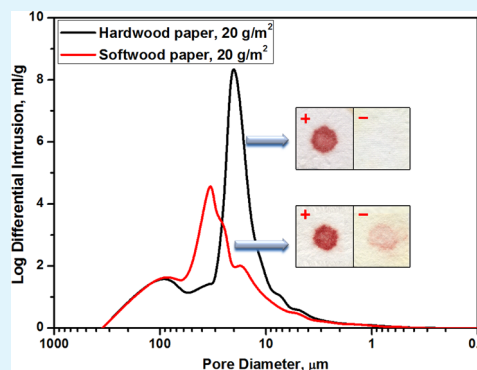
<sup>†</sup>Department of Chemical Engineering, Monash University, Clayton Campus, Clayton, VIC 3800, Australia

<sup>‡</sup>China National Pulp and Paper Research Institute, Beijing 100102, China

## S Supporting Information

**ABSTRACT:** In this work, we investigated the influence of paper structure on the performance of paper-based analytical devices that are used for blood analysis. The question that we aimed to answer is how the fiber type (i.e., softwood and hardwood fibers) influences the fiber network structure of the paper, which affects the transport of red blood cells (RBCs) in paper. In the experimental design, we isolated the influence of fiber types on the paper structure from all other possible influencing factors by removing the fines from the pulps and not using any additives. Mercury porosimetry was employed to characterize the pore structures of the paper sheets. The results show that papers with a low basis weight that are made with short hardwood fibers have a higher porosity (i.e., void fraction) and simpler pore structures compared with papers made with long softwood fibers. RBC transport in paper carried by saline solution was investigated in two modes: lateral chromatographic elution and vertical flow-through. The results showed that the complexity of the paper's internal pore structure has a dominant influence on the transport of RBCs in paper. Hardwood fiber sheets with a low basis weight have a simple internal pore structure and allow for the easy transport of RBCs. Blood-typing sensors built with low basis weight hardwood fibers deliver high-clarity assays. Softwood fiber papers are found to have a more complex pore structure, which makes RBC transport more difficult, leading to blood-typing results of low clarity. This study provides the principle of paper sheet design for paper-based blood analysis sensors.

**KEYWORDS:** paper-based diagnostic sensors, paper structure, hardwood fiber, softwood fiber, blood typing, mercury porosimetry



## 1. INTRODUCTION

Paper-based microfluidic devices and paper-based sensors have attracted a lot of attention because of their potential applications in point-of-care, immunoassays, food-quality testing, environmental monitoring, and disease screening in resource-limited areas.<sup>1–10</sup> Paper made of cellulose fibers demonstrates significant advantages over other substrates, such as silicon and glass, when used in the manufacturing of low-cost, disposable, and flexible diagnostic devices.<sup>1,2,11–13</sup> Paper-based sensors use the hydrophilic nature of the cellulose fiber network to transport homogeneous aqueous liquids by capillary wicking. To control the direction of liquid wicking on paper, previous publications reported a variety of methods to pattern the paper.<sup>1,14–17</sup> By physically and chemically functionalizing paper and patterned paper devices, many routine chemical and biological assays can be performed using paper-based devices without the need for sophisticated analytical equipment.<sup>1,9–11</sup> More recently, paper-based microfluidic diagnostics has evolved from analyzing samples of very simple matrices to analyzing samples of more complex matrices, such as animal and human blood samples.<sup>18–20</sup> Paper-based device design has increasingly involved the use of a colloid suspension, such as metal nanoparticles and encapsulated functional nanoparticles, as the reaction media or indicator

system.<sup>21,22</sup> Although several methods of using paper to separate and analyze heterogeneous samples have been demonstrated, the physicochemical properties of paper that are best-suited for analyzing a heterogeneous sample are not yet fully understood.<sup>1</sup> Paper is a material with a three-dimensional porous structure that is formed by multiple layers of cellulosic fibers.<sup>23,24</sup> It has been used for a long time as a filtration medium for separating solid and colloidal particles from heterogeneous fluids. To better utilize the filtration property of the paper to design high-performance paper sensors for complex sample analysis, a detailed understanding of the fiber network structure and particle transport behavior in paper is necessary.

Our group has developed a series of paper-based fluidic devices for blood typing; these devices work based on filtration and chromatographic separation principles.<sup>8,18,19,25</sup> Whole human blood is composed of a continuous plasma phase with red blood cells (RBCs) in a suspension state. The blood group is classified on the basis of the inherited differences (polymorphisms) in the antigens on the surface of the RBCs.<sup>26–28</sup>

**Received:** September 26, 2014

**Accepted:** November 18, 2014

Whereas the biochemical basis of a paper-based blood-typing assay is the hemagglutination of RBCs by their corresponding grouping antibodies, the mechanism of interpreting the assay result relies on the transport behaviors of agglutinated RBC lumps and nonagglutinated free RBCs within the porous fiber network of the paper. Paper-based blood-typing devices are fabricated by simply imbibing blood group antibody solutions into the fiber network of a paper. In a blood-typing assay, a blood sample is allowed to imbibe into the paper that has been treated with the antibodies. This design concept allows the hemagglutination to occur inside the fiber network of the paper. For a positive assay, hemagglutination makes RBCs agglutinate via the intercellular cross-linking by their corresponding antibody molecules. The agglutinated RBC lumps are then immobilized primarily by mechanical entrapment in the porous structure of paper. In contrast, no hemagglutination occurs in a negative assay; nonagglutinated RBCs remain stably dispersed in the plasma phase and can move through porous fiber network of paper, with plasma occurring as a single suspension phase.<sup>18,25,29</sup> To display the blood-typing result, the assay is subjected to either a buffer elution in a chromatographic tank or a buffer rinsing step to allow a small volume of buffer to penetrate the paper. Buffer elution or buffer rinsing is intended to flush out free RBCs from the fiber network. Because only nonagglutinated RBCs are free in the fiber network and agglutinated RBC lumps are not, a chromatographic elution or buffer rinsing can provide visual evidence of the occurrence of hemagglutination: a negative assay should show no blood color on the paper, whereas a positive result should show a strong blood color.<sup>18,19</sup>

A successful blood-typing assay on paper must differentiate a positive assay from a negative one with high clarity. In our investigation, we observed that blood-typing assay clarity is dependent on the type of paper selected. Visually, low clarity means that a negative assay may carry a faint to moderate blood color, whereas a positive assay occasionally gives a low density of the blood color; these observations may lead to an ambiguous assay result. To improve the clarity of the paper-based blood-typing assays, paper structures must be characterized and their influence on the movements of RBCs must be understood. This understanding will provide key information not only for selecting the right papers to fabricate blood-typing devices but also for fabricating paper-based devices for other blood analyses.

A paper sheet is often considered as an infinite network in its lateral dimensions but finite in the vertical (or *z*) direction.<sup>24</sup> Because paper-based blood-typing devices typically adopt two different designs, i.e., the lateral chromatographic flow design<sup>8,18</sup> and the vertical flow-through design,<sup>19,25</sup> the paper structure may influence the sample flow and the RBC separation of these flow modes differently, due to the anisotropic structural characteristics of paper.

In an actual papermaking process, a variety of chemical additives are used to improve the paper sheet properties, which include the wet and dry strength and printability additives. These additives include cationic starch, sodium carboxymethyl cellulose (CMC), and cationic polymers, such as polyacrylamide (PAM) and poly(diallyl dimethylammonium chloride) (PDADMAC).<sup>13,30,31</sup> Wood pulps also contain a fraction of fine fibrous and granular particles known as fines. However, for the papers that are used for blood typing, the charges carried by additives may affect the transport behavior of RBCs in fiber networks because RBCs are negatively charged in the plasma

environment.<sup>28</sup> Fines may also interact with fibers and RBCs. Because of the above factors, no commercial paper possesses the optimized properties for blood-typing assays.

In this work, we investigate the effect of paper structure on the performance of paper-based blood-typing devices. Papers with different basis weights were made using different fibers. To clearly identify the influence of the paper's physical structures on its blood-typing performance, no chemical additives were used and the fine particles in the pulp were removed in this study. The paper sheet properties were characterized with apparent thickness and apparent bulk measurements and with mercury intrusion porosimetry. Blood-typing assays by lateral chromatographic elution and vertical flow-through modes were investigated to study the red blood cell transport behavior in the papers' internal porous structure and the paper-based sensor performance.

## 2. EXPERIMENTAL SECTION

**2.1. Materials.** Eucalyptus hardwood bleached kraft pulp and northern softwood bleached kraft pulp were obtained from the National Institute of Standards and Technology (Gaithersburg, MD). The properties of these pulps were retrieved from the reports of NIST standard reference materials 8495 and 8496. Standard blotting paper with a basis weight of 280 g/m<sup>2</sup> was obtained from Fibrosystem AB and used as the absorbent paper for making handsheets. Blood samples were collected from adult volunteers with known blood groups through Red Cross Australia. All blood samples were stabilized with anticoagulant additives, stored in Vacutainer test tubes containing heparin, citrate, and EDTA at 4 °C and used within 7 days of collection. ALBAclone anti-A (Z001), anti-B (Z011), and anti-D (Z039) monoclonal grouping reagents were sourced commercially from Alba Bioscience Ltd. Anti-A and anti-B are a transparent cyan and a transparent yellow solution, respectively, whereas anti-D is a colorless solution. Monoclonal grouping reagents were also kept at 4 °C. Analytical grade NaCl from Sigma-Aldrich was used to prepare the physiological saline solution.

**2.2. Methods.** Hardwood and softwood fibers were obtained by disintegrating hardwood and softwood pulps using a Messmer standard pulp disintegrator for 7500 revolutions. The fibers were then thoroughly washed with a 150-mesh to remove the fines. Handsheets with basis weights of 20, 35, and 50 g/m<sup>2</sup> were made with hardwood and softwood fibers. Handsheets (20 g/m<sup>2</sup>) with different contents of hardwood and softwood fibers were also made. TAPPI (Technical Association of the Pulp and Paper Industry) standard method T205 was followed for making the handsheets. All handsheets were conditioned at 23 °C and 50% relative humidity for 24 h before measuring their physical properties. The sheet basis weight, apparent thickness, and apparent bulk were measured following the TAPPI standard method T220. The terms "thickness" and "bulk" used below indicate the "apparent thickness" and "apparent bulk". The mercury intrusion measurements were performed using an AutoPore IV 9500 instrument (Micromeritics).

For the lateral chromatographic elution test, paper handsheets were cut into 100 × 30 mm<sup>2</sup> strips. Ten microliters of antibody solution was spotted 2 cm from the shorter side of the paper strip and allowed to be absorbed completely over 30 s. An aliquot of 1 μL of whole blood sample was dropped onto the center of the antibody spot and allowed to react with the antibody reagent for 30 s. Then, the paper strip was suspended in a physical saline solution in a chromatographic tank to allow elution for 90 s; the distance between the blood spot and the level elution buffer was kept at 10 mm. The paper strip was then removed from the chromatographic tank and suspended in a fume cupboard to be dried in air at room temperature for 10 min. The dried paper strip was then scanned using a scanner (Epson Perfection 2450) for image analysis.

For the vertical flow-through saline-rinsing blood-typing test, handsheets were cut into 10 × 10 mm<sup>2</sup> paper squares. The testing paper was prepared by adding 10 μL of antibody solution to the paper



surface and allowing it to dry in air for 3 min. One microliter of whole blood sample was introduced onto the paper and allowed to react with the antibody reagent for 30 s. The testing paper was then transferred onto a sheet of blotting paper to perform the saline rinsing. Rinsing was performed by introducing a total of 30  $\mu\text{L}$  of saline solution onto the center of the blood spot for two applications; the absorbing power of the blotting paper assisted the rinsing buffer to penetrate through the testing paper. The rinsed blood-testing paper was allowed to dry in the fume cupboard for 10 min. A scan of the dried testing paper was then obtained.

The optical density values of blood spots of the positive and negative assays were assessed and reported as the mean  $\pm$  SD (standard deviation). Unpaired two-tailed *t* tests were used to compare the mean optical density values for the analysis of different blood samples with different testing modes. One-way analysis of variance (ANOVA) was applied to compare the mean red color optical density in more than two groups. The statistical analysis was performed using the GraphPad Prism (version 6) software with *P* < 0.05 considered significant.

### 3. RESULTS AND DISCUSSION

**3.1. Isolation of the Paper Physical Structure from the Influence of Chemical Additives and Fines.** To gain a precise understanding of the influence that the paper sheet physical structure has on its bloodtyping performance, we formed handsheets using well-characterized softwood and hardwood pulps, but without using any additives. Fines were also removed because their contribution to RBC transport should be investigated separately.

Handsheets with basis weights of 20, 35, and 50  $\text{g}/\text{m}^2$  were made with hardwood and softwood fibers, respectively. Figure 1a shows that the apparent thickness of the handsheets increased substantially with the increase in sheet basis weight. For hardwood handsheets, when the basis weight was increased from 20 to 50  $\text{g}/\text{m}^2$ , the thickness increased from 84.9 to 171.9  $\mu\text{m}$ , representing an increase of 102.5%. For handsheets made from softwood fibers, a similar trend can be observed. This trend is intuitively appreciable because the number of fiber layers increases with the basis weights of handsheets. Figure 1a also shows that all of the hardwood handsheets have greater apparent thickness compared with the softwood handsheets of the same basis weight. Figure 1b shows that for each basis weight, hardwood sheets have a higher bulk value than do the softwood sheets. The bulk of a paper is defined as the reciprocal of the sheet density and has a unit of cubic centimeters/gram.<sup>32</sup> Additionally, the bulk of the hardwood and softwood handsheets decreased from 4.13 to 3.36  $\text{cm}^3/\text{g}$  and from 3.88 to 3.07  $\text{cm}^3/\text{g}$ , respectively, as the sheet basis weights increased to 50  $\text{g}/\text{m}^2$ . The data in Figure 1b indicate that the volume of voids in a hardwood sheet was higher than that in a softwood sheet of the same basis weight. It also indicates that the fiber network became denser as the sheet basis weight increased.

Figure 2 shows the thickness and bulk of handsheets made of different blends of hardwood and softwood fibers, all with a basis weight of 20  $\text{g}/\text{m}^2$ . The thickness of the handsheets increases with the content of hardwood fibers to 50% at first and then levels off. It, however, is only suggested because the error bars of some data sets are large. Detailed handsheet data can be found in Table S3 in the Supporting Information (SI). By varying the sheet thickness and bulk through controlling the content of different fibers, the structure of the paper network can be varied in a controlled manner. This provides the possibility to investigate the influence of the paper's physical structure on the transportation and immobilization of RBCs, without any interference from chemical additives.

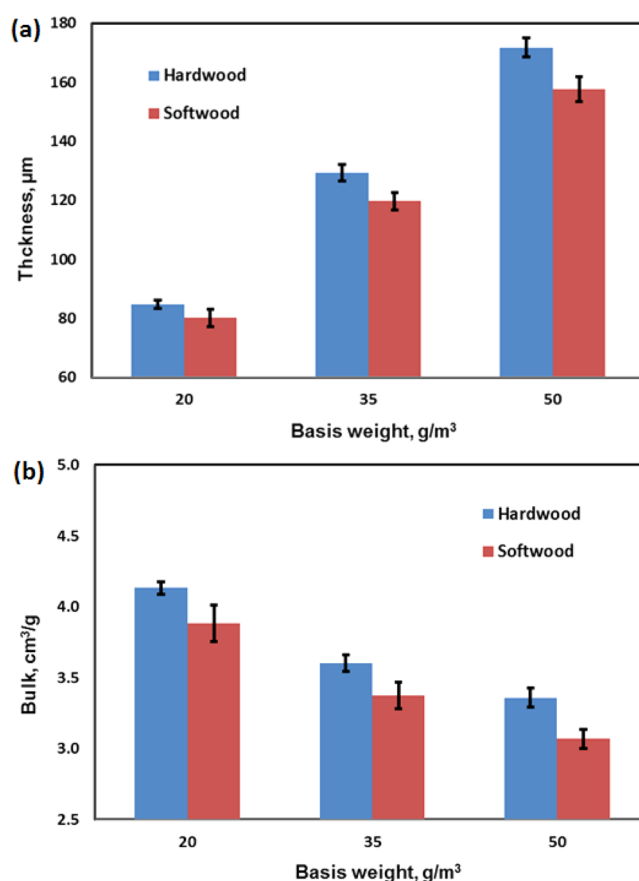


**Figure 1.** Apparent thickness (a) and apparent bulk (b) of hardwood and softwood handsheets of different basis weights.

**3.2. Characterization of Pore Size Distribution of Paper.** Mercury porosimetry was used to characterize the pore size distribution of handsheet samples. Figure 3a shows the pore size distributions of hardwood handsheets of different basis weights. The data show similar bimodal patterns. Such a pattern has been reported previously.<sup>33</sup> Silvy et al. attributed the low-intensity peak of larger pore diameters to the pores located on the surface of the paper and the high-intensity peak of smaller pore diameters (between 10 and 30  $\mu\text{m}$ ) to pores inside the sheets.<sup>33</sup> Our results show that both peaks for hardwood 20  $\text{g}/\text{m}^2$  paper are higher than those of papers with higher basis weights; this finding indicates that papers with lower basis weight have a more porous surface and internal structures. This finding is in agreement with the sheet bulk results shown in Figure 1b.

The sizes of the surface pores of hardwood paper are centered at approximately 100  $\mu\text{m}$  and range from 45 to 200  $\mu\text{m}$ . Because RBCs have the shape of biconcave disks, with a diameter of 6–8  $\mu\text{m}$  and a thickness of 2  $\mu\text{m}$ ,<sup>29</sup> they can easily pass through the surface pores of hardwood paper. Furthermore, the integral of the log differential intrusion plot over a certain pore size range gives the cumulative mercury intrusion volume; it reflects the pore volume corresponding to the pore size range of the material being tested.<sup>34</sup> Because the 20  $\text{g}/\text{m}^2$  hardwood handsheet has the highest volume of surface pores, it could therefore be hypothesized to have a greater capability to allow for the lateral transportation of free RBCs via chromatographic elution.

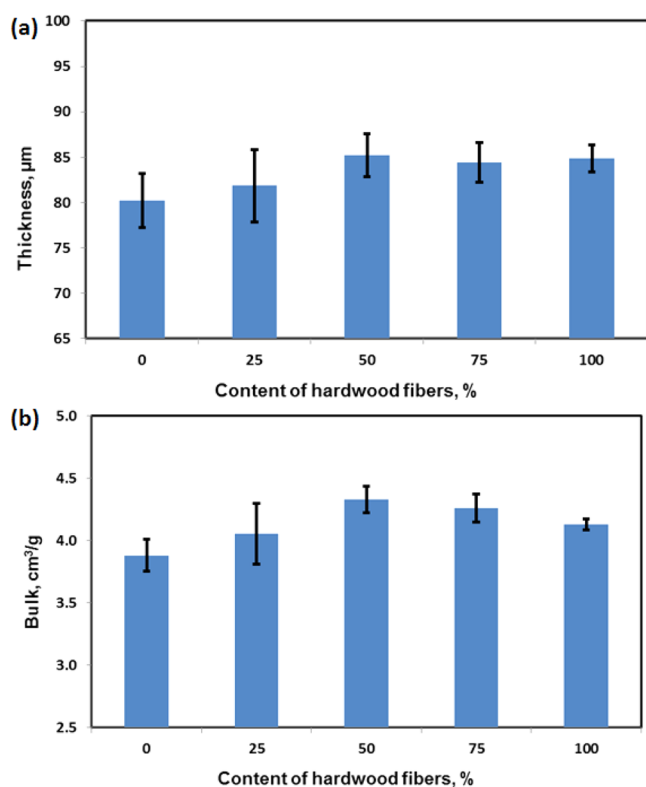


**Figure 2.** Apparent thickness (a) and apparent bulk (b) of handsheets with different content of hardwood and softwood fibers (basis weight of all sheets was 20 g/m<sup>2</sup>).

Figure 3a also shows that the internal pores of hardwood handsheets with basis weights of 20, 35, and 50 g/m<sup>2</sup> are centered at 20, 18, and 10 μm, respectively. Among these handsheets, the 20 g/m<sup>2</sup> one has an internal volume of 8.4 mL/g, while the internal volumes of the 35 and 50 g/m<sup>2</sup> sheets are much lower, being 4.7 and 4.2 mL/g, respectively. In addition, the high-intensity peak of the 20 g/m<sup>2</sup> hardwood handsheet is narrower than those of higher basis weights. These findings suggest that low basis weight handsheets have more uniform internal pore size distribution, which is a desirable sheet property for separation. It is noted, however, that the internal pore size distribution of the 50 g/m<sup>2</sup> hardwood sheet has a shoulder, suggesting that the internal structure is formed by pores of two sizes. We hypothesized that the internal pore structure of the 50 g/m<sup>2</sup> hardwood sheet was less uniform and more complex. One explanation of this observation is that sheets of high basis weight contain more fibers, which contribute to more fiber–fiber bonding; this leads to a more complex internal pore structure of the sheet. We hypothesize that RBC transport in complex pore structures would be more difficult. This effect is discussed in more detail below.

Internal pores with diameters smaller than 8 μm would not provide easy transport pathways to free RBCs. Although it is known that red cells can pass through veins with smaller diameters than those of RBCs under pressure through cell deformation,<sup>35,36</sup> no report has shown that this would also occur for RBCs traveling in a porous network under no external pressure.

In summary, hardwood handsheets of lower basis weights could have the potential to transport free RBCs more efficiently via both chromatographic elution and flow-through modes

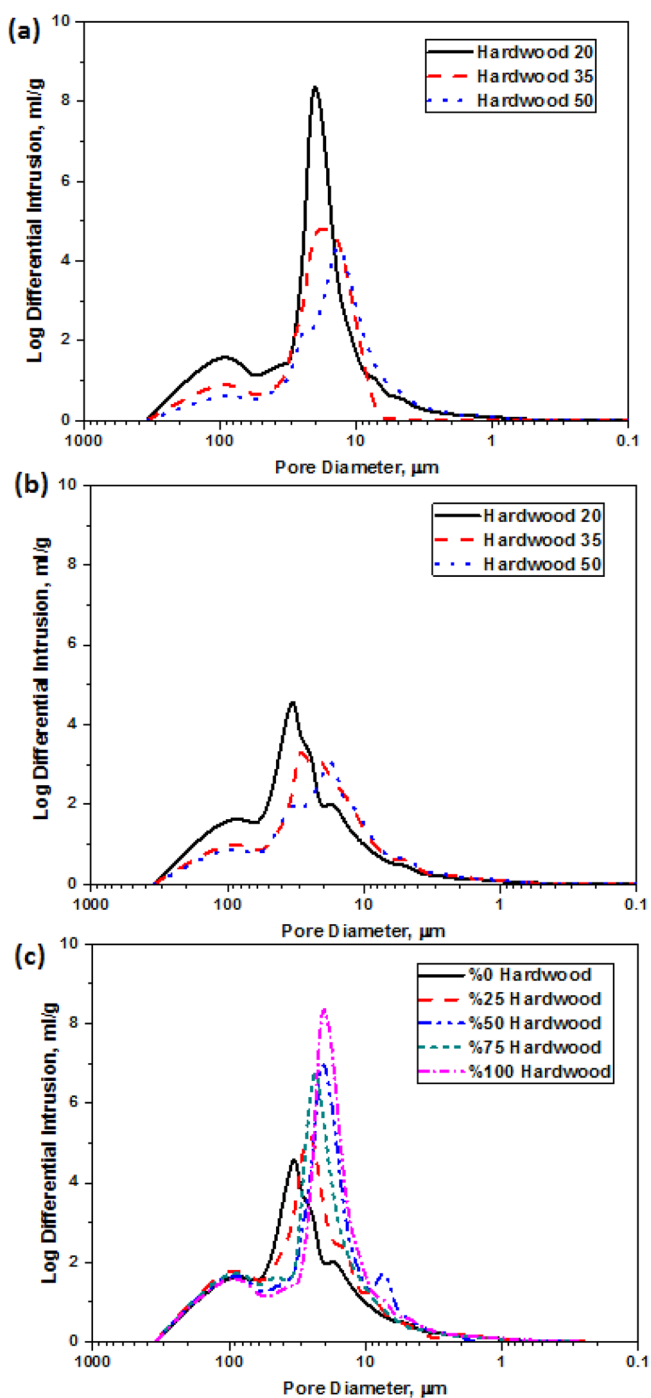


**Figure 3.** Pore size distributions of (a) hardwood paper with different basis weights, (b) softwood paper with different basis weights, and (c) paper with different content of hardwood and softwood fibers (basis weight of 20 g/m<sup>2</sup>).

because of their large surface volume and internal pores that have uniform sizes.

The pore size distributions of softwood papers are illustrated in Figure 3b. The first (left) peak corresponds to surface pores; the second peak with more than one shoulder corresponds to the internal pores. The pore volume of softwood handsheets decreases as the basis weight increases; this trend is similar to that observed for hardwood sheets. This trend indicates that sheets of higher basis weights contain more fibers and therefore more fiber–fiber bondings, which leads to denser sheets (see

also Figure 1b). This finding is in agreement with the sheet bulk data in Figure 1b.

The first peak of surface pores of softwood paper is also centered at approximately 100  $\mu\text{m}$ , similar to that of the hardwood paper. The most interesting information in Figure 3b, however, is that the mercury intrusion results show more than one peak in the region of internal pores, indicating that the internal pore structures of the softwood sheets are more complicated than those of hardwood sheets and that mercury intrusion into the softwood handsheets has met a hierarchical internal structure. This can be clearly observed from the four peaks (shoulders) of the intrusion curve for the internal pore region of the 20  $\text{g/m}^2$  softwood sheet. At the end of each step of the hierarchical structure, the rate of mercury intrusion slowed down, but the rate increased again when mercury intruded into the pores of the next hierarchical step. This could make the transport of RBC in softwood sheets more difficult. The mercury intrusion results are discussed with respect to the RBC elution results below.

The pore size distributions of papers made by blending hardwood and softwood fibers in different proportions were also analyzed using mercury porosimetry, and the results are presented in Figure 3c. The basis weight of all of the sheets made with mixed fibers was 20  $\text{g/m}^2$ . The results show that mixing short and long fibers in different proportions does not change the size or volume of the surface pores. Thus, the surface pores are dominantly determined by the basis weight of the sheets and sheet-forming conditions, but not by the fibers. Figure 3c also shows three expected trends. First, as the percentage of long softwood fibers in the handsheets increases, the overall pore volume of the sheets decreases. This trend is supported by the conclusion of the previous section that long softwood fibers form denser sheets. Second, the pore size of handsheets increases with an increase in the percentage of softwood fibers. This trend can be explained as follows: the pore size of a network structure formed with larger fibers (both in length and in width) is larger than that formed with smaller fibers. Third, the internal sheet structure becomes increasingly complex as the percentage of long fibers is increased to above 50%. This trend is supported by the increased fiber network hierarchical structure with the increase of long fibers in the network.

With the above insights into the handsheet surface and internal structures, we have made hypotheses concerning RBC transport behavior in different sheets. Tests of these hypotheses are presented below.

**3.3. Effect of the Physical Structure of Paper on Lateral Elution Blood-Typing Performance.** In the lateral chromatographic elution blood-typing test, blood was spotted onto a handsheet treated with grouping antibody reagents; the spotted sheet was then chromatographically eluted by physical saline solution in a chromatographic tank for 90 s. A blood sample spotted on its corresponding antibody will agglutinate and become immobilized on the same spot in paper and resist saline elution; this signifies a positive test result. Conversely, a blood sample spotted onto noncorresponding antibodies will not agglutinate; RBCs remain free and can be eluted away by the saline buffer, leaving behind no, or a very faint, blood spot. Such an assay signifies a negative result. The critical criterion of a high-performance blood-typing device is the ability to distinguish a positive result from a negative result with high clarity. Both surface and internal pores of paper affect the fixation and transport of agglutinated and free RBCs.

From Figure 4a, the positive and negative results for the 20  $\text{g/m}^2$  hardwood paper had the highest clarity judged by naked

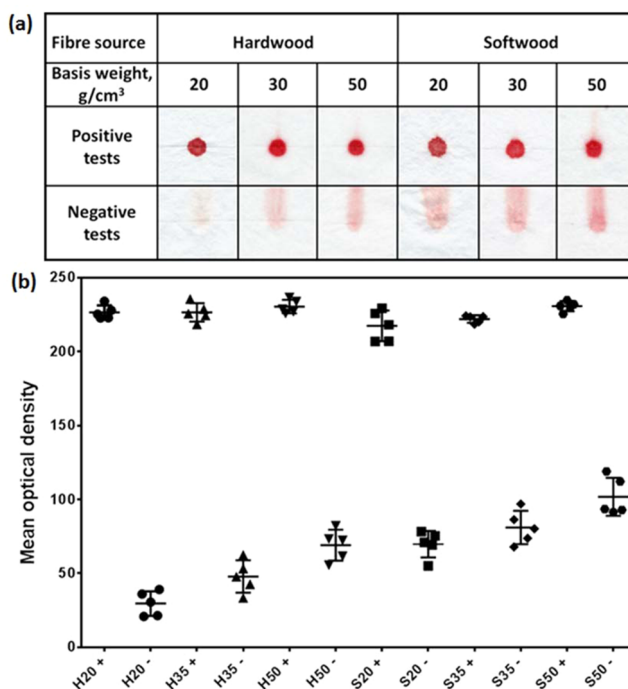


**Figure 4.** Lateral chromatographic elution blood-typing tests using papers of different basis weights: (a) scanned images of testing results and (b) mean optical densities of positive (+) and negative (−) tests. H, hardwood fibers; S, softwood fibers. The numbers after H and S are the basis weights of papers in  $\text{g/m}^2$ .

eye, whereas the results for the 50  $\text{g/m}^2$  softwood sheet had the lowest clarity. Quantitative analysis of optical density of the blood spotting area is given in Figure 4b and Table S3 in the SI. The optical densities of all positive tests were high and not significantly affected by either sheet basis weight or fiber type. However, the optical density of all negative tests increased substantially with an increase in sheet basis weight. In addition, the scanned images of chromatographically eluted blood spots on handsheets containing different percentages of softwood fibers (Figure 5a) show that although the positive tests on all sheets have high optical density (Table S4, SI), the optical density of negative results increases with the increase in softwood fiber content; this reduces the clarity of the negative tests. Therefore, for sheets of the same basis weight, their chromatographic elution performance reduces as the content of the softwood fiber in the sheet increases.

To interpret the above results, the following points are considered. First, the reason why positive tests are less affected by the physical structure of paper sheets is because the RBC reacted with the corresponding antibody and agglutinated into large aggregates. Our previous confocal microscopy study revealed that agglutinated RBC aggregates were immobilized inside the fiber network through entrapment in interfiber gaps and adhesion to the fiber surface.<sup>29,40</sup> Those immobilized RBC aggregates could not be moved by capillary-driven buffer elution. Therefore, the physical properties of paper sheets have a weak influence on the clarity of positive tests performed using the chromatographic elution method.

Second, the physical structure of the paper substrate plays a significant role in the elution of nonagglutinated RBCs in a



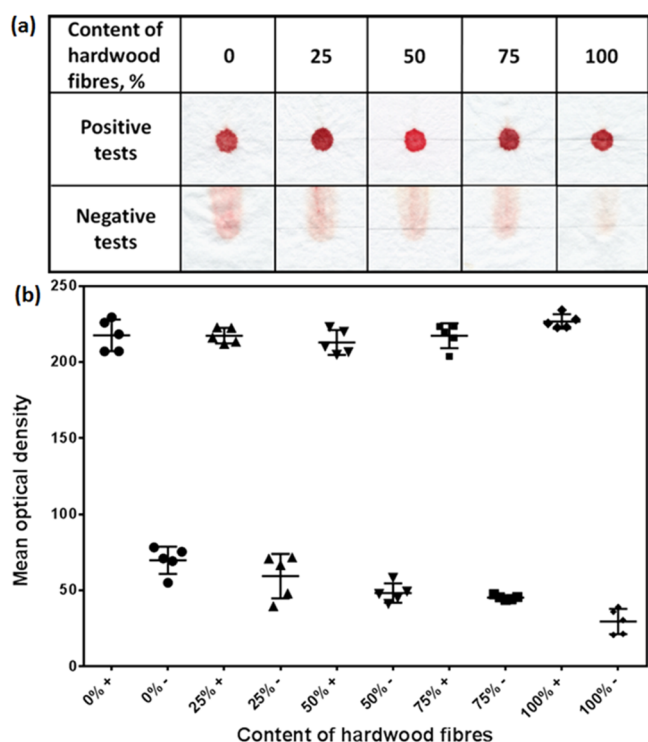


**Figure 5.** Lateral chromatographic elution blood-typing tests using paper with different content of hardwood fibers: (a) scanned images of testing results and (b) mean optical densities of positive (+) and negative (−) tests.

negative test using the chromatographic elution method. Mercury intrusion results of handsheets made with different fibers and mixed fibers showed that most internal pores of all sheets are sufficiently large for free RBCs to pass through. However, the internal pore structures became more complicated as the content of softwood fibers increased (Figures 3c and 5) and as the sheet basis weight increased (Figures 3a,b and 4). Because the movement of RBCs in the fiber network is driven by the capillary flow of the plasma phase, it will be slowed down when the network becomes more complex.

Roberts et al.<sup>37</sup> showed that the penetration of aqueous liquid in paper was by film flow. V-shaped microgrooves formed by the interfiber gaps constitute a major group of channels for liquid transport in paper. Their model shows that liquid wicking along a fiber gap is interrupted or stopped when the liquid wicking front hits the discontinuity of a V-groove channel. Roberts et al. showed that fiber–fiber crossing points could be points of discontinuity, which could cause the liquid wicking front to stop and then change to another channel to continue the wicking.<sup>37</sup> In our study of blood wicking in paper, RBCs are likely to be caught at the fiber–fiber crossing points where the buffer wicking front hits points of discontinuity. This will increase the chance for more and more RBCs to be left behind the buffer wicking front, reducing the clarity of a negative blood-typing assay by chromatographic elution.

Softwood fibers are approximately three times longer and are thicker than hardwood fibers.<sup>38</sup> In a paper sheet, a single softwood fiber may have more fiber–fiber crossing points than a single hardwood fiber because of the greater length of the former. He et al. and Batchelor et al. proposed a new analytical model that links the paper sheet cross-sectional properties of the fibers in the sheet to the number of fiber–fiber crossing

points per unit length of fiber; their modeling work concluded that the number of fiber–fiber crossing points along a single softwood fiber in a sheet is greater than that along a hardwood fiber.<sup>39</sup> This greater number leads to a larger number of liquid flow discontinuities along a single softwood fiber than a single hardwood fiber. Because of the greater width of a softwood fiber compared with a hardwood fiber, the fiber–fiber contact area of two crossing softwood fibers is greater than those of two crossing hardwood fibers. Therefore, fiber–fiber crossings formed by softwood fibers present more substantial discontinuities to the liquid flow and RBC migration. In this study, the observed more complex internal pore structures of softwood fiber sheets agree with the above analysis. Therefore, buffer wicking in paper sheets with higher softwood fiber content will meet a greater number of discontinuities. This creates more obstacles to the elution of free RBCs, resulting in negative elution blood typing with low clarity. Increasing the sheet basis weight has a similar effect.

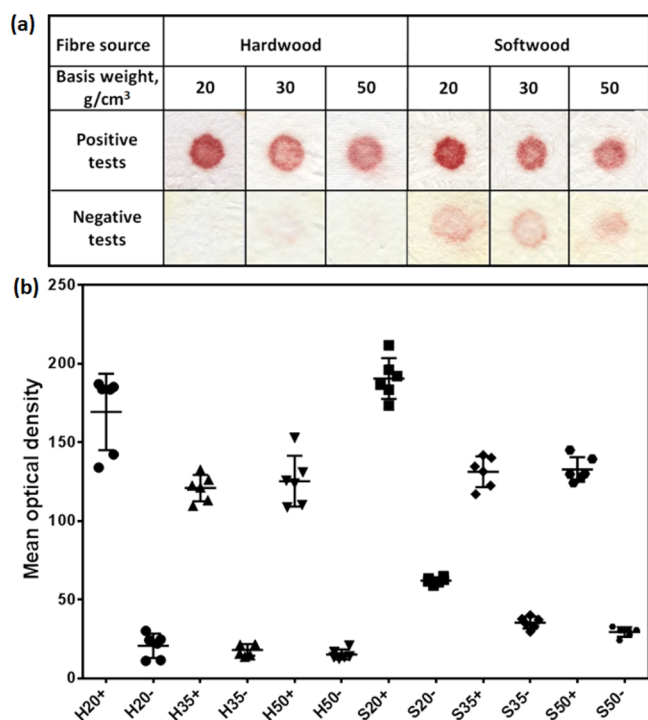
In summary, a paper's physical structure affects the clarity of positive tests of chromatographic elution blood typing relatively weakly, but it affects the clarity of negative tests significantly. Our investigation shows that paper sheets of low basis weight and high hardwood fiber content provide greater assay clarity for chromatographic elution blood typing. The results from this study provide a guide for the future investigation of paper chemical effects on elution blood typing.

**3.4. Effect of Paper Physical Structure on Vertical Flow-Through Blood-Typing Performance.** An advantage of the flow-through test over the lateral elution test in practical blood-typing application is its rapidness; test results can be read immediately after rinsing. The mechanism of buffer rinsing and buffer elution is different, and the influence of paper properties on the clarity of flow-through rinsing results is thus different.

For the buffer rinsing method, the buffer does not just enter the pores in a paper sheet by capillary wicking. Instead, when a drop of buffer is added to the blood spot on paper surface, it floods the blood spot. Because the agglutination of RBCs by their corresponding antibodies is a reversible process, some large lumps of agglutinated RBCs may dissociate into smaller ones or even to free RBCs when flooded by buffer and be flushed away by the rinsing buffer. Figure 6a shows that the color densities of positive assays obtained using the rinsing method are weaker than those obtained using the elution method for the same handsheets, whereas the clarity of negative assays was improved.

The antibody concentration in the paper sheet is likely to be the major factor affecting the color density of positive assays. Because buffer rinsing can cause the dissociation of agglutinated RBCs, a higher antibody concentration in the sheet will resist such dissociation by shifting the equilibrium toward the RBC agglutination. In the antibody treatment of the sheets, the same quantity of antibody solutions was added to sheets of different basis weights, which have different thickness (Figure 1a). Our experimental observation showed no significant difference in sizes of antibody-wetted areas on sheets of different basis weights. Considering that low basis weight sheets have low thickness, the antibody would be distributed in a smaller volume; the antibody concentration in low basis weight sheets is likely to be higher than that in high basis weight sheets. Because the RBC agglutination is controlled by the equilibrium involving the antibody concentration, it is expected that the RBC agglutination on the 20 g/m<sup>2</sup> sheets would be the strongest. The results of optical density for positive tests in





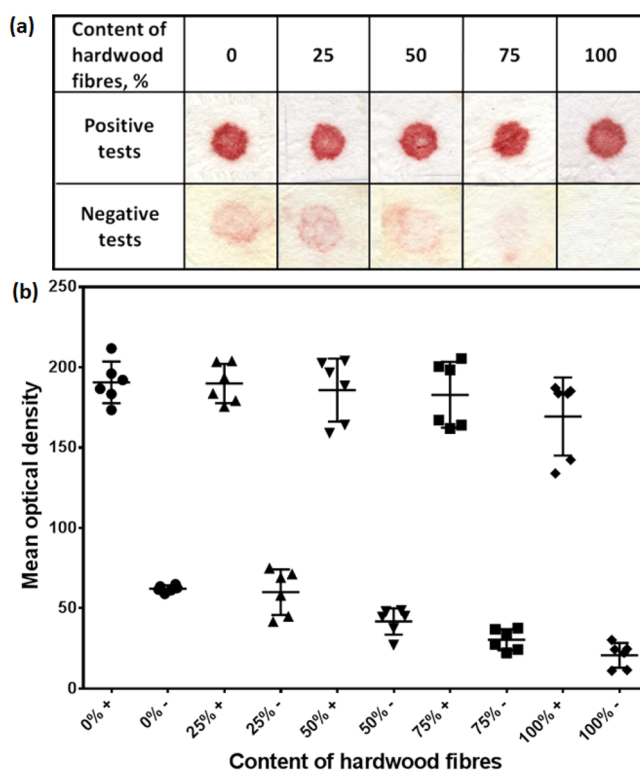
**Figure 6.** Vertical flow-through blood-typing tests using paper of different basis weights: (a) scanned images of testing results and (b) mean optical densities of positive (+) or negative (−) tests. H, hardwood fibers; S, softwood fibers. The numbers after H and S are basis weight of papers in g/m<sup>2</sup>.

Figure 6 and Table S5 (SI) support this analysis. For the rinsing method, the blood spot color densities of positive assays on sheets of different basis weights are different. This trend is different from that observed for the elution method. The slightly higher optical density of a positive result on 20 g/m<sup>2</sup> softwood than on 20 g/m<sup>2</sup> hardwood sheets can be attributed to the higher complexity of the internal pore structure in the softwood sheet compared with the hardwood sheet; complex pore structures make the movement of agglutinated RBCs in fiber network difficult.

For negative assays, hardwood fiber sheets show higher clarity than do softwood fiber sheets. This result can also be attributed to the structures of the fiber network. The less complex pore structures of hardwood fibers allow easy movement of RBCs with the rinsing buffer to travel through the sheets. Again, the more complex pore structure of the softwood fiber sheets makes RBC movement more difficult.

The blood-typing assay performances of all 20 g/m<sup>2</sup> mixed fiber sheets are shown in Figure 7. According to the above analysis, it can be understood that the color density of all positive assays is not significantly dependent on fiber mixing. However, the color density of negative assays is affected by the content of softwood fibers because of the increasing complexity in the sheet pore structure as the softwood fiber content increases.

In summary, the future design of paper sheets for buffer rinsing or flow-through blood-typing sensors will need to follow the principle using a low basis weight sheet with low content of softwood fibers.



**Figure 7.** Vertical flow-through blood-typing tests using paper of different content of hardwood fibers: (a) scanned images of testing results and (b) mean optical densities of positive (+) or negative (−) tests.

#### 4. CONCLUSIONS

In this study, we identified two important paper sheet physical properties that significantly influence the RBC transport behavior in paper: the fiber type and the sheet's internal pore structures. These properties must be controlled in paper sheet design for blood analysis applications. Low basis weight papers made with hardwood fibers have high porosities (i.e., the void fraction) and a simple internal pore structure. These properties, particularly the simple internal pore structure, allow the easy transport of RBCs in paper. Sensors made with such paper deliver high-clarity assay results. However, papers made with softwood fibers have lower porosity, and mercury porosimetry data revealed more complex sheet internal pore structures. Complex pore structures do not allow the easy transport of RBCs; thus, paper sheets made of softwood fibers have an inferior blood-typing performance compared with sheets made of hardwood fibers. Our analysis suggests that the number of fiber–fiber contacts along a single fiber in a sheet is likely to be a significant factor that affects the RBC transport. This analysis is made on the basis of the aqueous liquid flow pattern in paper that was previously reported. The liquid penetration front in a fiber network may be slowed down when it hits a discontinuity in its flow path, and fiber–fiber contacts in paper were identified by Roberts et al. as discontinuities for liquid penetration. Softwood fibers are much longer and thicker than hardwood fibers; the number of fiber–fiber contacts on a single softwood fiber is therefore greater than those on a single hardwood fiber in a paper sheet. RBC transport in softwood paper is therefore more difficult. The finding of this work will be used as a guide for future paper sheet design for paper-based blood analysis sensors.

For future work, more pulping and papermaking parameters including refining and addition of papermaking chemicals could be investigated.

## ■ ASSOCIATED CONTENT

### ● Supporting Information

Basis weight, apparent thickness, and bulk of handsheets; statistical analysis of mean optical density of positive or negative lateral chromatographic elution blood-typing tests; and statistical analysis of mean optical density of positive or negative vertical washing blood typing tests (Tables S1–S6). This material is available free of charge via the Internet at <http://pubs.acs.org>.

## ■ AUTHOR INFORMATION

### Corresponding Author

### Notes

The authors declare no competing financial interest.

## ■ ACKNOWLEDGMENTS

This work is supported by Australian Research Council Grants (ARC DP1094179 and LP110200973). The authors thank Haemokinesis for its support through an ARC Linkage Project. L.L. thanks the Monash University Research and Graduate School and the Faculty of Engineering for postgraduate research scholarships.

## ■ REFERENCES

- (1) Li, X.; Ballerini, D. R.; Shen, W. A Perspective on Paper-Based Microfluidics: Current Status and Future Trends. *Biomicrofluidics* **2012**, *6*, 11301–1130113.
- (2) Abe, K.; Kotera, K.; Suzuki, K.; Citterio, D. Inkjet-Printed Paper Fluidic Immuno-Chemical Sensing Device. *Anal. Bioanal. Chem.* **2010**, *398*, 885–893.
- (3) Delaney, J. L.; Hogan, C. F.; Tian, J.; Shen, W. Electrogenerated Chemiluminescence Detection in Paper-Based Microfluidic Sensors. *Anal. Chem.* **2011**, *83*, 1300–1306.
- (4) Delaney, J. L.; Doeven, E. H.; Harsant, A. J.; Hogan, C. F. Use of a Mobile Phone for Potentiostatic Control with Low Cost Paper-Based Microfluidic Sensors. *Anal. Chim. Acta* **2013**, *790*, 56–60.
- (5) Zhu, Y.; Xu, X.; Brault, N. D.; Keefe, A. J.; Han, X.; Deng, Y.; Xu, J.; Yu, Q.; Jiang, S. Cellulose Paper Sensors Modified with Zwitterionic Poly(carboxybetaine) for Sensing and Detection in Complex Media. *Anal. Chem.* **2014**, *86*, 2871–2875.
- (6) Joo-Hyung, K.; Seongcheol, M.; Hyun, U. K.; Gyu-Young, Y.; Jaehwan, K. Disposable Chemical Sensors and Biosensors Made on Cellulose Paper. *Nanotechnology* **2014**, *25*, 092001.
- (7) Kang, T.-K. Tunable Piezoresistive Sensors Based on Pencil-on-Paper. *Appl. Phys. Lett.* **2014**, *104*, 073117–073117–3.
- (8) Khan, M. S.; Thouas, G.; Shen, W.; Whyte, G.; Garnier, G. Paper Diagnostic for Instantaneous Blood Typing. *Anal. Chem.* **2010**, *82*, 4158–4164.
- (9) Nery, E. W.; Kubota, L. T. Sensing Approaches on Paper-Based Devices: A Review. *Anal. Bioanal. Chem.* **2013**, *405*, 7573–7595.
- (10) Santhiago, M.; Nery, E. W.; Santos, G. P.; Kubota, L. T. Microfluidic Paper-Based Devices for Bioanalytical Applications. *Bioanalysis* **2014**, *6*, 89–106.
- (11) Pelton, R. Bioactive Paper Provides a Low-Cost Platform for Diagnostics. *Trends Anal. Chem.* **2009**, *28*, 925–942.
- (12) Biermann, C. J. *Handbook of Pulping and Papermaking*, 2nd ed.; Academic Press: New York, 1996.
- (13) Ek, M.; Gellerstedt, G.; Henriksson, G. *Paper Chemistry and Technology*; Walter de Gruyter: Berlin, 2009.
- (14) Li, X.; Tian, J.; Nguyen, T.; Shen, W. Paper-Based Microfluidic Devices by Plasma Treatment. *Anal. Chem.* **2008**, *80*, 9131–9134.
- (15) Li, X.; Tian, J.; Garnier, G.; Shen, W. Fabrication of Paper-Based Microfluidic Sensors by Printing. *Colloids Surf., B* **2010**, *76*, S64–S70.
- (16) Martinez, A. W.; Phillips, S. T.; Butte, M. J.; Whitesides, G. M. Patterned Paper as a Platform for Inexpensive, Low-Volume, Portable Bioassays. *Angew. Chem.* **2007**, *119*, 1340–1342.
- (17) Ballerini, D.; Li, X.; Shen, W. Patterned Paper and Alternative Materials as Substrates for Low-Cost Microfluidic Diagnostics. *Microfluid. Nanofluid.* **2012**, *13*, 769–787.
- (18) Al-Tamimi, M.; Shen, W.; Zeineddine, R.; Tran, H.; Garnier, G. Validation of Paper-Based Assay for Rapid Blood Typing. *Anal. Chem.* **2012**, *84*, 1661–8.
- (19) Li, M. S.; Tian, J. F.; Al-Tamimi, M.; Shen, W. Paper-Based Blood Typing Device That Reports Patient's Blood Type “in Writing”. *Angew. Chem. Int. Ed.* **2012**, *51*, S497–S501.
- (20) Li, H.; Han, D.; Pauletti, G. M.; Steckl, A. J. Blood Coagulation Screening Using a Paper-Based Microfluidic Lateral Flow Device. *Lab Chip* **2014**, *14*, 4035–4041.
- (21) Lee, C. H.; Tian, L.; Singamaneni, S. Paper-Based SERS Swab for Rapid Trace Detection on Real-World Surfaces. *ACS Appl. Mater. Interfaces* **2010**, *2*, 3429–3435.
- (22) Noor, M. O.; Krull, U. J. Paper-Based Solid-Phase Multiplexed Nucleic Acid Hybridization Assay with Tunable Dynamic Range Using Immobilized Quantum Dots as Donors in Fluorescence Resonance Energy Transfer. *Anal. Chem.* **2013**, *85*, 7502–7511.
- (23) Ek, M.; Gellerstedt, G.; Henriksson, G. *Paper Products Physics and Technology*; Walter de Gruyter: Berlin, 2009.
- (24) Niskanen, K. J. *Paper Physics*; Fapet Oy: Helsinki, Finland, 1999.
- (25) Jarujamrus, P.; Tian, J. F.; Li, X.; Siripinyanond, A.; Shiowatana, J.; Shen, W. Mechanisms of Red Blood Cells Agglutination in Antibody-Treated Paper. *Analyst* **2012**, *137*, 2205–2210.
- (26) Daniels, G.; Reid, M. E. Blood Groups: The Past 50 Years. *Transfusion* **2010**, *50*, 281–289.
- (27) Duguid, J. K. M.; Bromilow, I. M. New Technology in Hospital Blood Banking. *J. Clin. Pathol.* **1993**, *46*, S85–S88.
- (28) Daniels, G.; Bromilow, I. M. *Essential Guide to Blood Groups*; Wiley-Blackwell: Chichester, UK, 2010.
- (29) Li, L.; Tian, J.; Ballerini, D.; Li, M.; Shen, W. A Study of the Transport and Immobilisation Mechanisms of Human Red Blood Cells in a Paper-Based Blood Typing Device Using Confocal Microscopy. *Analyst* **2013**, *138*, 4933–4940.
- (30) Paulapuro, H. *Papermaking Part 1, Stock Preparation and Wet End*, 2nd ed.; Fapet: Helsinki, Finland, 2008; Vol. 8.
- (31) Alén, R. *Papermaking Chemistry*; Fapet: Helsinki, Finland, 2007; Vol. 4.
- (32) Levlin, J.; Soderhjelm, L. *Pulp and Paper Testing*; Fapet: Helsinki, Finland, 1999; Vol. 17.
- (33) Silvy, J.; Pannier, C.; Veyre, J. *16th EUCEPA Conference Proceedings*; Paper Industry Technical Association: Bury, UK, 1976.
- (34) Webb, P. A.; Orr, C. *Analytical Methods in Fine Particle Technology*; Micromeritics Instrument Corp.: Norcross, GA, 1997.
- (35) Reinhart, W. H.; Chien, S. Roles of Cell Geometry and Cellular-Viscosity in Red-Cell Passage through Narrow Pores. *Am. J. Physiol.* **1985**, *248*, C473–C479.
- (36) Gong, X.; Sugiyama, K.; Takagi, S.; Matsumoto, Y. The Deformation Behavior of Multiple Red Blood Cells in a Capillary Vessel. *J. Biomech. Eng.* **2009**, *131*, 074504–074504.
- (37) Roberts, R. J.; Senden, T. J.; Knackstedt, M. A.; Lyne, M. B. Spreading of Aqueous Liquids in Unsized Papers is by Film Flow. *J. Pulp Pap. Sci.* **2003**, *29*, 123–131.
- (38) Fardim, P. *Chemical Pulping*; Fapet: Helsinki, Finland, 1999; Vol. 6.
- (39) He, J.; Batchelor, W.; Johnston, R. An Analytical Model for Number of Fibre–Fibre Contacts in Paper and Expressions for Relative Bonded Area (RBA). *J. Mater. Sci.* **2007**, *42*, S22–S28.
- (40) Batchelor, W. J.; He, J.; Sampson, W. W. Inter-Fibre Contacts in Random Fibrous Materials: Experimental Verification of Theoretical Dependence on Porosity and Fibre Width. *J. Mater. Sci.* **2006**, *41*, 8377–8381.

# Control Performance of Paper-Based Blood

## Analysis Devices through Paper Structure Design

Lizi Li<sup>†</sup>, Xiaolei Huang<sup>‡</sup>, Wen Liu<sup>‡</sup>, Wei Shen<sup>\*†</sup>

<sup>†</sup>Department of Chemical Engineering, Monash University, Clayton Campus, VIC 3800, Australia

<sup>‡</sup>China National Pulp and Paper Research Institute, Beijing 100102, China

**Table S1.** Basis weight, thickness and bulk of hardwood and softwood handsheets.

<i>Type of paper</i>	<i>Basis weight (g/m<sup>2</sup>)</i>	<i>Thickness (μm)</i>	<i>Bulk (cm<sup>3</sup>/g)</i>
<b>H20</b>	20.5	84.85 ± 1.46	4.13 ± 0.04
<b>H35</b>	35.4	129.40 ± 2.77	3.60 ± 0.06
<b>H50</b>	51.2	171.88 ± 3.19	3.36 ± 0.07
<b>S20</b>	20.5	80.20 ± 2.99	3.88 ± 0.13
<b>S35</b>	35.6	119.8 ± 2.91	3.37 ± 0.09
<b>S50</b>	51.4	157.8 ± 4.15	3.07 ± 0.07

**Table S2.** Basis weight, thickness and bulk of handsheets made from different content of hardwood and softwood fibers.

<i>Content of</i>	<i>Basis weight (g/m<sup>2</sup>)</i>	<i>Thickness (μm)</i>	<i>Bulk (cm<sup>3</sup>/g)</i>
<i>hardwood fibers</i>			
<b>0%</b>	20.5	80.20 ± 2.99	3.88 ± 0.13
<b>25%</b>	20.2	81.84 ± 4.00	4.06 ± 0.24
<b>50%</b>	19.7	85.20 ± 2.38	4.33 ± 0.11
<b>75%</b>	19.8	84.40 ± 2.16	4.26 ± 0.11
<b>100%</b>	20.5	84.85 ± 1.46	4.13 ± 0.04

**Table S3.** Mean optical density of positive or negative lateral chromatographic elution blood typing tests using paper with different basis weights. Standards deviation is from five measurements.

<i>Type of paper</i>	<i>Positive test</i>	<i>Negative test</i>	<i>Difference</i>	<i>P value</i> <sup>1</sup>
<b>H20</b>	226.7 ± 2.1	29.5 ± 3.7	197.2 ± 4.3	< 0.0001
<b>H35</b>	226.7 ± 2.8	47.8 ± 4.9	178.8 ± 5.6	< 0.0001
<b>H50</b>	230.5 ± 2.1	69.0 ± 4.7	161.5 ± 5.1	< 0.0001
<b>S20</b>	217.5 ± 4.6	69.7 ± 4.0	147.8 ± 6.1	< 0.0001
<b>S35</b>	222.1 ± 1.1	81.0 ± 5.0	141.1 ± 5.2	< 0.0001
<b>S50</b>	230.9 ± 1.5	101.8 ± 5.8	129.1 ± 6.0	< 0.0001
	<b>P value</b> <sup>2</sup> = 0.0116	<b>P value</b> <sup>2</sup> < 0.0001		

P value<sup>1</sup> is from unpaired two-tailed t test. P value<sup>2</sup> is from one way ANOVA. P value<0.05 considered significant.

**Table S4.** Mean optical density of positive or negative lateral chromatographic elution blood typing tests using paper made from different content of hardwood fibers. Standards deviation is from five measurements.

<i>Content of hardwood fibers</i>	<i>Positive test</i>	<i>Negative test</i>	<i>Difference</i>	<i>P value</i> <sup>1</sup>
<b>0%</b>	217.5 ± 4.6	69.7 ± 4.0	147.8 ± 6.1	< 0.0001
<b>25%</b>	217.3 ± 2.3	59.3 ± 6.5	158.0 ± 6.9	< 0.0001
<b>50%</b>	212.9 ± 3.7	48.2 ± 2.8	164.6 ± 4.6	< 0.0001
<b>75%</b>	217.3 ± 3.6	45.2 ± 0.7	172.0 ± 3.7	< 0.0001
<b>100%</b>	226.7 ± 2.1	29.5 ± 3.7	197.2 ± 4.3	< 0.0001
	<b>P value</b> <sup>2</sup> = 0.1040	<b>P value</b> <sup>2</sup> < 0.0001		

P value<sup>1</sup> is from unpaired two-tailed t test. P value<sup>2</sup> is from one way ANOVA. P value<0.05 considered significant

**Table S5.** Mean optical density of positive or negative vertical washing blood typing tests using paper with different basis weights. Standards deviation is from six measurements.

<i>Type of paper</i>	<i>Positive test</i>	<i>Negative test</i>	<i>Difference</i>	<i>P value</i> <sup>1</sup>
<b>H20</b>	169.4 ± 9.9	20.6 ± 3.1	148.7 ± 10.4	< 0.0001
<b>H35</b>	121.0 ± 3.4	18.1 ± 1.5	102.9 ± 3.8	< 0.0001
<b>H50</b>	125.3 ± 6.6	15.1 ± 1.3	110.2 ± 6.7	< 0.0001
<b>S20</b>	190.6 ± 5.3	62.1 ± 0.8	128.5 ± 5.4	< 0.0001
<b>S35</b>	131.3 ± 4.0	35.4 ± 1.5	95.9 ± 4.3	< 0.0001
<b>S50</b>	132.8 ± 3.2	29.4 ± 1.2	103.4 ± 3.4	< 0.0001
	<b>P value</b> <sup>2</sup> < 0.0001	<b>P value</b> <sup>2</sup> < 0.0001		

P value<sup>1</sup> is from unpaired two-tailed t test. P value<sup>2</sup> is from one way ANOVA. P value < 0.05 considered significant

**Table S6.** Mean optical density of positive or negative vertical washing blood typing tests using paper made from different content of hardwood fibers. Standards deviation is from five measurements.

<i>Content of hardwood fibers</i>	<i>Positive test</i>	<i>Negative test</i>	<i>Difference</i>	<i>P value</i> <sup>1</sup>
<b>0%</b>	190.6 ± 5.3	62.1 ± 0.8	128.5 ± 5.4	< 0.0001
<b>25%</b>	189.9 ± 5.0	60.0 ± 5.8	129.9 ± 7.6	< 0.0001
<b>50%</b>	185.8 ± 8.0	41.8 ± 3.4	144.1 ± 8.7	< 0.0001
<b>75%</b>	182.9 ± 8.4	30.3 ± 2.7	152.6 ± 8.8	< 0.0001
<b>100%</b>	169.4 ± 9.9	20.6 ± 3.1	148.7 ± 10.4	< 0.0001
	<b>P value</b> <sup>2</sup> = 0.2995	<b>P value</b> <sup>2</sup> < 0.0001		

P value<sup>1</sup> is from unpaired two-tailed t test. P value<sup>2</sup> is from one way ANOVA. P value < 0.05 considered significant

**This page is intentionally blank**



## Short communication

## Superhydrophobic surface supported bioassay – An application in blood typing

Lizi Li<sup>1</sup>, Junfei Tian<sup>1</sup>, Miaosi Li, Wei Shen\*

Department of Chemical Engineering, Monash University, Clayton Campus, VIC 3800, Melbourne, Australia

## ARTICLE INFO

## Article history:

Received 8 September 2012

Received in revised form 15 January 2013

Accepted 18 January 2013

Available online 30 January 2013

## Keywords:

Superhydrophobic surface

Liquid drop micro reactor

Bioassay

Blood typing

Digital image analysis

## ABSTRACT

This study presents a new application of superhydrophobic surfaces in conducting biological assays for human blood typing using a liquid drop micro reactor. The superhydrophobic substrate was fabricated by a simple printing technique with Teflon powder. The non-wetting and weak hysteresis characteristics of superhydrophobic surfaces enable the blood and antibody droplets to have a near-spherical shape, making it easy for the haemagglutination reaction inside the droplet to be photographed or recorded by a digital camera and then analyzed by image analysis software. This novel blood typing method requires only a small amount of blood sample. The evaluation of assay results using image analysis techniques offers potential to develop high throughput operations of rapid blood typing assays for pathological laboratories. With the capability of identifying detailed red blood cell agglutination patterns and intensities, this method is also useful for confirming blood samples that have weak red blood cell antigens.

Crown Copyright © 2013 Published by Elsevier B.V. All rights reserved.

## 1. Introduction

The superhydrophobic phenomenon and fabrication of artificial superhydrophobic surfaces have attracted intense research in recent years. The strong water-repellent property of superhydrophobic surfaces forces water droplets to assume large contact angles ( $>150^\circ$ ) and can be designed to have very weak hysteresis on those surfaces [1–4]. Superhydrophobic surfaces have many practical applications such as self-cleaning [5,6], anti-wetting [7], water-repellence [8,9], oil–water separation [10], anti-freezing [4] and fluid-drag reduction [11].

While numerous studies have been directed towards the fabrication and applications of superhydrophobic surfaces for water-repellence, anti-wetting and oil–water separation, some research works have focused on utilizing the water droplet supported by superhydrophobic surfaces for practical applications. The non-wetting and weak hysteresis characteristics of superhydrophobic surfaces enables a lab-on-chip analytical sensor to be designed; aqueous droplets containing analytes can be manipulated for analytical purposes, such as sample storage, transport, mixing and splitting on a lab-on-chip device [12]. More recently, several researchers explored the use of aqueous droplets on superhydrophobic pedestals as a micro-scale reactor to perform chemical reactions and the growth of crystals [13,14].

The near-spherical shape of an aqueous droplet on a superhydrophobic surface allows for a sufficient elevation of its centre of gravity so that a micro-scale physical transformation or biochemical reaction occurring inside the droplet can be clearly observed and recorded from the side view. The superhydrophobic surface supported micro-scale analytical or diagnostic reactors require materials of low-cost and are easy to be transformed into an automated high volume biochemical assays. To date, however, there is little information about superhydrophobic surface supported biochemical assays in literature.

To clearly observe a living reaction inside an aqueous droplet from the side view, the droplet needs to have a sufficient height on the supporting surface; for this reason a hydrophobic surface or a superhydrophobic surface is required. Eq. (1) and Fig. 1(a) describe the height of a droplet and its contact angle with the supporting surface.

$$h = R[1 + \sin(\theta - 90^\circ)] \quad (1)$$

where  $h$  is the height of the drop,  $R$  is the radius of the drop and  $\theta$  is the contact angle of the drop on the surface. If the gravity effect is neglected, the height of a drop on a surface can be calculated by Eq. (1). Fig. 1(b) shows the plot of the droplet height and its contact angle with the supporting surface. For a droplet having a radius of 1.68 mm ( $\sim 20 \mu\text{L}$ ) on a hydrophobic surface ( $\theta = 120^\circ$ ), the height is 2.52 mm. For the same droplet on a superhydrophobic surface ( $\theta = 150^\circ$ ), the height of the droplet increases 3.13 mm. The difference in droplet height on superhydrophobic and hydrophobic surfaces is moderate, and further increase in contact angle beyond  $150^\circ$  results in only a very small increase in droplet height. Therefore, for the purpose of only acquiring side views of

\*

<sup>1</sup> Lizi Li and Junfei Tian contributed equally as co-first authors.



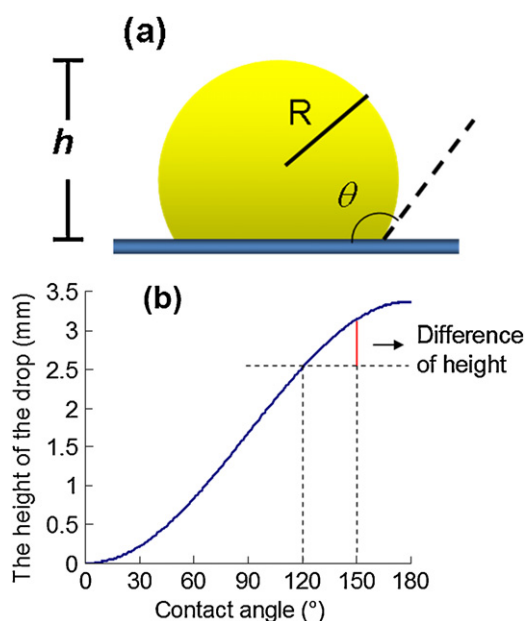


**Fig. 1.** (a) Scheme of the side-view profile of a water droplet on a (super-) hydrophobic surface ( $R$  and  $h$  are the radius and the height of the droplet, respectively;  $\theta$  is the contact angle); (b) a plot of the height of a 20  $\mu\text{L}$  droplet on a supporting surface with respect of its contact angle with the surface (gravity effect is not considered). The red line shows the difference of the heights of water droplets on a hydrophobic surface ( $\theta = 120^\circ$ ) and a superhydrophobic surface ( $\theta = 150^\circ$ ).

a droplet, a highly hydrophobic surface would be sufficient. However, a significant advantage of using superhydrophobic surface for biochemical assay is that the liquid sample can easily roll off the surface after test; this prevents the surface from being contaminated. For some assays, this advantage may be important, since the superhydrophobic supporting surface may be reused. This highly useful function of superhydrophobic surfaces needs to be further explored to enable chemical and biological reactions, and biochemical assays to be conducted in a high throughput capacity and at low cost.

In this study, we demonstrate the use of superhydrophobic surfaces for biological assays through making observations of the haemagglutination reaction of human red blood cells (RBC) and blood typing assay. Accurate and rapid typing of human blood is not only of great importance for blood transfusion and transplantation medicine [15], but also critically important for blood banking, and for screening or cross-checking donors' blood samples. For the later, in particular, high throughput methods are required to process large number of samples rapidly. Although the lateral flow and the Gel Card technologies are the mainstream technologies currently in use in hospitals and pathological laboratories, diagnostic industry has never stopped exploring new technologies [16,18–21,24–26]. In this work superhydrophobic substrate was fabricated by using a simple contact printing method developed in our laboratory [17]; the substrate is inexpensive and disposable, suitable for use as a laboratory consumable item. In a blood typing application, the haemagglutination reaction inside the blood sample droplet can be imaged by using a digital camera and suitable software can be used for the blood type identification. The use of digital camera allows photos of an assay to be kept for retrieval and analysis, and it has the potential to reveal detailed agglutination process if camera with high magnification is used. Further automation in assay result evaluation will provide a new potential method for rapid blood typing assays of high throughput operation, with the capability of providing magnified photo and video footage of the agglutination reaction,

which will be of a significant diagnostic aid to the identifying of blood samples whose RBCs carry weak antigens.

## 2. Material and methods

Teflon powder with an average particle size of 35  $\mu\text{m}$  was obtained from Sigma–Aldrich. The polymer film used in this study was a commercial overhead transparency (Xerox). A UV curable flexographic post-print varnish (UV 412) was received as a gift from Flint Inks (Flint Group Australia). Six blood samples (type A+, A–, B+, AB+, O+ and O–) were received from a pathological laboratory, following the ethical protocols. All blood samples were stored in Vacutainer® test tubes containing lithium–heparin anticoagulant at 4 °C and used within 5 days of collection. Epiclone™ anti-A, anti-B and anti-D monoclonal grouping reagents were sourced commercially from the Commonwealth Serum Laboratory, Australia. Anti-A and anti-B are colour-coded cyan and yellow solutions respectively, while anti-D is a clear colourless solution. All monoclonal grouping reagents were also stored at 4 °C.

### 2.1. Fabrication of superhydrophobic Teflon powder surface on polymer film

The superhydrophobic surface on polymer film was fabricated by a contact printing method developed in our laboratory [17]. A thin layer of UV curable flexographic post-print varnish was uniformly transferred onto the transparency film with a roller. Teflon powder was then dusted onto the film and adhered to the uncured varnish. The film was then passed through a UV curing station. Upon curing, the UV varnish tightly glued the Teflon powder particles on the film. The micron-scale roughness of Teflon particles on the film formed the required superhydrophobic surface.

### 2.2. Observation of haemagglutination reaction inside the blood sample drop

Blood samples of two types, A+ and B+, were chosen to demonstrate the time dependency of haemagglutination reaction with anti-B solution inside near-spherical blood droplets supported by the superhydrophobic surface. 10  $\mu\text{L}$  of each blood sample was placed on the superhydrophobic surface using a micropipette (Eppendorf research®). The same volume of anti-B solution was then injected into the blood droplet with a micropipette, and gently stirred with the micropipette-head. The droplets were then monitored for haemagglutination reaction for 180 s with a digital microscopy camera (Moticam 2500); photographs were taken at 30 s intervals from the beginning of the blood sample and antibody mixing.

### 2.3. Blood typing assay on superhydrophobic surfaces

The experimental procedure of performing a blood typing assay is similar to observing the haemagglutination reaction except that three droplets of each blood sample were taken and mixed with three different antibody reagents; anti-A, anti-B and anti-D. The sample blood type can be identified from the pattern of the haemagglutination reaction(s) with the three antibodies. Photos of the sample droplets taken by the camera provide clear identification of the occurrence of a haemagglutination reaction.

A simple colour density measurement method is presented in this study to digitally determine the changes of colour intensities of the blood sample droplets after being mixed with antibody solutions. This method can potentially be used to automate this blood typing assay for high throughput applications.



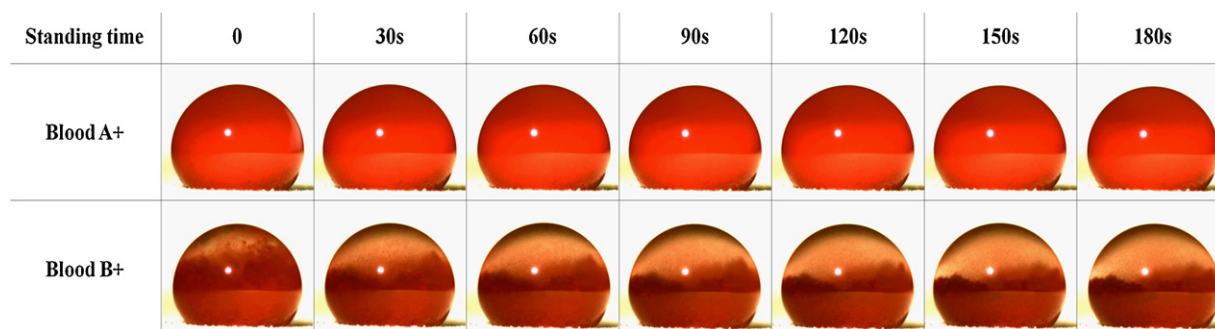


**Fig. 2.** Photos of two 10  $\mu$ L blood droplets (A+ and B+) mixed with 10  $\mu$ L anti-B reagent. Haemagglutination was immediately observed inside the droplet of B+ blood sample (second row), due to the specific interaction between anti-B and the B-antigen carried by RBCs of the B+ sample. There was, however, no haemagglutination in the droplet of A+ blood sample during the entire 180 s standing time (first row), since anti-B is not a specific antibody to the antigen carried by the RBCs of the A+ sample.

### 3. Results and discussion

#### 3.1. Contact angle characterization of the superhydrophobic Teflon powder surface

Contact angle measurements were used to characterize the printed Teflon powder surface. Water, a blood sample and antibody solutions were used as liquids for contact angle measurements. Contact angles for water, blood (A+), anti-A, anti-B and anti-D with the Teflon powder surface were determined to be  $158.6^\circ \pm 1.0^\circ$ ,  $153.1^\circ \pm 2.2^\circ$ ,  $154.1^\circ \pm 3.2^\circ$ ,  $155.8^\circ \pm 1.3^\circ$  and  $148.5^\circ \pm 0.2^\circ$ , respectively. This data is the average of 5 measurements and the standard deviations are also given.

From the contact angle data of water with the surface it can be seen that the printed Teflon powder surface was superhydrophobic since the water contact angle was significantly higher than  $150^\circ$ . The blood and antibody solutions also showed contact angles greater than or close to  $150^\circ$ . The only liquid that has the lower than  $150^\circ$  contact angle was the anti-D solution. The slightly lower contact angle of anti-D solution compared to that of the other antibody solutions may be related to its formulation being different from other antibody solutions. However, it can be found that such a small difference in contact angle between the blood sample and the antibody solutions means that there is a negligible difference in the practical application of observing haemagglutination reactions inside the sample droplets.

#### 3.2. Observation of haemagglutination inside the blood sample droplet

To observe the haemagglutination reaction inside blood sample droplets, anti-B was introduced into two blood samples of A+ and B+ types. As anti-B was introduced into the drop of blood sample type B+, the specific antibody-antigen interaction resulted in an immediate haemagglutination of RBCs – a clear separation of agglutinated RBC lumps from the plasma phase can be observed inside the blood sample drop immediately after the anti-B introduction (Fig. 2).

As time progressed to 90 s, the agglutination reaction led to the clearing of the top part of B+ sample droplet. Further standing of the sample to 180 s showed little further change in RBC separation. In contrast to the reaction of B+ blood sample with anti-B, the mixing of A+ blood sample with anti-B (a non-specific antibody) resulted in no haemagglutination reaction and therefore no separation of the RBCs inside the sample droplet (Fig. 2). Haemagglutination of RBCs is the indication of the occurrence of specific interactions between the antigen present on the surface of the red blood cells and the corresponding antibody present or added in the plasma phase. Therefore haemagglutination of RBCs in the presence

of blood typing antibodies provides identification of the blood type of the sample. Results in Fig. 2 provide rapid and clear identification of the blood types of the samples. With the use of a digital camera, it is also possible for the captured images to be digitally analyzed to identify the blood types of the samples in an automated way for high throughput blood typing service application. Depending on the assay, the superhydrophobic substrate may be disposed of after use, or reused after allowing the sample drop to roll off the surface.

#### 3.3. Blood typing using superhydrophobic surfaces as a low-cost supporting substrate

The clear observation of haemagglutination reaction inside a blood sample droplet shows that a superhydrophobic substrate in general can be used to support micro reactors for biochemical assays. We further demonstrate the use of superhydrophobic surface for ABO and RhD blood typing assays. The use of superhydrophobic surfaces for blood typing may offer significant economic advantage, since the cost of such a surface is low.

Recently, low-cost paper- and thread-based blood typing platforms have been reported [18–21]. Paper- and thread-based blood typing devices greatly reduce the cost and the time required for performing blood typing assays; they are particularly suitable for making user-operated devices for developing countries. As an alternative platform, superhydrophobic surface-based blood typing assays offer the following advantages: (1) Superhydrophobic surfaces combined with an imaging system allow automated high throughput equipment to be built at a moderate to low cost. (2) Such equipment provides detailed visual haemagglutination patterns of samples, which may be further used for evaluation of haemagglutination reaction through image analysis. (3) Haemagglutination reactions inside the sample drop provide the possibility of extracting the plasma phase from the samples for other assays.

Six blood samples were assayed using the superhydrophobic surface supported blood typing assay. For each blood sample, three sample droplets were placed on the superhydrophobic surface; these droplets were respectively mixed with anti-A, anti-B and anti-D following the protocol described in Section 2. The samples droplets were then observed for haemagglutination reactions. Fig. 3 shows images of the assaying results of the six blood samples; haemagglutination reaction can be easily identified from the photos taken from the side view of the droplets. Based on the pattern of haemagglutination reactions in Fig. 3, blood types of the samples were identified as being A+, A–, B+, AB+, O+ and O–. These results were in total agreement with the blood typing results obtained by the pathological laboratory using the Gel Card technology.

To explore the possible automation of using the superhydrophobic surface supported bioassay for high throughput blood typing

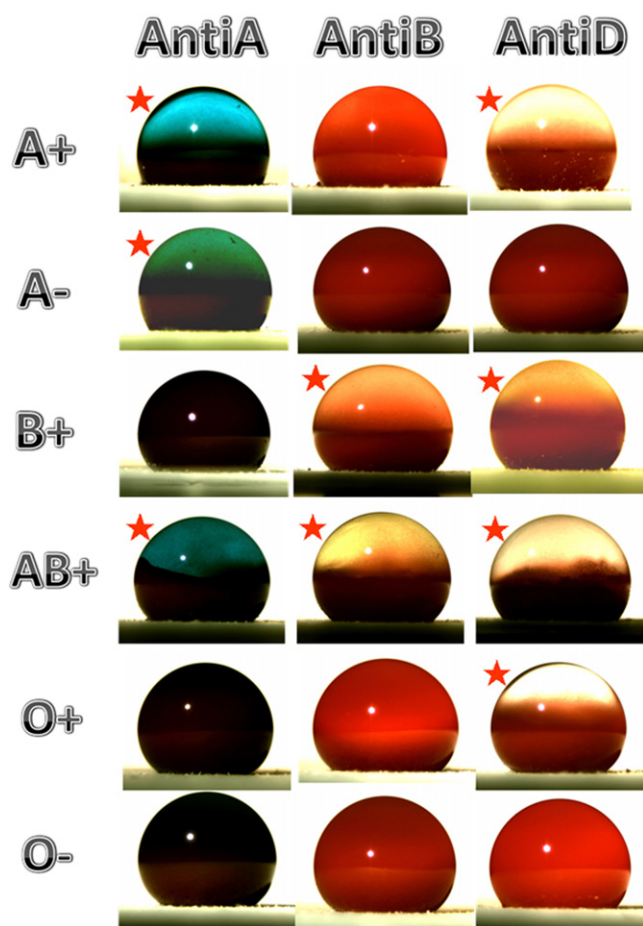


**Fig. 3.** Photos of the blood agglutination of the six blood samples (A+, A−, B+, AB+, O+ and O−) when they are respectively mixed with three antibodies (Anti-A, Anti-B and Anti-D) on superhydrophobic surface. The red star represents blood aggregation was found in that photo. The blood type can be determined by observing the aggregation of blood with different antibodies.

assays, images in Fig. 4 were digitally processed and identification of haemagglutination via image analysis was pursued by using Adobe Photoshop. The image analysis was performed on a standard square of 5 mm × 5 mm in the top part of the droplet image; the average colour intensity of the magenta channel was measured from the square. The choice of measuring the magenta channel is based on its large dynamic range [22], which is capable of providing more accurate measurement of the sample. Table 1 shows the magenta intensity of the analyzed area of each image. The magenta colour intensity measured from the images of the sam-

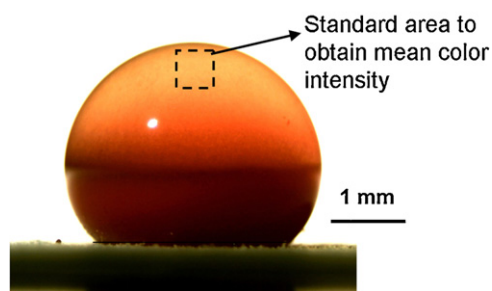


**Fig. 4.** Illustration of the measurement of colour intensity (magenta channel). The blood aggregation can be detected by comparing the colour intensity of the standard area in the images of different drops. From the identified aggregation of blood caused by their corresponding antibodies, the type of blood can be determined.

**Table 1**

The magenta intensity of the standard area in each image of Fig. 3.

	Anti-A	Anti-B	Anti-D
A+	7.18 ± 0.75	219.52 ± 0.13	0.06 ± 0.04
A−	70.22 ± 2.93	253.04 ± 0.53	253.23 ± 0.26
B+	225.36 ± 0.28	101.52 ± 1.98	94.81 ± 0.76
AB+	147.52 ± 1.63	61.63 ± 1.89	6.38 ± 1.89
O+	219.65 ± 0.57	253.79 ± 0.41	0.23 ± 0.15
O−	220.10 ± 1.60	252.39 ± 0.67	252.80 ± 0.04

ple drops shows strong contrast; samples with haemagglutination correspond to colour intensity values much lower than saturation, whereas samples with no haemagglutination show magenta colour intensity close to saturation.

In order for the haemagglutination status to be evaluated digitally, a colour intensity threshold of 180 was introduced to differentiate haemagglutination from non-haemagglutination. This threshold level was chosen as it is numerically around 40 above the highest colour intensity of the non-agglutinated sample and around 40 below the lowest colour intensity of the agglutinated sample. With this threshold level it is possible to digitally identify the haemagglutination reaction in a blood sample drop after the addition of antibody solution. The combination of the superhydrophobic supporting surface, the simple camera system and the software system presents a design concept of an automated blood typing device capable of high throughput analysis of blood samples. The digitized results obtained using this system can deliver direct blood typing result and also can be transmitted by mobile phone [23] or other electronic devices to a remote facility should it be necessary.

#### 4. Conclusion

In this study we investigated a new application of using superhydrophobic surfaces to conduct biological assays. By using a superhydrophobic surface as a supporting surface for liquid droplets, a human blood typing assay was conducted. The non-wettable property of the superhydrophobic surface by blood samples and antibody solutions makes the blood and antibody droplets assume a near spherical shape, providing an excellent side view for the haemagglutination reaction to be observed inside the droplet. By observing the presence or absence of the haemagglutination reaction, specific antibody–RBC interactions can be identified; this method can be used for rapid blood typing. By using a camera and a simple image analysis system, haemagglutination inside the blood sample droplets can be digitally identified. This capability potentially makes the superhydrophobic surface supported blood typing assay suitable for high throughput assay applications. We believe that the superhydrophobic surface supported micro reactor concept can be developed into more applications for chemical or biological assays.

#### Acknowledgements

This work is supported by Australian Research Council Grants (ARC LP0990526 and LP110200973). Authors thank Haemokinesis for its support through an ARC Linkage Project. The authors would like to specially thank Dr. Emily Perkins, Department of Chemical Engineering and Mr Hansen Shen, student of the Faculty of Law of Monash University for proof reading the manuscript. Lizi Li, Junfei Tian and Miaosi Li thank Monash University Research and Graduate School and the Faculty of Engineering for their postgraduate research scholarships.

## Appendix A. Supplementary data

Supplementary data associated with this article can be found, in the online version, at <http://dx.doi.org/10.1016/j.colsurfb.2013.01.049>.

## References

- [1] X. Hong, X.F. Gao, L. Jiang, Application of superhydrophobic surface with high adhesive force in no lost transport of superparamagnetic microdroplet, *J. Am. Chem. Soc.* 129 (2007) 1478–1479.
- [2] X. Zhang, F. Shi, J. Niu, Y. Jiang, Z. Wang, Superhydrophobic surfaces: from structural control to functional application, *J. Mater. Chem.* 18 (2008) 621–633.
- [3] A. Tuteja, W. Choi, M. Ma, J.M. Mabry, S.A. Mazzella, G.C. Rutledge, G.H. McKinley, R.E. Cohen, Designing superoleophobic surfaces, *Science* 318 (2007) 1618–1622.
- [4] X. Yao, Y. Song, L. Jiang, Applications of bio-inspired special wettable surfaces, *Adv. Mater.* 23 (2011) 719–734.
- [5] R. Bossey, Self-cleaning surfaces – virtual realities, *Nat. Mater.* 2 (2003) 301–306.
- [6] V.A. Ganesh, H.K. Raut, A.S. Nair, S. Ramakrishna, A review on self-cleaning coatings, *J. Mater. Chem.* 21 (2011) 16304–16322.
- [7] T.L. Sun, L. Feng, X.F. Gao, L. Jiang, Bioinspired surfaces with special wettability, *Acc. Chem. Res.* 38 (2005) 644–652.
- [8] X.M. Li, D. Reinhoudt, M. Crego-Calama, What do we need for a superhydrophobic surface? A review on the recent progress in the preparation of superhydrophobic surfaces, *Chem. Soc. Rev.* 36 (2007) 1350–1368.
- [9] P. Roach, N.J. Shirtcliffe, M.I. Newton, Progress in superhydrophobic surface development, *Soft Matter* 4 (2008) 224–240.
- [10] L. Feng, Z. Zhang, Z. Mai, Y. Ma, B. Liu, L. Jiang, D. Zhu, A super-hydrophobic super-oleophilic coating mesh film for the separation of oil and water, *Angew. Chem.* 116 (2004) 2046–2048.
- [11] H. Mertaniemi, V. Jokinen, L. Sainiemi, S. Franssila, A. Marmur, O. Ikkala, R.H.A. Ras, Superhydrophobic tracks for low-friction, guided transport of water droplets, *Adv. Mater.* 23 (2011) 2911–2914.
- [12] B. Balu, A.D. Berry, D.W. Hess, V. Breedveld, Patterning of superhydrophobic paper to control the mobility of micro-liter drops for two-dimensional lab-on-paper applications, *Lab Chip* 9 (2009) 3066–3075.
- [13] B. Su, S. Wang, Y. Song, L. Jiang, A miniature droplet reactor built on nanoparticle-derived superhydrophobic pedestals, *Nano Res.* 4 (2011) 266–273.
- [14] B. Su, S. Wang, J. Ma, Y. Song, L. Jiang, Clinging-microdroplet patterning upon high-adhesion, pillar-structured silicon substrates, *Adv. Funct. Mater.* 21 (2011) 3297–3307.
- [15] G. Daniels, M.E. Reid, Blood groups: the past 50 years, *Transfusion* 50 (2010) 281–289.
- [16] J.K.M. Duguid, I.M. Bromilow, New technology in hospital blood banking, *J. Clin. Pathol.* 46 (1993) 585–588.
- [17] J. Tian, X. Li, W. Shen, Printed two-dimensional micro-zone plates for chemical analysis and ELISA, *Lab Chip* 11 (2011) 2869–2875.
- [18] M.S. Khan, G. Thouas, W. Shen, G. Whyte, G. Garnier, Paper diagnostic for instantaneous blood typing, *Anal. Chem.* 82 (2010) 4158–4164.
- [19] M. Al-Tamimi, W. Shen, R. Zeineddine, H. Tran, G. Garnier, Validation of paper-based assay for rapid blood typing, *Anal. Chem.* 84 (2012) 1661–1668.
- [20] D.R. Ballerini, X. Li, W. Shen, An inexpensive thread-based system for simple and rapid blood grouping, *Anal. Bioanal. Chem.* 399 (2011) 1869–1875.
- [21] T. Arbatan, L. Li, J. Tian, W. Shen, Liquid marbles as micro-bioreactors for rapid blood typing, *Adv. Healthcare Mater.* 1 (2012) 80–83.
- [22] A.W. Martinez, S.T. Phillips, E. Carrilho, S.W. Thomas, H. Sindi, G.M. Whitesides, Simple telemedicine for developing regions: camera phones and paper-based microfluidic devices for real-time, off-site diagnosis, *Anal. Chem.* 80 (2008) 3699–3707.
- [23] J.L. Delaney, C.F. Hogan, J. Tian, W. Shen, Electrogenated chemiluminescence detection in paper-based microfluidic sensors, *Anal. Chem.* 83 (2011) 1300–1306.
- [24] M. Li, J. Tian, M. Al-Tamimi, W. Shen, Paper-based blood-typing device that reports patient's blood type in writing, *Angew. Chem. Int. Ed.* 51 (2012) 5497–5501.
- [25] P. Jarujamrus, J. Tian, X. Li, A. Siripinyanond, J. Shiowatana, W. Shen, Mechanisms of antibody and red blood cell interactions in paper-based blood typing devices, *Analyst* 137 (2012) 2205–2210.

**This page is intentionally blank**

# Liquid Marbles as Micro-bioreactors for Rapid Blood Typing

Tina Arbatan, Lizi Li, Junfei Tian, and Wei Shen\*

Due to their unique properties, liquid marbles have been the subject of a collection of studies in the past decade, centered on fundamental research on their properties, as well as their practical applications.<sup>[1–37]</sup> These liquid droplets, enwrapped with solid powder while having no direct contact with the supporting substrate, may be exploited for a wide range of applications ranging from, but not limited to, the displacement of a small volume of liquid without any leak left behind,<sup>[2]</sup> water surface pollution detection,<sup>[13]</sup> gas detection, gas–liquid reactions,<sup>[8,30,31]</sup> and, last but not the least, preparation of microreactors.<sup>[7,30,31,34]</sup> With numerous powder types available, the fabrication options of liquid marbles seem to be infinite. This enables the design of tailor-made liquid-marble-based systems for intended applications.

To our knowledge, fabrication of microreactors by forming liquid marbles for the purpose of containing chemical reactions at the micrometer scale has been proposed by only a limited number of studies. For instance, Xue et al.<sup>[34]</sup> have shown that a liquid marble coated with magnetic powder can be used as a miniature chemical reactor to either encapsulate the reagents in a single marble, or in two separate marbles, which could coalesced afterwards to trigger the reaction. The authors used fluorinated decyl polyhedral oligomeric silsesquioxane and magnetic powder aggregates to generate stable liquid marbles capable of encapsulating liquids of either high or low surface tension. They also demonstrated a chemiluminescence reaction between hydrogen peroxide and bis (2,4,6-trichlorophenyl) oxalate and a dye to prove the concept of the controllable liquid marble microreactors.

Tian et al.<sup>[30,31]</sup> showed that the porous nature of the liquid-marble shell could be used to allow gases to transport through the marble shell. They demonstrated the use of liquid marbles formed with gas-reactive indicator solutions to detect gases. Bormashenko et al.<sup>[8]</sup> have also reported the use of polyvinylidene fluorid particles of micrometer size for fabrication of a liquid marble microreactor containing ammonia acetate, acetic acid, and acetylacetone, which is then exposed to formaldehyde vapor to trigger the reaction.

In this study we present the use of liquid marble as micro-bioreactors for biological reactions and diagnostic assays. We choose human blood grouping (ABO and Rh) as the biological system to demonstrate the use of liquid marble as a micro-bioreactor in practical diagnosis involving human blood, which is the most biologically informative human body fluid. The significant advantages of liquid marble micro-bioreactor are: First, it requires relatively small amount of samples and reagents. Second, it reduces biohazards, since the power-wrapped biological sample makes no contact to the surface of the supporting substrate. Third, the control of the bioreactions can be made by either coalescing marbles containing different reagents or by injecting into the marble of different reagents. Fourth, marbles are low in cost and therefore disposable. The construction of the micro-bioreactors for this work is simple; in each blood grouping test three drops ( $3 \times 10 \mu\text{L}$ ) of a blood sample were used to prepare three “blood marbles”. Three antibody solutions (Anti-A, Anti-B and Anti-D) were injected into the three blood marble to initiate the test. Subsequently, ABO and Rh blood grouping is studied by monitoring whether or not haemagglutination reaction occurs inside each of the blood marble micro-bioreactor.

The presence or absence of certain antigens on the surface of a red blood cell (RBC) is an intrinsic biological property which determines a person's blood group. On the other hand, antibodies existing in the blood plasma are available to protect the body when threatened by hostile antigens. According to Landsteiner's Law, when an RBC possesses certain antigens on its surface, the corresponding antibody is absent in the blood plasma and vice versa.<sup>[38]</sup> Blood grouping is a basic yet essential test to be performed prior to a blood transfusion to avoid the consequences of incompatibility, which may lead to a fatal haemolytic reaction. A few examples of the current techniques of blood grouping include dry instant blood typing plate.<sup>[39]</sup> Microplate-based techniques,<sup>[40–42]</sup> and integrated microfluidic biochips are among other options of blood grouping.<sup>[43]</sup> Recently, interesting progress has been made in the fabrication of low-cost, disposable and easy to use paper-based<sup>[44]</sup> and thread-based<sup>[45]</sup> blood typing devices. The liquid marble micro-bioreactor method we report herein has the same advantages in terms of, low-cost, disposability, not relying on any medical facilities.

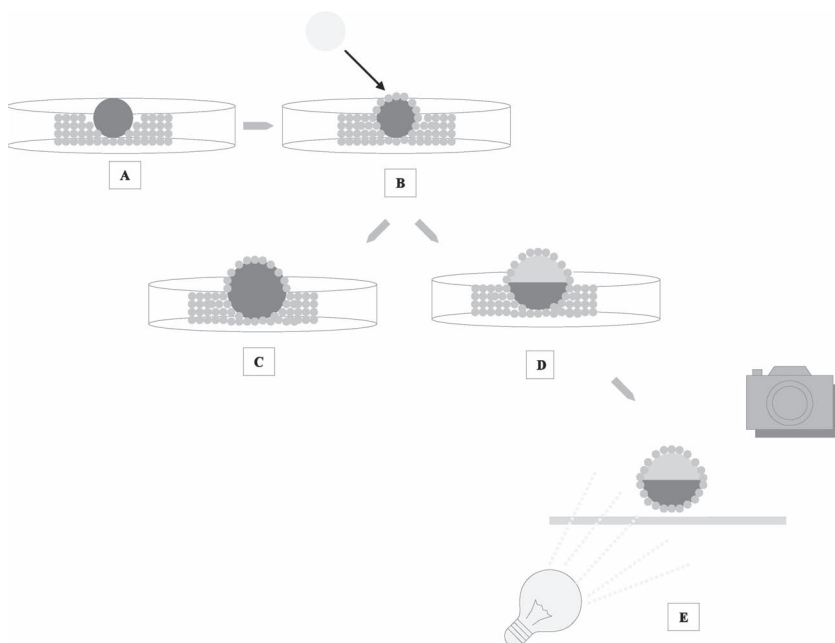
The microreactors in this work were made by coating blood drops with hydrophobic powder of precipitated calcium carbonate (PCC). An antibody solution was subsequently injected into the micro-bioreactors to test for haemagglutination. **Scheme 1** shows the schematic illustration of the steps of the experiment. Before the antibody injection, all blood marbles were

T. Arbatan, L. Li, J. Tian, Prof. W. Shen  
Austrian Pulp and Paper Institute  
department of Chemical Engineering Monash University  
Wellington road, Clayton, 3168, Australia



DOI: 10.1002/adhm.201100016





**Scheme 1.** The Schematic illustration of the steps of microreactor preparation and blood-type identification. A) Blood (10  $\mu\text{L}$ ) is placed on a hydrophobic PCC powder bed to form the blood marble. B) An antibody solution (10  $\mu\text{L}$ ) is injected inside the blood marble to complete the preparation of the microreactor. C) When the corresponding antigens are not present on the surface of RBCs, no separation is visible. D) When the corresponding antigens are present, RBC agglutination reaction will take place; this will result in the separation of marble color into two distinct light (top) and dark (bottom) parts.

in a homogeneous red color. Immediately after the injection of antibody solution into the blood marbles, strong darkening of the marbles injected with Anti-A was observed. This is because commercial Anti-A solution is color-coded with a blue dye for identification purpose (Figure 1). If haemagglutination reaction occurs, the initial uniform red color of the blood marble separates into two clearly discernible parts of light- and dark-red colors due to the precipitation of the agglutinated RBCs to the bottom of the marble. The appearance of such color separation of a blood marble signals the agglutination reaction, indicating the presence of the corresponding antigen on the surface of RBCs. On the other hand, if color separation of the blood marble does not occur, it indicates that the corresponding antigens are absent. The blood grouping results of A+, B+, O+ and O- samples can be seen in (Figure 1). It is worth noting that due to the strong red color of the blood samples, if the haemagglutination does not occur, even by providing a strong backlighting, the blood marble micro-bioreactor will still remain uniformly dark-red in color and opaque. On the other hand, if haemagglutination reaction occurs, a lighter-colored upper part develops when agglutinated RBCs settle to the lower part of the marble.

This method requires three blood marble micro-bioreactors to determine the blood group (ABO RhD) of a blood sample. The interpretation of the blood

grouping test result can be made following this example: For a blood marble made of a B+ sample, injections of Anti-B and Anti-D solutions will cause the separation of uniformly red-colored marbles into a light-red (top) and dark-red (bottom) parts. However, the injection of Anti-A will not change the color uniformity of the marble, as no haemagglutination will occur between a B+ sample and anti-A (Figure 1).

According to the literature, blood surface tension is lower than that of water.<sup>[46]</sup> This might explain the higher than usual deformation of the blood marbles, compared with the pure water marble. Further study of the physical properties of blood marbles can be done in our future investigations. Nevertheless, based on our observations, blood marble micro-bioreactor has the potential to be used rapid blood typing tests. Only a few seconds of gentle shaking of the marble containing the blood and antibody mixture is enough to initiate the haemagglutination reaction. Whilst the main powder used for this study was PCC treated with stearic acid,<sup>[47]</sup> we have also used PTFE powder (100  $\mu\text{m}$  particle size) (Figure 2) just to demonstrate the feasibility of using other powders for the same

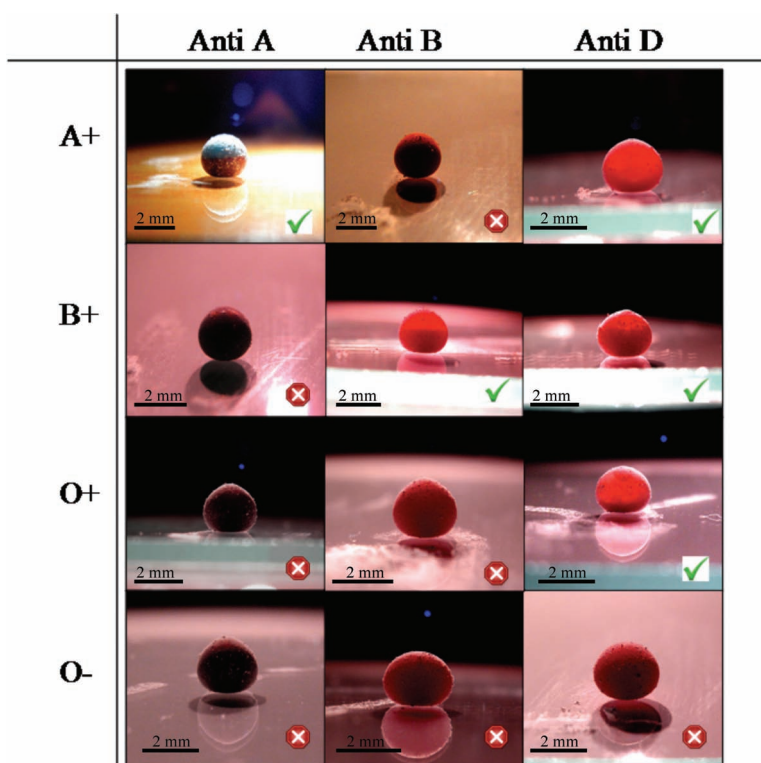


**Figure 1.** Summary of blood typing results after the corresponding antibodies are injected into the marble microreactor (20  $\mu\text{L}$ ). Green ticks are added to the photos where the separation of agglutinated RBC is observed. The cross signs are added to photos where agglutination caused color separation is not observed.

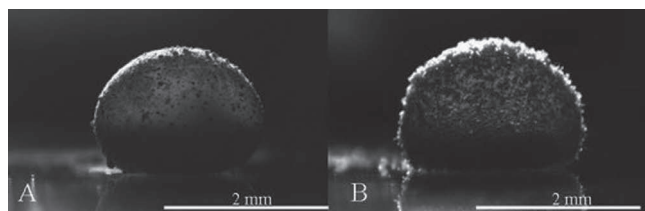


**Figure 2.** A) A blood marble (20  $\mu$ L) micro-bioreactor made of A+ blood and hydrophobic PCC powder after the injection of Anti-A solution. B) A blood marble (20  $\mu$ L) micro-bioreactor made of A+ blood and PTFE powder after the injection of Anti-A solution.

application. The two powders used in this work are just examples of the numerous powder type options that can be used for the same purpose.

The choice of PCC was made mainly because of its low cost, availability, environmental compatibility, and ease of hydrophobization. PCC crystallites are about 1  $\mu$ m in length but clusters containing a few crystallites can have large sizes of several micrometers. Further aggregations of the clusters can be seen on the surface of the blood marble. However, the color change caused by haemagglutination is clearly visible. Since only a minute amount of powder is needed to form a marble, and considering the low-cost of the PCC powder, this method can be regarded as one of the most inexpensive methods suitable for ABO and Rh blood typing. Furthermore, after the blood typing test, the used marble micro-reactor can be burnt to eliminate any potential biohazards. We believe that this study may open a new door for the further biological applications of using liquid marble as micro-bioreactors.

## Experimental Section

Four blood samples of known types were acquired and stored in Vacutainer test tubes containing lithium-heparin anticoagulant from a pathological laboratory. Precipitated calcium carbonate powder (Precarb 100, BASF, which was then treated in-house with stearic acid) was used as the coating powder.<sup>[46]</sup> To prepare a blood marble, a drop of blood was placed on the hydrophobic PCC powder bed inside a Petri dish using a micropipette. The Petri dish was then shaken gently to allow the PCC particles to cover the blood drop uniformly. The same method was used to prepare PTFE coated marbles; a contact angle measurement system (Dataphysics OCA230, Germany) was used to take images of both marbles after haemagglutination inside the marbles has occurred. Epiclone Anti-A (color-coded blue), Anti-B (color-coded yellow) and Anti-D (colorless) monoclonal grouping reagents were acquired commercially from Commonwealth Serum Laboratory, Australia. The same volume of an as-received antibody was then injected into a blood marble using the micropipette, which finally constructed the micro-bioreactor for the RBC agglutination reaction to take place. This procedure was repeated three times to prepare three microreactors containing the same blood sample, but different antibodies. The blood type was then determined based on the method described above. Photos were taken using a Mju 9010 Olympus digital camera. A spatula was used to transfer the microreactor onto a microscope glass slide and a suitable lighting condition was provided with a light source (Microlight 150, Fibreoptic lightguides, Australia).

## Acknowledgements

The authors would like to acknowledge Dr. Mohammad al-Tamimi for kindly providing the blood samples. Monash University postgraduate

scholarships, as well as funding received from ARC LP0989823, are gratefully acknowledged.

Received: November 4, 2011

Published online: December 15, 2011

- [1] T. Arbatan, W. Shen, *Langmuir* **2011**, *27*, 12923.
- [2] P. Aussillous, D. Quere, *Nature* **2001**, *411*, 924.
- [3] P. Aussillous, D. Quéré, *Proc. Royal Soc. A: Math. Phys. Eng. Sci.* **2006**, *462*, 973.
- [4] U. Bangi, S. Dhere, A. Venkateswara Rao, *J. Mater. Sci.* **2010**, *45*, 2944.
- [5] P. S. Bhosale, M. V. Panchagnula, *Langmuir* **2010**, *26*, 10745.
- [6] P. S. Bhosale, M. V. Panchagnula, H. A. Stretz, *Appl. Phys. Lett.* **2008**, *93*, 034109.
- [7] E. Bormashenko, R. Balter, D. Aurbach, *Appl. Phys. Lett.* **2010**, *97*, 091908.
- [8] E. Bormashenko, R. Balter, D. Aurbach, *Int. J. Chem. Reactor Eng.* **2011**, *9*, S10.
- [9] E. Bormashenko, Y. Bormashenko, A. Musin, *J. Colloid Interface Sci.* **2009**, *333*, 419.
- [10] E. Bormashenko, Y. Bormashenko, A. Musin, Z. Barkay, *ChemPhysChem* **2009**, *10*, 654.
- [11] E. Bormashenko, Y. Bormashenko, G. Oleg, *Langmuir* **2010**, *26*, 12479.
- [12] E. Bormashenko, Y. Bormashenko, R. Pogreb, O. Gendelman, *Langmuir* **2010**, *27*, 7.
- [13] E. Bormashenko, A. Musin, *Appl. Surf. Sci.* **2009**, *255*, 6429.
- [14] E. Bormashenko, R. Pogreb, A. Musin, R. Balter, G. Whyman, D. Aurbach, *Powder Technol.* **2010**, *203*, 529.
- [15] E. Bormashenko, R. Pogreb, G. Whyman, A. Musin, Y. Bormashenko, Z. Barkay, *Langmuir* **2009**, *25*, 1893.
- [16] E. Bormashenko, T. Stein, R. Pogreb, D. Aurbach, *J. Phys. Chem. C* **2009**, *113*, 5568.
- [17] M. Dandan, H. Y. Erbil, *Langmuir* **2009**, *25*, 8362.
- [18] D. Dupin, S. P. Armes, S. Fujii, *J. Am. Chem. Soc.* **2009**, *131*, 5386.
- [19] B. Edward, *Curr. Opin. Colloid Interface Sci.* **2011**, *16*, 266.
- [20] N. Eshtiaghi, J. J. S. Liu, K. P. Hapgood, *Powder Technol.* **2010**, *197*, 184.
- [21] N. Eshtiaghi, J. J. S. Liu, W. Shen, K. P. Hapgood, *Powder Technol.* **2009**, *196*, 126.
- [22] S. Fujii, S. Kameyama, S. P. Armes, D. Dupin, M. Suzuki, Y. Nakamura, *Soft Matter* **2010**, *6*, 635.
- [23] L. Gao, T. J. McCarthy, *Langmuir* **2007**, *23*, 10445.
- [24] S.-H. Kim, S. Y. Lee, S.-M. Yang, *Angew. Chem. Int. Ed.* **2010**, *49*, 2535.
- [25] P. McEleney, G. M. Walker, I. A. Larmour, S. E. J. Bell, *Chem. Eng. J.* **2009**, *147*, 373.
- [26] G. McHale, S. J. Elliott, M. I. Newton, D. L. Herbertson, K. Esmer, *Langmuir* **2008**, *25*, 529.
- [27] G. McHale, M. I. Newton, *Soft Matter* **2011**, *7*, 5473.
- [28] T. H. Nguyen, K. Hapgood, W. Shen, *Chem. Eng. J.* **2010**, *162*, 396.
- [29] D. Quéré, *Reps. Prog. Phys.* **2005**, *68*, 2495.
- [30] J. Tian, T. Arbatan, X. Li, W. Shen, *Chem. Commun.* **2010**, *46*, 4734.
- [31] J. Tian, T. Arbatan, X. Li, W. Shen, *Chem. Eng. J.* **2010**, *165*, 347.
- [32] A. Tosun, H. Y. Erbil, *Appl. Surf. Sci.* **2009**, *256*, 1278.
- [33] A. Venkateswara Rao, M. M. Kulkarni, S. D. Bhagat, *J. Colloid Interface Sci.* **2005**, *285*, 413.
- [34] Y. Xue, H. Wang, Y. Zhao, L. Dai, L. Feng, X. Wang, T. Lin, *Adv. Mater.* **2010**, *22*, 4814.
- [35] H. Zeng, *Appl. Phys. Lett.* **2010**, *96*, 114104.

- [36] N. Zhao, X.-Y. Zhang, Y.-F. Li, X.-Y. Lu, S.-L. Sheng, X.-L. Zhang, J. Xu, *Cell Biochem. Biophys.* **2007**, 49, 91.
- [37] Y. Zhao, J. Fang, H. Wang, X. Wang, T. Lin, *Adv. Mater.* **2010**, 22, 707.
- [38] K. Landsteiner, *Transfusion* **1961**, 1, 5.
- [39] D. Blakeley, B. Roser, B. Tolliday, C. Colaco, *The Lancet* **1990**, 336, 854.
- [40] F. Llopis, F. Carbonell-Uberos, M. C. Montero, S. Bonanad, M. D. Planelles, I. Plasencia, C. Riols, T. Planells, C. Carrillo, A. De Miguel, *Vox Sanguinis* **1999**, 77, 143.
- [41] F. Llopis, F. Carbonell-Uberos, M. D. Planelles, M. Montero, I. Plasencia, C. Carrillo, *Vox Sanguinis* **1996**, 70, 152.
- [42] J. H. Spindler, H. Klüter, M. Kerowgan, *Transfusion* **2001**, 41, 627.
- [43] D. S. Kim, S. H. Lee, C. H. Ahn, J. Y. Lee, T. H. Kwon, *Lab Chip* **2006**, 6, 794.
- [44] M. S. Khan, G. Thouas, W. Shen, G. Whyte, G. Garnier, *Anal. Chem.* **2010**, 82, 4158.
- [45] D. Ballerini, X. Li, W. Shen, *Anal. Bioanal. Chem.* **2011**, 399, 1869.
- [46] E. Hrnčir, J. Rosina, *Physiol. Res.* **1997**, 46, 319.
- [47] T. Arbatan, X. Fang, W. Shen, *Chem. Eng. J.* **2011**, 166, 787.



---

## **Appendix II**

***Published Co-Authored Papers Not Included in the  
Main Body of This Thesis***

---

**This page is intentionally blank**

# Strategy To Enhance the Wettability of Bioactive Paper-Based Sensors

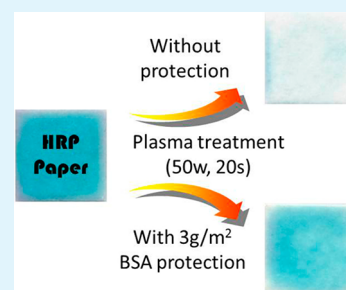
Junfei Tian,<sup>†</sup> Purim Jarujamrus,<sup>‡</sup> Lizi Li,<sup>†</sup> Miaosi Li,<sup>†</sup> and Wei Shen<sup>\*,†</sup>

<sup>†</sup>Department of Chemical Engineering, Monash University, Wellington Road, Clayton, Vic. 3800, Australia

<sup>‡</sup>Department of Chemistry and Center for Innovation in Chemistry, Faculty of Science, Mahidol University, Rama VI Road, Bangkok 10400

## S Supporting Information

**ABSTRACT:** This paper reports a potential method that can restore the wettability of bioactive paper-based sensors while maintaining their bioactivity. This study is driven by the need to increase the wettability of the antibody-loaded blood typing paper devices in order to increase the blood typing assaying speed using such paper devices. Plasma treatment is used to improve the wettability of bioactive paper; the protective effect of bovine serum albumin (BSA) to biomolecules against plasma deactivation is investigated. In the first stage, horseradish peroxidase (HRP) was used as a model biomolecule, because of the convenience of its quantifiable colorimetric reaction with a substrate. By using this protection approach, the inactivation of biomolecules on paper during the plasma treatment is significantly slowed down. This approach enables plasma treatment to be used for fabricating paper-based bioactive sensors to achieve strong wettability for rapid penetration of liquid samples or reagents. Finally, we demonstrate the use of plasma treatment to increase the wettability of antibody treated blood typing paper. After the treatment, the blood typing paper becomes highly wettable; it allows much faster penetration of blood samples into the plasma treated testing paper. Antibodies on the paper are still sufficiently active for blood typing and can report patients' blood type accurately.



**KEYWORDS:** paper-based, bioactivity, wettability, low-cost diagnostics, blood typing, plasma treatment

## INTRODUCTION

The recent rapid advancement in bioactive paper-based diagnostics has shown enormous promise of this new platform technology in improving human health in the developing world.<sup>1–5</sup> Some novel proof of concept studies focusing on specific diagnostic assays and methods of assay result transmissions have demonstrated that paper-based diagnostics have superior application potentials to many currently available technologies in obtaining rapid diagnoses under the unsupported field conditions.<sup>2,4,6</sup> Major research and development groups in this field have estimated that real applications of bioactive paper diagnostics are getting closer to becoming reality, although there are still hurdles to overcome.<sup>7–9</sup>

Among the engineering considerations of an up-scaled production of bioactive paper devices, a top priority is to retain all the required properties of the substrate and biomolecular materials in a fabrication process so that the performances of the fabricated devices are at their optimum. For most bioactive paper-based devices, paper wettability and paper bioactivity are two of the most important properties, which determine the performance of the devices. In the fabrication of some devices, it was found that the introduction of bioactive reagents can significantly reduce the wettability of bioactive paper, seriously compromising the performance of the device in a diagnostic test.

An example from our recent experience is the bioactive paper device for blood typing.<sup>6,10,11</sup> The working principle of a paper-based blood typing device relies on the introduction of blood

typing antibodies into the paper first. Penetration of antibody solution into the pores of the paper results in deposition of antibody molecules and an additive, such as BSA, on the fiber surface. The so-formed bioactive blood typing paper is expected to function when a blood sample is added onto the paper. First, the blood will redissolve the deposited antibody from the fiber surface into the blood serum. The dissolved antibody will be able to interact with the antigens on the surface of the red blood cells (RBCs). The antibody-RBC interaction may either cause agglutination of the red cells or have no effect on them. With the aid of saline washing, the agglutination or non-agglutination of RBCs will be revealed.<sup>6,10,11</sup>

This simple design has confronted an unexpected problem of reduced wettability of the antibody loaded paper by the blood sample when antibodies from commercial sources are used.<sup>10</sup> Figure 1 shows the degree of poor wetting of the antibody-loaded paper compared with paper without antibody. The poor wettability of the paper significantly reduces the speed of liquid penetration. An easy and upscalable solution for restoring the wettability of the paper could be by plasma treatment. In a plasma environment, energetic electrons, ions, and radical species impinge on the surface, leading to physical and chemical changes of the surface in three main ways: 1) Etching. Plasma treatment is used to remove materials from solid surfaces. 2)

**Received:** August 18, 2012

**Accepted:** November 14, 2012

**Published:** November 14, 2012



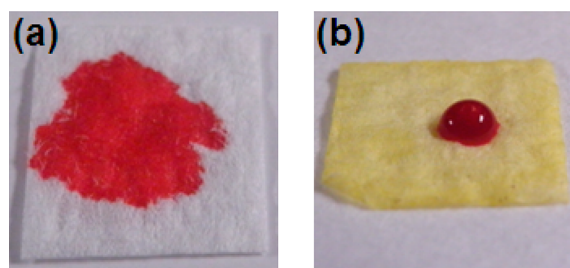


**Figure 1.** (a) 4  $\mu\text{L}$  of blood penetrates into untreated paper and (b) 4  $\mu\text{L}$  of blood stands on an antibody treated paper.

Activation. It is used to chemically and/or physically modify the surfaces so that the modified surfaces carry active species. 3) Coating. It is used to deposit a thin film of material on solid surfaces.<sup>12</sup> Martinez et al. and Abo et al. respectively demonstrated the use of plasma treatment as a step of  $\mu\text{PADs}$  fabrication to increase channel wettability.<sup>1,13</sup> Li et al. and Tian et al. also used plasma treatment to increase the wettability of the thread-based microfluidic device and V-groove microfluidic device on polymer film by removing the contaminant deposits on the surface.<sup>14,15</sup> In another study by Li et al., plasma treatment has been utilized as a patterning method to selectively etch hydrophilic patterns onto a piece of hydrophobic filter paper to create the  $\mu\text{PADs}$ .<sup>3</sup> After plasma treatment, the sample delivery channels and detection areas of these devices become highly wettable. Aqueous solution of biomolecules and detection reagents can be easily loaded into the paper by absorption, to form a complete sensor.

While plasma treatment is an easy and matured technology for surface treatment to increase materials' wettability, it can significantly reduce the activity of biomolecules.<sup>16–18</sup> Plasma treatment has been widely used as a method for biodecontamination.<sup>17,19,20</sup> Von Keudell showed that plasma treatment can efficiently inactivate a range of biocontaminants including micro-organisms, bacteria and proteins, etc.<sup>16</sup> Plasma treatment allows energetic particles to destroy or modify surface chemical bonding of materials, causing a variety of proteins to denature.

In our bioactive paper studies, however, we found that plasma treatment imposes a much weaker destructive effect on blood typing antibodies than expected. Blood typing antibodies do not lose their functions in blood typing assays. This surprising observation was found to be reproducible. One possible reason for this observation is the presence of certain protection additives in the antibody reagent. Based on the supplier's specification, the antibodies contain 1–5% BSA as a protection additive. There are reported bioactivity protection methods in the literature, but most of these methods focus on the protection of the activity and stability of proteins and enzymes from the inhibition induced by temperature, soluble additives, and even radiation.<sup>21–24</sup> In those methods, BSA is a widely used stabilizer that prevents the thermally induced inactivation of biomolecules. Moreover, BSA has also been reported to have a protection effect on enzyme activity from the inhibition caused by a toxicant. Our hypothesis is that BSA may contribute to the protection for antibody during the plasma treatment. If the destructive effect of plasma to biomolecules can be reduced through a simple method, then plasma treatment can be used to improve the wettability of bioactive papers; it will greatly improve the fabrication of low-cost sensors.

In this paper, we used horseradish peroxidase (HRP) as a model biomolecule to demonstrate the influence of plasma treatment to the activity of biomolecules on paper. The choice of HRP is based on the fact that its activity can be visually shown by using a suitable liquid substrate; HRP therefore provides an easy way to assess the activity loss of the biomolecule. We compared the activity of HRP paper loaded with a range of concentrations of HRP solutions before and after plasma treatment. The effect caused by plasma with increasing treatment time on the activity of HRP paper loaded with a given concentration of HRP solution was also studied. An effective strategy that can protect the biomolecules on paper from being deactivated by plasma treatment was investigated. This strategy offers a significant flexibility to the fabrication of bioactive paper based sensors; this flexibility allows the enhancement of the device's wettability and the addition of bioactivity to the paper to be performed in any desired sequence, effectively reducing practical fabrication constraints in device production.

## ■ EXPERIMENTAL SECTION

**Materials and Equipment.** Horseradish peroxidase (HRP) (Type I, lyophilized powder, 100 KU) was obtained from Sigma-Aldrich. HRP powder was dissolved in phosphate-buffered saline (PBS, pH 7.4) to make stock solution (1 mg/mL). A liquid substrate system of HRP, 3,3',5,5'-tetramethylbenzidine (TMB), was obtained from Sigma-Aldrich and used for HRP activity analysis. The activity of enzymatic paper containing HRP molecules can be calorimetrically assessed by using TMB substrate. After applying the liquid substrate to an HRP loaded enzymatic paper, the enzyme-catalyzed reaction will occur. The intensity of the blue color developed through this reaction reflects the activity of HRP in paper. The blue color of the reacted substrate was then scanned into a computer, and the activity of HRP was quantitatively analyzed using computer software.

Commercial antibody solutions of red blood cell antigens A, B, and D (Epiclone Anti-A, Anti-B, and Anti-D monoclonal grouping reagents) were obtained from CSL, Australia. Anti-A and Anti-B are color-coded blue and yellow solutions, respectively, whereas Anti-D is a clear solution. These antibodies are made of immunoglobulin M (IgM). Normal saline (0.85 g NaCl in 100 mL of deionized water (18.2 M $\Omega$  cm<sup>-1</sup>)) was used as diluent and washing solution in this study. Blood samples were collected from 3 adult volunteers; the samples were kept in standard plastic vials containing lithium heparin anticoagulant. Antibody solutions and blood samples were stored at 4 °C, and blood samples were used within 5 days.

Filter papers (Whatman grade 4) were cut into 1 cm  $\times$  1 cm squares for fabricating HRP and HRP-BSA paper. A Kleenex paper towel was cut into 5 mm  $\times$  5 mm squares which were used as the base substrate for making the blood typing device, while standard blotting papers (drink coaster blotting, 280 g/m<sup>2</sup>) were used to remove excess liquids during device preparation.

K1050X plasma asher (Quorum Emitech, U.K.) was used for plasma treatment. The vacuum level for the treatment was  $6 \times 10^{-1}$  mbar. The paper samples were always placed in the center of the chamber during the treatment for a consistent effect of treatment.

**Test of Activity of HRP Paper without Plasma Treatment.** HRP stock solution was diluted with to get serially diluted HRP standard solutions with the concentrations of 0, 1, 2, 3, and 4  $\mu\text{g/mL}$ . About 10 mL of HRP solution in a plastic Petri dish (I.D. = 8.5 cm) was used for soaking paper. Five filter paper squares were respectively soaked in each diluted HRP solution for 2 s. The wet paper squares were not blotted. They were put onto a piece of plastic film and dried in a fume hood for 20 min. After drying, each paper square received an addition of 15  $\mu\text{L}$  of TMB liquid substrate solution. These paper squares carrying TMB were then placed into a dark box for 2 min to develop color changes of the substrate on paper. Color intensity of scans of the filter paper squares was measured using Adobe Photoshop

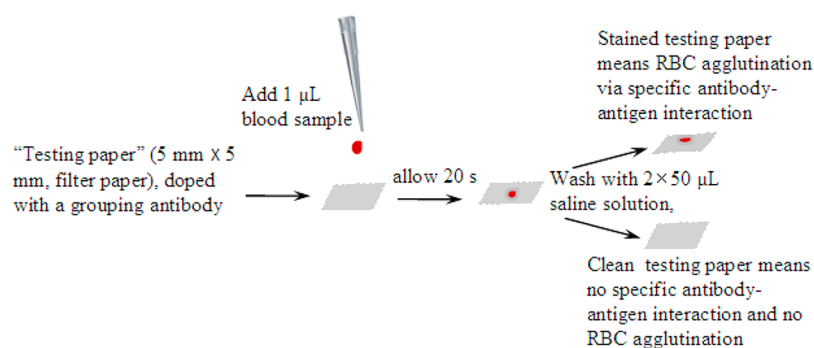


**Figure 2.** A schematic diagram showing blood typing test protocol using paper and result interpretation.

CS software; the calibration curve was then obtained. Error bars (relative standard deviation) were obtained from five repeats of the whole experiment.

**Test of Activity of HRP-BSA Paper without Plasma Treatment.** Seven filter paper squares (1 cm × 1 cm) were soaked in diluted HRP solution (4 µg/mL) and dried in a fume hood for 20 min. Then, 15 µL of BSA solution with the concentrations of 0.1%, 0.2%, 0.5%, 1%, 2%, 3%, and 4% (w/v) were deposited onto each square, respectively. After drying in the fume hood for 20 min, 15 µL of TMB liquid substrate solution was added onto each of the filter paper squares. These filter paper squares were then incubated for 2 min to allow the color development. Finally, the filter paper squares were scanned to get clear images. Error bars (relative standard deviation) were obtained from five repeats of the whole experiment.

**Test of Activity of HRP Paper after Plasma Treatment.** *Paper Loaded with Different Concentrations of HRP Solution Treated with Plasma for a Fixed Treatment Time.* HRP stock solution was diluted to standard solutions with the concentrations of 0, 1, 2, 3, and 4 µg/mL. Five filter paper squares (1 cm × 1 cm) were soaked in each diluted HRP solution and dried in a fume hood for 20 min. Then, the paper squares were plasma treated (50 W) for 60 s. Plasma treatment was activated in vacuum, with a background air pressure of  $6 \times 10^{-1}$  mbar. TMB liquid substrate was added to the paper squares following the same procedure used in the previous section.

*Paper Loaded with a Known Fixed Concentration of HRP Solution Treated with Plasma for Different Times.* Six filter paper squares (1 cm × 1 cm) were soaked in diluted HRP solution (4 µg/mL) and dried in a fume hood for 20 min. Then, the paper squares were plasma treated (50 W) for 0, 5, 10, 20, 40, and 60 s, respectively. TMB liquid substrate was added to the paper squares following the same procedure used in the previous section.

**Test of Activity of HRP-BSA Paper with Plasma Treatment.** *Paper Loaded with a Fixed Concentration of HRP Solution and BSA Solution Treated with Plasma for a Fixed Treatment Time.* Ten filter paper squares (1 cm × 1 cm) were soaked in diluted HRP solution (4 µg/mL) and dried in a fume hood for 20 min. Then, 15 µL of BSA solution with the concentration of 2% (w/v) was deposited onto these squares. After drying in the fume hood for 20 min, the paper squares were plasma treated (50 W) for 0, 5, 10, 20, 40, 60, 80, 100, 200, and 300 s, respectively. TMB liquid substrate was added to the paper squares following the same procedure used in the previous section.

*Paper Loaded with a Fixed Concentration of HRP Solution and Different Concentrations of BSA Solution Treated with Plasma for a Fixed Treatment Time.* Seven filter paper squares (1 cm × 1 cm) were soaked in diluted HRP solution (4 µg/mL) and dried in a fume hood for 20 min. Then, 15 µL of BSA solution with the concentration of 0.1%, 0.2%, 0.5%, 1%, 2%, 3%, and 4% (w/v) were deposited onto each paper square, respectively. After drying in the fume hood for 20 min, the paper squares were plasma treated (50 W) for 20 s. TMB liquid substrate was added to the paper squares following the same procedure used in the previous section.

**Quantification of the Activity of Bioactive Paper from Scanned Images.** After each test, the colored paper squares were imaged with a desktop scanner (Epson Perfection 2450, color photo setting), then imported into Adobe Photoshop software, and

converted into CMYK mode. The mean cyan intensity was obtained using the histogram function. This is because the cyan channel can provide a larger dynamic range than other channels and further increases the accuracy of the analysis of the developed color on the paper squares. The ultimate mean intensity value was generated by subtracting the measured average intensity of the colored paper squares from the mean intensity of the blank control.

**Blood Typing by Using Plasma Treated Testing Paper.** A 5 mm × 5 mm Kleenex paper square was cut and treated by doping it with 3.5 µL of undiluted (1×) commercial grouping antibody agent and allowed to dry in a fume hood for 10 min. This Kleenex paper square was then treated in a vacuum plasma reactor for 1 min, at an intensity of 50 W. The vacuum level for the treatment was  $6 \times 10^{-1}$  mbar. A further 3.5 µL of undiluted (1×) commercial grouping antibody agent was then introduced to the paper square (double dope). The plasma treatment was then repeated once again. The antibody-treated papers (with 2 × plasma treatments) are referred to as the “testing papers” and are shown as the white squares in Figure 2. The testing papers treated with Anti-A, Anti-B, and Anti-D are specifically referred to as “paper A”, “paper B”, and “paper D”, respectively.

A one-microliter blood sample was introduced onto the antibody treated testing paper (Figure 2). Most of the sample was absorbed by the testing paper. The nonabsorbed blood sample passed through the testing paper and was absorbed by blotting paper. Twenty seconds was given to allow interactions of RBCs with the antibody in paper. After that, the testing paper was placed onto another blotting paper. Two aliquots of 50 µL saline solution aliquot saline solution were gradually introduced by a micropipet onto the blood sample-loaded testing paper; the saline solution penetrated through the testing paper and was absorbed by the blotting paper underneath the testing paper. The testing paper was then separated from the blotting paper for visual inspection. Visible blood stain on the testing paper indicates that RBC agglutination occurred and the test is positive. On the other hand, if no blood stain is observable on the testing paper, RBC agglutination did not occur, and the test is negative. Following this principle an ideal testing-result-matrix is presented in Figure S1.

## RESULTS AND DISCUSSION

**Effect Plasma Treatment of HRP Activity.** Proteins, including enzymes, can be denatured when they are exposed to extreme conditions such as high temperature, mechanical forces, radiation, plasma treatment, chemicals, and many transition metal ions. Figures 3 (a) and 3 (b) clearly show that plasma treatment has the effect of deactivating the HRP paper. Since the TMB solution was added onto HRP paper, the blue color was developed resulting from the enzyme–substrate reaction (Figure 3 (a)). The HRP activity is indicated by the intensity of the blue color. Figure 3 (c) shows the activity of HRP paper treated with a series of concentrations of HRP solution. However, after 60 s plasma treatment (50 W), the blue color intensity was greatly reduced indicating a significant



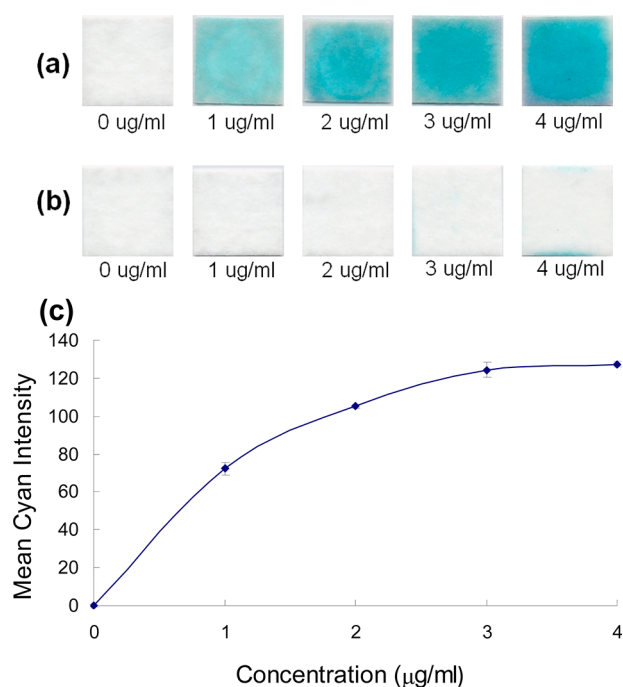


**Figure 3.** The comparison of the activities of a series of HRP paper squares (a) without plasma treatment and (b) with plasma treatment (50 W, 60 s); (c) measured mean cyan intensity of catalytic product on HRP paper. (a) First, paper squares were treated with different concentrations of HRP solution and dried in a fume hood. Then, 15  $\mu\text{L}$  TMB was added on the squares. Image was obtained after 2 min incubation. (b) First, paper squares were treated with different concentrations of HRP solution and dried in a fume hood. Then, these paper squares were treated with plasma (50 W) for 60 s. After that, 15  $\mu\text{L}$  TMB was added on the squares. Image was obtained after 2 min incubation.

loss of enzymatic activity (Figure 3 (b)). This observation clearly shows the devastating loss of HRP activity in paper by plasma treatment.

To quantify the effect of plasma treatment on the activity loss of HRP, the dried HRP paper, which was prepared by soaking the paper in 4  $\mu\text{g/mL}$  HRP solution, was chosen for further investigation; the paper squares were treated with plasma (50 W) for different times, and the HRP activity was measured in the same way. Figure 4 shows the rapid loss of HRP activity on paper with the increase of plasma treatment time. It can be seen from Figure 4 that there is a sharp decline of mean cyan intensity with the increasing treatment time from 0 to 10 s,

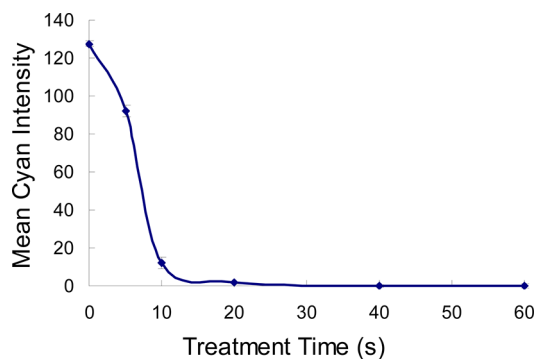


**Figure 4.** The effect of plasma treatment on the activity of HRP on paper.

showing that deactivation of HRP occurred in a very short time under plasma treatment. After 20 s of plasma treatment, HRP was almost completely deactivated. This study indicates the activity of HRP is extremely susceptible to plasma treatment.

**Protection of HRP from Total Inactivation Caused by Plasma Treatment.** The above results are in agreement with many studies reported in the literature that plasma treatment has devastating effects on activities of biointerfaces. In fabrication of low-cost diagnostic devices such as bioactive paper devices, however, it is ideal that bioactivities can be protected from total inactivation by plasma treatment. At least two scenarios can be perceived where such protection will be necessary. First, if bioactivities can be protected from plasma inactivation, then the fabrication process can be carried out with more flexibility; plasma treatment of the device does not have to be performed before the addition of bioactive reagents into the device. Second, the biochemical method used for protecting the plasma inactivation could be used as a method of patterning of bioactivity. In this study, however, we focus on proving the concept of using BSA to protect the bioactivity from total inactivation by plasma treatment.

In order to quantitatively evaluate the protective action of BSA against the inactivation of HRP paper caused by plasma treatment, a range of concentrations of BSA solution was prepared to create a protective layer over the HRP paper. In order to understand the addition of BSA to the activity of HRP on the paper, HRP activities on paper with and without BSA were compared. It can be seen from Figure 5 (a) that the

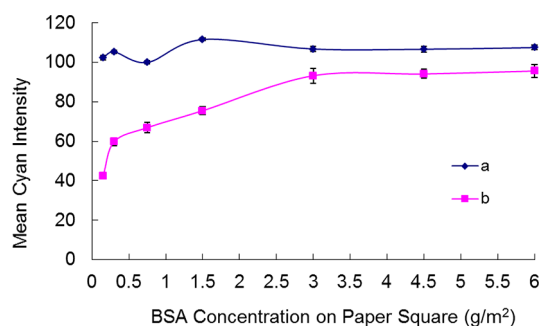


**Figure 5.** The protective action of BSA on HRP paper: (a) untreated HRP-BSA paper and (b) plasma (50 W, 20 s) treated HRP-BSA paper. Filter paper squares were soaked in 4  $\mu\text{g/mL}$  HRP solution. After drying, these squares were dosed with 15 mL of different concentrations of BSA solution. After drying in a fume hood for 20 min, HRP-BSA paper was fabricated. The calibration curve to convert color intensity to equivalent concentration of HRP solution ( $\mu\text{g/mL}$ ) can be seen in Figure S3.

addition of a BSA layer over the HRP paper slightly reduced the activity of HRP, nevertheless the HRP still remain active. A possible reason for this observation may be that the protective layer of BSA slows down the penetration of the TMB solution, which restricted the accessibility of TMB to the HRP molecules that are covered by the BSA layer. Therefore, the shorter reaction time led to a slightly weaker development of color.

The most interesting result can be seen in Figure 5(b), which clearly shows that HRP molecules on the HRP-BSA paper retain a substantial level of activity after plasma treatment (50 W, 20 s). Compared with Figure 4, the inactivation of HRP on paper is significantly slowed down. This result suggests that the protection layer of BSA offers protection to HRP in paper against damage by plasma treatment. The effect of protection

could be improved with the increase of the concentration of BSA up to approximately 2 wt %. Fifteen microliters of 2 wt % BSA solution can provide a BSA layer with the concentration of 3 g/m<sup>2</sup> on paper square. Further increase of BSA concentration solution beyond 2 wt % offers little improvement of the protection of HRP in paper. The results show that a stable protection layer which was made of 2 wt % BSA solution offers a significant level of protection to HRP against plasma deactivation of HRP although such protection is not 100%. The HRP activity that survived the plasma treatment shows that BSA offers a practical means to protect the bioactivity in paper, and the level of protection is sufficient to maintain its bioactive function. The possible mechanism of the protection of HRP by BSA may be due to the physical barrier effect of BSA which shields the HRP molecules from the direct exposure to the energetic particles in the plasma environment.

Kylián et al. studied the plasma etching of a deposited BSA layer on a silica surface. They found that the deposited BSA layer can be etched away by plasma treatment.<sup>25</sup> However, the reduction of BSA layer under the plasma treatment was not instantaneous; instead, it was shown to be a gradual process with the increase of the amount of plasma treatment (i.e., intensity  $\times$  time).

Figure 6 compares the stability between HRP paper and HRP-BSA paper under plasma treatment. With increasing

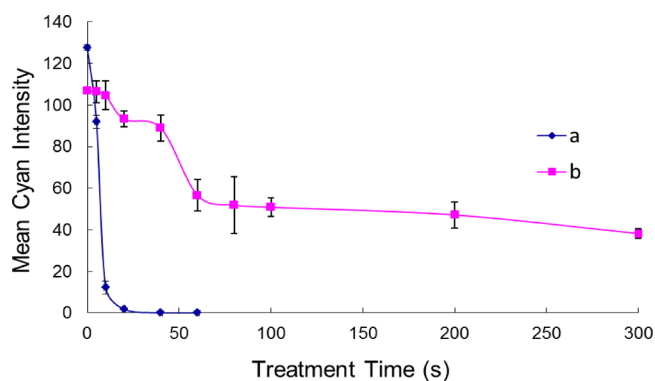


**Figure 6.** The stability of HRP paper (a) and HRP-BSA paper (b) under plasma treatment (50 W). Filter paper squares were soaked in 4  $\mu$ g/mL HRP solution. After drying, these squares were treated with 15 mL of BSA solution (2 wt %). After drying in fume hood for 20 min, the preparation of an HRP-BSA paper sample was completed. The calibration curve to convert color intensity to equivalent concentration of HRP solution ( $\mu$ g/mL) can be seen in Figure S4.

treatment time, the intensity of developed cyan color of the catalytic product on HRP-BSA paper was reduced. The trend shown by Figure 6 (b) indicates that the activity of the HRP-BSA paper underwent slower loss with the increase of plasma treatment time, compared with the HRP paper without BSA. This result shows that BSA has a positive protection effect on HRP activity against plasma treatment. Normally, 20–30 s of plasma treatment (50 W) can significantly improve the wettability of low-wettable paper. After 20–30 s of plasma treatment at 50 W, the measurement of HRP catalyzed color change shows that greater than 70% of color intensity can still be observed. This color intensity corresponds to near 40% of enzyme activity. Even after 300 s of plasma treatment at 50 W, measurement of HRP catalyzed color change shows that greater than 40% of color intensity can still be observed indicating that there is still an amount of enzyme molecules remaining active.

This finding shows the stability of HRP-BSA paper is greatly improved over HRP paper, whose activity was almost completely lost after 20 s of plasma treatment at 50 W.

**Plasma Treatment of Papers Carrying Blood Grouping Antibodies.** We return to the practical application of improving blood wettability of blood typing paper that carries the blood typing antibodies. As was mentioned earlier, when blood typing antibodies from stated source are introduced on the paper, the blood wettability of the paper reduces significantly (Figures 7 (a) and 7 (b)). Such a reduction in

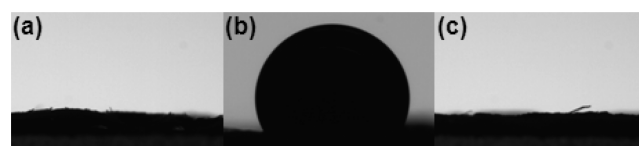


**Figure 7.** Profile of blood in/on (a) paper; (b) antibody paper (contact angle = 122.2°); and (c) plasma treated antibody paper. (a) Kleenex paper square without any treatment. (b) Kleenex paper square treated by adding antibody solution twice. (c) Kleenex paper square treated using the same treatment procedure as blood typing paper. Four microliters of blood was deposited onto each paper square respectively. After 3 s, images were taken to compare the status of blood sample on each paper. Blood penetrated into paper (a) and plasma treated antibody paper (c) in less than 3 s. However, water does not completely penetrate into antibody paper (b) within 30 s.

blood wettability negatively impacts on the performance of the blood typing paper, since slow penetration of sample will slow down the assaying speed. The most effective way to overcome this problem is to restore the wettability of the paper.

Blood typing antibodies from stated source contain 1–5% BSA as the stabilization reagent.<sup>10</sup> Because of the hydrophobic nature of BSA, its adsorption on cellulose fiber surfaces will reduce wettability. However, based on our study of the HRP-BSA system, the wettability of the paper carrying blood typing antibodies should be restored by plasma treatment and the blood typing antibody molecules should still be active. Followed by this hypothesis, paper carrying blood typing antibodies were plasma treated for 60 s at 50 W. After the treatment, the blood wetting of the paper was restored; a blood sample can completely penetrate into the treated paper within 3 s (Figure 7 (c)). This level of wettability fulfills the blood penetration requirement of blood typing paper.

Figure 8 shows the blood typing results using the plasma treated papers (50 W, 60 s). These results show that plasma treatment can be used as a method to improve the wettability of bioactive papers, provided that appropriate protection measures are taken to prevent the plasma deactivation of the biomolecules.

## CONCLUSION

The concept of using plasma treatment to improve the wettability of bioactive paper for rapid spreading and penetration of liquid sample into paper was investigated. Plasma treatment is shown to rapidly deactivate HRP molecules on paper. In this study, we found that BSA can act as a molecular chaperone to protect HRP in paper against inactivation caused by plasma treatment. The successful protection of biomolecules by BSA enables plasma treatment to be used as a part of the fabrication process for the mass production of paper-based sensors in which strong wettability of bioactive areas such as detection areas on a device is

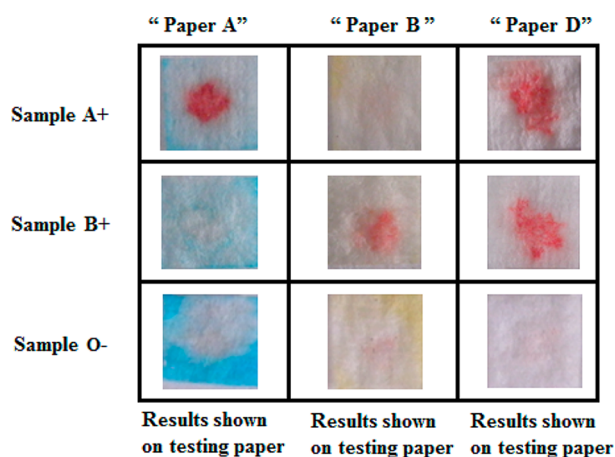


**Figure 8.** Testing of blood types using testing papers treated with  $2 \times 3.5 \mu\text{L}$  of commercial antibodies. Paper A, Paper B, and Paper D, all showing expected results ( $1 \mu\text{L}$  blood sample, plasma treatment).

required. We also demonstrated a real bioactive paper application of blood typing paper. Plasma treatment of antibody loaded papers greatly increases the blood penetration rate into the paper and at the same time leaves a sufficient level of antibody activity to agglutinate RBCs that carry the corresponding antigens. Plasma treatment of the blood typing papers shows that this method may be further developed into a fabrication step in mass production of bioactive paper diagnostics where devices must have a high level of wettability and sufficient bioactivity. This study shows that the sequence of plasma treatment and the introduction of bioactive reagents onto paper may no longer be an engineering restriction in sensor production. These two fabrication steps can be implemented in any sequence to suit the engineering of the best production efficiency.

## ■ ASSOCIATED CONTENT

### Supporting Information

Four figures: (1) Figure S1. A schematic of an ideal blood typing testing-result-matrix of antibody-specific agglutination of RBCs on testing paper; (2) Figure S2. A schematic of the process for evaluating the protection of HRP paper by BSA from plasma treatment; (3) Figure S3. The protective action of BSA on HRP paper. (a) Untreated HRP-BSA paper; (b) Plasma (50 W, 20 s) treated HRP-BSA paper; (4) Figure S4. The stability of HRP paper (a) and HRP-BSA paper (b) under plasma treatment (50 W). This material is available free of charge via the Internet at <http://pubs.acs.org>.

## ■ AUTHOR INFORMATION

### Corresponding Author

[Redacted]

### Notes

The authors declare no competing financial interest.

## ■ ACKNOWLEDGMENTS

This work is supported by Australian Research Council Grant (ARC DP1094179 and LP110200973). Authors thank Haemokinesis for its support through ARC Linkage Project. The authors would like to specially thank Dr. E. Perkins in the Department of Chemical Engineering, Monash University for proofreading the manuscript. J.T., L.L., and M.L. thank Monash University Research and Graduate School and the Faculty of

Engineering for their postgraduate research scholarships. P.J. is grateful for the research grants from the Thailand Research Fund (TRF) through the Royal Golden Jubilee PhD Program (RGJ) and Center of Excellence for Innovation in Chemistry (PERCH-CIC), Commission on Higher Education, Ministry of Education.

## ■ REFERENCES

- (1) Martinez, A. W.; Phillips, S. T.; Butte, M. J.; Whitesides, G. M. *Angew. Chem., Int. Ed.* **2007**, *46*, 1318–1320.
- (2) Martinez, A. W.; Phillips, S. T.; Whitesides, G. M.; Carrilho, E. *Anal. Chem.* **2010**, *82*, 3–10.
- (3) Li, X.; Tian, J.; Nguyen, T.; Shen, W. *Anal. Chem.* **2008**, *80*, 9131–9134.
- (4) Pelton, R. *TrAC, Trends Anal. Chem.* **2009**, *28*, 925–942.
- (5) Tian, J.; Shen, W. *Chem. Commun.* **2011**, *47*, 1583–1585.
- (6) Li, M.; Tian, J.; Al-Tamimi, M.; Shen, W. *Angew. Chem., Int. Ed.* **2012**, *51*, S497–S501.
- (7) Mukhopadhyay, R. *Chem. World* **2010**, *7*, 50–53.
- (8) McMaster University Daily News. <http://dailynews.mcmaster.ca/article/bioactive-paper-closer-to-commercialization/> (accessed Nov 5, 2012).
- (9) Paper Money Web site. <http://www.globalpapermoney.org/bioactive-paper-research-receives-added-funding-for-bioactive-paper-development-cms-5380> (accessed Nov 5, 2012).
- (10) Jarujamrus, P.; Tian, J.; Li, X.; Siripinyanond, A.; Shiwatana, J.; Shen, W. *Analyst* **2012**, *137*, 2205–2210.
- (11) Al-Tamimi, M.; Shen, W.; Zeineddine, R.; Tran, H.; Garnier, G. *Anal. Chem.* **2011**, *84*, 1661–1668.
- (12) Pykönen, M.; Silvaani, H.; Preston, J.; Fardim, P.; Toivakka, M. *Colloids Surf., A* **2009**, *352*, 103–112.
- (13) Abe, K.; Suzuki, K.; Citterio, D. *Anal. Chem.* **2008**, *80*, 6928–6934.
- (14) Li, X.; Tian, J.; Shen, W. *ACS Appl. Mater. Interfaces* **2010**, *2*, 1–6.
- (15) Tian, J.; Kannangara, D.; Li, X.; Shen, W. *Lab Chip* **2010**, *10*, 2258–2264.
- (16) von Keudell, A.; Awakowicz, P.; Benedikt, J.; Raballand, V.; Yanguas-Gil, A.; Opretzka, J.; Flötgen, C.; Reuter, R.; Byelykh, L.; Halfmann, H.; Stapelmann, K.; Denis, B.; Wunderlich, J.; Muranyi, P.; Rossi, F.; Kylián, O.; Hasiwa, N.; Ruiz, A.; Rauscher, H.; Sirghi, L.; Comoy, E.; Dehen, C.; Challier, L.; Deslys, J. P. *Plasma Processes Polym.* **2010**, *7*, 327–352.
- (17) Rauscher, H.; Kylián, O.; Benedikt, J.; von Keudell, A.; Rossi, F. *ChemPhysChem* **2010**, *11*, 1382–1389.
- (18) Fumagalli, F.; Kylián, O.; Amato, L.; Hanuš, J.; Rossi, F. *J. Phys. D: Appl. Phys.* **2012**, *45*, 135203.
- (19) Birmingham, J. G.; Hammerstrom, D. J. *IEEE Trans. Plasma Sci.* **2000**, *28*, 51–55.
- (20) Rossi, F.; Kylián, O.; Hasiwa, M. *Plasma Processes Polym.* **2006**, *3*, 431–442.
- (21) Eremin, A. N.; Budnikova, L. P.; Sviridov, O. V.; Metelitsa, D. I. *Appl. Biochem. Microbiol.* **2002**, *38*, 151–158.
- (22) Gronczewska, J.; Biegniewska, A.; Ziętara, M. S.; Skorkowski, E. *Comp. Biochem. Physiol., Part C: Toxicol. Pharmacol.* **2004**, *137*, 307–311.
- (23) Marini, I.; Moschini, R.; Corso, A.; Mura, U. *Cell. Mol. Life Sci.* **2005**, *62*, 3092–3099.
- (24) D'Souza, S. E.; Altekar, W.; D'Souza, S. F. *World J. Microbiol. Biotechnol.* **1997**, *13*, 561–564.
- (25) Kylián, O.; Benedikt, J.; Sirghi, L.; Reuter, R.; Rauscher, H.; von Keudell, A.; Rossi, F. *Plasma Processes Polym.* **2009**, *6*, 255–261.

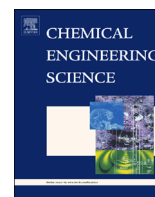




Contents lists available at [SciVerse ScienceDirect](http://www.sciencedirect.com)

# Chemical Engineering Science

journal homepage: [www.elsevier.com/locate/ces](http://www.elsevier.com/locate/ces)



## Charge transport between liquid marbles



Miaosi Li<sup>a</sup>, Junfei Tian<sup>a</sup>, Lizi Li<sup>a</sup>, Aihua Liu<sup>b</sup>, Wei Shen<sup>a,\*</sup>

<sup>a</sup> Department of Chemical Engineering, Monash University, Wellington Road, Clayton, 3800, Victoria, Australia

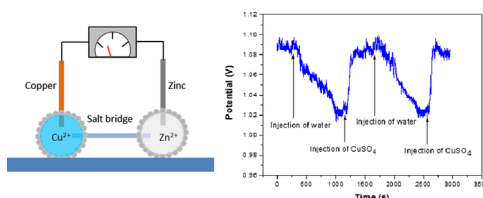
<sup>b</sup> Laboratory for Biosensing, Qingdao Institute of Bioenergy & Bioprocess Technology, and Key Laboratory of Bioenergy, Chinese Academy of Sciences, 189 Songling Road, Qingdao 266101, China

### HIGHLIGHTS

- Liquid marble was studied as micro reactors.
- Charge and mass transport properties of liquid marble were explored.
- Sample mixing profiles inside a liquid marble were achieved.
- The study indicates that nutrient refilling and waste removal can be realized.
- Liquid marble has the potential use for electric stimulation and reaction monitoring.

### GRAPHICAL ABSTRACT

A Daniell Cell was made with liquid marbles. The sample mixing profiles inside liquid marbles were studied and the transport of electric charge and energy between the liquid marble cells was demonstrated. Only microlitres of electrolytes are required to construct an electric cell, showing the liquid marbles can form micro electrochemical reactors.



### ARTICLE INFO

#### Article history:

Received 8 January 2013

Received in revised form

28 March 2013

Accepted 3 April 2013

Available online 18 April 2013

#### Keywords:

Chemical reactors

Interface

Electrochemistry

Transport processes

Liquid marbles

Continuous sample flow

### ABSTRACT

Recent studies on liquid marble applications have shown the possibilities of using liquid marbles as biochemical or biological reactors. These potential applications of liquid marbles generate further interests in the investigation of materials and energy transport between liquid marbles to enable the control and manipulation of the biochemical and biological reactions inside them. In this study, the transport of electric charges between liquid marbles containing electrolyte solutions is demonstrated through a Daniell cell made with liquid marbles. Potential and current comparisons of the Daniell cells made using liquid marbles and solutions in beakers are made. Results show that charge transport between liquid marbles driven by electrochemical reactions is possible. Furthermore, the solution mixing conditions inside a liquid marble is also investigated experimentally and through modeling. The results offer a preliminary appraisal of the internal conditions of liquid marbles as a biological reactor.

© 2013 Published by Elsevier Ltd. All rights reserved.

### 1. Introduction

Liquid marble as an interesting interface phenomenon has inspired an abundance of intensive research in recent years after the pioneer study by Quéré and Aussillous was reported in 2001. (Aussillous and Quéré, 2001, 2006; Bormashenko et al., 2009a, 2009b; Dandan and Erbil, 2009; Gao and McCarthy, 2007; Bangi et al., 2010; Rao et al., 2005; Quéré and Aussillous, 2002) A liquid marble is

formed from a liquid drop coated with hydrophobic powder particles; the loosely packed hydrophobic particles form the shell of the liquid marble which prevents any direct contact between the liquid it enwraps and any surface outside the shell. Liquid marbles can therefore maintain a near spherical shape stably on a supporting surface. (Newton et al., 2007; Bormashenko et al., 2009; Dandan and Erbil, 2009) This interesting property has attracted many studies that focused on the fundamental physics (Bormashenko et al., 2009a, 2009b, 2009c, 2011a, 2011b; Aussillous and Quéré, 2006; Dandan and Erbil, 2009; Dupin et al., 2009; Fujii et al., 2010; Arbatan and Shen, 2011; Bormashenko, 2011, 2012; Bajwa et al., 2012; McHale and Newton, 2011) and potential applications (Bormashenko, 2011, 2012; Bajwa et al., 2012; McHale and Newton, 2011; Hapgood et al., 2009;

Bormashenko and Musin, 2009; Zhang et al., 2006; Yao et al., 2011; Tian et al., 2010a, 2010b; Arbatan et al., 2012) of liquid marbles. Among a variety of possible applications, the use of liquid marble as micro reactors has been explored by several groups (Tian et al., 2010a, 2010b; Arbatan et al., 2012; Bormashenko and Balter, 2011). Newton et al. (2007) reported on using the charged Teflon sticks to move liquid marble, demonstrating that motions of marbles can be individually controlled. Bormashenko et al. (2008) investigated the incorporation of  $\text{Fe}_2\text{O}_3$  nanoparticles in water encapsulated within a polyvinylidene fluoride liquid marble to create a ferrofluidic marble that can be magnetically manipulated. Zhao et al. (2010) showed that liquid marbles enwrapped with hydrophobic  $\text{Fe}_3\text{O}_4$  nanoparticles can be further controlled by “opening” and “closing” the upper surface of the marble. These reports of liquid marble control further demonstrate that liquid marbles can be used as micro reactors. Tian et al. showed that the porous shell of liquid marbles can be used as micro reactors to detect gas or emit gas (Tian et al., 2010). Bormashenko et al. (2011) also showed that porous liquid marble shells enable gas-triggered reactions to occur inside the liquid marble. More recently, Arbatan et al. (2012a) demonstrated the use of liquid marble as a micro-bioreactor for blood typing. These reports have shown that liquid marbles can be used as micro reactors to carry out chemical and biochemical reactions by either coalescing two marbles containing different reactants into a single marble, or facilitating reactions within one liquid marble while relying on external materials to transport into the liquid marble.

Recently, we have developed new applications of using liquid marbles as biological micro-reactors. (Arbatan et al., 2012b; Tian et al., 2013) Liquid marble can provide one of the simplest micro biological reactors to facilitate the formation of tumor cell spheroids (Arbatan et al., 2012b). The use of liquid marble micro biological reactor for tumor cell spheroid growth is easy and highly efficient: cell aggregation could be clearly observed after 24 h; numerous spheroids formed in a single marble; the yield of cells formation was very high. The confined liquid space inside liquid marble and the hydrophobic marble shell discourage the cell adhesion onto the marble shell, making them to aggregate and forming spheroids. It is possible that the liquid marble method may become a complementary but much more efficient method than the “hanging drop” method that is widely used in biological laboratories for cell spheroid growth, allowing *in vitro* studies of tumor and cancer physiology to be carried out much more easily. Liquid marble also provides a suitable micro-environment for the culturing of microorganisms. This application took advantage of the porous nature of the liquid marble shell; gaseous materials can pass through it, allowing for efficient respirable micro reactors (Tian et al., 2013). The environment in this respirable bioreactor made the growth of aerobic cell more rapidly than that through the traditional way, in the McCartney bottle with shaking incubation. These studies show that the unique structure of liquid marble

provides unexpected advantages over the traditional methods in facilitating biological processes.

In order to explore the full capability of using liquid marble as micro reactors, a wide range of the liquid marble properties must be further investigated. These properties include the movement of liquid marbles as reactant reservoirs; the marble shell compatibility with reactant contained by the liquid marble; and the mass, charge, and energy transport abilities between liquid marbles. It is generally known that stimulations by electric current or potential can be used as a means to manipulate biochemical and biological processes. For this reason, charge transportation between liquid marbles driven by electrochemical processes attracts our attention. The ability to use liquid marbles to transport electric charge between liquid marbles is the first step to the future design of liquid marble micro reactors with functions of generating electric current or potential as the reaction control and monitoring mechanisms. In this study we formed a Daniell cell with liquid marbles and used this micro reactor to investigate the continuous sample flow through liquid marble and sample mixing conditions inside a liquid marble. We envisage that the ability to transport electric charge between liquid marbles will lead to the possible material transport, driven by external electric potential, between liquid marbles for filtration and separation applications in future.

## 2. Experimental section

A liquid marble Daniell cell was used to demonstrate the conversion of chemical energy into electric energy and the transport of electric charges between liquid marbles. A Daniell cell consists of two half cells of  $\text{Zn(s)}|\text{ZnSO}_4$  ( $\alpha_1$ , M) and  $\text{Cu(s)}|\text{CuSO}_4$  ( $\alpha_2$ , M). Zinc and Copper electrodes are immersed in zinc sulfate and copper sulfate solutions, respectively. A salt bridge connects the two half cells to enable the continuity of the electric current flow. Fig. 1(a) shows a typical Daniell cell, ([http://commons.wikimedia.org/wiki/File:Galvanic\\_Cell.Svg](http://commons.wikimedia.org/wiki/File:Galvanic_Cell.Svg)) while Fig. 1(b) illustrates our design of a liquid marble micro Daniell cell. John Frederic Daniell invented the Daniell cell in 1836; one of his original ideas was to eliminate the generation of  $\text{H}_2$  gas by a Voltaic pile. This property of the Daniell cell is well suited for the liquid marble micro Daniell cell, since gas generation may compromise the integrity of the marbles.

Two 50  $\mu\text{L}$  droplets of 0.1 M solutions of copper sulfate and zinc sulfate (both are of AR, Sigma-Aldrich) were rolled over a bed of Polytetrafluoroethylene powder (100  $\mu\text{m}$ , Sigma-Aldrich), respectively, to form two liquid marbles. A 0.2 mm copper wire and a 0.2 mm zinc wire (purity > 99%) were used as electrodes and inserted into the copper sulfate and zinc sulfate marbles, respectively, to form two half cells. An agar salt bridge was prepared to provide electric connection between the two liquid marble half

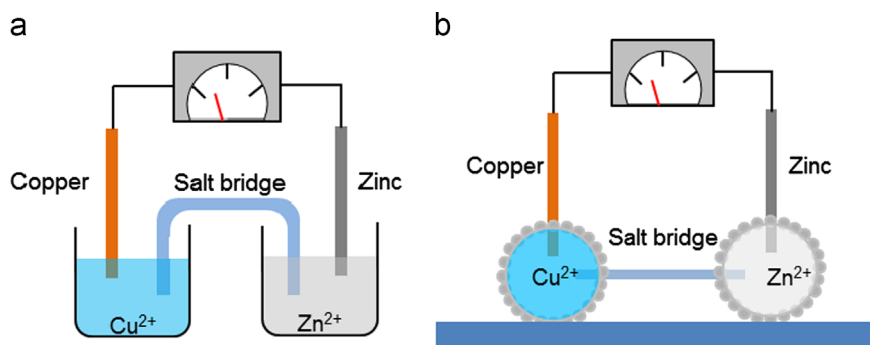


Fig. 1. Schematic of a typical “solutions-in-beakers” Daniell cell (a), ([http://commons.wikimedia.org/wiki/File:Galvanic\\_Cell.Svg](http://commons.wikimedia.org/wiki/File:Galvanic_Cell.Svg)) and a liquid marble micro Daniell cell (b).

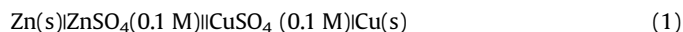
cells. The salt bridge was made by first heating a mixture of 3% agar in 1 M KNO<sub>3</sub> (w/v) to prepare the agar salt solution. The heated agar salt solution was then filled into a polyethylene tube of 1 mm inner diameter and allowed to cool to room temperature in the tube to form gel. The salt bridge was then put onto a support of suitable height. The two ends of the salt bridge were then inserted into the copper sulfate and the zinc sulfate liquid marbles, respectively, forming a micro liquid marble Daniell cell (Fig. 1(b)). As a comparison, the traditional Daniell Cell made in beakers (Fig. 1(a)) was also formed. The same electrolyte solution, salt bridge and electrode were used in this cell.

To demonstrate the use of a liquid marble as a realistic micro reactor, two micro syringe pumps were used to introduce and withdraw electrolyte solutions from one of the liquid marbles of the Daniell cell. When the two pumps were set at the same flow rate (2  $\mu$ L/s), the size of the liquid marble was kept constant and the electrolyte solution flowed through the marble continuously. From measuring the potential variation of the Daniell cell, an experimental evaluation of the sample mixing condition inside the marble was obtained. The data of potential variation measured per second was recorded by a portable data acquisition module (ADVANTECH, USB-4711 A). Mathematical modeling of the sample mixing process was employed to understand the results of the experimental Daniell cell potential change and the solution mixing condition inside the liquid marble.

### 3. Results and discussions

#### 3.1. Liquid marble Daniell cell potential and charge transport between liquid marbles

The liquid marble Daniell cell can be written as:



The potential of the liquid marble Daniell cell and the current flow through the cell from the cathode to anode was measured using a multimeter (LG, Korea) and was compared with the standard Daniell cell potential, which was calculated using the Nernst Eq. (2), as well as with a Daniell cell formed using beakers shown in Table 1. The calculation of the cell potential also

considers the ion activity coefficient and the Debye–Hückel equation (Eq. (3)) was used Debye and Hückel (1923)

$$E_{\text{Cell}} = E_{\text{Cu}^{2+}/\text{Cu}}^{\ominus} - E_{\text{Zn}^{2+}/\text{Zn}}^{\ominus} + \frac{RT}{nF} \ln \frac{a_{\text{Cu}^{2+}}}{a_{\text{Zn}^{2+}}} \quad (2)$$

$$\ln \gamma_i = -0.509 Z_i^2 \sqrt{I} \quad (3)$$

where  $E_s$ : Standard potential of Daniell cell (1) calculated by the Nernst equation;  $E_b$ : measured potential of Daniell cell (1) made with the electrolyte solutions in beakers (Fig. 1 (a));  $E_m$ : Potential of the liquid marble micro Daniell cell (1).

The effect of liquid marble size on cell potential was investigated. The liquid droplet volumes ranged from 30  $\mu$ L to 100  $\mu$ L are appropriate for making liquid marble cell. This is because that it is difficult to fit the salt bridge and an electrode to a liquid marble smaller than 30  $\mu$ L, whereas liquid marble greater than 100  $\mu$ L loses its spherical shape due to gravity. The electric potentials of Daniell cell (1) formed by liquid marbles of the sizes of 30, 50, 80 and 100  $\mu$ L were tested, the potential difference fell in narrow range of  $\pm 0.006$  V compared with the value reported in Table 1.

The potential of the Daniell cell formed using beakers is the sum of the electrode potentials and the potentials at the interface between the solution and salt bridge; it is therefore slightly different from the standard Daniell cell potential calculated by the Nernstian equation, which does not consider the latter. The potential of the liquid marble Daniell cell ( $E_m$ ) is closely comparable with that of the Daniell cell formed using beakers ( $E_b$ ). This indicates that electric charge transport between the two liquid marble half-cells can be facilitated by the salt bridge and liquid marbles can be used to form electric cells and micro electrochemical reactors. To visually demonstrate the electric charge transport, we used liquid marble Daniell cells to build a battery to power an LED. Since the potential of one liquid marble cell is less than 1.1 V, three cells (4) were connected in series to form a battery pack that has a potential of higher than 3 V.



A schematic of the battery system which is formed with three liquid marble cells is illustrated in Fig. 2(a). The actual liquid marble battery system is shown in Fig. 2(b) the copper electrode of one liquid marble is connected with the zinc electrode of the next liquid marble. An LED is connected to the liquid marble battery series and turned on.

Further investigation of liquid marble Daniell cells was carried out by varying the electrolyte concentrations of each liquid marble. In the first study, we monitored the potential and current change of a liquid marble Daniell cell (5) as a function of the concentration of ZnSO<sub>4</sub> solution (varied from 0.005 to 0.5 M), whilst the concentration of

**Table 1**  
Comparison of potentials of different Daniell cells with the standard Daniell cell potential calculated by the Nernst equation.

Potential (V)	$E_s$	$E_b$	$E_m$
	1.100	$1.091 \pm 0.002$	$1.085 \pm 0.004$

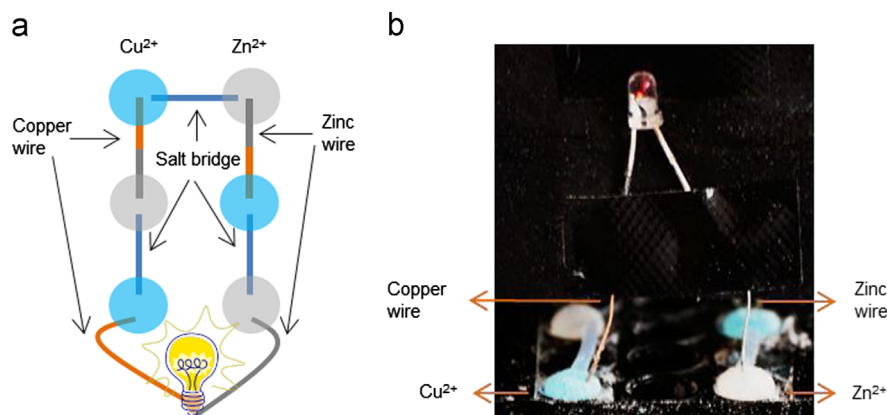


**Fig. 2.** (a) Schematic of a battery pack formed by liquid marble Daniell cells; (b) LED powered by the liquid marble battery pack.

CuSO<sub>4</sub> solution was held constant at 0.1 M. The potential and current changes of the liquid marble Daniell cell was compared with the potential changes of Daniell cell made using beakers.

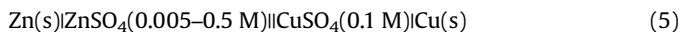


Fig. 3 shows the potential (a) and current (b) variations as functions of the Zn<sup>2+</sup> concentration in the Daniell cell (5) formed with liquid marbles (triangle points) and with beakers (circular points), respectively. Error bars of each data point were calculated from 8 parallel measurements of 8 cells. Numerical data of cell potentials, currents, standard deviation and standard error of the measurements can be found in the supporting information. The data show that both the cell potential and current increased as the Zn<sup>2+</sup> concentration increased from 0.005 to 0.2 M, but dropped slightly as the Zn<sup>2+</sup> concentration further increased to 0.5 M. This is possibly due to a large change of the ionic activity of Zn<sup>2+</sup> in high concentration ZnSO<sub>4</sub> solutions.

The potential and current change of a liquid marble Daniell cell (6) was also monitored as a function of the concentration of CuSO<sub>4</sub> solution (varied from 0.005 to 0.5 M), while the concentration of ZnSO<sub>4</sub> solution was held unchanged at 0.1 M.

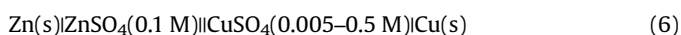


Fig. 4 shows the potential (a) and current (b) variations as functions of the Cu<sup>2+</sup> concentration variation of the Daniell cell (6) formed with liquid marbles and with beakers, respectively. Error bars of each data point were also calculated from 8 parallel measurements of 8 cells and numerical data are presented in ESI.

A major difference between cell (6) and cell (5) was that the potential and current of cell (6) increase monotonically as the Cu<sup>2+</sup> concentration increased from 0.005 to 0.500 M. This is most likely due

to the ionic activities of Cu<sup>2+</sup> in high concentration CuSO<sub>4</sub> solutions being different from the ionic activities of Zn<sup>2+</sup> in high concentration ZnSO<sub>4</sub> solutions. Data comparison of cell potentials and currents of cell (5) and cell (6) indicates that there is no significant difference between the Daniell cells formed by liquid marbles and by beakers.

### 3.2. Sample flow control in liquid marble micro reactor

The ability to control the inward and outward sample flows will enable liquid marbles to be used as a realistic micro reactor. Here we demonstrate the use of liquid marble Daniell cell as a micro reactor to monitor the sample flow into and out of a liquid marble. Through monitoring the potential variation of the liquid marble Daniell cell, a preliminary evaluation of the sample mixing condition inside a liquid marble micro reactor can be obtained.

A micro syringe pump was used to pump water and 0.5 M CuSO<sub>4</sub> solution into the CuSO<sub>4</sub> marble of the Daniell cell (4) in alternation at a rate of 2 μL/s; another micro syringe pump withdrew the solution from the CuSO<sub>4</sub> marble at the same pumping rate so that the size of the CuSO<sub>4</sub> marble was kept unchanged. In this process the concentration of ZnSO<sub>4</sub> in the ZnSO<sub>4</sub> marble was kept unchanged at 0.1 M and the ZnSO<sub>4</sub> liquid marble was kept in a sealed container to prevent the concentration change of ZnSO<sub>4</sub> due to water evaporation. The whole experimental setup is illustrated in Fig. 5(a).

The Daniell cell (4) showed a potential of 1.09 V; the cell potential oscillates around 1.09 V as one syringe pump introduced the 0.5 M CuSO<sub>4</sub> solution into the CuSO<sub>4</sub> marble, while the other pump withdrew of the solution out of the marble at the same rate. In this process the amplitude of potential oscillation was ~0.01 V. At 250 s after the experiment began, the introduction of CuSO<sub>4</sub> to

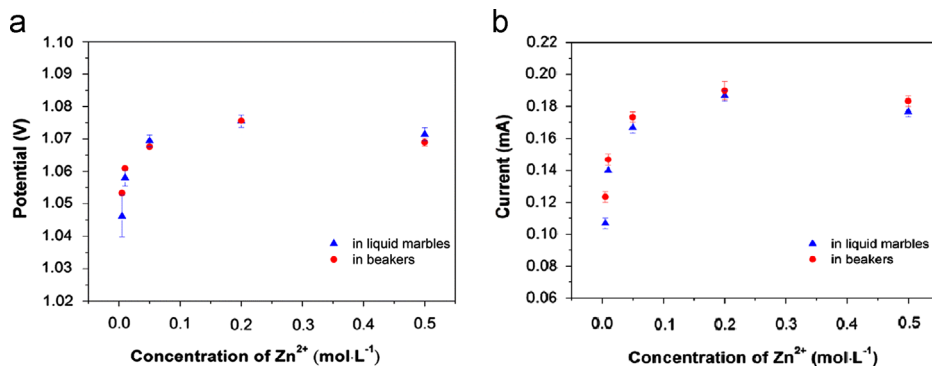


Fig. 3. Potential (a) and current (b) variations of Daniell cell (5) formed with liquid marbles (triangle points) and with beakers (circular points), error bars were calculated from 8 parallel measurements (see ESI).

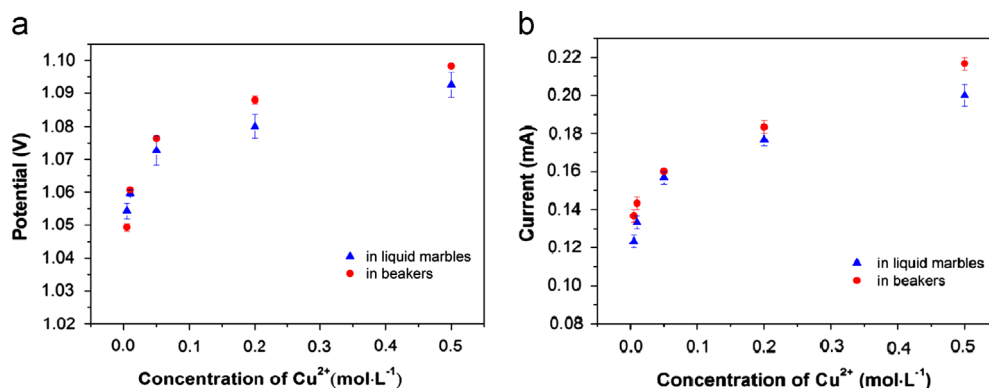
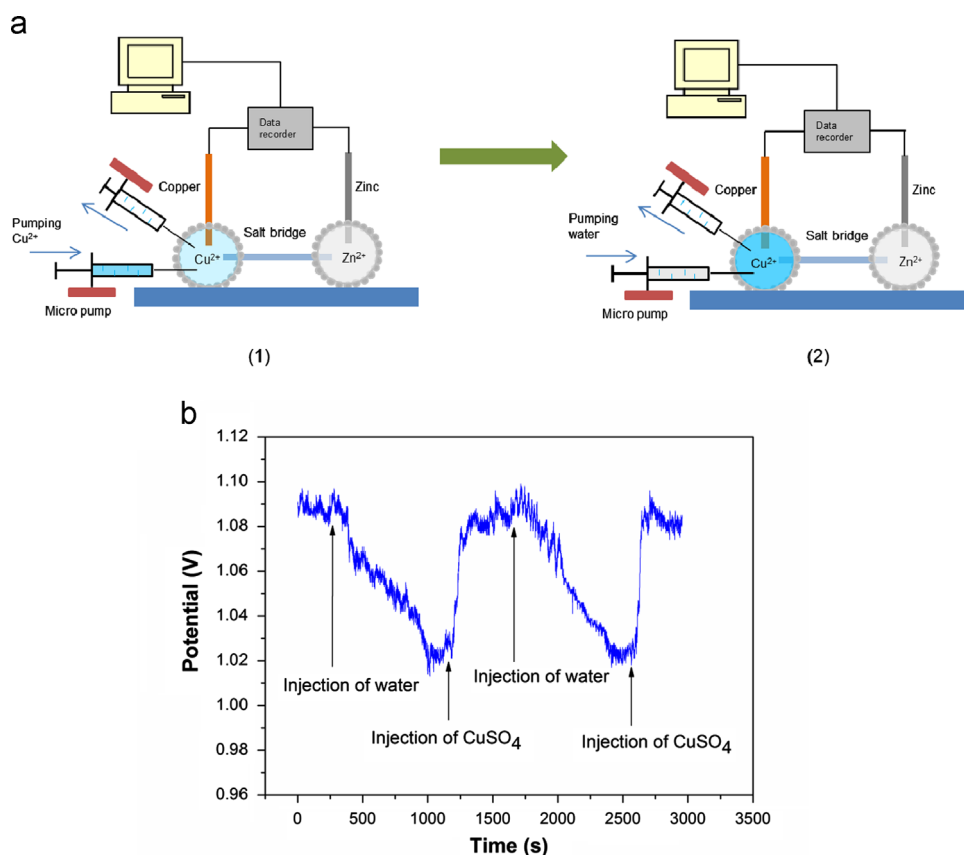


Fig. 4. Potential (a) and current (b) variations of Daniell cell (6) formed with liquid marbles (triangle points) and with beakers (circular points), error bars were calculated from 8 parallel measurements (see ESI).



**Fig. 5.** (a) Experimental set up of sample flow in out of a liquid marble holding  $\text{CuSO}_4$  solution: (1) water is introduced into the liquid marble containing 0.5 M  $\text{CuSO}_4$  while the mixed solution is withdrawn from the liquid marble by two micropumps with the same rate of 2  $\mu\text{L/s}$ ; (2) 0.5 M  $\text{CuSO}_4$  is then pumped into the same liquid marble while the mixed solution is withdrawn from the liquid marble. (b) Potential variation of liquid marble Daniell cell through the entire pumping process of two cycles.

the  $\text{CuSO}_4$  marble was stopped and was replaced with the introduction of water. As water was pumped into the  $\text{CuSO}_4$  marble, the potential of the Daniell cell began to drop from 1.09 V, and reached a flat-bottom valley of around 1.025 V after 750 s (Fig. 5(b)). Further introduction of water did not cause further decreases of cell potential. By using the Nernst equation and the standard Nernst Potential  $E_s$  of the cell (Table 1), the  $\text{Cu}^{2+}$  concentration in the  $\text{CuSO}_4$  marble can be calculated. However, since the use of Nernst equation for cell potential calculation may be affected by the presence of interface potential between the solution and salt bridge, calculation error is unavoidable. We expect, however, that using the measured liquid marble potential  $E_m$  in Table 1 to calculate the  $\text{Cu}^{2+}$  concentration in the  $\text{CuSO}_4$  marble is justifiable and would minimize potential error. This calculation thus gives the  $\text{Cu}^{2+}$  concentration in the  $\text{CuSO}_4$  marble to be  $1.99 \times 10^{-4}$  M.

From 200 s after the cell potential reached the valley, the solution introduction was switched back to 0.5 M  $\text{CuSO}_4$ . The cell potential recovered much more rapidly initially compared with its decrease when water was introduced. After around 100 s of rapid increase, the cell potential increase slowed down and after a further 400 s the potential reached the level before the introduction of water. A repeat of such a cycle was performed and the results showed the pattern of potential change was reproducible.

A simple mathematical simulation was conducted to get a preliminary sample mixing appraisal inside the marble. The simulation considered a fixed-volume reactor with one solution inlet and one outlet. The reactor was fed with a 0.5 M  $\text{CuSO}_4$  solution; the inlet solution was assumed to have instantaneous mixing with the solution inside the marble. The mixed solution was withdrawn from the reactor via the outlet at the same flow

rate as that of the inlet; this ideal solution flow system was used to simulate the potential changes of the liquid marble Daniell cell as a function of time.

Eq. (7) describes the  $\text{Cu}^{2+}$  mass flow rate; integration of Eq. (7) leads to the concentration of  $\text{Cu}^{2+}$  as a function of time,  $\text{Cu}^{2+}(t)$ , in the  $\text{CuSO}_4$  marble (Eq. (8)). By Substituting Eq. (8) into the Nernst equation, a relationship of cell potential as a function of time (Eq. (9)) is obtained.

$$\frac{dm(\text{Cu}^{2+})}{dt} = c(\text{Cu}^{2+})_{en} \nu_{en} - \frac{m(\text{Cu}^{2+})}{V_{mar}} \nu_{ex} \quad (7)$$

$$c_{\text{Cu}^{2+}}(t) = \frac{\frac{c(\text{Cu}^{2+})_{en} \nu_{en} V_{mar}}{\nu_{ex}} - e^{\frac{-(t-A)\nu_{ex}}{V_{mar}}}}{V_{mar}} \quad (8)$$

$$E(t) = E^\circ \left( \frac{\text{Cu}^{2+}}{\text{Cu}} \right) + \frac{RT}{nF} \ln c_{\text{Cu}^{2+}}(t) - E^\circ \left( \frac{\text{Zn}^{2+}}{\text{Zn}} \right) - \frac{RT}{nF} \ln c_{\text{Zn}^{2+}} \quad (9)$$

where  $m(\text{Cu}^{2+})$  is mass of  $\text{Cu}^{2+}$  in the liquid marble;  $c(\text{Cu}^{2+})_{en}$  is concentration of  $\text{Cu}^{2+}$  of the inlet solution into the liquid marble;  $\nu_{en}$  and  $\nu_{ex}$  are volume flow rates of the inlet and outlet solutions, respectively;  $V_{mar}$  is the volume of the liquid marble; A is constant resulted from the integration.

A plot of the liquid marble Daniell potential as a function of time using Eq. (9) is shown in Fig. 6. This plot simulates two cycles of changing inlet solution from water to 0.5 M  $\text{CuSO}_4$  at the flow rate of 2  $\mu\text{L/s}$ . At time = 0, reactor contained 0.5 M  $\text{CuSO}_4$  solution; as water is added into the reactor the Daniell cell, potential decreases linearly with time from 1.09 V to 1.02 V; this is in good qualitative agreement with the experimental result, although the slopes of the simulation and experimental curves differ



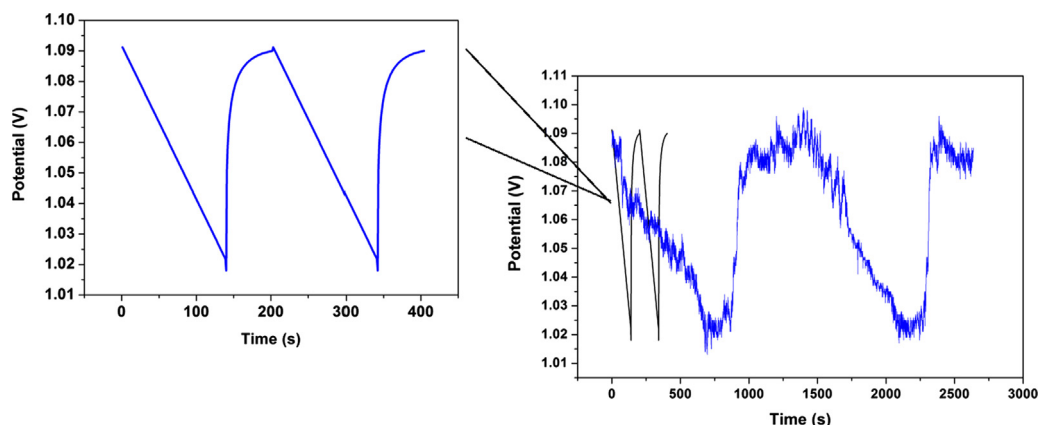


**Fig. 6.** Mathematical simulation of sample mixing appraisal inside the liquid marble: a plot simulation of the liquid marble Daniell potential as a function of time obtained from the Nernst equation (Eq. (9) overlaid by the experimental data).

significantly, which will be discussed below. From the simulation equations, the linear decrease in cell potential with time only occurs when the  $\text{Cu}^{2+}$  concentration of the inlet solution is zero. Simple manipulations of Eqs. (7)–(9) will lead to a relationship shown in Eq. (10), given that  $v_{en}=v_{ex}$ :

$$E(t) = A' + \frac{RT}{nF} \ln \left[ c(\text{Cu}^{2+})_{en} + e^{-(t+A)/V_{mar}} \right] \quad (10)$$

In the beginning of the cycle the inlet solution is water and  $c(\text{Cu}^{2+})_{en}$  equals to zero; Eq. (10) shows that this condition leads the cell potential to decrease linearly with time. When the inlet sample was switched from water to the 0.5 M  $\text{Cu}^{2+}$  solution, the variable of the natural logarithm term in Eq. (10) underwent a step change— $c(\text{Cu}^{2+})_{en}$  was abruptly changed from 0 to 0.5 M. This step change of the concentration caused a rapid recovery of the potential in the beginning of the change of  $c(\text{Cu}^{2+})_{en}$  to 0.5 M. Since  $c(\text{Cu}^{2+})_{en} \neq 0$ , the cell potential change with time is linear and the exponential function becomes dominant only as time increases (Eq. (10)).

The qualitative agreement of the experiment result with the mathematical simulation shows that sample mixing inside the liquid marble has occurred. Two points require further comments. First, because of the small size of the liquid marble, the position of the electrode is unavoidably very close to the inlet and outlet solutions. The electrode potential therefore shows significant oscillation, which may be caused by disturbance of the electric double layer around the electrode. Second, the much longer experimental cycle compared to the simulation indicates that sample mixing inside liquid is not instantaneous (Liu and Vecitis, 2012). The concentration of  $\text{Cu}^{2+}$  at sample inlet is expected to be quite different from that at locations close to the shell of the marble. For this reason, the  $c(\text{Cu}^{2+})_{ex}$  is expected to be higher than the simulation value, which is based on the assumption of instantaneous mixing. This is likely the major factor responsible for the much slower experimental sample mixing result than the simulation. Because of the slow sample flow rate, sample mixing inside liquid marble is likely to be dependent considerably upon diffusion. The simulation work provides a preliminary understanding of mass transfer and mixing conditions inside liquid marble; this understanding will trigger further engineering ideas to improve the sample mixing which is useful for the future applications using liquid marbles as a micro reactor.

#### 4. Conclusion

In this study we demonstrated the electric charge transport between liquid marbles by forming a Daniell cell using liquid marbles

and a salt bridge. Charge transport is a relevant property for using liquid marbles to build micro reactors. Only microlitres of electrolytes are required to construct a Daniell cell and a battery pack that can power a LED. The potential and current of the liquid marble Daniell cell are in good agreement with that of the Daniell cell formed with  $\text{CuSO}_4$  and  $\text{ZnSO}_4$  solutions in beakers. Our investigation also showed that the potential of the liquid marble Daniell cell can be used to monitor the change in  $\text{Cu}^{2+}$  concentration in the liquid marble. With this idea in mind, we set up a system that provides a continuous flow of  $\text{Cu}^{2+}$  solutions of different concentrations through the  $\text{CuSO}_4$  marble of the Daniell cell and monitored the cell potential by measuring the Daniell cell potential; the results obtained were used as the preliminary evaluation of the sample mixing condition inside a liquid marble. Mathematical modeling shows that sample mixing inside a liquid marble caused by the continuous flow of sample solutions is not instantaneous, but the pattern of sample concentration change inside the marble under the continuous sample flow follows the pattern of mathematical modeling. This study provides the first insights of charge transportation, liquid flow and mixing behavior inside liquid marbles. These insights are useful for designing future liquid marble micro reactors for biochemical and biological applications.

#### Acknowledgment

Australian Research Council funding (DP1094179) is gratefully acknowledged. ML JT and LL would like to thank Monash University and the Faculty of Engineering for their postgraduate scholarships.

#### Appendix A. Supplementary Information

Supplementary data associated with this article can be found in the online version at <http://dx.doi.org/10.1016/j.ces.2013.04.003>.

#### References

- Arbatan, T., Shen, W., 2011. *Langmuir* 27, 12923.
- Arbatan, T., Li, L., Tian, J., Shen, W., 2012a. *Adv. Healthcare Mater.* 1, 80.
- Arbatan, T., Al-Abboodi, A., Sarvi, P.P.Y.C., Shen, W., 2012b. *Adv. Healthcare Mater.* 1, 467–469.
- Aussillous, P., Quéré, D., 2001. *Nature* 411, 924.
- Aussillous, P., Quéré, D., 2006. *Proc. R. Soc. London, Ser. A* 462, 973.
- Bajwa, A., Xu, Y., Hashmi, A., Leong, M., Ho, L., Xu, J., 2012. *Soft Matter* 8, 11604–11608.
- Bangi, U.K.H., Dhare, S.L., Rao, Venkateswara A., 2010. *J. Mater. Sci.* 45, 2944.
- Bormashenko, E., 2011. *Curr. Opinion Colloid Interface Sci.* 16, 266.

- Bormashenko, E., 2012. *Soft Matter* 8, 11018–11021.
- Bormashenko, E., Balter, R., Aurbach, D., 2011. *Int. J. Chem. React. Eng.* 9, S10.
- Bormashenko, E., Musin, A., 2009. *Appl. Surf. Sci.* 255, 6429.
- Bormashenko, E., Pogreb, R., Bormashenko, Y., Musin, A., Stein, T., 2008. *Langmuir* 24, 12119.
- Bormashenko, E., Bormashenko, Y., Musin, A., 2009a. *J. Colloid Interface Sci.* 333, 419.
- Bormashenko, E., Bormashenko, Y., Musin, A., Barkay, Z., 2009b. *ChemPhysChem* 10, 654.
- Bormashenko, E., Pogreb, R., Whyman, G., Musin, A., 2009c. *Colloids Surf. A* 351, 78.
- Bormashenko, E., Bormashenko, Y., Pogreb, R., Gendelman, O., 2011. *Langmuir* 27, 7.
- Bormashenko, E., Pogreb, R., Musin, A., 2011b. *J. Colloid Interface Sci.* 366, 196.
- Dandan, M., Erbil, H.Y., 2009. *Langmuir* 25, 8362.
- Debye, P., Hückel, E., 1923. The theory of electrolytes. I. Lowering of freezing point and related phenomena. *Phys. Z.* 24, 185–206.
- Dupin, D., Armes, S.P., Fujii, S., 2009. *J. Am. Chem. Soc.* 131, 5386.
- Figure was adapted from the original diagram from Wikimedia: ([http://commons.wikimedia.org/wiki/File:Galvanic\\_Cell.Svg](http://commons.wikimedia.org/wiki/File:Galvanic_Cell.Svg)).
- Fujii, S., Kameyama, S., Armes, S.P., Dupin, D., Suzuki, M., Nakamura, Y., 2010. *Soft Matter* 6, 635.
- Gao, L., McCarthy, T.J., 2007. *Langmuir* 23, 10445.
- Hapgood, K.P., Farber, L., Michaels, J.N., 2009. *Powder Technol.* 188, 248.
- Liu, H., Vecitis, C.D., 2012. *J. Phys. Chem. C* 116, 374–383.
- McHale, G., Newton, M.I., 2011. *Soft Matter* 7, 5473.
- Newton, M.I., Herbertson, D.L., Elliott, S.J., Shirtcliffe, N.J., McHale, G., 2007. *J. Phys. D: Appl. Phys.* 40, 20.
- Quéré, D., Aussillous, P., 2002. *Chem. Eng. Technol.* 25, 925.
- Rao, A.V., Kulkarni, M.M., Bhagat, S.D., 2005. *J. Colloid Interface Sci.* 285, 413.
- Tian, J., Arbatan, T., Li, L., Shen, W., 2010a. *Chem. Eng. J.* 65, 347.
- Tian, J., Arbatan, T., Li, X., Shen, W., 2010b. *Chem. Commun.* 46, 4734.
- Tian, J., Fu, N., Chen, D., Shen, W., 2013. *Colloids Surf. B* 106, 187–190.
- Yao, X., Gao, J., Song, Y., Jiang, L., 2011. *Adv. Funct. Mater.* 21, 4270.
- Zhang, C., Xu, J., Ma, W., Zheng, W., 2006. *Biotechnol. Adv.* 24, 243.
- Zhao, Y., Fang, J., Wang, H., Wang, X., Lin, T., 2010. *Adv. Mater.* 22, 707–710.

**This page is intentionally blank**



# Paper-based device for rapid typing of secondary human blood groups

Miaosi Li · Whui Lyn Then · Lizi Li · Wei Shen

Received: 26 September 2013 / Revised: 4 November 2013 / Accepted: 6 November 2013 / Published online: 28 November 2013  
© Springer-Verlag Berlin Heidelberg 2013

**Abstract** We report the use of bioactive paper for typing of secondary human blood groups. Our recent work on using bioactive paper for human blood typing has led to the discovery of a new method for identifying haemagglutination of red blood cells. The primary human blood groups, i.e., ABO and RhD groups, have been successfully typed with this method. Clinically, however, many secondary blood groups can also cause fatal blood transfusion accidents, despite the fact that the haemagglutination reactions of secondary blood groups are generally weaker than those of the primary blood groups. We describe the design of a user-friendly sensor for rapid typing of secondary blood groups using bioactive paper. We also present mechanistic insights into interactions between secondary blood group antibodies and red blood cells obtained using confocal microscopy. Haemagglutination patterns under different conditions are revealed for optimization of the assay conditions.

**Keywords** Bioactive paper · Blood typing · Secondary blood groups · Confocal microscopy · Haemagglutination

## Introduction

Blood groups were discovered at the beginning of the twentieth century, and for many years they have been considered the best human genetic markers since they carry a significant amount of information for mapping the human genome. To date, 30 blood group systems, including 328 authenticated blood groups, have been classified [1, 2]. The discovery of the ABO blood groups by Landsteiner made blood transfusion

feasible. The later discovery of the RhD antigens led to the understanding and subsequent prevention of haemolytic disease of the newborn (HDN) [3–5]. Although the ABO and RhD groups are the most important systems in transfusion medicine, many other blood group antibodies are also capable of causing haemolytic transfusion reactions or HDN. These blood groups, known as minor or secondary blood groups, are also of great clinical and biological importance in blood transfusion and transplantation [5, 6]. Each of these blood groups contains unique subtype antigens and has a different weight of distribution in the human population [7]. Furthermore, secondary blood groups do not follow the second part of Landsteiner's law—"If an agglutinin is absent in the red cells of a blood, the corresponding agglutinin must be present in the plasma"—which is true only of the ABO groups. Although antibodies A and B are naturally present in human blood serum corresponding to the antigens which they lack, the Rh and secondary antibodies in serum are generated only as a result of an immunization response triggered by transfused red blood cells (RBCs) that carry secondary antigens, or by fetal RBCs leaking into the maternal circulation during pregnancy or during birth [5]. Table 1 summarizes the common secondary blood groups and their subtype antigens. Among these blood groups, some antibodies, such as M, N, Lewis and Lutheran system antibodies, are inactive below 37 °C and are therefore not considered clinically important [5]. Others, however, are as clinically significant as primary blood groups. The mismatching of these blood groups may cause immediate and severe haemolytic transfusion reactions and HDN.

Accurate and rapid identification of human secondary blood groups is important for blood banking and medical procedures under either laboratory or field conditions [8]. Routine minor blood grouping methods rely primarily on the haemagglutination reactions between antigens and antibodies that are performed either manually or by automatic means

M. Li · W. L. Then · L. Li · W. Shen (✉)  
Department of Chemical Engineering, Monash University,  
Wellington Rd, Clayton, VIC 3800, Australia

**Table 1** Common secondary blood group systems

Secondary blood group systems	Antigens
Rh	D <sup>a</sup> , C, c, E, e
Kell	K, k
P	P <sup>1</sup>
Kidd	Jk <sup>a</sup> , Jk <sup>b</sup>
MNS	M, N, S, s
Lewis	Le <sup>a</sup> , Le <sup>b</sup>
Lutheran	Lu <sup>a</sup> , Lu <sup>b</sup>

\* Group D is one of the blood groups in the Rh system, but it is not considered as a secondary blood group

[9, 10]. Currently, the commonly used method for secondary blood grouping is based on a gel card test procedure, which requires concentrated RBCs and centrifugation [9]. Because there are a large number of antigens in secondary blood groups, a full identification of the antigens in those groups using this procedure is expensive and requires central laboratory conditions. Other methods, such as slide techniques, although of low cost and equipment-free, are insensitive and therefore are not recommended for initial or definitive antigen determinations, particularly when dealing with neonatal samples [5]. Investigations into novel techniques for rapid and low-cost secondary blood group typing diagnostics are therefore necessary and significant, especially for use in less-industrialized areas, for home care, and for local and temporary blood banking in disaster-response missions.

Recent research on the use of bioactive paper for human blood typing has established a new method for identifying haemagglutination of RBCs [11–16] which relies on using fibre networks in paper with controlled pore sizes to filter out and retain the agglutinated RBC lumps. When a blood sample is introduced onto a piece of paper pretreated with the corresponding grouping antibody, haemagglutination will occur, leading to the formation of agglutinated RBC lumps inside the fibre network [17]. The agglutinated lumps of RBCs are captured by the fibre network and cannot be removed by chromatographic elution with phosphate-buffered saline (PBS) or saline solution, leaving a clearly visible bloodstain on the paper. Conversely, if a blood sample is introduced onto paper treated with non-corresponding grouping antibodies, haemagglutination will not occur and free RBCs can be easily washed out of the fibre network, leaving no discernible stain. This phenomenon forms the foundation of using paper to make low-cost, rapid and user-friendly devices for ABO and RhD blood typing assays [16].

The antigens of some secondary blood groups are found to be less antigenic than the primary blood groups [18]. Those antigens show weaker interactions with their corresponding antibodies, resulting in increased difficulty in their identification in blood grouping assays. Different antibodies [e.g. immunoglobulin G (IgG) instead of immunoglobulin M (IgM)]

available to certain secondary RBC group antigens present further difficulties in blood grouping assays. Although the capabilities of IgG and IgM antibodies in the typing of secondary blood groups have been well understood, RBC responses to bonding with those antibodies are not. In this study, we investigate the secondary blood group antibody–RBC interactions in the fibre network of paper for the purpose of designing highly efficient paper-based secondary blood grouping devices. The confocal microscopy method we developed for paper-based blood grouping assays [17] was used to obtain mechanistic details of RBC behaviour in the interactions with secondary blood group antibodies. Our results elucidate (1) the differences in antibody-specific RBC haemagglutination caused by primary and secondary blood group antibodies, (2) the responses of RBCs to bonding with IgG and IgM antibodies, (3) the time-dependent antibody–antigen interactions in secondary blood grouping, and (4) a concept of secondary blood group assay result reporting using symbols. The protocols and conditions of assaying have also been established and are discussed. The outcome of this work provides microscopic details for the engineering of low-cost, sensitive, specific and rapid paper-based blood grouping devices for secondary human blood groups.

## Experimental

### Materials and appliances

The paper substrate used in this study was Kleenex paper towel (Kimberly-Clark, Australia). Alkyl ketene dimer (AKD; wax 88 Konz) as a paper hydrophobization reagent was obtained from BASF. AR grade *n*-heptane was obtained from Sigma-Aldrich (Australia); it was used to formulate an inkjet-printable solution for patterning text on paper through the formation of hydrophobic borders. Blood samples were sourced from Red Cross Australia (Sydney). They were stored at 4 °C and used within 7 days of collection. All antibodies were purchased from Alba Bioscience (Edinburgh, UK). The 0.9 % (w/v) NaCl saline solution and the PBS were prepared with AR grade NaCl (Univar) and phosphate (Sigma-Aldrich), using Milli-Q water. Fluorescein isothiocyanate (FITC; isomer I, product number F7250, from Sigma-Aldrich) was used for labelling RBCs [17, 19, 20]. Anhydrous dimethyl sulfoxide (Merck, Australia) was used to dissolve the FITC. Anhydrous D-glucose was provided by Ajax Finechem (Australia).

A reconstructed Canon inkjet printer (Pixma iP3600) was used to print the AKD–*n*-heptane solution onto a Kleenex paper sheet to form the required patterns defined by the hydrophilic–hydrophobic contrast. A series of micropipettes (Eppendorf Research®, 2.5–50 µL) were used to transfer antibodies, blood samples and saline solutions onto the paper device.

A Nikon Ai1Rsi confocal microscope in the Melbourne Centre for Nanofabrication was used to obtain the confocal micrographs. The objective lens used for imaging was a  $\times 60$  oil immersion lens.

### Symbol patterning onto paper

In our previous work for ABO and RhD blood group tests [16], the fabrication of a paper-based blood grouping device involved patterning letters and symbols as hydrophilic sites for RBC and antibody interactions, surrounded by hydrophobic borders, onto paper. It was done with inkjet printing of AKD onto paper to selectively hydrophobize it. The hydrophobic–hydrophilic contrast allows unambiguously legible text patterns of agglutinated blood to be displayed. Following the international convention, the blood types of the ABO group are reported directly with letters, whereas Rh and other secondary blood groups are reported with the symbol “+” or “-” to indicate either their presence or their absence in RBCs. In this work, for patterning paper for secondary blood grouping, we used “+” and “-” to indicate either a positive or a negative assay result. The symbol consists of a vertical hydrophilic channel and an overlapping horizontal bar printed with water-insoluble ink, as shown in Fig. 1.

An assay for identifying multiple secondary blood groups was performed by introducing 2.5  $\mu\text{L}$  of the corresponding antibodies onto the vertical section of the symbols, and allowing the antibodies to dry under ambient conditions. Two and half microlitres of a blood sample was then introduced onto the vertical channel of all the symbols; a predetermined reaction time was allowed for the antibodies to interact with the RBCs. Subsequently, two 30- $\mu\text{L}$  aliquots of saline solution were introduced onto the vertical section of the cross symbol to wash out the non-agglutinated RBCs.

After washing, the results can be directly read from the device—“+” indicating positive and “-” indicating negative.

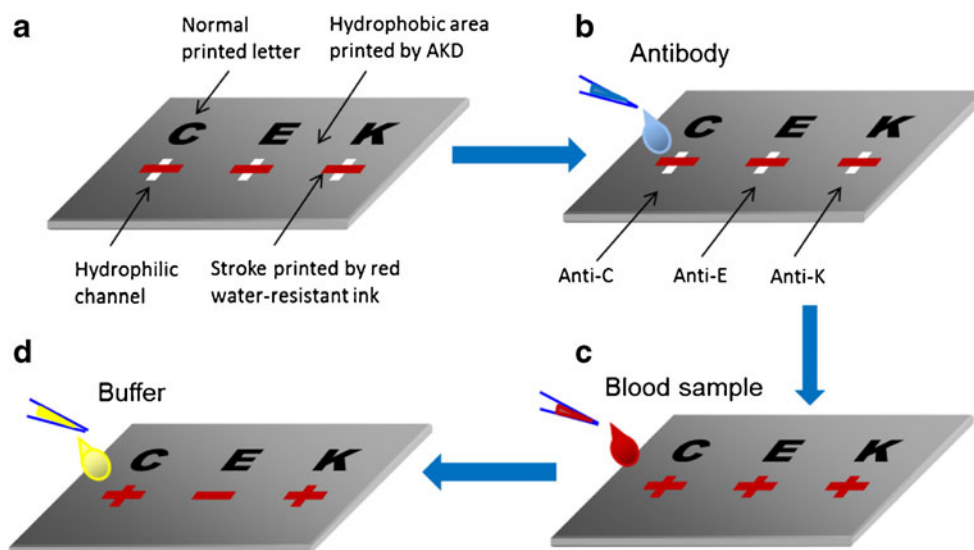
For confocal imaging, RBCs were labelled with FITC using the method reported by Li et al. [17], Hauck et al. [19] and Hudetz et al. [20]. The whole blood sample was first centrifuged at 1,300g relative centrifugal force for 3 min to separate the RBCs from the plasma. The plasma layer was then removed and the RBC layer was washed once with physical saline solution (PSS). FITC was dissolved in dimethyl sulfoxide at a high concentration (40 mg/mL), and was then diluted with CellStab solution to 0.8 mg/mL. This FITC solution and a D-glucose solution in PBS were then added to the RBCs until the concentrations of FITC and D-glucose reached 0.5 mg/mL and 0.4 mg/mL, respectively. This RBC suspension was then incubated in the dark for 2 h to allow FITC to attach onto the cell surface. After incubation, the RBC suspension was washed 13 times with PSS to remove unattached FITC and the RBCs were then resuspended at a haematocrit of around 35 % for further use.

Kleenex paper towel was cut into 10 mm  $\times$  10 mm pieces for use as the test substrate. Ten microlitres of antibody solution was dropped onto paper pieces and allowed to dry, and then 6  $\mu\text{L}$  of labelled RBCs was dropped onto them. A preset reaction time was allowed. Then, 20  $\mu\text{L}$  of PSS was pipetted onto the sample and the sample was immediately placed onto a glass slide for confocal imaging.

### Results and discussion

Following the testing procedure illustrated in Fig. 1, a number of secondary blood groups can be assayed on a paper strip; the typical assay results of one blood sample are shown in Fig. 2 by putting the assay papers together. Gel card tests of the same

**Fig. 1** Design, fabrication, testing procedures and result reporting of paper diagnostics for secondary blood group typing. AKD alkyl ketene dimer



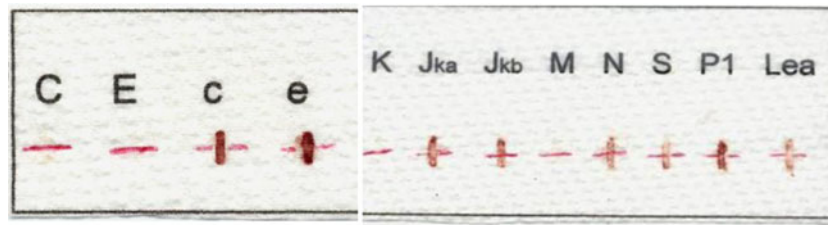


**Fig. 2** Paper-based blood group assay designed for identifying 12 antigens in six secondary blood group systems. The blood grouping assay was performed under the same conditions: the reaction time was 30 s and the washing of free red blood cells (RBCs) was done using 0.9 % NaCl

physical saline solution. Reference assays using mainstream technology (gel card) showed that the secondary blood group systems of this blood sample were C(-), E(-), c(+), e(+), K(-), Jka(+), Jkb(+), M(+), N(+), S(+), P1(+), and Lea(+)

blood sample performed in the laboratory of Red Cross Australia were used to compare the results with the results obtained using our paper-based assays.

Two observations can be made. First, with the exception of blood group M, the secondary blood grouping results reported by our paper-based assays matched the gel card results. Second, like the gel card tests, where the clarity of the results of secondary blood groups is less consistent than that of primary blood groups, on paper-based assays the colour intensity of antigen-positive RBCs differs significantly despite all tests being conducted under the same conditions. These results suggest that paper-based sensors are capable of performing assays for secondary blood grouping, and the reaction conditions of secondary blood group antigens and antibodies differ. To further understand the antigen–antibody interactions of secondary blood groups, and to optimize the assay conditions, we focused on the influence of the following factors on RBC agglutination: the antibody–antigen reaction time, antibody types, and washing conditions. Microscopic information obtained with confocal microscopy was compared with information obtained from the visual assays to study the interactions of RBCs in paper.

#### The effect of the interaction period

The bonding of ABO and RhD antigens with their corresponding antibodies normally occurs instantaneously [16]; therefore, haemagglutination can be visually identified within 30 s [17]. This reaction time, however, is not sufficient for some secondary blood group antigens as they are less antigenic. As a result, the time required for secondary blood group agglutinations to

be visually identifiable ranges from 30 s to 3 min, depending on the antibody–antigen pair. For example, blood groups C and E have strong interactions with their corresponding antibodies within 30 s, whereas blood groups c and e would show false-negative results if the same interaction time of 30 s were allowed. We found that longer interaction times (i.e. 2–3 min) must be allowed for secondary blood groups to improve the clarity of the results (Fig. 3). However, a prolonged reaction time can lead to false-positive results, as excessive exposure of a blood sample to the atmosphere causes aggregation of RBCs. Our study showed that a reaction time up to 3 min is appropriate and adequate for the unambiguous identification of the weaker haemagglutinations.

Confocal microscopy was used to gain a microscopic understanding of haemagglutination processes of RBCs carrying secondary blood group antigens. For comparison, haemagglutination of RBCs by corresponding primary and secondary blood group antibodies was investigated to show the differences in the strength of RBC agglutination. Figure 4 shows four confocal microscopy images taken with a  $\times 60$  oil immersion lens. RBCs carrying D(+) (primary) and E(+) (secondary) antigens showed rapid agglutination within 30 s after contact with their corresponding antibodies. RBCs carrying primary blood group D antigens interacted strongly with their corresponding antibodies, leading to strong deformation of RBCs, which formed large lumps; individual RBCs in the lump could not be identified (Fig. 4a). RBCs carrying secondary blood group E antigens showed weaker agglutination than the RBCs carrying group D antigens. Although E(+) RBCs also formed lumps on reacting with the E antibody, cell

**Fig. 3** Increasing degrees of haemagglutination of secondary blood group e in antibody-treated paper as a function of time

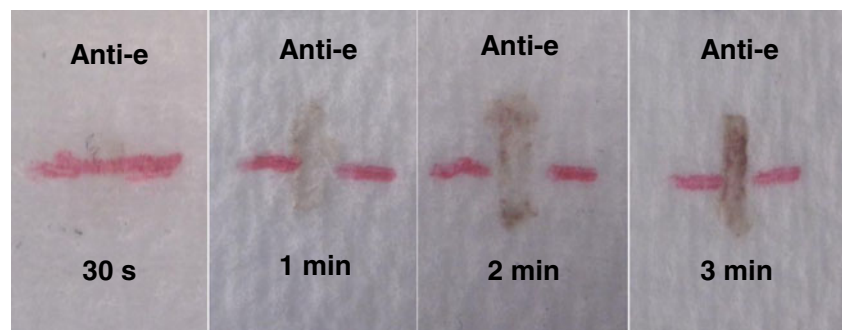
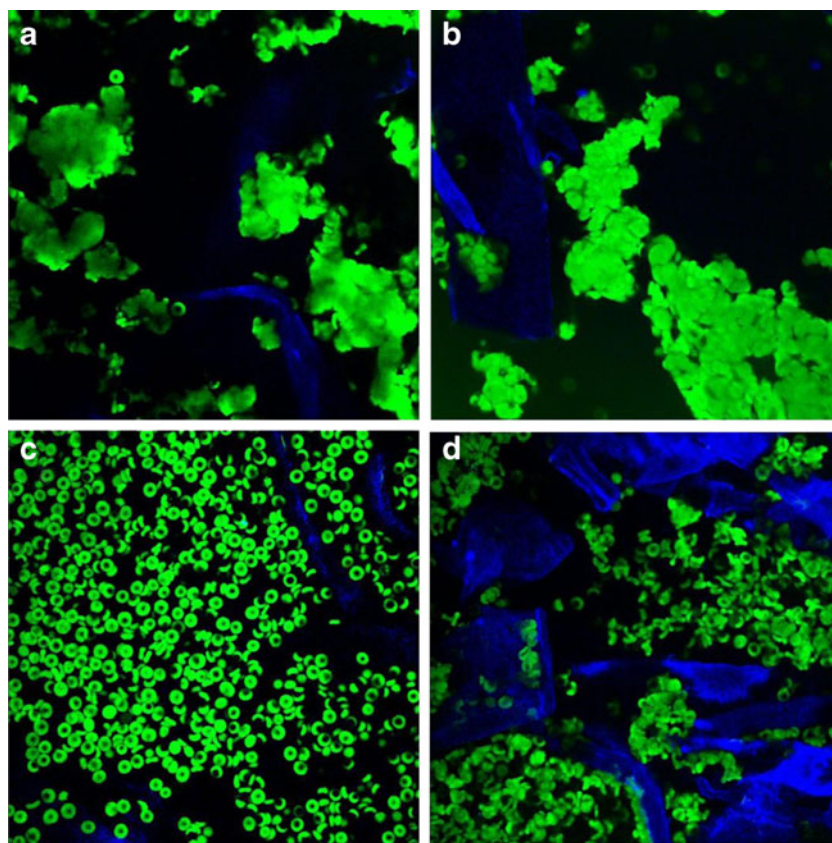




**Fig. 4** Haemagglutination behaviour of three blood groups investigated by confocal imaging ( $\times 60$  oil immersion lens): **a** RBCs of primary blood group D(+) agglutinated by D antibodies within 30 s; **b** RBCs of secondary blood group E(+) agglutinated by E antibodies within 30 s; **c** RBCs of secondary blood group e(+) did not show any sign of agglutination after reacting with e antibody for 30s; **d** blood group e(+) RBCs showed clear agglutination when reacting with e antibody for 3 min



deformation was less severe than that of the D(+) RBCs (Fig. 4b). The e(+) RBCs showed even weaker agglutination; no agglutination was observable for 30 s of reaction time (Fig. 4c). However, when 3 min of reaction time was allowed, the e(+) RBCs clearly showed agglutination, even though the degree of agglutination was much weaker than for RBCs of the D(+) and E(+) groups (Fig. 4d). These results correlate with the visual assays performed on paper (Fig. 3). More importantly, the confocal microscopy results confirmed the time-dependent haemagglutination reaction of some secondary blood groups. Table 2 summarizes the reaction time required by different secondary blood groups.

#### The effect of antibody structure

Although some commercial antibodies for secondary blood grouping can easily identify the corresponding secondary blood group antigens through RBC haemagglutination, others

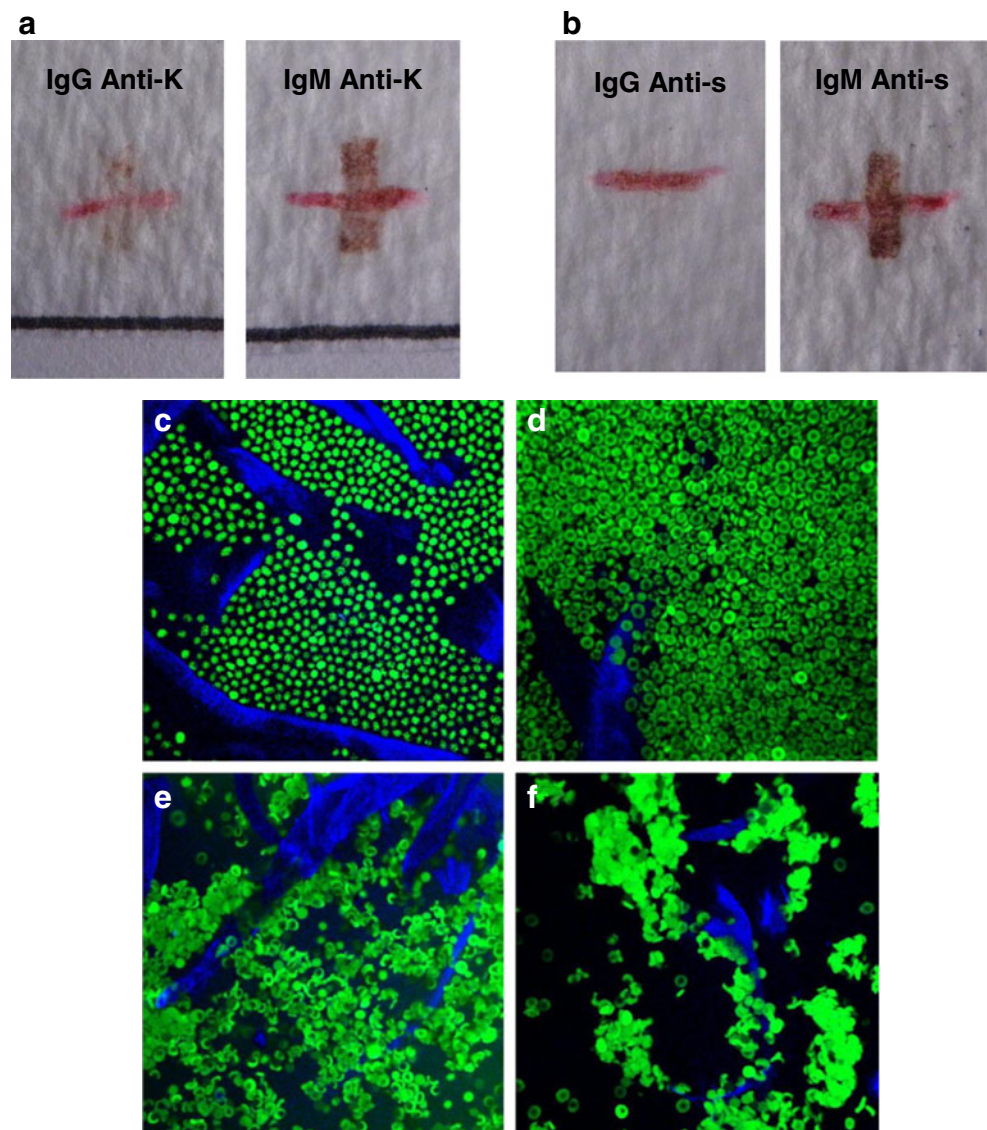
cannot. This is partially due to the structure of antibodies; the IgM and IgG antibodies show a strong performance contrast in causing haemagglutination of RBCs. The commercial products of IgM are monoclonal immunoglobulin which has a pentameric form; each monomer has two binding sites, and IgM therefore has ten sites in total. IgG antibodies, however, are monomers with only two binding sites in total. The molecular dimension of an IgM molecule is also greater than that of an IgG molecule, being 30 nm and 14 nm, respectively [5]. Consequently, the distance between the two binding sites of an IgG molecule is too small to allow it to simultaneously bind with antigens on two RBCs and cause direct agglutination. Generally, IgM antibodies will directly agglutinate antigen-positive RBCs, whereas most IgG antibodies require potentiators or anti-human globulin to effect agglutination [5].

For secondary blood grouping on paper, the IgM antibodies can simultaneously bind to antigens on two RBCs, thus producing sufficiently large agglutinated RBC lumps that can be

**Table 2** Agglutination reaction time required by each secondary blood group for the Alba Bioscience antibodies specified in this study

	Blood groups										
	C	c	E	e	K	k	Jk <sup>a</sup>	Jk <sup>b</sup>	P <sup>1</sup>	S	s
Required reaction period	30 s	3 min	30 s	3 min	2 min	30 s	2 min	2 min	30 s	2 min	2 min

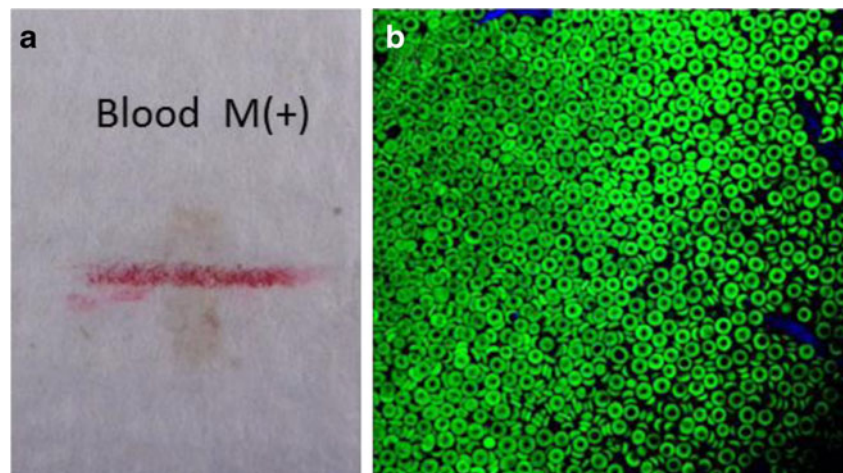
**Fig. 5** Comparison of the effect of antibody structures (IgG and IgM) on the visual identification of the test results: **a** for K antigen test; **b** for s antigen test. The confocal images show details of the haemagglutination behaviours of K(+) and s(+) on paper treated with different antibodies: **c** anti-K IgG, **d** anti-s IgG, **e** anti-K IgM and **f** anti-s IgM. The reaction times of all assays were 2 min and a  $\times 60$  oil lens was used



immobilized in the porous structure of paper. In contrast, agglutination reactions between IgG and RBC antigens

without anti-human globulin are either extremely weak or do not occur at all, leading to false-negative results. The example

**Fig. 6** **a** Visual assay of an M(+) blood sample on paper and **b** confocal image of the same sample. A commercial anti-M IgM obtained from human sera was used for the assay and a reaction time of 3 min was allowed





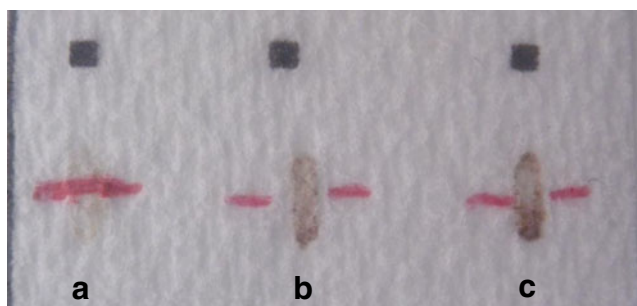


**Fig. 7** Identification for agglutinated RBCs of blood group c washed with distilled water (a), 0.9 % NaCl (b), and phosphate-buffered saline (c). An RBC–antibody interaction time of 2 min was allowed

of K antigen in the Kell system is used to illustrate the different performance of antibodies with different structures. Both IgM and IgG antibodies corresponding to K antigen are commercially available. Figure 5a shows a distinct difference in RBC agglutination patterns: whereas IgM causes strong agglutination of the K-positive sample, IgG shows little or no effect. Another example of detecting s antigen (of the MNS system, Table 1) using IgM and IgG antibodies also shows results very similar to those of the K antigen in the Kell system, confirming that the different structures of antibodies can lead to extremely different agglutination behaviours (Fig. 5b).

Confocal microscopy was used to capture the agglutination patterns of the K(+) and s(+) RBCs by IgM and IgG antibodies. Figure 5c and d show agglutination patterns of K(+) and s(+) RBCs after they had been introduced onto papers treated with anti-K IgG and anti-s IgG, respectively. In both cases, no discernible RBC agglutination could be observed. An interesting observation was that K(+) RBCs show strong deformation and crenation when mixed with anti-K IgG. This is because the commercial anti-K IgG reagent was directly obtained and prepared from a donor's plasma. The impurity of the antibody solution might have caused the RBC deformation. After a drop of 10  $\mu$ L CellStab solution had been added to the paper, the RBCs regained their natural biconcave disc shape (result not presented), but agglutination of RBCs never occurred. In contrast, when K(+) and s(+) RBCs were introduced onto papers treated with anti-K IgM (Fig. 5e) and anti-s IgM (Fig. 5f), agglutination of RBCs was clearly observed

under the confocal microscope. The confocal microscopy results also show that anti-s IgM causes a stronger degree of agglutination than anti-K IgM (Fig. 5e, f); these results concur with the visual assay on the paper surface (Fig. 5a, b). They provided a clear understanding of the effects of antibody structures on the efficiency of RBC agglutination; such effects were further confirmed on a microscopic level.

In another study, antibody–antigen interactions of secondary blood group M were investigated using confocal microscopy. The motivation of this investigation was to understand why a false-negative result was observed for this blood group in our screening test (Fig. 2). A repeat of the assay on paper showed no RBC agglutination, even though a reaction time of 3 min was allowed (Fig. 6a). The confocal image showed that M(+) RBCs could not be agglutinated by anti-M IgM (Fig. 6b). Although anti-M is IgM antiserum, it is considered as a naturally occurring antibody in the human body, rather than an antibody generated by immunoreactions [21]. This type of antibody is a cold-reacting antibody which is not active at 37  $^{\circ}$ C, and therefore is regarded as clinically insignificant [5, 21]. In general, the detection of anti-M can be disregarded for transfusion purposes.

#### The effect of washing conditions

The selection of the washing solution affects the result of secondary blood grouping assays. Firstly, water cannot be used to remove the non-agglutinated blood because of the osmotic effect. Under osmotic pressure, water penetrates into the RBC through its membrane, causing RBC haemolysis by bursting. The agglutinated RBCs therefore can also be removed from the paper (Fig. 7, test a). Secondly, the pH is also an important factor in washing. Under normal circumstances, a washing solution with a pH of about 7 is acceptable because RBCs carry a negative charge and at pH 7–7.5 most antibody molecules have weak positive charges. This enhances the attraction between the RBCs and antibody molecules during the first stage of interaction. Significant lowering of the pH increases the dissociation of the antigen–antibody complexes. This influence of pH levels on the assay result was found to be much more important for secondary blood groups than for primary blood groups; this is due to the weaker antibody–

**Table 3** Secondary blood group typing data obtained using paper devices

	Blood type										
	C	E	c	e	P <sup>1</sup>	K	k	Jk <sup>a</sup>	Jk <sup>b</sup>	S	s
Antibody type	IgM	IgM	IgM	IgM	IgM	IgM	IgM	IgM	IgM	IgM	IgM
Reaction period	30 s	30 s	3 min	3 min	30 s	2 min	30 s	2 min	2 min	2 min	2 min
Number of samples	127	127	127	127	79	79	19	30	30	11	11
Matching with the laboratory results (%)	100	100	100	100	100	100	100	100	100	100	100

antigen interactions of secondary blood groups. Figure 7 (tests b and c) shows the washing of the agglutinated RBCs from the paper. Our results show that for the best results of secondary blood grouping assays, PBS should be used for washing.

Five clinically important secondary blood group systems, including 11 blood groups, have been tested under their optimum conditions. Each blood group involved from 11 to more than 100 samples and all test results using the bioactive-paper devices matched the results obtained in a pathology laboratory using gel card technology. Details of the samples tested are presented in Table 3. The accuracy of this paper diagnostic assay for the blood samples studied was 100 %.

## Conclusion

We have shown in this study that paper-based diagnostics are capable of testing various clinically important secondary blood types. Compared with the typing of primary blood groups, the major challenges in secondary blood group assaying were identified to be the antibody–RBC interaction time, the antibody types, and the pH of the washing buffer. Visual observation of the agglutination pattern on paper was used to evaluate the degree of agglutination under the conditions of the investigation, and confocal microscopy was used to obtain microscopic information on the agglutination patterns in a fibre network at a cellular level. The microscopic and macroscopic results presented in this work establish a detailed understanding of secondary blood grouping in paper. First, RBCs carrying some secondary blood group antigens require a longer time to react with their corresponding antibodies in order to form a sufficient level of agglutination for unambiguous visual identification on paper. Second, the types of antibodies are important in secondary blood group typing. This work confirmed, at a cellular level, that whereas IgM antibodies are able to cause direct agglutination of RBCs, IgG antibodies are unable to do this. In that case an indirect method must be used. Third, the pH of the washing buffer must be maintained at neutral, or at a slightly basic level, to prevent the undesirable dissociation of the agglutinated RBC lumps during washing.

This work is the first research on using paper-based diagnostics for secondary blood group typing. Of the 11 clinically important secondary blood groups we investigated in this study (Table 3), the results obtained by paper-based devices showed a 100 % match with the mainstream gel card technology. The design concept of the paper assay allows both professionals and non-professionals to easily understand and perform the assay.

**Acknowledgments** This work was supported by the Australian Research Council (ARC). Funding received from the ARC through grants DP1094179 and LP110200973 is gratefully acknowledged. The authors thank Haemokinesis for its support through the ARC Linkage Project. The authors also thank John Zhu of the Melbourne Centre for Nanofabrication for confocal imaging and technical help, and Hansen

Shen for proofreading the manuscript. M.L., W.L.T. and L.L. thank the Monash University Research and Graduate School and the Faculty of Engineering for postgraduate research scholarships.

## Reference

- Daniels G (2002) Human blood groups, 2nd edn. Blackwell, Oxford
- Daniels G, Reid ME (2010) Blood groups: the past 50 years. *Transfusion* 50(2):281–289
- Avent ND, Reid ME (2000) The Rh blood group system: a review. *Blood* 95(2):375–387
- Westhoff CM (2004) The Rh blood group system in review: a new face for the next decade. *Transfusion* 44(11):1663–1673
- Daniels G, Bromilow I (2007) Essential guide to blood groups. Wiley-Blackwell, Hoboken
- Daniels G, Poole J, de Silva M, Callaghan T, MacLennan S, Smith N (2002) The clinical significance of blood group antibodies. *Transfus Med* 12:287–295
- Thakral B, Saluja K, Sharma RR, Marwaha N (2010) Phenotype frequencies of blood group systems (Rh, Kell, Kidd, Duffy, MNS, P, Lewis, and Lutheran) in north Indian blood donors. *Transfus Apher Sci* 43(1):17–22
- Malomgré W, Neumeister B (2009) Recent and future trends in blood group typing. *Anal Bioanal Chem* 393(5):1443–1451
- Harmening DM (1999) Modern blood banking and transfusion practices, 4th edn. Davis, Philadelphia
- Li L, Tian J, Ballerini D, Li M, Shen W (2013) Superhydrophobic surface supported bioassay—an application in blood typing. *Colloids Surf B: Biointerfaces* 106:176–180
- Pelton R (2009) Bioactive paper provides a low-cost platform for diagnostics. *Trends Anal Chem* 28(8):925–942
- Li X, Tian J, Shen W (2009) Paper as a low-cost base material for diagnostic and environmental sensing applications. In: 63rd Appita annual conference and exhibition, Melbourne 19–22 April 2009. Appita, Melbourne, pp 267–271
- Ballerini D, Li X, Shen W (2012) Patterned paper and alternative materials as substrates for low-cost microfluidic diagnostics. *Microfluidics Nanofluidics* 13(5):769–787
- Khan MS, Thouas G, Shen W, Whyte G, Garnier G (2010) Paper diagnostic for instantaneous blood typing. *Anal Chem* 82(10):4158–4164
- Al-Tamimi M, Shen W, Zeineddine R, Tran H, Garnier G (2011) Validation of paper-based assay for rapid blood typing. *Anal Chem* 84(3):1661–1668
- Li M, Tian J, Al-Tamimi M, Shen W (2012) Paper-based blood typing device that reports patient's blood type “in writing”. *Angew Chem Int Ed* 51:5497–5501
- Li L, Tian J, Ballerini D, Li M, Shen W (2013) A study of the transport and immobilisation mechanisms of human red blood cells in a paper-based blood typing device studied using confocal microscopy. *Analyst* 138:4933–4940
- Dean L (2005) Blood groups and red cell antigens. National Center for Biotechnology Information, Bethesda
- Hauck EF, Apostel S, Hoffmann JF, Heimann A, Kempinski O, Cereb J (2004) Capillary flow and diameter changes during reperfusion after global cerebral ischemia studied by intravital video microscopy. *Blood Flow Metab* 24:383–391
- Hudetz AG, Feher G, Weigle CGM, Knuese DE, Kampine JP (1995) Video microscopy of cerebrocortical capillary flow: response to hypotension and intracranial hypertension. *Am J Physiol Heart Circ Physiol* 268:H2202–H2210
- Mais DD (2009) ASCP quick compendium of clinical pathology, 2nd edn. ASCP Press, Chicago





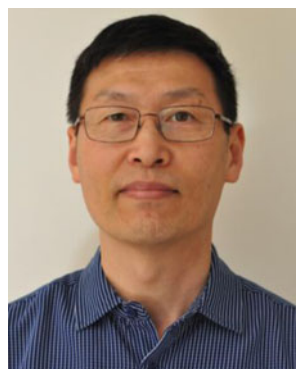
**Miaosi Li** is a PhD student with the Australia Pulp and Paper Institute in the Department of Chemical Engineering, Monash University, Australia. Her current research is focused on the development of user-friendly diagnostic sensors for the purpose of blood analyses and other biochemical analyses for developing countries.



**Lizi Li** is a PhD student in the Department of Chemical Engineering, Monash University, Australia. Her current research interests include the optimization of paper structure and surface chemistry for high-performance paper-based blood typing devices and the development of superhydrophobic surface supported bioassays.



**Whui Lyn Then** is a PhD candidate with BioPRIA in the Department of Chemical Engineering, Monash University, Australia, researching antigen–antibody interactions on paper diagnostics with special focus on paper-based diagnostics for blood typing applications.



**Wei Shen** is Head of the Surface Engineering Group of the Department of Chemical Engineering, Monash University, Australia. His research interest is focused on paper-based and thread-based analytical devices for diagnostic and environmental applications. The group's aim is to use low-technology innovations to create high-performance devices for real-life analysis.

**This page is intentionally blank**

# Red blood cell transport mechanisms in polyester thread-based blood typing devices

Azadeh Nilghaz<sup>1</sup> · David R. Ballerini<sup>1</sup> · Liyun Guan<sup>1</sup> · Lizi Li<sup>1</sup> · Wei Shen<sup>1</sup>

Received: 24 March 2015 / Revised: 7 June 2015 / Accepted: 10 June 2015  
© Springer-Verlag Berlin Heidelberg 2015

**Abstract** A recently developed blood typing diagnostic based on a polyester thread substrate has shown great promise for use in medical emergencies and in impoverished regions. The device is easy to use and transport, while also being inexpensive, accurate, and rapid. This study used a fluorescent confocal microscope to delve deeper into how red blood cells were behaving within the polyester thread-based diagnostic at the cellular level, and how plasma separation could be made to visibly occur on the thread, making it possible to identify blood type in a single step. Red blood cells were stained and the plasma phase dyed with fluorescent compounds to enable them to be visualised under the confocal microscope at high magnification. The mechanisms uncovered were in surprising contrast with those found for a similar, paper-based method. Red blood cell aggregates did not flow over each other within the thread substrate as expected, but suffered from a restriction to their flow which resulted in the chromatographic separation of the RBCs from the liquid phase of the blood. It is hoped that these results will lead to the optimisation of the method to enable more accurate and sensitive detection, increasing the range of blood systems that can be detected.

**Keywords** Polyester thread · Low-cost · Blood typing · Diagnostic · Confocal microscopy

## Introduction

Worldwide collection of blood exceeds 108 million units annually, with the collected blood used for the treatment of blood loss and of many other medical conditions [1]. However, blood cannot simply be transfused between any two people; because of the existence of blood types, there must be donor–recipient compatibility [2]. Without screening, one in three transfusions would result in acute haemolytic reaction [3] with catastrophic results including shock and renal failure, often resulting in death [4].

Blood type is defined by the expression of antigens on the surface of the red blood cells (RBCs) [5], and is usually identified using specific antibodies against these antigens which induce agglutination of the RBCs [6]. Techniques based on haemagglutination include the tube [7], slide [8], and microplate tests [9, 10] and the column agglutination system [11, 12]. Although highly accurate and specific, these techniques are expensive, requiring specialised equipment and trained personnel. Disposable point-of-care systems including lateral-flow devices [13] and bedside test cards [14] avoid high costs, but always require that the user handle or reconstitute antibody reagents or perform pre-treatments on the blood.

Low-cost ways of diagnosing blood type and disease are necessary for impoverished regions [15], and rapid, point-of-care-oriented devices are also highly important for medical emergencies when a second of delay can be the difference between life and death. For both of these applications diagnostics need to be easy to interpret and use, preferably with minimal requirements for training of users.

Published in the topical collection *Fiber-based Platforms for Bioanalytics* with guest editors Antje J. Bäumner and R. Kenneth Marcus.

**Electronic supplementary material** The online version of this article (doi:10.1007/s00216-015-8845-5) contains supplementary material, which is available to authorized users.

✉ Wei Shen

<sup>1</sup> Australian Pulp and Paper Institute, Department of Chemical Engineering, Monash University, Clayton, Melbourne, Victoria 3800, Australia

Recent research has found thread to be an exceptional substrate for fabricating low-cost microfluidic diagnostics, because of its flexibility, ready-made capillary channel structure, strength, low liquid volume requirements, and low cost [16–22]. A polyester thread-based blood typing diagnostic was prototyped which had several unique advantages over earlier paper-based methods [23]. This device enabled the identification of blood type in a single step via a chromatographic separation of the blood cells and serum, which could be easily visually identified by the user. Polyester threads were soaked in antibody solution and dried, and, upon addition of positive blood, agglutination of the RBCs occurred, followed by separation of the plasma and RBC phases, creating a visible band on the thread. The advantages of this method were that it was rapid (<1 min), did not require dilution or pretreatment of blood, and only tiny volumes (~2 µL) were needed, which could be obtained by finger prick. Previous paper-based tests required greater volumes of blood because of higher substrate absorbency, necessitating venepuncture [24]. Furthermore, operation of the thread-based test did not require the washing with saline or other reagents needed in paper tests [25, 26], and therefore no handling of other liquids by users was necessary.

Although polyester thread-based diagnostic devices were effective, the mechanisms responsible were unknown. Recently Li et al. investigated the mechanism behind paper blood typing, using a confocal microscope to view the systems at the cellular scale [27]. Results revealed RBC aggregates mechanically locked within the structure of the paper. The structures of thread and paper differ greatly, with thread having longer, narrower channels resulting from its tightly-packed parallel fibres, as opposed to the many criss-crossed fibres of paper. It is therefore highly likely that dissimilar mechanisms are responsible. The reduced volume of the pores is likely to force RBCs to aggregate in a more organised fashion because of the limited space available for movement. This work studies what occurs on the polyester thread at a deeper level, investigating the main differences between the paper and polyester thread methods by use of confocal microscopy. It is hoped that this study will lead to a greater understanding of the phenomena underlying this new diagnostic method, enabling further optimisation.

## Materials

Polyester (polyethylene terephthalate) threads were kindly donated by the School of Fashion and Textiles, RMIT University, Melbourne. All blood samples were acquired from adult volunteers of known blood group via Dorevitch Pathology, Australia. Samples were stored in Vacutainer tubes containing heparin, citrate, and EDTA and refrigerated at 4 °C, and used within 10 days of collection. Epiclone™ anti-A, anti-

B, and anti-D monoclonal-antibody grouping reagents were purchased from Commonwealth Serum Laboratories, Australia. Anti-A and anti-B are transparent solutions, coloured blue (Patent Blue; E131) and yellow (Tartrazine; E102), respectively, for identification purposes, whereas anti-D is a clear, colourless solution. Antibody reagents were also stored at 4 °C. Physiological saline solution (PSS, 0.9 %) and phosphate-buffered saline solution (PBS, pH 7.4) were prepared from analytical-grade NaCl, KCl, Na<sub>2</sub>HPO<sub>4</sub>, and KH<sub>2</sub>PO<sub>4</sub>, all of which were obtained from Sigma–Aldrich. Anhydrous D-glucose was provided by AJAX Chemicals Ltd., Australia. Fluorescein isothiocyanate (FITC, isomer I) and rhodamine B (also from Sigma–Aldrich) were used for labelling RBCs and staining the plasma phase, respectively. Anhydrous dimethyl sulfoxide (DMSO, from MERCK Chemicals Ltd, Australia) was used to dissolve the FITC at 40 mg mL<sup>-1</sup>. The solution of FITC dissolved in DMSO was then added to ID-CellStab red-cell stabilisation solution (BioRad, Australia) at a volume ratio of 20 µL mL<sup>-1</sup>, to give a solution of FITC concentration 0.8 mg mL<sup>-1</sup>. Rhodamine B was dissolved in PBS at a concentration of 5 ppm. For the oil lenses, type FF fluorescence microscopy immersion oil from Cargille Laboratories, USA, was used. Samples were fixed using Objektträger microscope slides and covers from Knittel Glass, Germany.

## Methods

### Preparation of antibody-impregnated thread

Polyester thread was selected for its excellent colour-display properties, which aid in the identification of the chromatographic separation of the blood phases. Polyester fibres are also solid and impermeable to liquid, meaning that liquid absorption by the thread is only possible because of the voids between fibres; as a result, less liquid is needed to saturate the threads [28]. A JEOL JSM-7001F FEGSEM, provided by the Monash Centre for Electron Microscopy, was used to capture the scanning electron micrograph of the thread. Threads had a fibre thickness of ~13 µm and a roughly circular cross section. Threads used were given an initial plasma treatment, as described by Li et al., to remove surface contaminants, greatly increasing wettability and homogenizing the wicking rate along the thread [16–19]. Threads were treated with antibody via soaking in the grouping reagent followed by blotting to remove excess solution. After drying under a fume hood for 10 min, antibody-coated threads were ready to be used.

### Blood-sample staining

RBCs and blood plasma do not fluoresce (unlike polyester) making it necessary to use fluorescent stains or dyes to impart

fluorescence to these substances. To stain the RBCs a commonly used biological staining compound, FITC, was used. FITC contains the isothiocyanate group which is reactive towards nucleophiles including the amine and sulfhydryl groups commonly found on proteins, enabling it to effectively stain RBCs. This compound has absorption and emission-spectrum maxima at approximately 494 nm and 526 nm, respectively [29], enabling it to be excited by the 488 nm laser used. It was also desired to dye the plasma phase of the blood sample for some experiments, to show the migration of plasma independently from the RBCs. To achieve this another fluorescent compound, rhodamine B, was added to the PBS used to resuspend the RBCs after the final wash. This dye has absorption and emission-spectrum maxima at approximately 557 nm and 578 nm, respectively [29], enabling excitement by the 561 nm laser.

A whole blood sample (1 mL) was centrifuged at 1300g for 3 min. The plasma and buffy coat were then removed from the top layers. The remained RBCs were resuspended to 45 % haematocrit using FITC stain mixed in ID-CellStab ( $0.8 \text{ mg mL}^{-1}$ ). Glucose solution ( $40 \text{ }\mu\text{L}$ ,  $10 \text{ mg mL}^{-1}$ ) was then added to the RBCs before incubating for 2.5 h. Afterwards, the RBCs were washed 10 times to remove unbound FITC from the cells. The RBCs were then resuspended to 45 % haematocrit with ID-CellStab.

To investigate inclusion of FITC and DMSO in the RBC-antigens activities, the FITC-stained RBCs were examined in the presence of specific and nonspecific antibodies under a confocal microscope. The confocal microscopy images reveal that the stained RBCs form aggregates in the presence of specific antigen–antibody solutions despite the FITC stain and rhodamine B dye, as shown in Fig. S1a in the Electronic Supplementary Material (ESM), and ESM Fig. S1b reveals that no haemagglutination forms when the antibody is nonspecific.

### Confocal microscope use

Antibody-treated threads were immobilised in folded polypropylene films with lodging slits to aid testing, and a micropipette (Eppendorf research  $0.1\text{--}2.5 \text{ }\mu\text{L}$ ) was used to dispense a  $2\text{-}\mu\text{L}$  blood sample onto the centre of the threads, which was allowed to react and dry for 5 min. Thread samples were then placed onto glass slides and saturated with immersion oil for confocal imaging. A Nikon Ai1Rsi confocal microscope with  $40\times$  Nikon Plan Fluor oil iris objective lens was used for generating the confocal micrographs. Excitation lasers with wavelengths of 405 nm, 488 nm, and 561 nm were used for excitation of the polyester, FITC, and rhodamine B, respectively. Polyester emission was displayed at 450 nm, FITC at 525 nm, and rhodamine B at 595 nm. Micrographs were captured at a resolution of  $2048\times 2048$  ( $4.2 \text{ Mpx}$ ) and transferred to Fiji image-processing-suite software for post processing.

## Results and discussion

### Confirming the original hypothesis of blood phase locations

In the original study [23], it was hypothesised that three distinct zones were formed on the positive testing threads. The three zones can be seen in Fig. 1d, and are:

1. a RBC dosing zone, which had the deep crimson colour of blood because of the presence of a large number of RBCs;
2. a yellowish separation zone, where it was hypothesised that plasma had separated from the whole blood and wicked further along the thread; and
3. a dry zone which no blood or plasma had reached, which remained coloured only by the non-fluorescent blue dye [30], Patent Blue, added to the antibody solution for identification purposes.

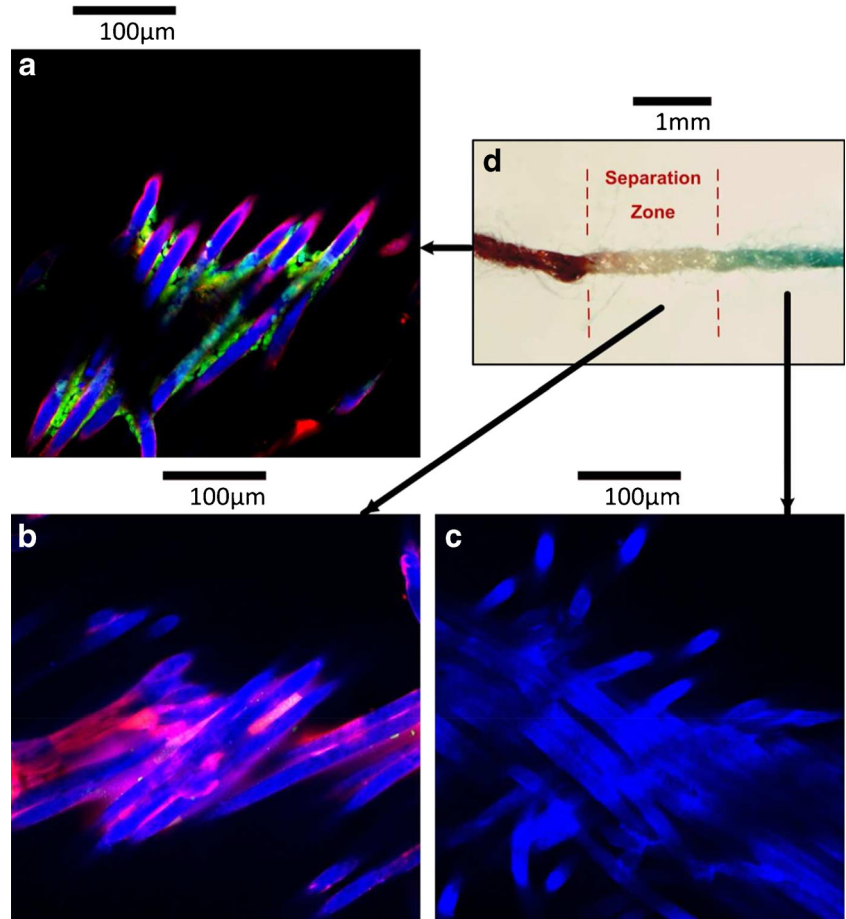
To investigate whether the original hypothesis was correct, a study was performed using the confocal microscope. A blood sample was prepared using FITC stain for the RBCs and rhodamine B dye to mark the location of plasma. This blood was added to threads treated with antisera, and the separation of the plasma phase from the RBCs was observed as expected. Three separate confocal micrographs were captured at different positions along the thread: one for each distinct zone identified above. As a control, laser power levels and detector sensitivities were kept constant at each location.

Figure 1a shows the image captured by the confocal microscope in the region where the blood was dispensed. FITC-stained cells appear green, rhodamine B dye appears red, and polyester appears blue, the colour of its autofluorescence. The image clearly shows a mass of RBCs on and between the fibres of the polyester, surrounded by the plasma phase, as expected. Figure 1b shows the separation zone of the thread device at the cellular level. We clearly see evidence that the plasma phase has reached this area, with the red colour of rhodamine B present on and between the fibres of the thread. Unlike the image of the dosing zone, there are no RBCs visible at all in this region, confirming the original hypothesis that the blood undergoes a separation of phases. Figure 1c shows the final region that was viewed, the dry zone. The appearance of the thread in this region is identical to that of the unused test threads. In this figure we see only the blue colour of the plain polyester fibres, with no green or red visible, suggesting that neither the RBCs nor plasma penetrated this far.

The results of this investigation confirm the original hypothesis that the band formed on the thread between the dosing zone and dry zone is caused by a separation of phases of the blood sample, which enables the plasma phase to penetrate further along the length of the thread than the RBCs.



**Fig. 1** Images of the thread-based blood-typing diagnostic, showing a positive result for detection of the A-antigen on the surfaces of RBCs from a sample of whole blood of type A+. The separation of phase which acts as an indicator of blood type is clearly visible in part (d) (this photograph was not produced with stained or dyed blood), with un-wet, separated, and red-cell zones easily distinguishable. Parts (a) to (c) show confocal micrographs of the three zones, where (a) is the dosing region, (b) is the separation zone, and (c) is the un-wet antibody-treated thread



### Mechanisms of separation

Using the confocal microscope to investigate RBC behaviour in polyester thread treated with nonspecific antibodies revealed that cells were free to migrate within the channels of the thread as individuals. In Fig. 2, cells can be seen in large numbers, with many individual cells visible. The large number of cells present seems to result in the packing together of RBCs in some parts of the image, but it remains clear that there is no cell agglutination. This is to be expected, because RBCs carry a slight negative charge resulting from the presence of the carboxyl group of sialic acids in the cell membrane, causing them to be repelled by each other over short distances [31].

In samples dispensed onto threads with antibodies specific to the cell antigens, the confocal microscope revealed interesting haemagglutination behaviour of RBCs. The cells no longer appeared as individuals, instead appearing as members of small-to-large aggregates. It was expected that these aggregates would take the form of large, irregular lumps, similar to those seen with paper typing [27]. Instead, the cells appeared to form large sheet-like structures between and around the fibres of the thread. These planar bodies wrapped around fibres and spread out between them, filling the spaces between

the fibres. Almost all of the cells existed as part of an aggregate of many cells bound together, with very few RBCs observed as individuals or even within small groups because of

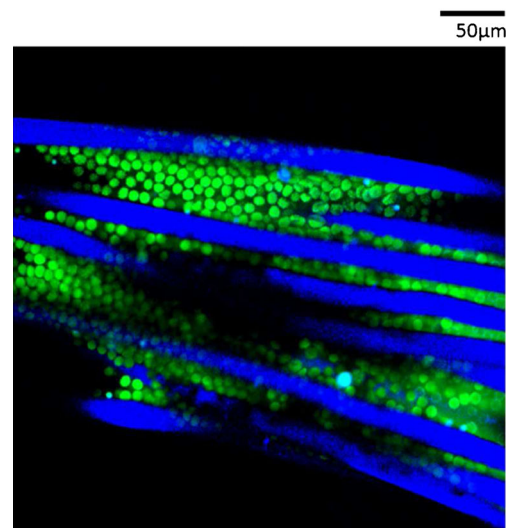
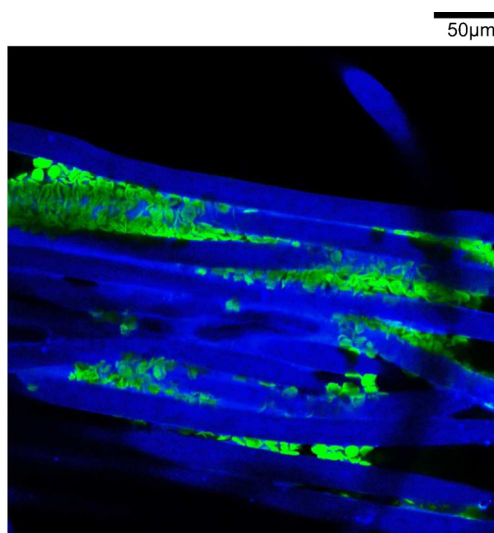


**Fig. 2** Non-agglutinated FITC-stained O- blood on anti-D-antibody-treated polyester thread. Despite the large number of RBCs visible, it is still possible to observe that the cells are not bound together, instead moving through the channels as individual cells

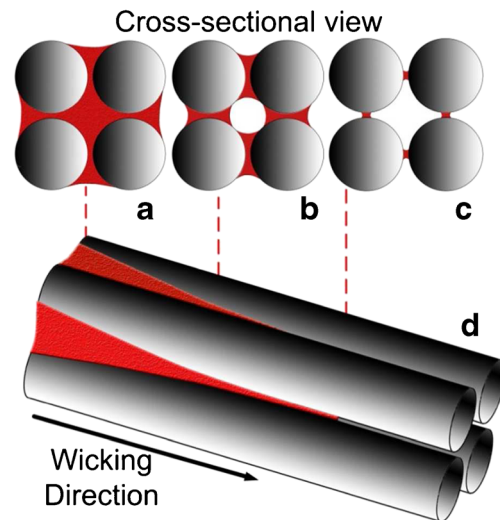
the powerful agglutinating ability of the antibody solutions used. It seems likely that this sheet-like formation of cells is a result of the narrow, parallel channels found in the threads. Agglutination occurring in this confined space is unable to form three-dimensional aggregates, because there is simply not enough space for RBCs to flow over each other.

Figure 3 below shows that the RBC aggregates are adsorbed to the fibre surfaces to some extent or are wrapped around them. The flat, planar shape of the aggregates means that, in the first step, negatively charged RBCs are attracted to the blood-typing antibodies, which have slightly positive charges. While blood plasma redissolved the antibody from the thread surface, specific antibody–antigen reaction occurred and large lumps of RBC aggregates formed. This results in a chromatographic separation of the phases, where the RBCs are analogous to the solute, the plasma to the mobile phase, and the thread to the stationary phase, and hence results in visible separation.

As liquid wicks in thread it does so via film wetting, with the thickness of the wicking liquid layer being extremely thin at the wicking front. This type of wetting was studied in detail by Roberts et al. [32] for paper substrates. Roberts et al. found that Laplace film thickening led liquid to be drawn into the corners formed between intersecting paper fibres. This effect would encourage the formation of 3D aggregates of RBCs, as has been seen in paper blood typing. The thread's structure does not include crossed fibres or corner sections, but rather parallel fibres. It is likely that wetting in these pores occurs, as illustrated in Fig. 4 below. Based on the work by Roberts et al., Khan et al. [33] and Tian et al. [34] have experimentally modelled liquid-penetration behaviour in V-grooves, simulating liquid movement in inter-fibre open capillaries similar to those illustrated in Fig. 4d. Their work provided a more



**Fig. 3** Agglutinated FITC-stained A+ blood on anti-A-antibody-treated thread. Sheet-like structures composed of agglutinated RBCs can be seen, wrapped around fibres and occupying the spaces between them



**Fig. 4** Illustration of film-wetting behaviour at the approaching wicking front on thread, showing four hypothetical fibres. (a) Cross-section of the flow at the saturated end of the thread. (b) Cross-section of the partially wet fibres not far from the wicking front. (c) Cross-section of the fibres at the wicking front, showing very small degree of coverage by the wetting liquid. (d) View of the fibres from the side, showing the oncoming wicking front

quantitative understanding of liquid-penetration rate and imaging-based information regarding the liquid wicking front in V-shaped open capillaries. The imaging result of this study (Fig. 2) is in good agreement with those modelling studies.

RBC aggregates will form in the regions where the blood sample first wicks and redissolves the antibody. Because of film wetting in thread this location is in the narrow spaces directly between adjacent fibre surfaces, as seen in Fig. 4a. Because of the narrowness of this area it would be difficult for rotund, three-dimensional aggregates to form. At this location cells cannot flow over each other, but instead must move lengthways along the fibre in the thin film. This may explain why the cells aggregate to form sheets rather than the more rotund, three-dimensional forms previously observed in paper substrates.

Because of the confined space between the sheets of agglutinated RBCs and the fibre surfaces, movement of aggregate lumps alongside the fibres is inhibited. The effects of any weak forces of attraction between the aggregates and the fibres are intensified because of their high facial-area-to-volume ratio, in a similar fashion to the way in which direct dye molecules adsorb strongly to flat substrates. Because the liquid phase of the blood sample is not subject to this kind of attraction, it remains able to move through the pores of the thread easily, resulting in the separation effect observed.

### Comparison with paper

Although the polyester thread and paper-based blood typing methods share many commonalities, there are several

important differences between them. Our results reveal that such difference is primarily linked to the fibre-network morphology in paper and thread, and to a lesser degree to the chemical composition of the materials.

Fibres in paper are more fibrilized than those in polyester thread; this is because these fibres are refined during the papermaking process. The microfibrils torn off the fibre walls increase the fibre surface area, leading to inter-fibre bonding via hydrogen bonding and entanglement of microfibrils. In contrast, microfibrillation is much less substantial on fibres in a thread; this leads to much weaker bonding between fibres in thread. The film flow of liquid in the fibre matrix of paper means that the liquid wicking front follows the capillaries defined by inter-fibre gaps [32]. Because fibres in a paper sheet are randomly oriented, fibre-gap capillaries are not continuous, but are obstructed by “corners” formed by fibres laying across one another. The sizes of pores close to the paper surface are several tens of micrometers, allowing the formation of 3D RBC aggregates. At the same time the corners provide mechanical anchoring sites to immobilize large, agglutinated RBC lumps. The flat and ribbon-shaped paper fibres, usually 20–30  $\mu\text{m}$  in width, can also immobilize smaller RBC aggregates [27].

In contrast with paper, the synthetic polymer fibres of polyester are produced by extrusion, giving them a more rounded shape and circular cross-section. The polymer fibres are highly regular, cylindrical in shape, and solid, making them impervious to liquid absorption. Their width is only  $\sim 12 \mu\text{m}$ , much smaller than that of paper fibres. Polyester thread has long parallel pores as a result of having a core made up of mostly parallel fibres, with some outer fibres wound around the core (Fig. 5). Within the core there is little criss-crossing of fibres, and hence the structure lacks the corners seen in paper. The capillary channels in which the blood flows are longer, with

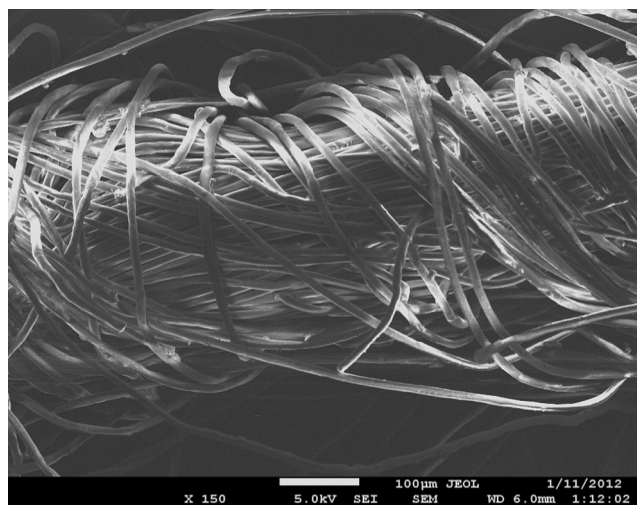


**Fig. 5** Scanning electron micrograph of the polyester thread used in the thread-based method, at 150 $\times$  magnification. A small proportion of outer polyester fibres wrap around a central core of axially orientated fibres

fewer interruptions to flow from cross-fibres. Additionally, comparing the apparent voidage between the two substrates reveals that threads have much more regularly orientated and densely packed fibres with less space between, meaning there is less empty space for the RBCs to travel and aggregate in. This is probably the main factor which makes RBC aggregates more flat and ribbon-shaped in polyester thread than within the structure of paper.

The difference in shape and absorbance between paper and polyester thread means that a greater volume of blood and separated plasma is needed to perform single-step blood typing tests on paper. Paper, being planar, has a circular wicking front, with the volume of paper that must be wet for the wicking front to advance increasing proportionally to the square of the wetting distance. This means that the wetting front slows substantially as the spot of blood wicks through the paper. This effect is compounded by the higher absorbency of the cellulose fibres of the paper compared with polyester thread; even when cut into thin strips, the volume of blood required to wet a long length of paper is substantial. Thread, in contrast, has a linear structure with very small cross-section, meaning that small volumes can result in long penetration distances. The low absorbency of the polyester thread selected further increases the ultimate penetration distance. This greater penetration distance results in the separation of phases being much more visibly prominent, making thread a superior substrate for the chromatographic separation of agglutinated blood from plasma phase and thus making it possible to type a low volume of blood in a single step.

## Conclusions

The polyester thread-based blood typing method shows great promise as a diagnostic for blood grouping in impoverished regions and in emergencies. The addition of the fluorescent dye rhodamine B to the plasma phase of FITC-stained blood enabled us to investigate the locations of the whole-blood phases independently of one another, and was an improvement to the previously reported technique. As a result, this technique was able to confirm the original hypothesis regarding the separation of the whole-blood samples into the constituent phases in different sections of the thread.

A surprising contrast with the mechanisms which occur on paper was found. Agglutinated aggregates are not rotund in the structure of the polyester thread as they are within the paper-fibre matrix, but rather experience restricted flow along the length of the thread, which results in their separation from the faster-wicking plasma phase. This resistance to flow is probably caused by a combination of chromatography separation, weak forces of attraction between agglutinated RBCs and antibodies, and confined space between fibres.



It is hoped that the results of this study can be used to further optimise the thread-based blood typing method to improve the accuracy or sensitivity of the device, possibly enabling it to detect other blood systems which have weaker haemagglutination reactions. On the basis of the mechanisms proposed, it is expected that changes to variables including the chemical composition of the fibre material, the fibre shape and thickness, the tightness of fibre twisting, and chemical treatments to the fibre could be investigated to meet these objectives.

**Acknowledgments** The authors would like to thank The Melbourne Centre for Nanofabrication (MCN) for providing world-class facilities, including the confocal microscope used in the study. We also thank Dr John Zhu of the MCN for his guidance and instruction in the use of the confocal microscope. The authors also thank Dr Lijing Wang of the School of Fashion and Textiles, RMIT University, for kindly providing the thread samples and Dr Ying Hui Ngo for her assistance in capturing SEM images of the thread used, and the Monash Centre for Electron Microscopy for providing SEM facilities. The research scholarships of Monash University and the Department of Chemical Engineering are gratefully acknowledged.

## References

- World Health Organization (2014) <http://www.who.int/mediacentre/factsheets/fs279/en/> visited on November 2014
- Watkins WM (2001) The ABO blood group system: historical background. *Transfus Med* 11:243–265
- Daniels G, Bromilow I (2007) *Essential guide to blood groups*. Blackwell Publishing Ltd, Oxford
- Joshi V (2006) *Anatomy and physiology for nursing and health care*. BI Publications, New Delhi
- Malomgré W, Neumeister B (2009) Recent and future trends in blood group typing. *Anal Bioanal Chem* 393:1443–1451
- Dean L (2005) *Blood groups and red cell antigens*. National Center for Biotechnology Information (NCBI), Bethesda
- Estridge BH, Reynolds AP, Walters NJ (2000) *Basic medical laboratory techniques*. Delmar Cengage Learning, Albany
- Pramanik D (2010) *Principles of physiology*. Academic Publishers, Kolkata
- Llopis F, Carbonell-Uberos F, Montero MC, Bonanad S, Planelles MD, Plasencia I, Riola C, Planells T, Carrillo C, De Miguel A (1999) A new method for phenotyping red blood cells using microplates. *Vox Sang* 77:143–148
- Llopis F, Carbonell-Uberos F, Planelles MD, Montero M, Puig N, Atienza T, Alba E, Montoro JA (1997) A monolayer coagglutination microplate technique for typing red blood cells. *Vox Sang* 72:26–30
- Langston MM, Procter JL, Cipolone KM, Stroncek DF (1999) Evaluation of the gel system for ABO grouping and D typing. *Transfusion* 39:300–305
- LaPierre Y, Rigal D, Adam J, Josef D, Meyer F, Greber S, Drot C (1990) The gel test: a new way to detect red cell antigen-antibody reactions. *Transfusion* 30:109–113
- Plapp FV, Rachel JM, Sinor LT (1986) Dipsticks for determining ABO blood groups. *Lancet* 327:1465–1466
- Giebel F, Picker SM, Gathof BS (2008) Evaluation of four bedside test systems for card performance, handling and safety. *Transfus Med Hemother* 35:33–36
- Yager P, Edwards T, Fu E, Helton K, Nelson K, Tam MR, Weigl BH (2006) Microfluidic diagnostic technologies for global public health. *Nature* 442:412–41816
- Nilghaz A, Ballerini DR, Fang XY, Shen W (2014) Semiquantitative analysis on microfluidic thread-based analytical devices by ruler. *Sensors Actuators B Chem* 191:586–594
- Nilghaz A, Ballerini DR, Shen W (2013) Exploration of microfluidic devices based on multi-filament threads and textiles: a review. *Biomicrofluidics* 7:051501–051516
- Ballerini DR, Li X, Shen W (2011) Flow control concepts for thread-based microfluidic devices. *Biomicrofluidics* 5:14105
- Li X, Tian J, Shen W (2009) Thread as a versatile material for low-cost microfluidic diagnostics. *ACS Appl Mater Interfaces* 2:1–6
- Safavieh R, Mirzaei M, Qasaimeh MA, Juncker D (2009) Yarn based microfluidics: from basic elements to complex circuits, in *MicroTAS, The thirteenth International Conference on Miniaturized Systems for Chemistry and Life Sciences 2009*. The Chemical and Biological Microsystems Society, Jeju
- Safavieh R, Zhou GZ, Juncker D (2011) Microfluidics made of yarns and knots: from fundamental properties to simple networks and operations. *Lab Chip* 11:2618–2624
- Reches M, Mirica KA, Dasgupta R, Dickey MD, Butte MJ, Whitesides GM (2010) Thread as a matrix for biomedical assays. *ACS Appl Mater Interfaces* 2:1722–1728
- Ballerini DR, Li X, Shen W (2011) An inexpensive thread-based system for simple and rapid blood grouping. *Anal Bioanal Chem* 399:1869–1875
- Khan MS, Thouas G, Shen W, Whyte G, Garnier G (2010) Paper diagnostic for instantaneous blood typing. *Anal Chem* 82:4158–4164
- Li M, Tian J, Al-Tamimi M, Shen W (2012) Paper-based blood-typing device that reports patient's blood type "in writing". *Angew Chem Int Ed Engl* 51:5497–5501
- Al-Tamimi M, Shen W, Zeineddine R, Tran H, Garnier G (2011) Validation of paper-based assay for rapid blood typing. *Anal Chem* 84:1661–1668
- Li L, Tian J, Ballerini D, Li M, Shen W (2013) A study of the transport and immobilisation mechanisms of human red blood cells in a paper-based blood typing device using confocal microscopy. *Analyst* 138:4933–4940
- Fourné F (1999) *Synthetic fibers: machines and equipment, manufacture, properties: handbook for plant engineering, machine design, and operation*. Hanser/Gardner Publications, Cincinnati
- Sauer M, Hofkens J, Enderlein J (2010) *Handbook of fluorescence spectroscopy and imaging: from ensemble to single molecules*. Wiley, USA
- Tellier F, Steibel J, Chabrier R, Blé FX, Tubaldo H, Rasata R, Chambrion J, Duportail G, Simon H, Rodier JF, Poulet P (2012) Sentinel lymph nodes fluorescence detection and imaging using Patent Blue V bound to human serum albumin. *Biomed Opt Express* 3:2306–2316
- Fernandes HP, Cesar CL, Barjas-Castro MDL (2011) Electrical properties of the red blood cell membrane and immunohematological investigation. *Rev Bras Hematol Hemoter* 33:297–301
- Roberts RJ, Senden TJ, Knackstedt MA, Lyne MB (2003) Spreading of aqueous liquids in unsized papers is by film flow. *J Pulp Pap Sci* 29:123–131
- Khan M, Kannangara D, Garnier G, Shen W (2011) Effect of liquid droplet impact velocity on liquid wicking kinetics in surface V-grooves. *Chem Eng Sci* 66:6120–6127
- Tian J, Kannangara DS, Li X, Shen W (2010) Capillary driven low-cost V-groove microfluidic device with high sample transport efficiency. *Lab Chip* 10:2258–2264